



**A University of Sussex DPhil thesis**

Available online via Sussex Research Online:

<http://sro.sussex.ac.uk/>

This thesis is protected by copyright which belongs to the author.

This thesis cannot be reproduced or quoted extensively from without first obtaining permission in writing from the Author

The content must not be changed in any way or sold commercially in any format or medium without the formal permission of the Author

When referring to this work, full bibliographic details including the author, title, awarding institution and date of the thesis must be given

Please visit Sussex Research Online for more information and further details

# *N*-Heterocyclic Carbene-Palladium and -Copper Complexes in Cross-Coupling Reactions

**Christopher W. D. Gallop**

Supervisors: Dr E. M. E. Viseux and Dr O. Navarro

Submitted to the University of Sussex in part fulfilment of the requirements of the  
degree of Doctor of Philosophy, September 2014

**Declaration**

I hereby declare that the work presented in this thesis was carried out at the University of Sussex under the supervision of Dr E. M. E. Viseux and Dr O. Navarro between the dates of October 2010 and September 2014. The work presented in this thesis is my own, unless otherwise stated, and has not been submitted in whole or in part form for the award of another degree.

Christopher W. D. Gallop

September 2014

## ABSTRACT

Chapter 1 gives the reader a background on cross-coupling reactions, in particular palladium mediated couplings. Furthermore the importance of ligands, including phosphines and *N*-heterocyclic carbenes (NHC), in such cross-coupling reactions is explored.

Chapter 2 provides a background to the reductive lithiation of phosphines, followed by an account of our investigation of BINAP functionalisation by means of reductive elimination.<sup>1</sup> The reaction was examined by experimental means and through the use of density functional theory to predict <sup>31</sup>P NMR chemical shifts.

Chapter 3 provides background on the Heck reaction and selected developments over the years, with particular reference to the use of aryl chlorides in the reaction. A brief discussion of NHC based palladium complex sets the scene for our investigation of a new class of (NHC)-Pd catalysts developed by the Navarro group. Complexes of type (NHC)PdCl<sub>2</sub>(TEA) (TEA = triethylamine) have been tested for their activity in the Heck reaction, focusing on the scope of the reaction with electron-deficient aryl chlorides and electron-rich aryl bromides.<sup>2</sup>

Chapter 4 gives an account of the discovery and developments of the Sonogashira reaction. Particular attention is paid to non-classical systems such as palladium-only and copper-only protocols. Herein our investigation into the use of collaborative (NHC)-Pd and (NHC)-Cu in Sonogashira reactions is presented.<sup>3</sup> Notable features of this system are the low catalyst loadings and the synthetically convenient conditions in which the reaction can be carried namely non-anhydrous solvents and in air.

**Publications:**

- (1) Gallop, C. W. D.; Bobin, M.; Hourani, P.; Dwyer, J.; Roe, S. M.; Viseux, E. M. *E. J. Org. Chem.* **2013**, 6522–6528.
- (2) Gallop, C. W. D.; Zinser, C.; Guest, D.; Navarro, O. *Synlett* **2014**, 2225–2228.
- (3) Gallop, C. W. D.; Chen, M.-T.; Navarro, O. *Org. Lett* **2014**, 3724–3727.

## ACKNOWLEDGEMENTS

This thesis is dedicated to my parents for all the love and support they have given me over the years, this one's for you nippers!

Thank you to my supervisors: Dr O. Navarro and Dr E. M. E. Viseux

I would also like to thank:

Prof. P. J. Parsons

Dr J. F. C. Turner

Dr I. R. Crossley

Dr H. Cox

Dr S. M. Roe

Dr I. J. Day

Dr A. Abdul-Sada

Alex, Paul and Barry

Chris Dadswell

Mick and Fran

Thank you to all of my friends who have kept me company throughout my undergraduate and postgraduate years at Sussex. There are far too many to name you all, but you know who you are!

Debbie, Sme, Cath, Charli, Jennie, Jason, Paul B. Tara, Kayla, Becky, Mariusz, Adam, Oran, Dan, Gavin, Tom, Jess (micro), Sandy, Alistair.

Not forgetting all members, past and present, of the Sussex Uni Trampolining club; the club has been such a huge part of life during my time at Sussex.

Neil, Val, Amy G., Liz, Hannah, Phil, Cia, Nicole, Chris, Danielle, Amy M., Jo B., Fran, Fisher, Emi, Livvi, Alice, Megan, Joe.

A special thanks to:

Dr L. J. Walsh (aka Justin Leeber), Dr J. A. Friggins,  
Dr L. Nicholls, Dr N. Trathen and Dr M. Renshaw.

Finally to my pico Jess, you have put up with me through all the highs and lows that come with doing a PhD, and next a PGCE! I couldn't do any of it without you by my side. Thank you.

## TABLE OF ABBREVIATIONS

acac	acetylacetonyl
BDE	bond dissociation
BDI	$\beta$ -diketiminate ligand
BINAP	2,2'-bis(diphenylphosphino)-1,1'-binaphthalene
BINOL	[1,1'-binaphthalene]-2,2'-diol
CAN	cerium ammonium nitrate
CCDC	Cambridge Crystallographic Data Centre
cod	cyclooctadiene
Cp*	pentamethylcyclopentadiene
Cy	cyclohexyl
DABCO	1,4-diazabicyclo[2.2.2]octane
dba	dibenzylideneacetone
DBTA	dibenzoyl tataric acid
DCE	1,2-dichloroethane
DFT	density functional theory
DIPEA	diisopropylethylamine
dippb	1,4-bis(diisopropylphosphino)butane
DMA	dimethylacetamide
DMEDA	<i>N, N'</i> -dimethylethylenediamine
DMSO	dimethylsulfoxide
dppe	1,2-bis(diphenylphosphino)ethane
dppf	1,1'-bis(diphenylphosphanyl)ferrocene
dpph	1,6-bis(diphenylphosphino)hexane
dppm	1,2-bis(diphenylphosphino)methane
ee	enantiomeric excess
GC	gas chromatography
GIAO	gauge-including atomic orbital method
HMBC	heteronuclear multiple-bond correlation
HOMO	highest occupied molecular orbital
LUMO	lowest occupied molecular orbital
MOM	methoxymethyl ether
n.d.	not determined

NBS	<i>N</i> -bromosuccinimide
NHC	<i>N</i> -heterocyclic carbene
NMP	<i>N</i> -Methyl-2-pyrrolidone
NMR	nuclear magnetic resonance
NSCCS	National Service for Computational Chemistry Software
ppm	parts per million
TBAB	tetrabutylammonium bromide
TBAE	tetrabutylammonium acetate
TBDPS	<i>tert</i> -butyldiphenylsilyl
TBS	<i>tert</i> -butyldimethylsilyl
TEA	triethylamine
TEM	transmission electron microscopy
TES	triethylsilyl
Tf	trifluoromethanesulfonate
THF	tetrahydrofuran
TMS	trimethylsilyl
Triphos	bis(diphenylphosphinoethyl)phenylphosphine
Xantphos	4,5-bis(diphenylphosphino)-9,9-dimethylxanthene



## CONTENTS

<b>1. Introduction .....</b>	<b>12</b>
<b>1.1 Cross-Coupling Reactions .....</b>	<b>12</b>
<b>1.2 Overview of Palladium Cross-Coupling Reactions .....</b>	<b>13</b>
1.2.1 Kumada-Corriu Cross-Coupling .....	14
1.2.2 Suzuki-Miyaura Cross-Coupling .....	15
1.2.3 Negishi Cross-Coupling .....	18
1.2.4 Stille Cross-Coupling .....	19
1.2.5 Hiyama Cross-Coupling .....	20
<b>1.3 Cross-Coupling Reactions Catalysed by Other Metals .....</b>	<b>21</b>
1.3.1 Nickel .....	22
1.3.2 Copper .....	23
1.3.3 Iron .....	24
1.3.4 Cobalt .....	27
1.3.5 Rhodium .....	29
<b>1.4 Ligands in Cross-Coupling .....</b>	<b>31</b>
1.4.1 Phosphines .....	32
1.4.2 <i>N</i> -Heterocyclic Carbenes .....	46
1.4.3 Palladacycles .....	61
1.4.4 Ligand-free systems .....	65
<b>1.5 References .....</b>	<b>67</b>
<b>2. Investigation into the Reductive Cleavage of BINAP .....</b>	<b>74</b>
<b>2.1 Background .....</b>	<b>74</b>
2.1.1 Synthesis of Phosphines .....	74
2.1.2 Investigation Aim and Initial Studies .....	85

<b>2.2</b>	<b>Results and Discussion.....</b>	<b>86</b>
2.2.1	Lithiation.....	86
2.2.2	Protonation.....	89
2.2.3	Silylation.....	91
2.2.4	<sup>31</sup> P NMR Calculations.....	93
2.2.5	Alkylation .....	97
2.2.6	Mechanistic Insights .....	104
<b>2.3</b>	<b>Conclusions.....</b>	<b>108</b>
<b>2.4</b>	<b>References.....</b>	<b>109</b>
<b>3.</b>	<b>(NHC)PdCl<sub>2</sub>(TEA) catalysts for the Mizoroki-Heck Reaction .....</b>	<b>111</b>
<b>3.1</b>	<b>Background .....</b>	<b>111</b>
3.1.1	Discovery of the Mizoroki-Heck Reaction .....	111
3.1.2	Mechanism.....	112
3.1.3	Use of Aryl Chlorides in the Mizoroki-Heck Reaction.....	119
3.1.4	Investigation Aim.....	133
<b>3.2</b>	<b>Results and Discussion.....</b>	<b>134</b>
<b>3.3</b>	<b>Conclusions.....</b>	<b>148</b>
<b>3.4</b>	<b>References.....</b>	<b>148</b>
<b>4.</b>	<b>Sonogashira Couplings Catalysed by Collaborative (NHC)-Copper and - Palladium Complexes .....</b>	<b>152</b>
<b>4.1</b>	<b>Background .....</b>	<b>152</b>
4.1.1	Discovery of the Sonogashira Reaction .....	152
4.1.2	Mechanism.....	153
4.1.3	Development of Alternative Sonogashira Protocols .....	154
<b>4.2</b>	<b>Investigation Aims .....</b>	<b>176</b>

<b>4.3</b>	<b>Results and Discussion.....</b>	<b>177</b>
<b>4.4</b>	<b>Conclusions.....</b>	<b>188</b>
<b>4.5</b>	<b>References.....</b>	<b>188</b>
<b>5.</b>	<b>Experimental Details.....</b>	<b>192</b>
<b>5.1</b>	<b>Investigation into the Reductive Cleavage of BINAP .....</b>	<b>192</b>
5.1.1	General Remarks.....	192
5.1.2	Computational Methods.....	192
5.1.3	General Procedure for the Lithiation of Phosphines .....	193
5.1.4	General Procedure for the Trapping of the Lithiated Solutions .....	193
5.1.5	General Procedure for the Alkylation of Binaphthylphospholes .....	193
<b>5.2</b>	<b>(NHC)PdCl<sub>2</sub>(TEA) catalysts for the Mizoroki-Heck Reaction .....</b>	<b>199</b>
5.2.1	General Remarks.....	199
5.2.2	General Procedure for the Heck couplings .....	199
<b>5.3</b>	<b>Sonogashira Couplings Catalysed by Collaborative (NHC)-Copper and -Palladium Complexes .....</b>	<b>214</b>
5.3.1	General Remarks.....	214
5.3.2	Preparation of Catalyst Stock Solutions.....	214
5.3.3	General Procedure for the Sonogashira Couplings .....	214
<b>5.4</b>	<b>References.....</b>	<b>224</b>

## APPENDICES

All appendices can be found on the compact disc that accompanies this thesis.

**A1.** NMR Spectra for Chapter 2

**A2.** Computational Data for Chapter 2

**A3.** Crystal Structures for Chapter 2

**A4.** NMR Spectra for Chapter 3

**A5.** NMR Spectra for Chapter 4

**A6.** Journal article - Investigation of the Reductive Cleavage of BINAP and Application to the Rapid Synthesis of Phospholes.

**A7.** Journal article - Mizoroki–Heck Reactions Catalysed by (*N*-Heterocyclic carbene) PdCl<sub>2</sub>(Et<sub>3</sub>N) Complexes.

**A8.** Journal article - Sonogashira Couplings Catalyzed by Collaborative (*N*-Heterocyclic Carbene)-Copper and -Palladium Complexes.

## CHAPTER 1

**1. Introduction****1.1 Cross-Coupling Reactions**

Cross-coupling reactions have become one of the most significant and convenient tools that the synthetic organic chemist use to construct molecules of interest. A traditional cross-coupling is the reaction of an organic electrophile with a nucleophilic organometallic reagent, and is a selective process catalysed by a transition metal typically from groups 8-10 (Figure 1.1). During this reaction the product  $R^1-R^2$  is formed and ideally no homocoupled side products ( $R^1-R^1$  and  $R^2-R^2$ ) are obtained. A variety of bonds can be assembled in this manner including C-C, C-N, C-O, C-H and C-S bonds. Consequently, the industrial application of cross-coupling reactions now ranges from the synthesis of electronic materials to natural products and pharmaceuticals.<sup>1</sup>

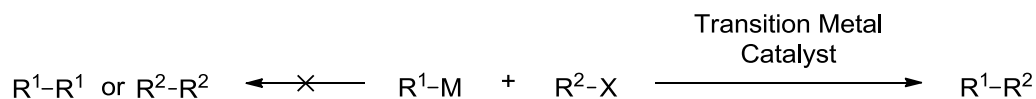


**Figure 1.1.** General scheme for a transition metal catalyzed cross-coupling.

Since the first discovery of cross-coupling reactions the scope of the organometallic species has been expanded and includes Mg, Li, Zn, B, Sn, Si or Cu; the identity of the organometallic coupling partner ( $R^1M$ ) generally determines the identity of the coupling reaction (see Figure 1.2). At the forefront of cross-coupling reactions are palladium-catalysed reactions, the significance of which was acknowledged in 2010 when Heck, Negishi and Suzuki were awarded the Nobel Prize for their contribution to this field of chemistry.<sup>2</sup>

## 1.2 Overview of Palladium Cross-Coupling Reactions

Mechanistically, all palladium cross-coupling reactions are generally accepted to involve three elementary steps: (1) the oxidative addition of an organic electrophile, the first coupling partner, to a palladium(0) centre to form a palladium(II) species; (2) the transmetalation of a nucleophilic organometallic reagent, the second coupling partner; finally (3) the reductive elimination which releases the product and regenerates the palladium(0) to restart the catalytic cycle (Figure 1.2).

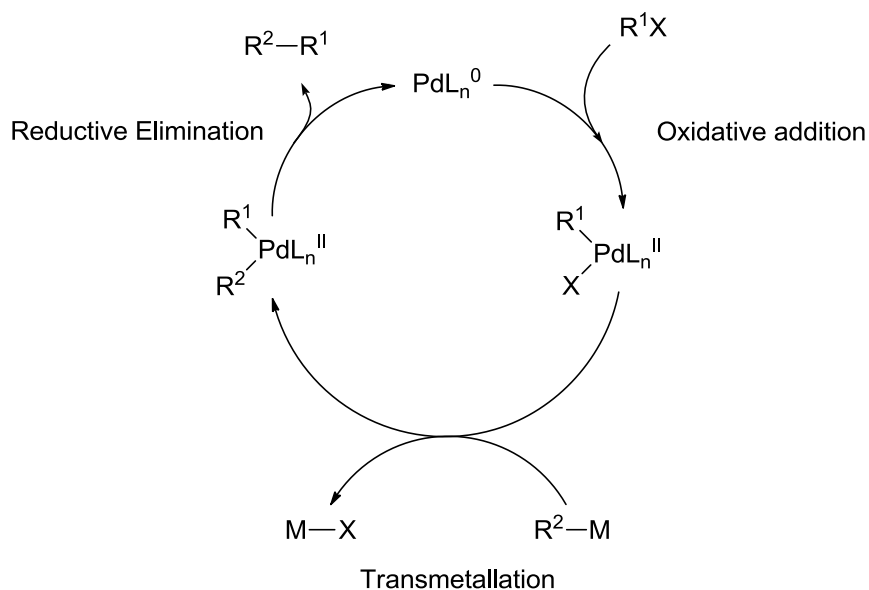
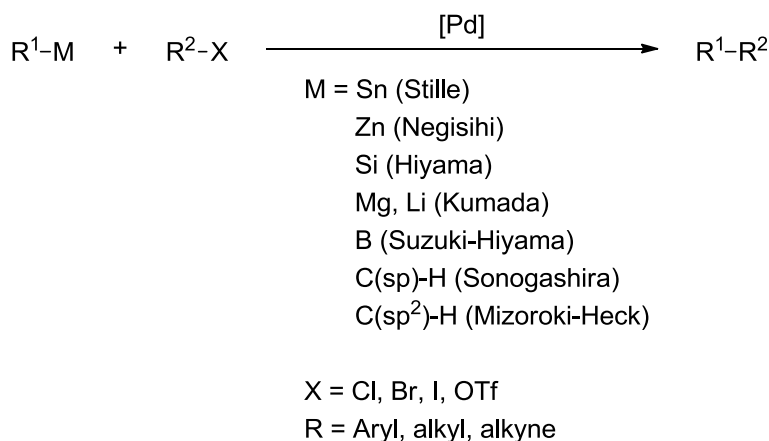


**Figure 1.2.** General catalytic cycle for a palladium(0) catalysed cross-coupling showing the three main common steps.

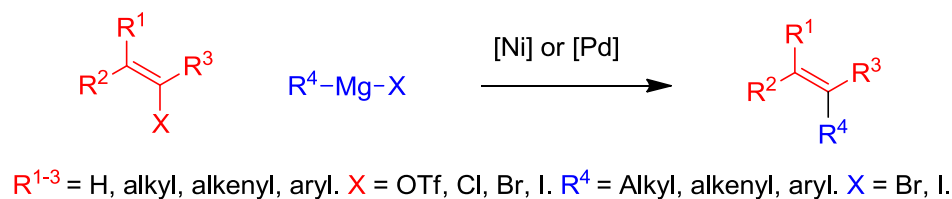
There are several cross-coupling reactions that are catalysed by palladium and they are determined by the type of nucleophile that they can couple with organic halides, these are summarised in Scheme 1.1. A short outline of these C-C bond forming reactions and an example of their use in synthesis are presented below. The Mizoroki-Heck reaction and Sonogashira reactions are the main focus of this work and are discussed in greater detail later on in Chapters 3 and 4.



**Scheme 1.1.** Summary of palladium(0) catalysed cross-coupling reactions, classified by the nucleophilic partner used.

### 1.2.1 Kumada-Corriu Cross-Coupling

The groups of Kumada and Corriu independently reported the coupling of Grignard reagents with aryl halides in 1972.<sup>3,4</sup>

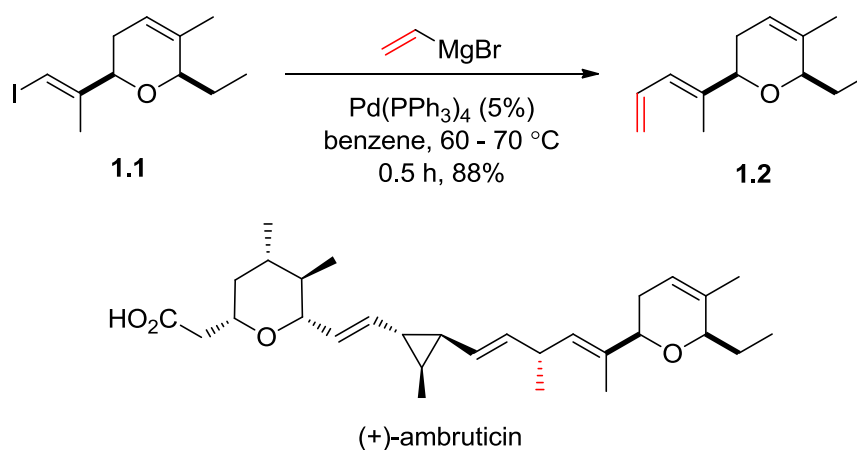


**Scheme 1.2** General scheme for a Kumada-Corriu coupling.

The availability of Grignard reagents makes this reaction a versatile method for C-C bond formation as alkyl (primary and secondary), aryl, alkenyl and allyl Grignard reagents are compatible with the coupling. Organolithium reagents can also be coupled when a Pd-based catalyst is used.<sup>5</sup> However the basic nature of these reagents can sometimes cause incompatibilities with coupling partners. In general this reaction tolerates coupling with chlorides fairly well, where others tend not to. For example, the first example of the Kumada coupling of unactivated aryl chlorides was reported by Nolan and Huang in 1999.<sup>6</sup> By utilising an (NHC)-Pd catalyst (NHC = *N*-heterocyclic carbene) they were able to couple PhMgBr and a range of electron rich aryl chlorides (including *ortho*-substitution), the only limitation being the synthesis of the demanding

tetra-*ortho*-substituted biaryls. The reactions proceeded at 80 °C and were generally complete in 3 - 5 hours, giving the desired biaryl product in good to excellent yields.

An example of the palladium-catalysed Kumada cross-coupling in synthesis can be seen in Jacobsen's total synthesis of the antifungal agent (+)-ambruticin.<sup>7</sup> Vinyl iodide **1.1** was coupling with vinyl magnesium bromide to install the diene functionality in **1.2** (Scheme 1.3).



**Scheme 1.3** Jacobsen's use of the Kumada coupling in the synthesis of (+)-ambruticin.

### 1.2.2 Suzuki-Miyaura Cross-Coupling

Suzuki and co-workers reported in 1979 the palladium-catalysed coupling of alkenylboranes with alkenyl halides which is known as the Suzuki-Miyaura coupling.<sup>8</sup>

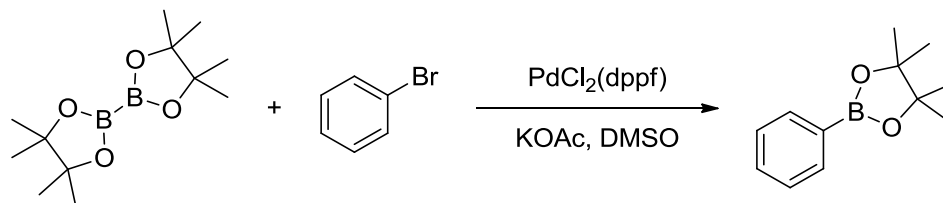


**Scheme 1.4.** General scheme for a Suzuki-Miyaura cross-coupling.

Organoboron reagents have several characteristics that make them an easy to handle substrate for cross-coupling reactions: they have good stability to air, moisture and heat; their compatibility with other functional groups is good; finally the boron-containing reagents, and any reaction by-products, are of low toxicity. The organoboron reagents can be easily prepared by either transmetalation reactions, for example treatment of a

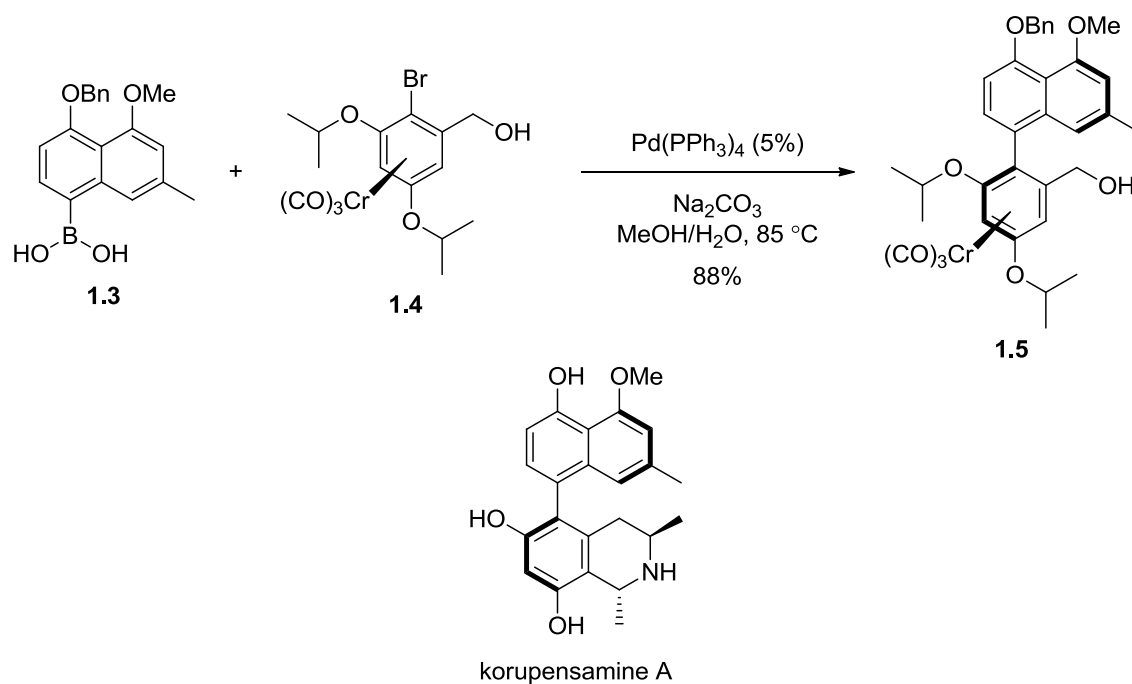


Grignard reagent with  $\text{B}(\text{OMe})_3$ , or a hydroboration of a alkene or alkyne.<sup>9</sup> Aryl boronic esters can also be synthesised directly from aryl halides using a palladium-catalysed cross-coupling protocol reported by Miyaura and co-workers (Scheme 1.5).<sup>10</sup>

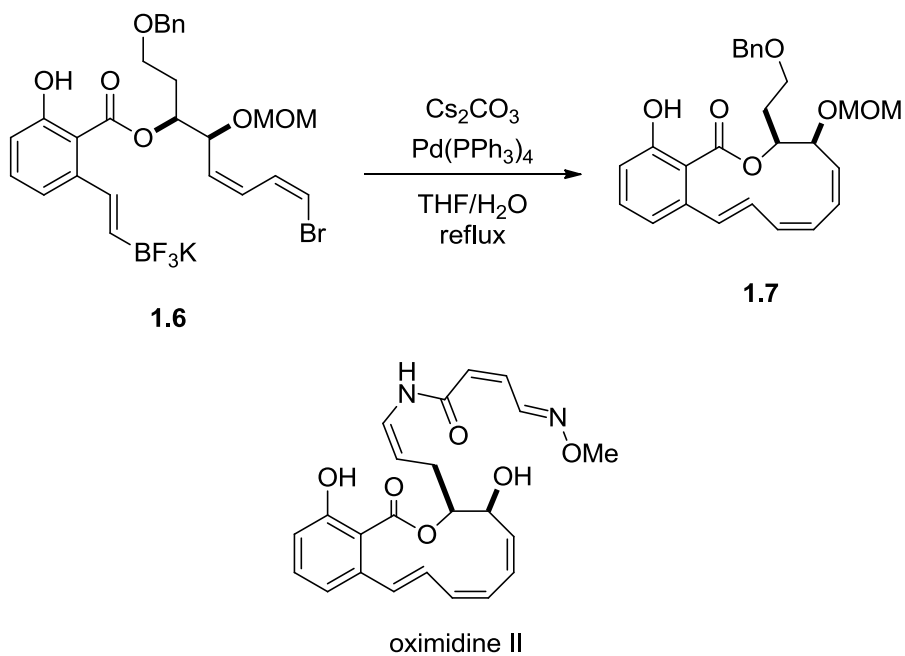


**Scheme 1.5** Miyaura's synthesis of arylboronic pinacol esters directly from aryl bromides.

Furthermore many different boronic acids and esters are commercially available. An interesting application is exemplified in Uemura's stereoselective synthesis of korupensamine A (Scheme 1.6).<sup>11</sup> A Suzuki-Miyaura coupling of boronic acid **1.3** with a single enantiomer of tricarbonylchromium-complexed aryl bromide **1.4** yielded the desired coupled product as a single atropisomer **1.5**, further steps in the synthesis gave korupensamine A. The use of potassium trifluoroborates in the Suzuki-Miyaura coupling was pioneered by Molander,<sup>12</sup> a strategy that his group then demonstrated in the total synthesis of oximidine II (Scheme 1.7).<sup>13</sup> The key step was the intramolecular Suzuki-Miyaura reaction of intermediate **1.6** to achieve the cyclisation of macrolactone **1.7**, which was further functionalised to yield oximidine II.



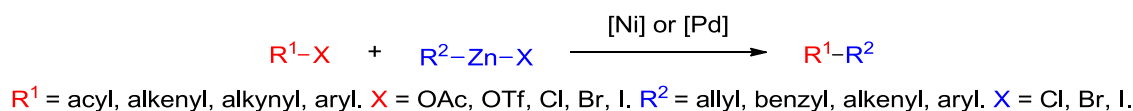
**Scheme 1.6** Uemura's example of a stereospecific Suzuki-Miyaura reaction used in the synthesis of korupensamine A.



**Scheme 1.7** Molander's synthesis of oximidine II incorporating a Suzuki-Miyaura coupling of a potassium trifluoroborate.

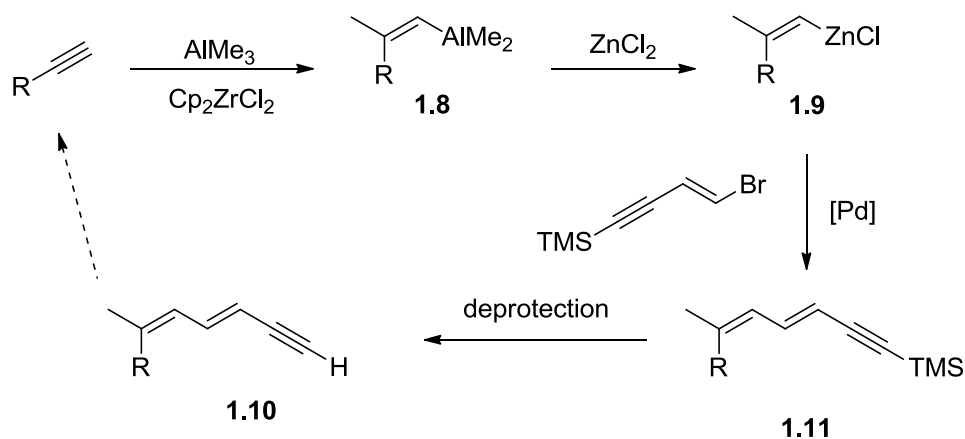
### 1.2.3 Negishi Cross-Coupling

Reported by Negishi in 1977,<sup>14</sup> the highly selective coupling of alkynylzinc reagents and alkenyl halides proved to be a useful alternative to the Kumada coupling. The reaction can be nickel- or palladium-catalysed and utilize an organo-aluminium, -zinc or -zirconium species, but the best results are usually obtained using organozinc reagents in the presence of a palladium catalyst.<sup>15</sup> The less electropositive zinc provides greater functional group tolerance than the more reactive Grignard and organolithium reagents.



**Scheme 1.8.** General scheme for a Negishi cross-coupling.

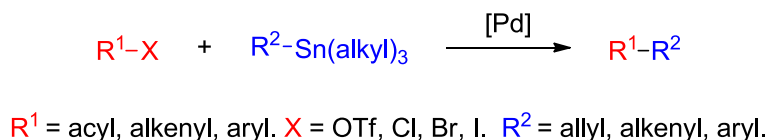
The organozinc reagents that are typically utilised in this reaction are diorganozinc compounds ( $\text{R}_2\text{Zn}$ ) or the more commonly used Grignard-equivalent organozinc halide ( $\text{RZnX}$ ). Organozinc halides can be prepared easily either by treatment of the organic halide with zinc dust or by transmetalation, treating an organolithium with  $\text{ZnCl}_2$  for example. Negishi has demonstrated the efficiency and stereoselectivity of this coupling reaction with the remarkable synthesis of various carotenoids.<sup>16</sup> The synthesis consists of 3 key steps: (1) the zirconium-promoted carboalumination of functionalised terminal alkynes; (2) the resulting alkenylaluminium species **1.8** can then undergo a transmetalation with  $\text{ZnCl}_2$ ; (3) the alkenylzinc reagent **1.9** can then undergo a Negishi coupling with the vinyl halide moiety of a protected enyne; TMS deprotection of **1.11** yields a terminal alkyne **1.10** (Scheme 1.9). At this stage the homologation can be continued or alternatively two alkenylzinc species joined by a dual Negishi coupling with (*E*)-1-bromo-2-iodoethene. Employing this strategy both symmetrical and unsymmetrical carotenoids could be synthesised.



**Scheme 1.9** Outline of Negishi's strategy for the synthesis of carotenoids, involving carboaluminations and cross-couplings. Dashed arrow represents the potentially iterative coupling.

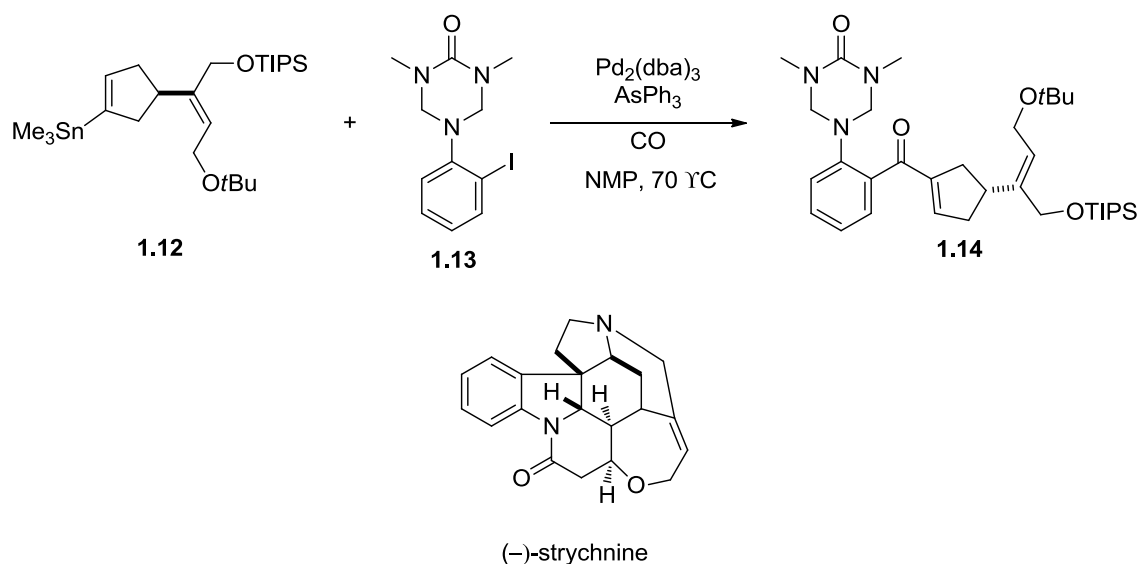
#### 1.2.4 Stille Cross-Coupling

The reaction of acid chlorides with organostannanes to yield ketones was reported in 1977 by Stille and co-workers<sup>17</sup> and they extended the scope of this coupling to alkyl and aryl chlorides the following year.<sup>18</sup> This reaction is known today as the Stille cross-coupling reaction.



**Scheme 1.10.** General scheme for a Stille cross-coupling.

The typical organostannane used for this reaction is  $\text{R-SnBu}_3$ , which is readily accessible by treatment of an organolithium or organomagnesium reagent with  $\text{Cl-SnBu}_3$ . A useful modification of the reaction is the incorporation of carbon monoxide to the reaction which yields aryl ketones without having to use the sensitive acid chloride functionality.<sup>19,20</sup> One application of this can be seen in Overman's total synthesis of (–)-strychnine.<sup>21</sup> Carbonylative Stille coupling of organostannane **1.12** and aryl iodide **1.13** gave the coupled product **1.14**, which was transformed into (–)-strychnine in subsequent steps (Scheme 1.11).

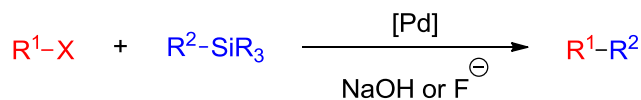


**Scheme 1.11** Overman's use of the carbonylative Stille coupling in the synthesis of (-)-strychnine.

Although the Stille cross-coupling has the advantages of wide functional group tolerance and mild conditions, it has the significant downsides of the toxicity of the stannane reagents and the difficulty of removing the tin by-product from the products. This aspect of the coupling makes it less appealing on an industrial scale. Furthermore, the advances in the Suzuki-Miyaura chemistry have meant that the Stille coupling is often overlooked in favour of the safer protocol.

### 1.2.5 Hiyama Cross-Coupling

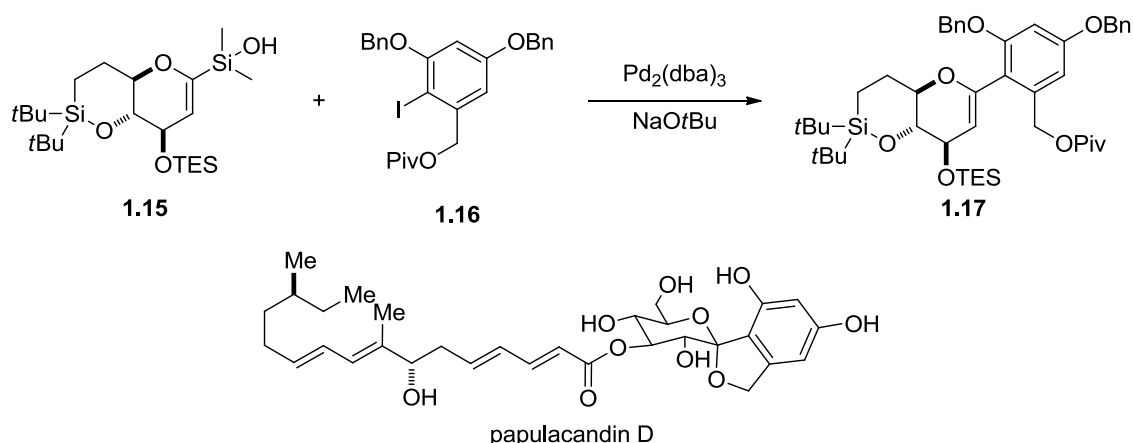
The coupling of an organosilane with an organohalide is known as the Hiyama cross-coupling and was first reported by Hiyama and co-workers in 1988.<sup>22</sup> Organosilanes themselves are not nucleophilic enough to undergo transmetalation with the palladium(II) species, so it is necessary to activate these substrates.



$\text{R}^1$  = alkyl, alkenyl, alkynyl, aryl.  $\text{X}$  = OTf, Cl, Br, I.  $\text{R}^2$  = alkynyl, alkenyl, aryl.  $\text{R}$  = Alkyl, Cl, F.

**Scheme 1.12.** General scheme for a Hiyama cross-coupling.

The addition of fluoride to activate the silane forms a five-coordinate silicate,<sup>23</sup> which can then undergo the necessary transmetalation step due to the enhanced nucleophilicity of this species compared to the silane. The fluoride anion can be replaced by a strong base such as NaOH if a dialkyldichlorosilane is used as the coupling partner.<sup>24</sup> This is advantageous as fluoride sources are incompatible with silyl protecting groups in the substrates. This can be particularly problematic in total syntheses as alcohols are often protected as silylethers. Another modification that has been made to the original conditions takes the form of the Denmark modification;<sup>25</sup> in which the use of silanols as the cross-coupling partner allows the reaction to be base-promoted. Denmark applied this modified coupling to the total synthesis of Papulacandin D.<sup>26</sup> To this end, silanol **1.15** and iodide **1.16** were coupled to give **1.17** in a 83% yield (Scheme 1.13).



**Scheme 1.13** Denmark's total synthesis of papulacandin D involving a modified Hiyama reaction.

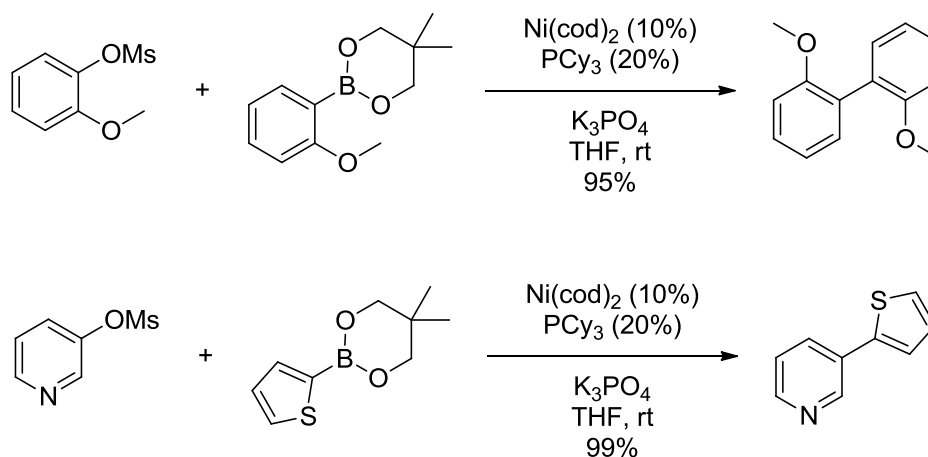
### 1.3 Cross-Coupling Reactions Catalysed by Other Metals

Although palladium is the most prevalent metal when it comes to catalysing cross-coupling reactions, there are other metals that are able to carry out this class of reaction.

### 1.3.1 Nickel

The use of nickel for cross-coupling reactions has long been known, with early examples of nickel-catalysed Kumada and Negishi couplings (see 1.2.1 and 1.2.3).<sup>27,28</sup> The majority of nickel-catalysed transformations require higher catalyst loadings compared to their palladium-catalysed counterparts, however the cheaper cost of nickel significantly counteracts this disadvantage. Fu's group have pioneered the use of nickel catalysts in three other cross-coupling reactions typically associated with palladium catalysts. The group reported that a Suzuki-Miyaura type cross-coupling could be achieved using  $\text{Ni}(\text{cod})_2$  with a phenanthroline based ligand. This allowed coupling between secondary alkyl bromides (or iodides) and a variety of different aryl boronic acids.<sup>29</sup> The coupled products could be obtained in good to modest yields. Fu then reported an example of the nickel-catalysed Hiyama coupling,<sup>30</sup> which made use of the same phenanthroline ligand but with  $\text{NiCl}_2$ -diglyme as the nickel source. Under these conditions, with the inclusion of CsF to activate the silicon reagent, trifluoroarylsilanes could be coupled with secondary aryl bromides in modest to good yields. The group reported an improvement to these conditions in a more recent paper.<sup>31</sup> By using an aminoalcohol-based ligand, norephedrine, higher yields could be obtained and the substrate scope of the secondary bromide could be significantly expanded. Finally, Fu's group have also reported a nickel-catalysed Stille coupling between secondary alkyl bromides and monoorganotin reagents ( $\text{RSnCl}_3$ ),<sup>32</sup> using  $\text{NiCl}_2$  with 2,2'-bipyridine as the ligand, results in moderate yields of the desired products.

A more recent example from the literature shows a  $\text{Ni}(\text{cod})_2/\text{PCy}_3$  catalyst system being used for a Suzuki-type cross-couplings between aryl mesylates/sulfamates and aryl neopentylglycolboronates at room temperature (Scheme 1.14).<sup>33</sup> The reaction showed good tolerance to electron-rich or electron-poor substituents regardless of the position on the ring, only diortho-substituted substrates proved challenging giving poor yields. The reaction also showed good tolerance to heteroaryl substrates.



**Scheme 1.14** Perec's conditions for nickel catalysed Suzuki-Miyaura reactions at room temperature.

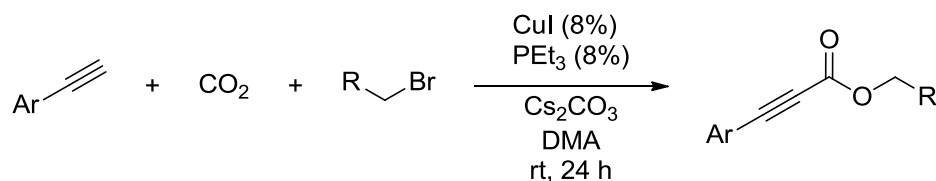
### 1.3.2 Copper

Pioneering examples of copper cross-coupling reactions were reported by Glaser in 1869,<sup>34</sup> this work was extended by Hay in 1962<sup>35</sup> to give us what is known today as the Glaser-Hay coupling; the coupling of two terminal acetylenes to form bisacetylenes. Another key study by Castro and Stephens showed that a stoichiometric amount of copper phenylacetylide could be coupled with aryl iodides to give the coupled bisarylacetylene as the product.<sup>36</sup> The most notable example of copper in cross-coupling reactions is as a co-catalyst in the Sonogashira coupling protocol, a catalytic example of the Castro-Stephens type reaction. This class of reaction, including copper-exclusive examples, will be discussed further in Chapter 4.

Inamoto and Kondo have recently reported that terminal acetylenes in the presence of an alkyl bromide and under an atmosphere of carbon dioxide can be transformed into alkyl-2-alkynoates by a CuI/PEt<sub>3</sub> catalytic system (Scheme 1.15).<sup>37</sup> The screening of a variety of different phenylacetylenes revealed that the reaction could generally tolerate electron-donating substituents present on the phenyl ring, but electron-withdrawing substituents proved problematic. Some of these problems could be overcome by performing the reaction at 50 °C with 2,2'-bipyridine as the ligand, in place of PEt<sub>3</sub>. Issues encountered for alkyl-substituted alkynes could also be avoided by

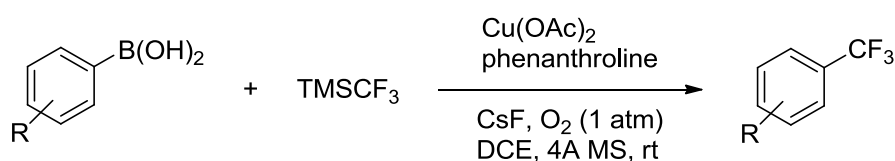


using these modified conditions. Attempts to incorporate alkyl chlorides and alkyl triflates proved unsuccessful.



**Scheme 1.15** Copper catalysed 3-component coupling reaction yielding alkyl-2-alkynoates.

In 2011 Buchwald and co-workers reported a convenient copper-catalysed protocol for trifluoromethylation. They found that aryl boronic acids could be coupled with  $\text{TMSCF}_3$  in the presence of a stoichiometric amount copper(II) salt and phenanthroline as a ligand (Scheme 1.16). While a previous example of this reaction reported the use of  $\text{Ag}_2\text{CO}_3$  as the oxidant,<sup>38</sup> Buchwald's group found that carrying out the reaction under an atmosphere of oxygen was sufficient to serve as the oxidant. The reaction displayed good tolerance towards the boronic acids, although the convenience and ease of operation of this protocol was somewhat offset by the low yields obtained due to the competing side reactions of protodeboration or halide transfer from the solvent.

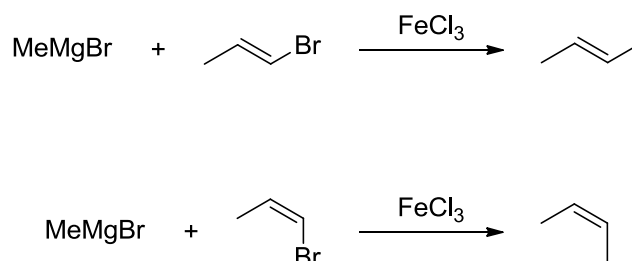


**Scheme 1.16** Buchwald's protocol for a copper catalysed trifluoromethylation cross-coupling reaction.

### 1.3.3 Iron

As with copper, iron catalysis is seeing a renewed interest in research in an effort to gain access to the high reactivity of privileged metals, such as palladium, at a fraction of the cost. The majority of iron-catalysed cross-coupling reactions lay in the coupling of organomagnesium reagents with a variety of different organic halides, and

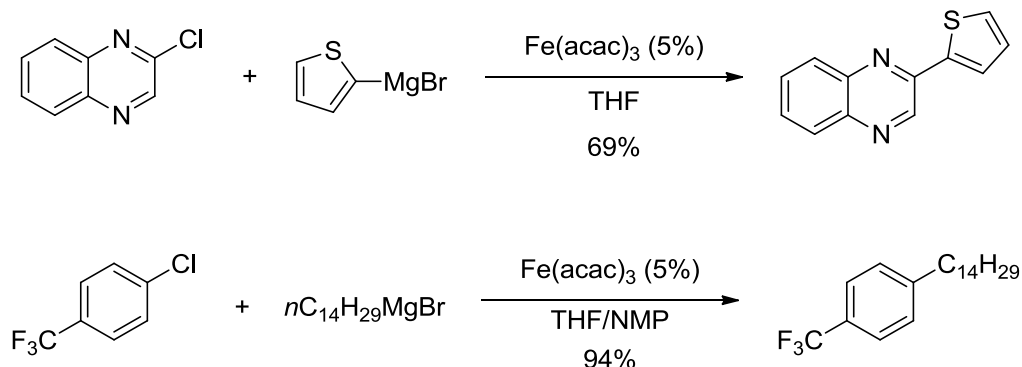
the scope of both components has been considerably broadened over the years. An early example of an iron-catalysed coupling of an alkyl Grignard reagent and an alkenyl bromide by Kochi in 1971,<sup>39</sup> predates the seminal paper for the palladium-related Kumada coupling. The reaction was shown to be stereospecific (Scheme 1.17), meaning there was no isomerisation of the carbon-carbon double bond during the coupling.



**Scheme 1.17** Retention of stereochemistry in Koichi's seminal report of an iron catalysed cross-coupling reaction.

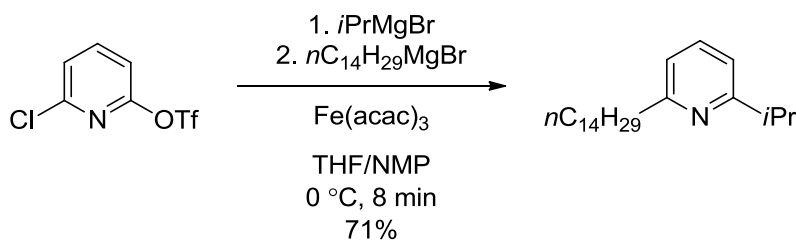
This protocol did have a downside however; the necessity for a large excess of the alkenyl halide reagent still only gave moderate yields. Cahiez and co-workers had noted that changing the nature of the iron catalyst had little effect to improve this situation, and instead set out on investigating various co-solvents.<sup>40</sup> Indeed the group found that by using NMP as an additive in THF the coupling between 1:1 equivalents of 1-bromoprop-1-ene and octylmagnesium chloride in the presence of 3% of  $\text{FeCl}_3$  could be achieved in a high yield of 87%, compared to 40% without the addition of NMP to the reaction mixture. Using this new protocol the group then demonstrated that alkenyl iodides, bromides and chlorides could all be coupled successfully. Most importantly of all, the reaction was tolerant of functional groups such as ketones, amides and esters without any significant by-products caused by addition to the carbonyl. A further publication by this group revealed that aryl based Grignard reagents were also compatible substrates for cross-coupling with alkenyl halides.<sup>41</sup> Work by Fürstner and co-workers demonstrated several major improvements to these iron-catalysed couplings by using  $\text{Fe}(\text{acac})_3$  as the iron source.<sup>42</sup> Alkyl Grignard reagents could be coupled with electron-poor (activated) aryl chlorides using this catalyst (Scheme 1.18); additionally,

alkyl and (hetero)aryl Grignard reagents could be coupled with heteroaryl chlorides in good and moderate yields respectively. At the time this paper was published aryl chlorides were problematic substrates for palladium-catalysed couplings.



**Scheme 1.18** Fürstner and co-worker's use of  $\text{Fe(acac)}_3$  to affect cross-couplings between Grignard reagents and (hetero)aryl chlorides.

The ability to perform consecutive additions in a single reaction proved to be a useful feature of this protocol. For example, the authors demonstrated this by the addition of two different Grignard reagents to a heteroaryl halide (Scheme 1.19). The reaction was completed in 8 minutes, despite being carried out at low temperatures, and a modest yield of 71% was obtained.



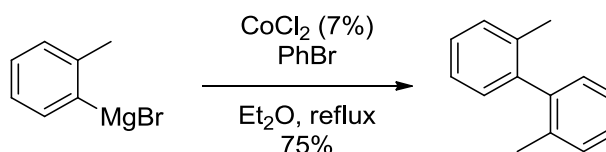
**Scheme 1.19** Fürstner and co-worker's demonstration of consecutive additions of two different Grignard reagents to 6-chloropyridin-2-yl triflate.

As a consequence of these developments, iron-catalysed couplings have been utilised towards the total synthesis of some natural products, as highlighted in Fürstner and Sherry's review.<sup>43</sup>

Recently the scope of iron catalysed cross-couplings has been expanded to include organoboron species for Suzuki-type couplings<sup>44,45</sup> and organozincs for Negishi-type couplings.<sup>46</sup> With the significant progress made in applying different nucleophilic coupling partners seen recently, iron catalysed cross-coupling reactions now represent a synthetically viable alternative to palladium mediated couplings.

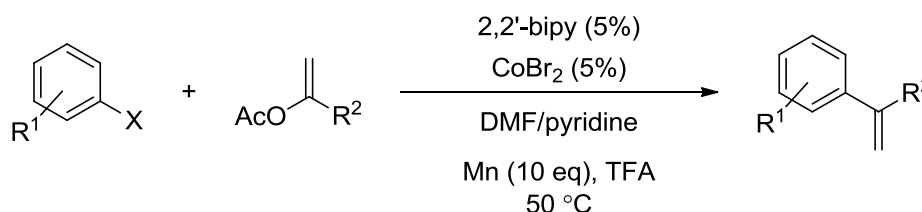
### 1.3.4 Cobalt

The first cobalt cross-coupling reaction was reported by Kharasch in 1941 in the form of a homocoupling reaction of aryl Grignard reagents.<sup>47</sup> For example treatment of *o*-tolylmagnesium bromide with  $\text{CoCl}_2$ , in the presence of bromobenzene as an oxidant, the corresponding biaryl could be obtained in a good yield (Scheme 1.20).



**Scheme 1.20** Kharasch's first example of a cobalt catalysed cross-coupling reaction.

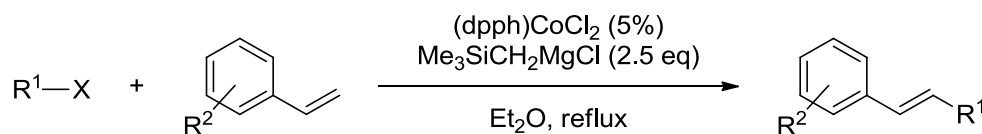
Cobalt has also been shown to catalyse the cross-coupling of vinyl acetates and aryl halides.<sup>48</sup> The authors reported that in the presence of  $\text{CoBr}_2$ , 2,2'-bipyridine as a ligand, manganese powder as a reducing agent with a trace of TFA as an activator and using a solvent mixture of DMF/pyridine (15/2), the reaction yielded a variety of  $\alpha$ -substituted styrenes in moderate to good yields (Scheme 1.21).



**Scheme 1.21** Gosmini's cobalt catalysed synthesis of  $\alpha$ -substituted styrenes.

The reaction was shown to work with a broad variety of electron-deficient and electron-rich aryl chlorides and bromides, providing it with a distinct advantage over similar palladium-catalysed protocols, which are often problematic with aryl chlorides. The authors noted that the large excess of manganese was necessary in order to keep the reaction times reasonable. This reaction represents a convenient synthesis of  $\alpha$ -substituted styrene, a class of alkene that can be elaborated further using the Mizoroki-Heck reaction. Furthermore, the vinyl acetate substrates can be easily formed by deprotonation of the desired ketone, forming an enolate, followed by trapping with acetyl chloride; this provides a convenient alternative to using a vinyl Grignard reagent.

The first example of a Mizoroki-Heck type coupling catalysed by a cobaloxime complex was reported by Branchaud in 1991.<sup>49</sup> Specialist photolysis equipment was necessary in order to initiate the reaction in this case. In 2002 Oshima and co-workers reported a more practical protocol for a cobalt-catalysed Mizoroki-Heck type reaction *via* a radical process.<sup>50</sup> Using cobalt phosphine complex  $\text{CoCl}_2(\text{dppe})$  with  $\text{TMSCH}_2\text{MgCl}$  as a reductant allowed for the coupling of styrenes with alkyl halides (Scheme 1.22). The reaction showed good generality for the alkyl halide. For example, the reaction of styrene with 1-adamantyl chloride gave the alkylated styrene in 90% yield. Primary and secondary chlorides and bromides also participated in the coupling, however using alkyl iodides only lead to mediocre yields. The functionalisation on the aryl ring of the styrene partner was also tolerated well, including amides, halides and methoxy groups.



**Scheme 1.22** Oshima's protocol for a cobalt catalysed Mizoroki-Heck type cross-coupling.

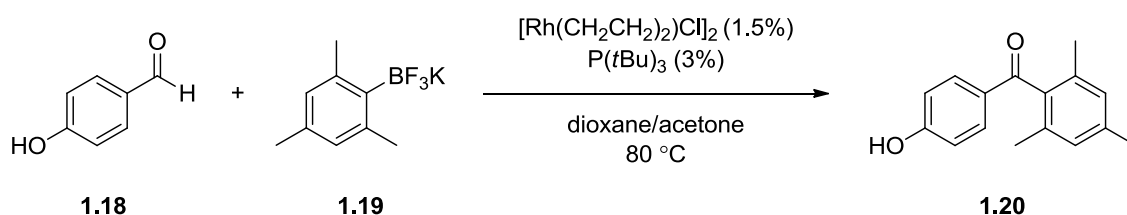
This cobalt catalysed protocol, which yields  $\beta$ -substituted styrenes, and the one described previously, which yields  $\alpha$ -substituted styrenes, are complimentary and

together provide a diverse methodology for the synthesis of highly functionalised styrenes.

It should be noted that cobalt, as with iron, has also been extensively studied in the coupling of organomagnesium reagents with various organic electrophiles, with similar examples to that of iron catalysed cross-coupling reactions. Cahiez has recently published a comprehensive review of this area.<sup>51</sup>

### 1.3.5 Rhodium

When considering metal catalysed processes, rhodium is typically associated with hydrogenation. Nevertheless, there are examples of cross-coupling reactions that are catalysed by rhodium. One example was reported by Darses and Genet, in which aryl aldehydes could be converted directly into ketones by coupling with aryl potassium trifluoroborates.<sup>52</sup> The reaction was catalysed by a Rh-P(*t*-Bu)<sub>3</sub> complex generated *in situ* and makes use of acetone as a convenient and inexpensive hydride acceptor. A variety of substituted benzaldehydes (including those with free -OH groups) were shown to participate in the coupling, as were the heteroaryl aldehydes furfural and its thiophene analogue.

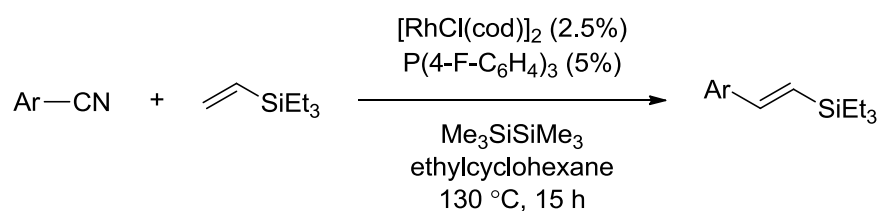


**Scheme 1.23** Genet and Darses' rhodium catalysed cross-coupling of aldehydes and aryl potassium tetrafluoroborates.

The potassium trifluoroborate reagent also showed good tolerance to the coupling, with both electron-donating and electron-withdrawing groups on the phenyl ring causing no issues. Most remarkably, the sterically hindered potassium trifluoroborate **1.19** can be successfully coupled with aldehyde **1.18** to yield ketone **1.20** with an 82% yield (Scheme 1.23). The transformation of an aldehyde to a ketone is classically performed

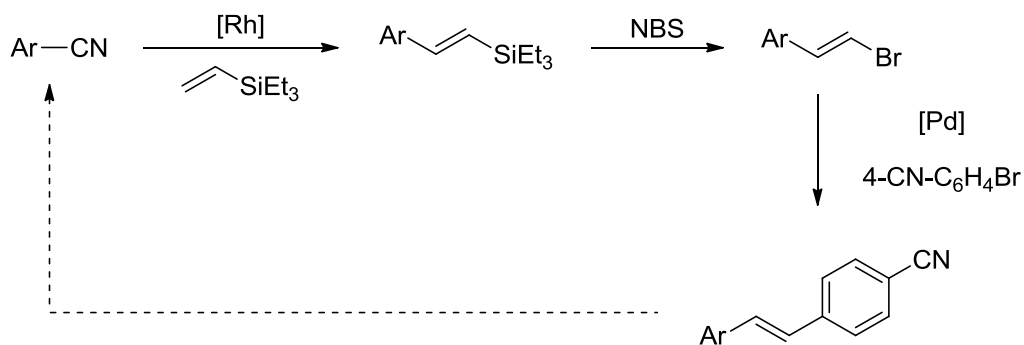
by umpolung chemistry, that is, protection of the aldehyde as a thioacetal, deprotonation of the  $\alpha$ -hydrogen, functionalisation with an organic electrophile and then thioacetal cleavage to give the desired ketone, although this route is not possible with an aryl electrophile.

Another example of rhodium-catalysed cross-coupling can be seen in Tobisu and Chatani's report of a Mizoroki-Heck type arylation of vinyl silanes with aryl cyanides (Scheme 1.24).<sup>53</sup> Treatment of a variety of aryl cyanides with vinyl triethylsilane in the presence of a Rh-phosphine catalyst formed *in situ* afforded the corresponding alkenes. The role of hexamethyldisilane was cited as both activating the Rh-Cl precatalyst to form the Rh-SiMe<sub>3</sub> active species, and as a hydride acceptor to regenerate the active species at the end of the catalytic cycle.



**Scheme 1.24** Tobisu and Chantani's rhodium catalysed Mizoroki-Heck type reaction of aryl nitriles and vinylsilanes.

Despite these kinds of functionalised vinyl silanes rarely being a synthetic target themselves, they do prove to be interesting synthetic intermediates. Performing Hiyama couplings with the silane moiety is one possibility, however the authors demonstrated that another possibility is the treatment of the vinyl silanes with NBS to yield the corresponding vinyl bromide. The bromide can then be utilized in different cross-coupling reactions. In this case, the authors chose to perform a Suzuki-Miyaura coupling with 4-CN-C<sub>6</sub>H<sub>4</sub>Br which allowed for a succinct and iterative synthesis of oligo(phenylenevinylene)s (Scheme 1.25).



**Scheme 1.25** Iterative synthesis of oligo(phenylenevinylene)s using rhodium and palladium catalysed cross-coupling reactions.

## 1.4 Ligands in Cross-Coupling

A ligand is a neutral molecule or ion that binds to a metal centre, typically by the donation of one or more electrons to a central metal atom. By changing the ligands coordinated to the metal centre the reactivity of the metal can be tuned. The change in reactivity is usually a combination of the steric environment that the ligands impart, in addition to their electronic influence on the metal centre. If this relationship can be well understood, the rational design of ligands and metal complexes for particular catalytic process becomes feasible. The role that ligands play in cross-coupling is therefore an important one, meaning that catalyst development is often synonymous with ligand development. The ideal ligand should be able to stabilise the catalytically active species in solution to allow high turnover numbers, but should not directly participate or interfere with the reaction.

The majority of palladium catalysed cross-coupling reactions are catalysed by a palladium(0) species that is formed from a suitable precatalyst, meaning there is usually an induction period in such reactions. Using a palladium(0) precatalyst would seem to be the most straightforward choice then, however these complexes have a tendency to be air sensitive such as the commonly used  $[\text{Pd}(\text{PPh}_3)_4]$ . Moreover, this precatalyst is coordinatively saturated and must lose at least two ligands in order to be able to generate the active  $(\text{PPh}_3)_2\text{Pd}(0)$  species. The time required for the loss of these ligands represents the induction period, which can result in long reaction times.  $\text{Pd}_2(\text{dba})_3$  and



$\text{Pd}(\text{dba})_2$  are commonly used as palladium(0) precatalysts, and can be activated by the addition of a ligand such as  $\text{PPh}_3$  to substitute the dba ligands.<sup>54</sup> However, the reality is not straightforward; the actual amount of the active  $\text{Pd}(\text{PPh}_3)_2$  is ill defined as dba is a comparable ligand to  $\text{PPh}_3$ .<sup>55</sup> Additionally, palladium(0) nanoparticles of varying size and catalytic activity may be generated under the reaction conditions.<sup>56</sup>

An alternative approach is to start with a palladium(II) salt such as  $\text{Pd}(\text{OAc})_2$  or  $\text{PdCl}_2$  and use a reducing agent in the presence of some suitable ligands that can stabilise the resultant palladium(0) species. The last two methods mentioned of generating palladium(0) are both examples of forming the catalyst *in situ*, and generally an excess of ligand to metal is used. The main disadvantage of *in situ* systems is that the identity of the active species is unpredictable, i.e. the ratio of ligand to metal is not fixed, making the rational improvement of *in situ* systems more difficult than well-defined systems. Well-defined systems typically only require the reduction of a  $\text{L}_2\text{Pd}(\text{II})$  precatalyst to the  $\text{L}_2\text{Pd}(0)$  active species. The characteristic feature being there is no net ligand substitution that needs to occur, only the removal of ligands. Well-defined precatalysts can be designed to make the activation step as predictable and facile as possible, reducing the induction time and removing some of the guesswork as to the identity of the active species.

There are several classes of ligand that dominate catalysis in general and some that are more specific to Pd catalysis, these will be discussed in the following sections.

#### 1.4.1 Phosphines

The association of phosphines with catalysis, especially tertiary phosphines, is such that it is difficult to describe the generalities about ligands in catalysis without the mention of phosphines. There are a wide range of commercially available phosphines: trialkyl and triaryl phosphines, trialkyl and triaryl phosphites  $[(\text{RO})_3\text{P}]$  and a variety of multidentate bridged diphosphines such as  $\text{Ph}_2\text{PCH}_2\text{PPh}_2$  (dppm) (Figure 1.3). BINAP is an axially chiral diphosphine and plays an important role as a ligand in enantioselective catalysis, as discussed in section 1.4.1.3.

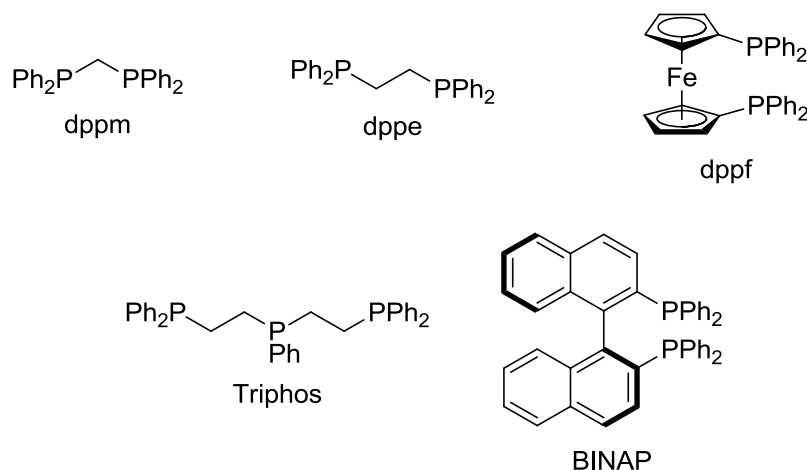


**Figure 1.3** Polydentate phosphine ligands commonly used in catalysis.

Phosphines bond to the metal centre through a mixture of  $\sigma$ -donor and  $\pi$ -acceptor interactions, this model of synergistic bonding applies to many bonding situations and has been developed from the Dewar-Chatt-Duncanson model for olefin-metal bonding.<sup>57-59</sup> The  $\text{R}_3\text{P-M}$  bond can be modeled as  $\sigma$ -donation from the phosphorus atom lone pair into a vacant metal based orbital and  $\pi$ -backbonding from filled metal d-orbitals into the  $\text{R-P}^*$  antibonding orbitals (Figure 1.4).

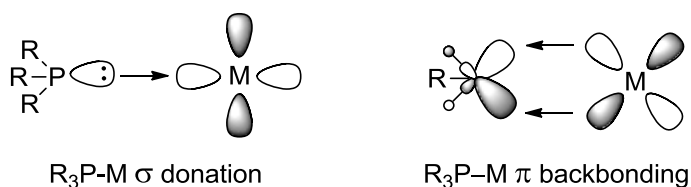


**Figure 1.4.** Model for phosphorus-metal bonding.

Pioneering work by Tolman has provided two models that are used to describe the steric and electronic properties of various phosphine ligands.<sup>60</sup> He proposed that the steric bulk of a phosphine can be determined from a simple space filling model of the phosphine and measuring the apex angle between the metal centre and the Van der Waals radii of the outermost atoms; a property that is now known as the Tolman cone angle (Figure 1.5).

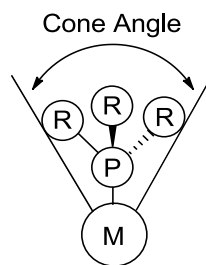


**Figure 1.5.** Tolman cone angle.

The electronic donating ability of phosphines was characterised by reacting the phosphine (L) with  $\text{Ni(CO)}_4$  to yield  $\text{LNi(CO)}_3$  and then measuring the CO stretching frequency of the resulting complex. The more electron donating the phosphine, the more electron density on the metal centre. This in turn results in more  $\pi$ -backbonding from the metal into the  $\pi^*$  antibonding orbitals of the CO ligands, weakening and lengthening the CO bond. A weaker CO bond is denoted by the lowering of the  $\nu_{\text{CO}}$  stretching frequency. Hence, more electron donating phosphines will result in lower  $\nu_{\text{CO}}$  values. These parameters give chemists a way of distinguishing different phosphines in terms of their sterics and electronics. In general bulkier phosphines can stabilise complexes with a lower coordination number in comparison to smaller phosphines, due to their ability to better shield the reactive metal centre. Furthermore, bulkier phosphines are generally more basic and electron donating,<sup>60</sup> for example the  $\text{pK}_{\text{a}}$  of  $\text{Cy}_3\text{P}$  is 9.70 whereas the  $\text{pK}_{\text{a}}$  of  $\text{Ph}_3\text{P}$  is 2.73.<sup>61</sup>

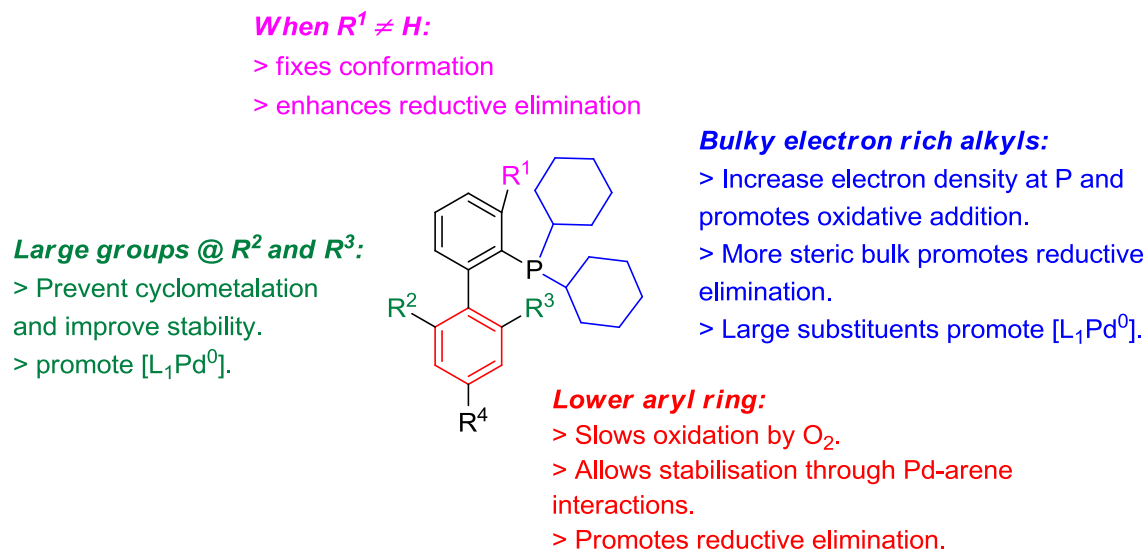
#### 1.4.1.1 Catalyst Activation

In palladium-catalysed cross-couplings, phosphines can also be used as a reducing agent in addition to acting as the ligand. The addition of a phosphine to a palladium(II) salt such as  $\text{Pd(OAc)}_2$  results in an  $\text{L}_2\text{Pd(0)}$  species and the corresponding phosphine oxide.<sup>62</sup> Because of this phosphines are used in excess to facilitate the *in situ* formation of the catalyst and is often how they are applied in cross-coupling reactions. More recently there has been a change of focus towards well-defined catalysts.<sup>63</sup> The reason for this are numerous: they can reduce the induction times; they are less likely to generate several different catalytic species (of varying activity and selectivity); it avoids

having to use an excess of the phosphine ligand as a sacrificial reducing agent and also separating the oxidised byproduct.

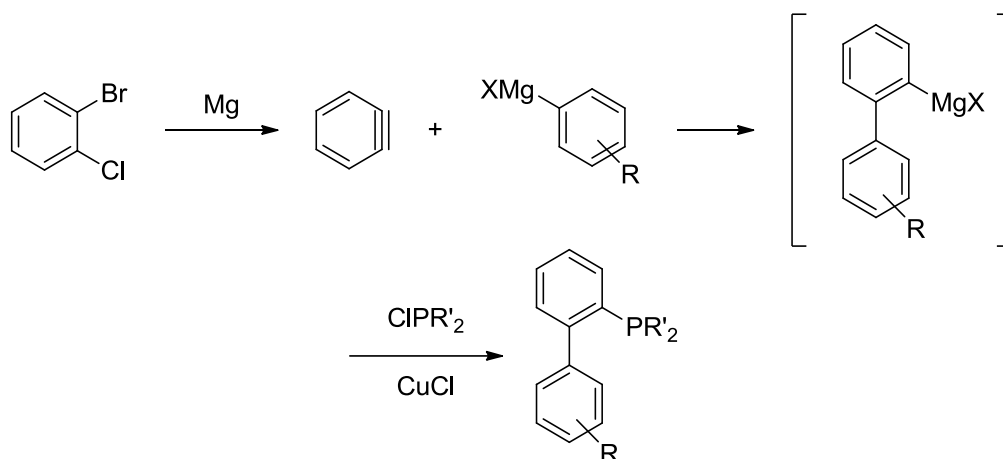
#### 1.4.1.2 Buchwald Ligands

Dialkylbiaryl phosphines are an important class of ligand for palladium catalysis introduced in 1998 by Buchwald and co-workers for room temperature Suzuki couplings of aryl chlorides.<sup>64</sup> The combination of strong electron-donor ability and significant steric environment of these Buchwald ligands can favour formation of the reactive LPd(0) species (in equilibrium with the L<sub>2</sub>Pd(0) species);<sup>65</sup> this has been cited as the reason for their ability to be able to activate challenging substrates such as unactivated aryl chlorides.<sup>66</sup> Moreover, these ligands also have good air and thermal stability so therefore do not require handling under inert gas.<sup>67</sup>



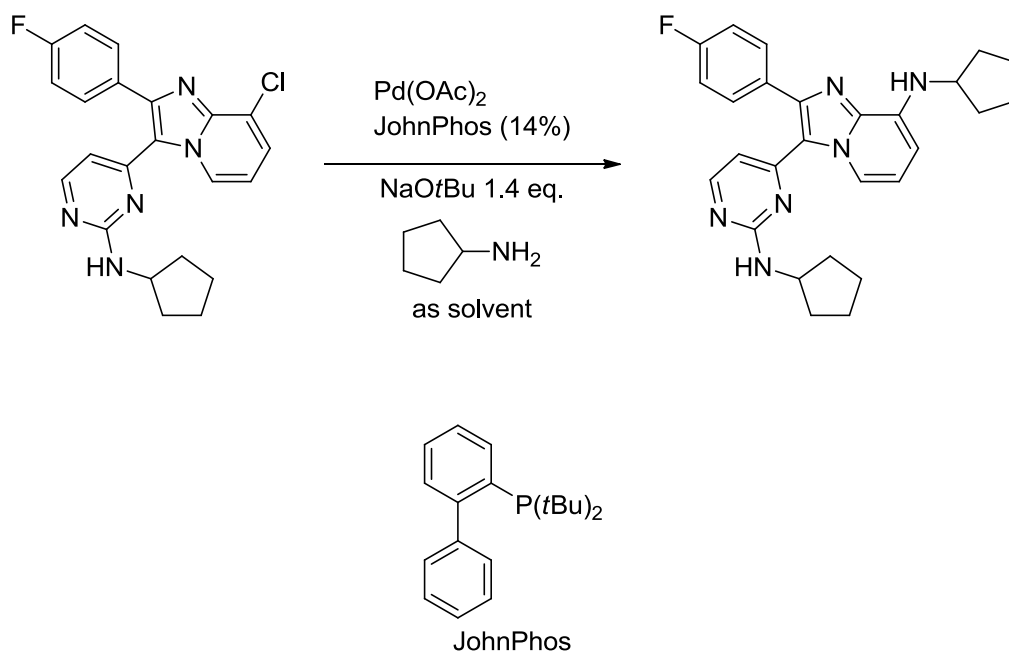
**Figure 1.6** Features of dialkylbiaryl phosphine ligands.<sup>66,67</sup>

Figure 1.6 is adapted from two reports and summarises the structural features of this class of phosphine that make them an efficient and modular ligand set for cross-coupling reactions.<sup>66,67</sup> A variety of different Buchwald ligands can be synthesised using the protocol illustrated in Scheme 1.26. An aryl Grignard reagent, or aryl lithium, undergoes addition to benzyne, the resulting intermediate can then be trapped using an appropriate dialkylchlorophosphine, a process that is enhanced with the use of CuCl.<sup>68</sup>



**Scheme 1.26** Synthesis of dialkybiaryl phosphines.

The use of Buchwald ligands in cross-coupling, particularly in amination reactions, can be seen in several important synthetic transformations, including total synthesis and in drug discovery.<sup>66</sup> One such example is the use of (*o*-biphenyl)P(*t*-Bu)<sub>2</sub> in the Buchwald-Hartwig amination coupling (Scheme 1.27) that GlaxoSmithKline used in their synthesis of imidazopyridines, which shows high potency against the herpes virus.<sup>69</sup> The production of Buchwald ligands and their application to the palladium-catalysed cross-coupling of hydrazones and aryl halides have both been established on an industrial scale.<sup>70</sup>



**Scheme 1.27** GlaxoSmithKline's use of Buchwald ligands for the synthesis of imidazopyridines.

#### 1.4.1.3 BINAP

2,2'-Bis(diphenylphosphino)-1,1'-binaphthyl (hereafter abbreviated to BINAP) is a chiral bisphosphine. Its chirality comes from being atropisomeric, which is a molecule that has two stereoisomers that are interconverted by rotation around a single bond. In the case of BINAP, this bond is connecting the two naphthalene units and the  $\text{PPh}_2$  groups hinder the rotation around this bond. When a single stereoisomer of BINAP is bound to a metal centre, the chirality in the binaphthyl backbone is translated through to the P-phenyl rings, which adopt *pseudo*-equatorial and *pseudo*-axial positions (Figure 1.7).<sup>71</sup> This creates a chiral environment that influences the orientation in which a substrate molecule (i.e. an alkene) will bind to the metal centre. This is often simplified to a quadrants diagram where the shaded areas represent space occupied by the axial phenyl rings; it is then easier to see that there is a favoured and disfavoured approach of the substrate molecule.<sup>72</sup>

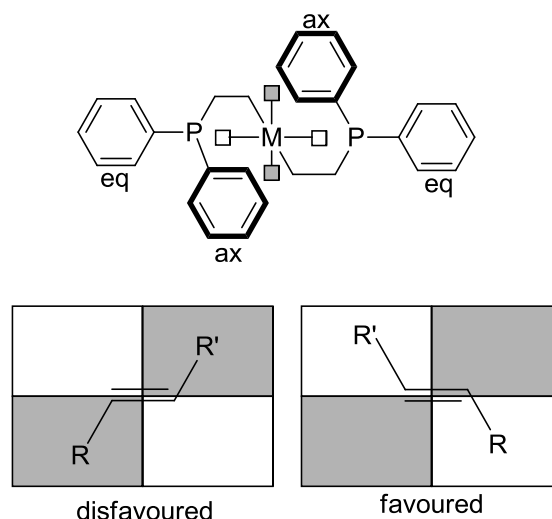
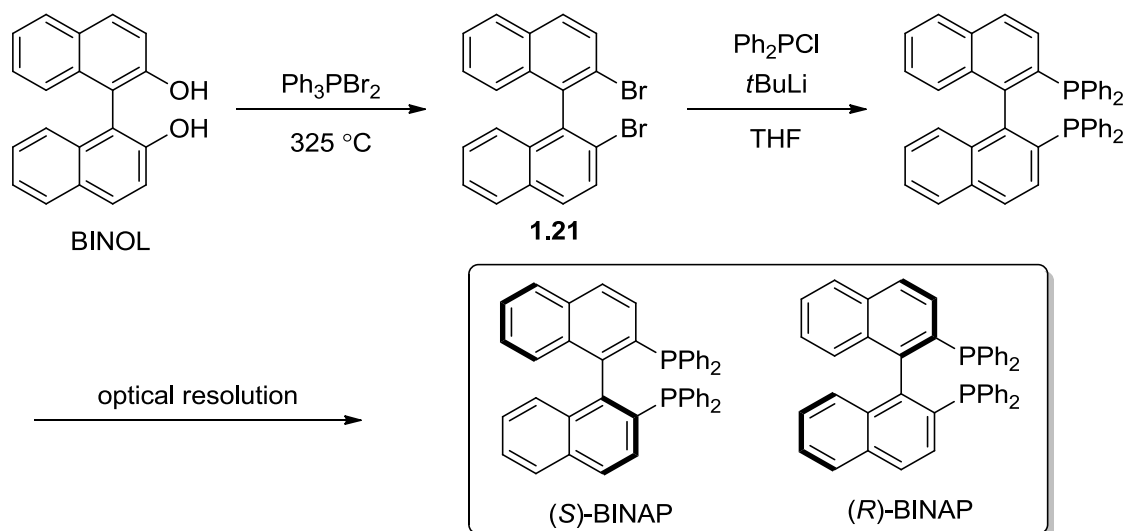


**Figure 1.7** Models used to explain how axially chiral ligands induce asymmetry. Shaded squares represent coordination sites occupied by the phenyl rings.

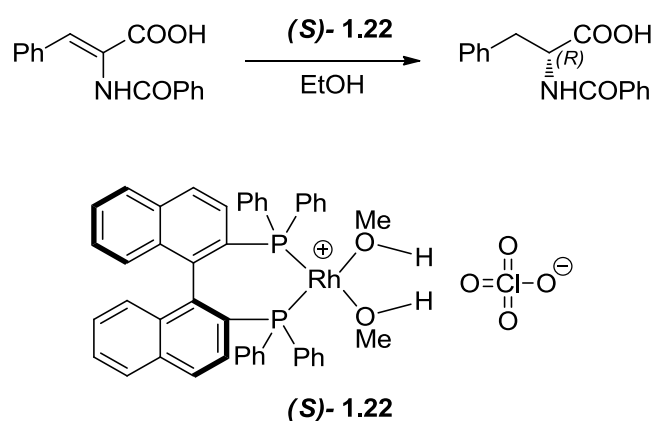
Therefore, BINAP is widely used as a ligand in asymmetric transformations including: hydrogenation of alkenes and ketones, isomerisation of allyl alcohols and amines, hydroboration, hydroamination, hydrosilylation, hydroacylation, aldol reactions and Michael reactions amongst others.<sup>71</sup>

BINAP was first synthesised by Noyori's group in 1980, and utilised for an asymmetric hydrogenation reaction.<sup>73</sup> The synthesis was achieved starting from racemic BINOL that was then transformed to the dibromide under forcing conditions with  $\text{Ph}_3\text{PBr}_2$ . The dibromide **1.21** then underwent lithium-halogen exchange upon treatment with *t*-BuLi, subsequent addition of two equivalents of  $\text{Ph}_2\text{PCl}$  gave BINAP as a racemate. In order to resolve the two atropisomers the group used a chiral palladium complex to form an adduct, which after fractional recrystallisation of the resultant diastereoisomers gave the separated (*R*) and (*S*) isomers of BINAP (Scheme 1.28).



**Scheme 1.28** The first synthesis and separation of the two atropisomers of BINAP.

Rhodium complex **1.22** was synthesised by treatment of  $[\text{Rh}((S)\text{-BINAP})(\text{norbornadiene})]\text{ClO}_4$  in methanol with an atmosphere of hydrogen at room temperature. The group demonstrated that both enantiomers of complex **1.22** could be used to affect an asymmetric hydrogenation of various  $\alpha$ -(acylamino)acrylic acids (Scheme 1.29).



**Scheme 1.29** First example of BINAP as a chiral auxiliary for an asymmetric hydrogenation reaction.

Although this catalyst was limited in its substrate scope, it sparked the development of other BINAP-metal complexes for enantioselective catalytic hydrogenation, such as



BINAP-Ru complexes,<sup>74</sup> which expanded the scope for alkene hydrogenations<sup>75,76</sup> and extended the reaction to the asymmetric hydrogenation of ketones.<sup>77</sup> Furthermore, it set the precedent for the development of BINAP and analogous atropisomeric chiral bidentate ligands,<sup>78,79</sup> with the SEGPHOS, SYNPHOS and BIPHEP being three of the most commonly used aside from BINAP (Figure 1.8).

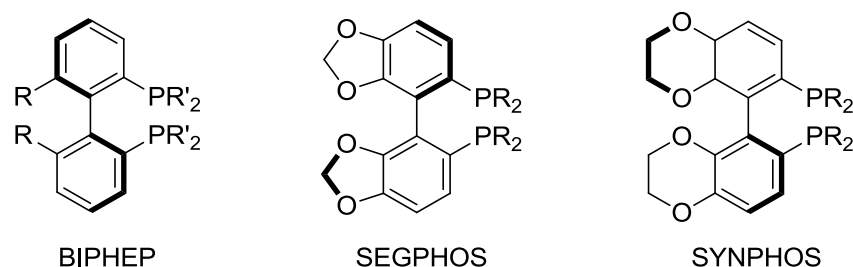
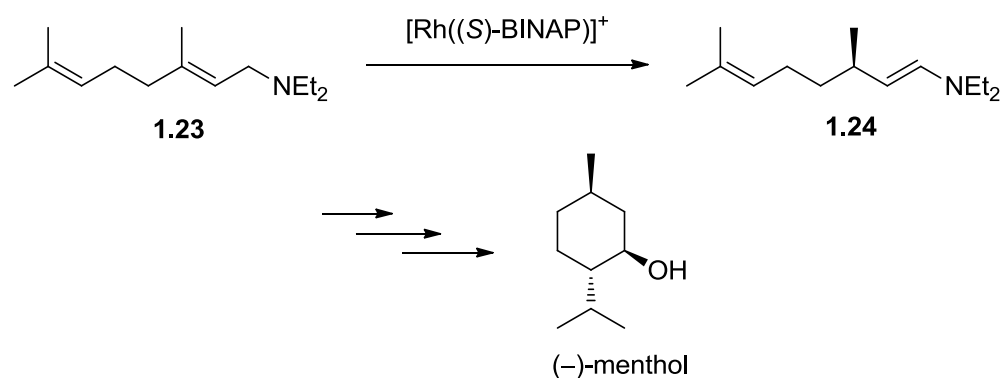


**Figure 1.8** General structures of BIPHEP, SEGPHOS and SYNPHOS ligands.

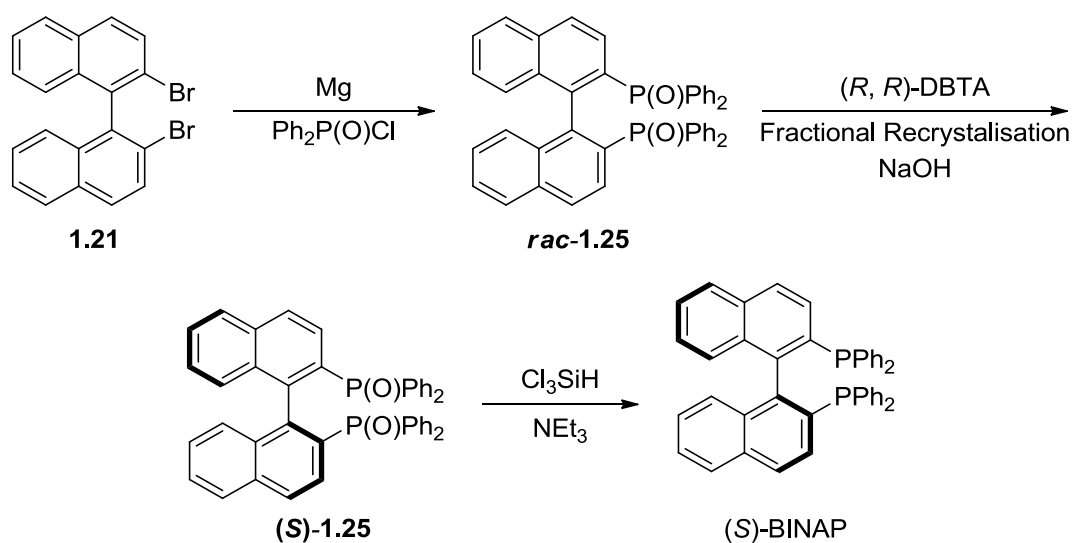
The success of BINAP as a chiral auxiliary has not only been restricted to research laboratories. Perhaps the most well known case of BINAPs use in an industrial scale synthesis is Takasago's (–)-menthol synthesis.<sup>74,80</sup> The key step in this ton scale synthesis is the asymmetric isomerisation of allyl amine **1.23** to (*R*)-citronellal enamine **1.24** in a 96-99% ee (Scheme 1.30).



**Scheme 1.30** - Takasago's industrial scale synthesis of (–)-menthol.

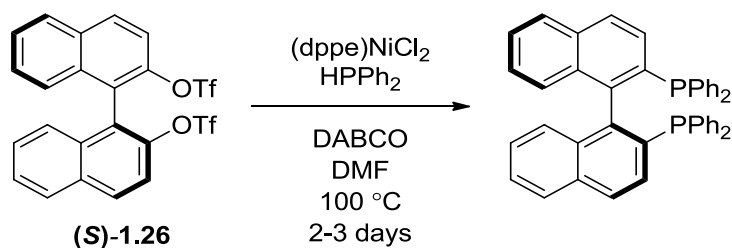
For processes on this large a scale to be feasible, an improved synthesis for BINAP was necessary. Takaya and Noyori, in collaboration with Takasago, developed a more practical synthesis of BINAP in 1986,<sup>81</sup> that Takasago used to synthesise BINAP on an

industrial scale (Scheme 1.31). The route was based on Noyori's original synthesis; dibromide **1.21** is transformed in the di-Grignard reagent (instead of the di-lithium) using magnesium which is then reacted with diphenylphosiny chloride to yield racemic BINAP as the diphosphine oxide *rac*-**1.25**. Fractional recrystallisation of the diastereomeric dibenzoyltartaric acid (DBTA) complexes gave enantiopure diphosphine oxides after treatment with a base, followed by reduction to yield a single BINAP isomer. However this method is still hampered by the difficult synthesis of the dibromo compound **1.21** which requires harsh conditions and gives only moderate yields.



**Scheme 1.31** Noyori's improved synthesis of chiral BINAP.

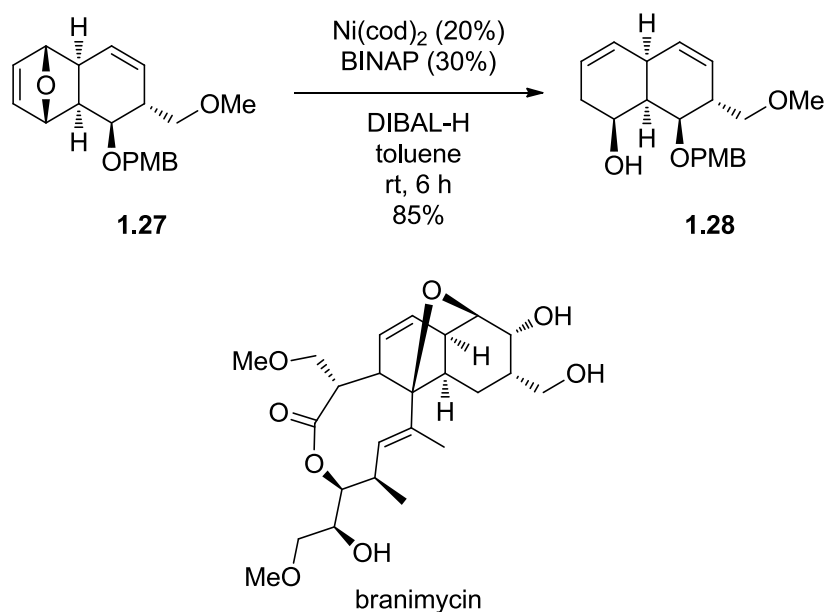
Another synthesis of BINAP, reported by Cai and co-workers at Merck,<sup>82</sup> bypassed this problematic step by converting chiral BINOL to the chiral ditriflate **1.26** using triflic anhydride (Scheme 1.32). The authors envisaged a transition metal-catalysed coupling approach to their synthesis, and the choice of a nickel-based catalyst was rationalised to avoid any potential catalyst poisoning once BINAP had formed. According to the hard-soft acid base theory, the harder nickel should not bind BINAP as strongly as other larger transition metals such as palladium or ruthenium. After screening several nickel catalysts and conditions, the authors successfully achieved the key step of this synthesis, a novel nickel-catalysed coupling reaction between triflate **1.26** and  $\text{HPPH}_2$ .



**Scheme 1.32** Cai's novel Ni catalysed phosphine insertion reaction for the synthesis of chiral BINAP.

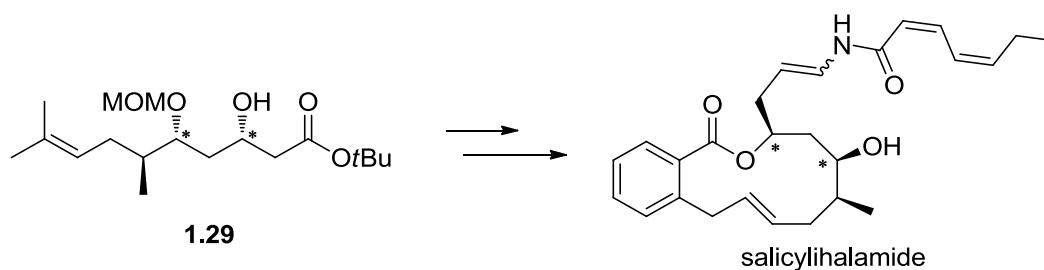
This synthesis presented several advantages: it is high yielding (~75%) and is only two steps starting from commercially available chiral BINOL. The severe disadvantage that this route has is the use of  $\text{HPPPh}_2$ , which on an industrial scale is less than ideal as it is volatile, flammable in contact with air and has a very characteristic stench. A modified version of this synthesis was reported by Laneman and co-workers at Monsanto, which utilised the safer  $\text{ClPPh}_2$  as the coupling partner.<sup>83</sup> The slightly lower yields obtained, compared to the previous synthetic route, were compensated for by the improved handling and price of the phosphorus reagent.

Some of the following examples show how important asymmetric transformations induced by BINAP are to synthetic chemists, particularly for total syntheses. Recently Mulzer's group reported the first total synthesis of the macrolactone antibiotic branimycin.<sup>84</sup> One of the key steps was the Ni-BINAP catalysed enantioselective ring opening of **1.27** to yield the desired cyclohexenol **1.28** (Scheme 1.33).



**Scheme 1.33** Mulzer's use of BINAP-Ni complex in the total synthesis of branimycin.

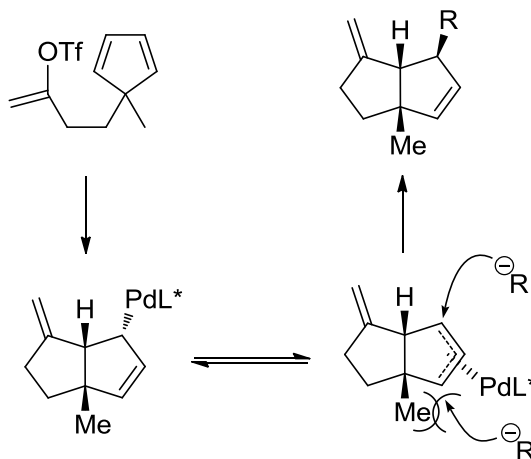
During Fürstner's total synthesis of salicyclihalamide,<sup>85</sup> the asymmetric hydrogenation of a  $\beta$ -ketoester was used twice to set the stereochemistry at the two centres indicated in compound **1.29** (Scheme 1.34).



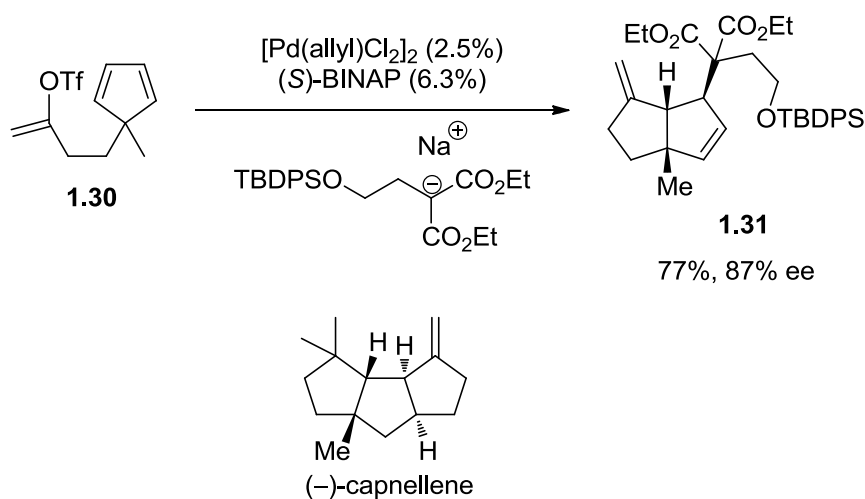
**Scheme 1.34** Fürstner's use of BINAP-Ru for the asymmetric hydrogenation during the total synthesis of salicyclihalamide.

The intramolecular asymmetric Mizoroki-Heck reaction is an important reaction in natural product synthesis, with BINAP being one of the prominent chiral auxiliaries used to effect these transformations.<sup>86</sup> An example of such a reaction can be seen in Shibasaki's work on developing an asymmetric Heck carbanion capture protocol.<sup>87</sup> Starting from *meso*-triflate **1.30** Shibasaki found that when the Heck reaction is performed with BINAP as a chiral ligand, the stereochemistry at the 5,5 fused ring

junction can be controlled. Furthermore, in the presence of the BINAP-Pd complex, the resultant  $\pi$ -allyl palladium complex could undergo selective addition of an anionic species (Scheme 1.35).



**Scheme 1.35** Mechanism of the Mizoroki-Heck carbanion capture protocol.

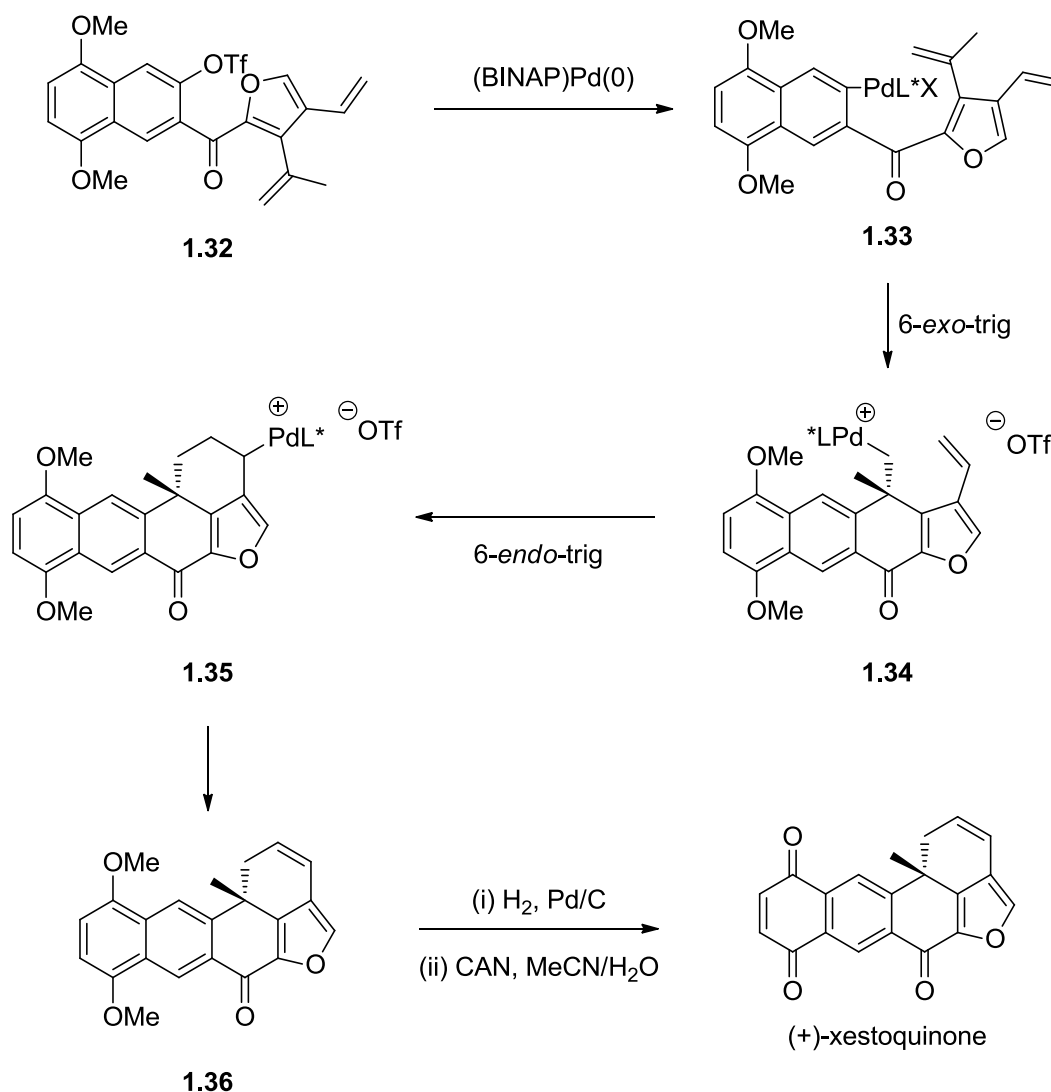


**Scheme 1.36** Shibasaki's key step featuring a Mizoroki-Heck carbanion capture protocol in the total synthesis of (-)-capnellene.

Shibasaki recognised the potential of the reaction, which was applied to the synthesis of (-)-capnellene; hence the transformation of **1.30** to **1.31** in a 77% with 87% ee formed one of the key transformations in the total synthesis (Scheme 1.36).

An elegant example of an asymmetric cascade Mizoroki-Heck reaction, which utilised BINAP as a chiral ligand, can be seen in Keay and co-workers' total synthesis of

(+)-xestoquinone.<sup>88</sup> During the last few steps of the synthesis (Scheme 1.37), achiral triflate **1.32** was treated with Pd<sub>2</sub>(dba)<sub>3</sub> (2.5%) and (*S*)-BINAP (10%), giving the oxidative addition product **1.33**. In order for **1.33** to be able to undergo the first cyclisation to yield **1.34**, the pendant alkene needs to be coordinated to the palladium centre. A vacant coordination site can be attained either by loss of the (*pseudo*)halide or one of BINAPs phosphine interactions. When the authors originally tried to use a bromide in place of triflate **1.32** an ee of 13% was recorded for the pentacycle product **1.36**. In the case of the bromide it is more likely that there is partial dissociation of the bisphospine, as the Pd-Br bond is less labile than the Pd-OTf bond, and consequently an inferior ee is obtained. In turn, **1.34** can then undergo either a 6-*endo*-trig or 5-*exo*-trig cyclisation. The authors report that the 6-*endo* product **1.35** was the dominant product, presumably due to the greater strain in the ring system resulting from the 5-*exo* cyclisation, which after β-hydride elimination yields the desired product **1.36** in 82% yield. Despite that the cascade cyclisation occurs with only a modest ee of 68%, the assembly of the pentacyclic ring system and quaternary stereocentre in one synthetic operation negates this. The synthesis of (+)-xestoquinone is then completed by hydrogenation of the remaining alkene followed by an oxidation to install the 1,4-naphthoquinone moiety.



**Scheme 1.37** Keay's asymmetric cascade Mizoroki-Heck reaction.

#### 1.4.2 *N*-Heterocyclic Carbenes

Today *N*-heterocyclic carbenes (NHCs) are normally associated with catalysis, either as organocatalysts themselves<sup>89</sup> or as ligands for metals in catalysis.<sup>90-94</sup> While the role of NHCs as ligands is now almost as prominent as phosphines, NHCs are relatively young in comparison. The most common of these NHCs are based on 5-membered heterocycles (Figure 1.9), such as imidazole and imidazoline, and will be the focus of this section. There are, however, many other varieties of NHCs, some of which are shown in Figure 1.10.<sup>94</sup>

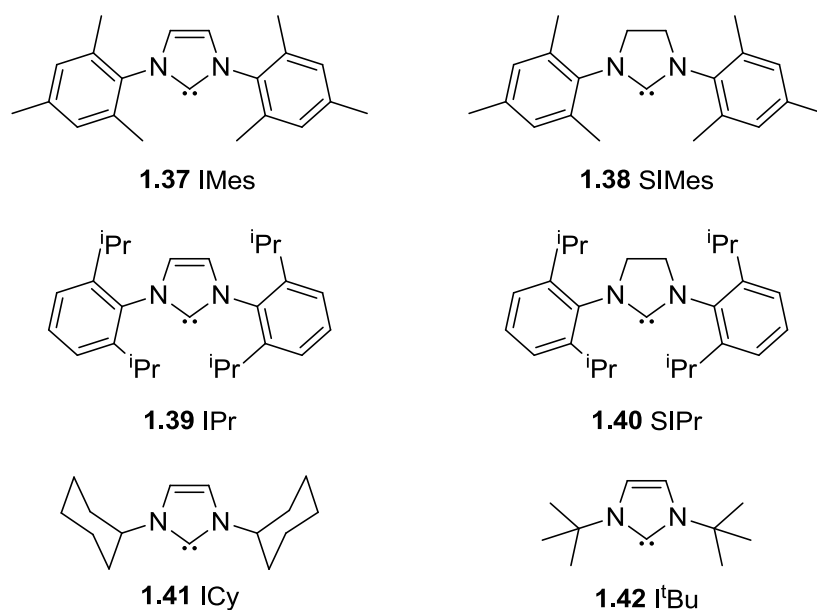


**Figure 1.9.** Some commonly used 5 membered-NHCs.

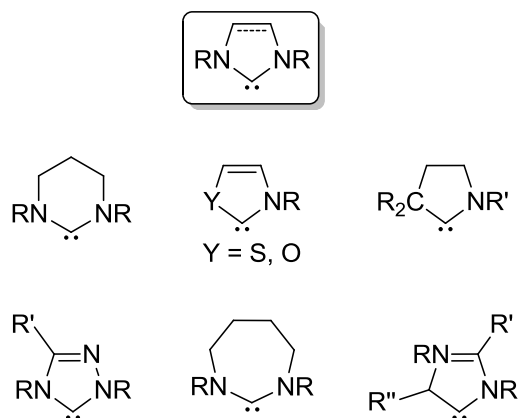
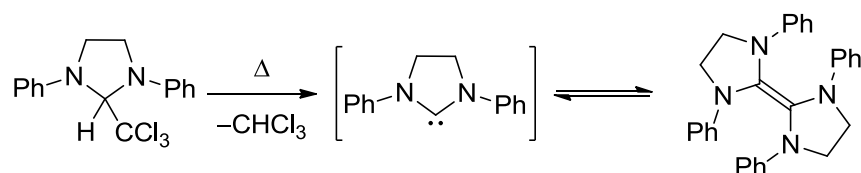


**Figure 1.10** Structural variety of NHCs.

#### 1.4.2.1 Discovery and Early Developments

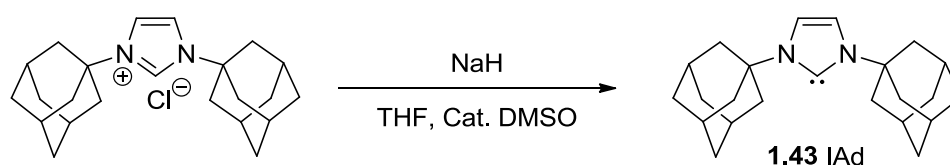
The first NHC was synthesised in 1968 by Wanzlick, however it was not isolable and rapidly dimerised (Scheme 1.38).<sup>95</sup>





**Scheme 1.38.** Synthesis and dimerisation of Wanzlick's first NHC.

Studies of the organometallic compounds of NHCs were furthered by Lappert and colleagues, showing that the nucleophilic lone pair could be trapped and coordinated to several different transition metals,<sup>96,97</sup> but isolating a stable NHC was the advance that was needed to ignite the investigation of NHCs as ligands. In 1991 Arduengo and co-workers synthesised the first stable NHC **1.43** by deprotonation of the corresponding imidazolium salt with sodium hydride (Scheme 1.39).<sup>98</sup>



**Scheme 1.39** The first isolable NHC IAd synthesised by Arduengo and co-workers.

The resulting crystalline carbene was stable in the absence of oxygen and moisture. The characteristics that granted the stability of IAd in comparison to those that Wanzlick was unable to isolate were not immediately obvious. The following year the same group reported four more stable NHCs (Figure 1.11, **1.37** and **1.44-1.46**), and two that were not stable (**1.48** and **1.49**).<sup>99</sup>

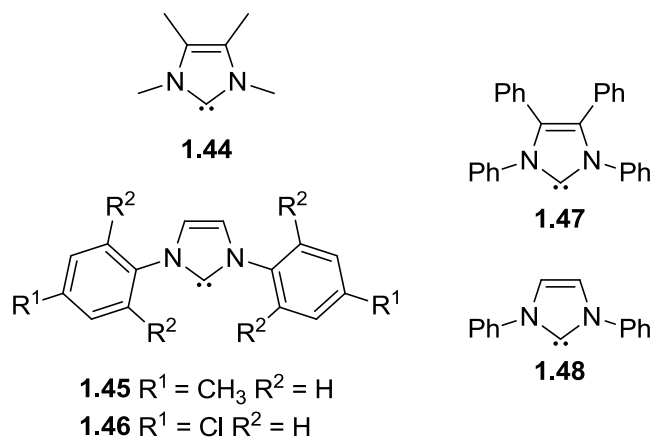


**Figure 1.11** Series of NHCs synthesised by Arduengo and co-workers.

By increasing the steric bulk of the nitrogen substituents it is relatively simple to appreciate how this can stabilise the reactive lone pair that is shielded within, and preventing it from dimerising. Whilst bulky substituents serve to kinetically stabilise the carbene (such in the case of IAd and IMes) the fact that **1.44** is an isolable solid but **1.47** is not, demonstrates that this stability cannot entirely be due to steric factors. The reality is that NHCs stability arrives from a combination of kinetic stability from sterics and thermodynamic stability from electronic factors.

#### 1.4.2.2 Electronic and Steric Considerations

The electronic structure of a cyclic NHC is characterised by the bent geometry of the carbenic carbon, due to the constraint of the 5-membered ring, the  $\sigma^2$  singlet state is favoured. Consequently, the frontier orbitals of the carbene are an  $sp^2$ -hybridised orbital ( $\sigma$ -lone pair, HOMO) and the remaining orthogonal p orbital ( $p_\pi$ , LUMO).<sup>94,100</sup> There are several possible configurations that the frontier molecular orbitals could be occupied in (shown in Figure 1.12). The  $\sigma^2$  singlet state is stabilised by a ‘push-pull’<sup>101</sup> mechanism: a combination of inductive electron withdrawal through the  $\sigma$ -framework by the nitrogen atoms flanking the carbene carbon and mesomeric donation of the nitrogen lone pairs into the unoccupied  $p_\pi$  orbital of the carbene carbon.

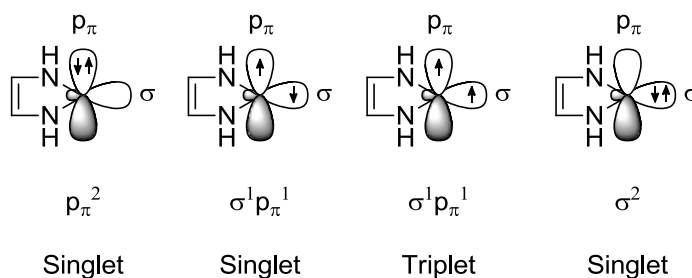


**Figure 1.12** Possibilities for the occupation of the frontier molecular orbitals for NHC based on imidazole.

Originally the unsaturated backbone was seen as a necessity in achieving a stable carbene, and intuitively this is a reasonable assumption as delocalisation of the  $6\pi$  electrons and aromaticity is associated with stability. The synthesis of the saturated NHC SIPr<sup>102</sup> (**1.38**) showed that this aromaticity only served as an additional source of stabilisation; the mesomeric donation of the nitrogen lone pair to the  $p_{\pi}$  carbene orbital can grant sufficient stabilisation of the free carbene providing the nitrogen substituents do not hinder this interaction. This could explain the instability of **1.47** and **1.48**, there is competition for the nitrogen lone pairs between the  $p_{\pi}$  carbene orbital and the  $\pi$  system of the unsubstituted phenyl rings, thus resulting in insufficient stabilisation of the free carbene.

NHCs behave as a typical 2-electron donor ligand and generally considered to be comparable if not stronger donors than the most donating tertiary phosphines.<sup>103</sup> Their donating ability can be determined in the same manner as developed by Tolman for phosphines, by measuring the CO stretching frequencies of appropriate M-L complexes.<sup>104,105</sup> Nolan and co-workers have reported these data for a vast range of different NHCs.<sup>106</sup> The 3 bonding contributions of the M-NHC bond are shown in Figure 1.13. The most dominant interaction is undoubtedly the  $\sigma$ -donation contribution, and until recently the  $\pi$  bonding modes were thought to be insignificant but have been shown to provide on average 10-20% of the NHC-M bonding interaction in the case of  $d^{10}$  metals.<sup>107</sup>

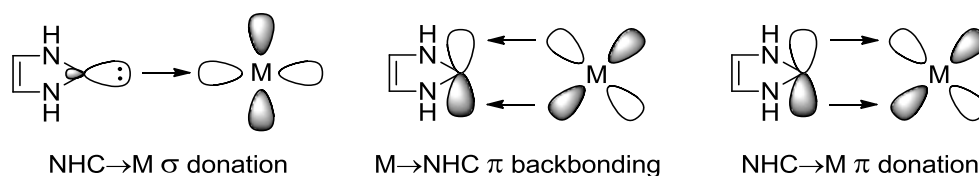


**Figure 1.13** Bonding interactions of the metal-NHC bond.

The strong electron donating properties of NHCs make them good ligands as they result in an electron-rich metal centre and show a low propensity to dissociate from the metal centre, resulting in a more stable active species that persists for longer during catalysis. In addition, the large steric environment usually associated with NHCs can often stabilise reactive low-valent metal species. Whilst the steric properties of phosphines can be summarised by the Tolman cone angle, such a description does not suffice for the steric parameters of NHCs.

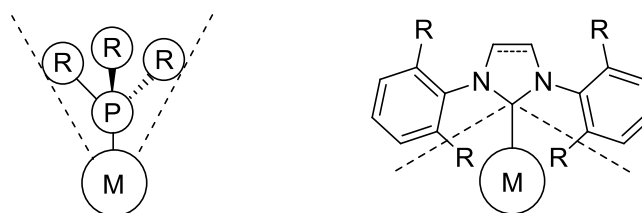


**Figure 1.14** Comparison of the steric environments imparted by phosphines and NHCs.

NHCs have a 'wrap around' character to the steric environment they impart on the metal centre due to the bulky N-substituent's that are angled inwards, whereas for phosphines the (bulky) substituents are angled away from the metal centre (Figure 1.14). In 2003 Nolan and Cavallo developed a method to quantify the steric properties of NHCs, namely the "percent buried volume" ( $\%V_{\text{bur}}$ ).<sup>108</sup> That is, the percentage of the volume of a sphere, representing the space around the metal, that is occupied by the ligand. They calculated the  $\%V_{\text{bur}}$  of commonly used imidazole (unsaturated) and imidazoline (saturated) based NHCs using the DFT optimised structures of the appropriate NHC. The model was formed by placing a metal atom at the centre of a

sphere with an arbitrary radius ( $r$ ) of 3 Å and the M-(NHC) bond distance was fixed at 2 Å ( $d$ ) (Figure 1.15).

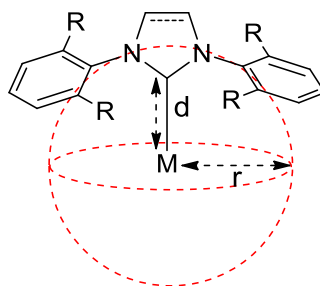


**Figure 1.15** Diagram illustrating the % $V_{\text{bur}}$  of NHC ligands.

In the same publication the authors determined the bond dissociation energies (BDE) of the (NHC)-M bond in a variety of ruthenium(II) complexes with general formula  $[\text{Cp}^*\text{Ru}(\text{NHC})\text{Cl}]$ . Comparison of the BDEs of these complexes and % $V_{\text{bur}}$  of their corresponding NHCs revealed a linear trend, an increase in (NHC)-Ru BDE of around  $12 \text{ kcal mol}^{-1}$  was observed when the steric bulk (% $V_{\text{bur}}$ ) of the NHC was decreased (37% to 21%). This demonstrated that the lability of the (NHC)-metal bond is strongly governed by its sterics. This model can also be used to compare NHCs to phosphines. A study by the same group examined the BDEs of the M-L and M-CO bonds in Ni complexes of the type  $[\text{LNi}(\text{CO})_3]$ , where the ligands were either phosphines or NHCs (Table 1.1).<sup>105</sup>

Ligand	% $V_{\text{bur}}$	BDE of Ni-CO	BDE of Ni-L
I'Bu	37	13.3	24.0
SI'Bu	38	10.3	21.8
IAd	37	7.6	20.4
IMes	26	28.3	41.1
SIMes	27	26.8	40.2
IPr	29	26.7	38.5
SIPr	30	25.6	38.0
ICy	23	27.0	39.6
PPh <sub>3</sub>	22	30.4	26.7
P( <i>t</i> -Bu) <sub>3</sub>	30	27.4	28.0

**Table 1.1** A comparison of ligand %  $V_{\text{bur}}$  and BDEs in complexes of type [LNi(CO)<sub>3</sub>]. BDEs given in kcal mol<sup>-1</sup>.<sup>105</sup>

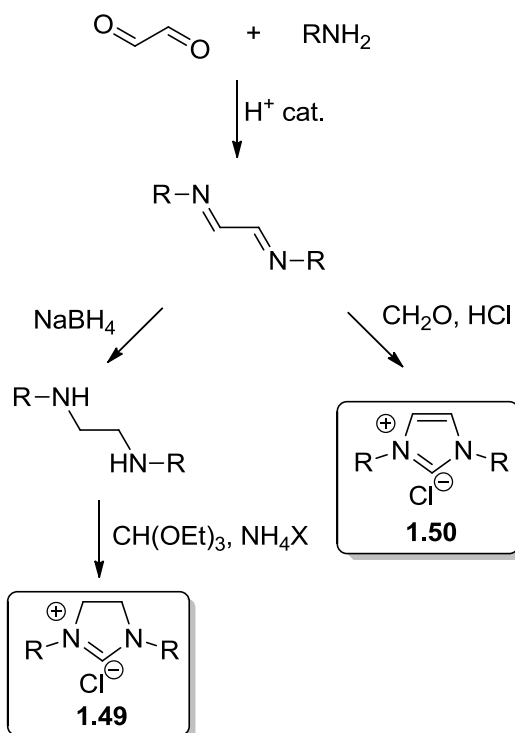
From these data several interesting comparisons can be made. When comparing saturated NHCs to their unsaturated analogues, the saturated NHCs have a slightly increased %  $V_{\text{bur}}$ , which is likely to be because the backbone of the 5-membered ring is flexible, whereas the unsaturated analogues are rigid. This is reflected in the BDEs for the Ni-L bond, the saturated NHCs BDE being lower than their unsaturated analogues and is most obvious when comparing the very bulky NHCs (I'Bu and SI'Bu). The BDE of the Ni-CO interaction of these complexes can be used as a measure of the electron donating ability of the attached ligand, and demonstrates that, in this case, saturated NHCs are more electron donating than their unsaturated versions. It also shows that NHCs are generally more donating than phosphines. For example P(*t*-Bu)<sub>3</sub> and SIPr have the same %  $V_{\text{bur}}$ , of 30, yet the SIPr complex has a Ni-CO BDE that is 1.8 KCal mol<sup>-1</sup> less than for the P(*t*-Bu)<sub>3</sub> complex; a similar trend is seen when comparing ICy and PPh<sub>3</sub>. With the exception of the exceeding bulky examples, NHCs form a more stable L-M complex than the phosphines. Again, comparing P(*t*-Bu)<sub>3</sub> and SIPr as they

have the same %  $V_{\text{bur}}$ , the Ni-SIPr interaction is 10 KCal mol<sup>-1</sup> more stable than for the Ni- P(*t*-Bu)<sub>3</sub> bond. The most bulky NHCs show the lowest Ni-CO BDEs signifying that they are the most electron donating ligands, despite being the least stable (low (NHC)-Ni BDEs).

The %  $V_{\text{bur}}$  model has been established as a convenient method to compare the steric properties of different classes of ligands. In a study carried out by Nolan and Clavier, around 700 crystal structures were analysed to calculate the %  $V_{\text{bur}}$  of a wide variety of monodentate phosphines, bidentate phosphines and NHCs in a number of metal complexes.<sup>109</sup> They showed that the steric parameters of the N-arylated NHCs, such as (S)IPr and (S)IMes, are flexible and can change depending on the nature of the metal complex and the presence of other ligands in the coordination sphere. The steric properties of the N-alkylated NHCs tend to be less varied and are independent of the metal centre.

#### 1.4.2.3 Synthesis of Commonly used NHCs

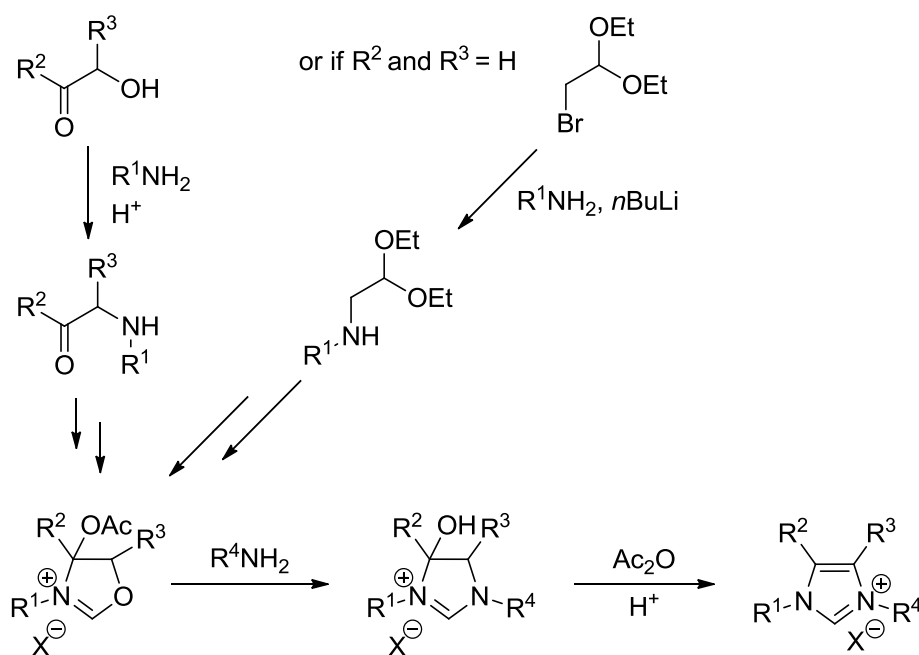
There are numerous routes that are available to synthesise a variety of different NHC precursors.<sup>110</sup> This has undoubtedly facilitated the diversity of NHCs and the extent to which they have been studied. Scheme 1.40 shows an example of a standard route to yield imidazolinium (**1.49**) and imidazolium (**1.50**) salts, which are precursors for saturated and unsaturated, commonly used NHCs respectively. The condensation of glyoxal with the desired aryl amine in the presence of an acid catalyst produces the corresponding diazobutadiene (DAD), the intermediate both saturated and unsaturated precursor salts. The reduction of the imine using NaBH<sub>4</sub> or LiAlH<sub>4</sub> yields the diamine, which after ring closure with triethylorthoformate in the presence of an ammonium salt yields the corresponding saturated NHC precursor salt **1.49**. The counterion can be varied depending on what ammonium salt is used, like NH<sub>4</sub>Cl, NH<sub>4</sub>Br or NH<sub>4</sub>BF<sub>4</sub> for example. Direct treatment of the DAD with paraformaldehyde under acidic conditions yields the unsaturated NHC precursor salt **1.50**.



**Scheme 1.40** Common routes to saturated and unsaturated NHC precursor salts.

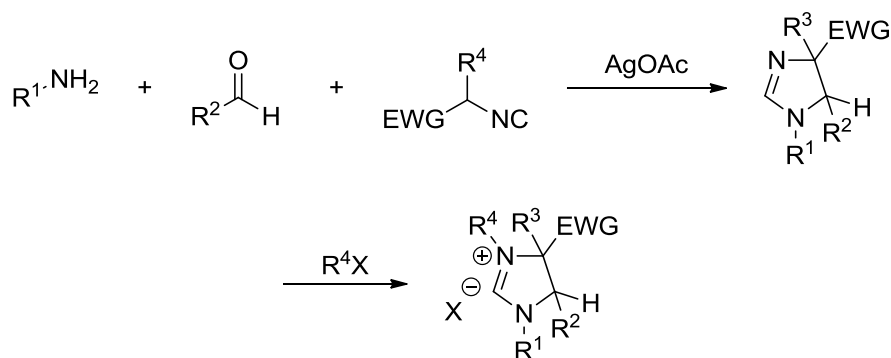
These synthetic routes work well for the synthesis of symmetrical carbenes, where the functionality on both nitrogen atoms is the same, but are not amenable for making unsymmetrical NHCs. A general approach to unsymmetrical imidazolium salts was reported by Fürstner in 2006.<sup>111</sup> This method tolerates a wide variety of anilines and amines, and is scalable (Scheme 1.41).





**Scheme 1.41** Fürstner's highly flexible synthesis of unsymmetrical imidazolium salts.

The key transformation in this synthesis is the reaction of an oxazolinium salt with an amine to yield the corresponding hydroxylated imidazolium salt, which after treatment with acetic anhydride under acidic conditions yields the desired NHC precursor. The oxazolinium intermediate can be synthesised from  $\alpha$ -hydroxyketones, or if  $R^2$  and  $R^3$  are protons then bromoacetaldehyde diethylacetal is used as the starting material. Orru and co-workers reported a similarly flexible route for the synthesis of unsymmetrical imidazolium salts.<sup>112</sup> The synthesis involves a silver-catalysed multicomponent reaction (MCR) of an aldehyde, isocyanide and an amine to yield highly substituted imidazolines (Scheme 1.42). The imidazolium salt is completed by quaternisation of the imidazoline using an appropriate alkyl electrophile, benzylbromide for example.



**Scheme 1.42** Orru's synthesis of imidazolinium salts *via* a silver catalysed MCR.

#### 1.4.2.4 NHCs In Catalysis

As discussed in the preceding sections, NHCs have desirable properties that make them good ligands for catalysis. In summary these are because they: (1) are usually more electron donating than phosphines; (2) form more stable complexes with metals than phosphines and (3) are customisable with regards to their steric and electronic properties. The first group to take advantage of NHCs as ancillary ligands for catalysis was that of Herrmann's in 1995,<sup>113</sup> only a short time after Arduengo's isolation of the first stable carbene IAd. Herrmann showed that a chelating bis-NHC palladium(II) complex could be used in Heck couplings between an acrylate and activated aryl chlorides and bromides. This opened the door for the investigation and development of NHC metal complexes as catalysts for homogeneous catalysis, particularly cross-coupling reactions.<sup>92</sup> The application of NHC based catalysts in examples of the Mizoroki-Heck and Songashira reactions will be discussed in greater detail in Chapters 3 and 4.

#### 1.4.2.5 NHC Design

One direction that the design of new NHCs has taken is towards developing ligands that are significantly bulky and strongly electron donating, with the goal of activating the most challenging aryl chlorides at mild temperatures in C-C cross-coupling reactions.<sup>91</sup> This is a fine balancing act, if the steric bulk of the ligand is excessive it will hinder the approach of the coupling partners, disfavours the oxidative addition step, particularly

if the aryl chloride has *ortho*-substituents, and the transmetalation step. The answer to this trade-off was the emergence of NHC ligands with “flexible bulk”,<sup>91</sup> that is, a ligand that could adapt and react to the sterics of the metal complex whilst accommodating the incoming aryl halide.

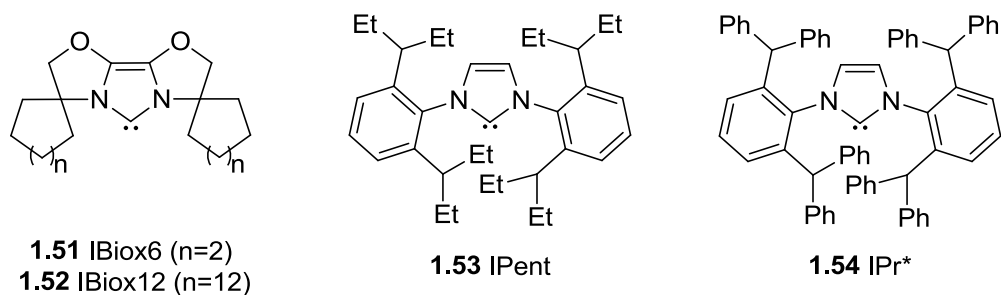
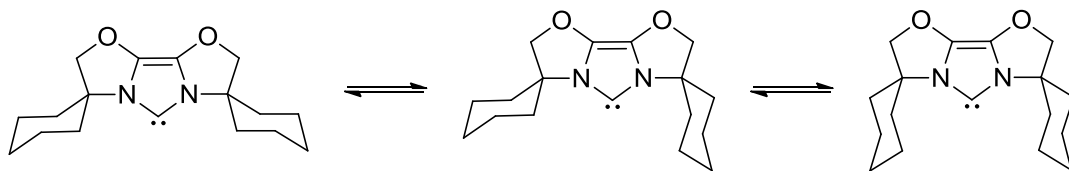


**Figure 1.16** NHCs with flexible sterics.

One of the first examples of such ligands were the IBiox NHCs reported by Glorius and co-workers in 2003 (Figure 1.16), where the authors showed that the steric flexibility of **1.51** originates from the ability of the cyclohexyl rings to flip conformation (Scheme 1.43).<sup>114</sup> The use of **1.51** with Pd(OAc)<sub>2</sub> allowed for the coupling of bulky chlorides, such as 2-chloro-1,6-dimethylbenzene, with phenyl boronic acids in good to excellent yields at room temperature. The synthesis of tri-*ortho*-substituted biaryl could also be achieved, albeit at slightly lower yields and much higher temperatures.



**Scheme 1.43** Steric flexibility of **1.51** achieved by change in confirmation of the cyclohexyl rings.<sup>115</sup>

2009 saw Organ and co-workers introduce IPent (**1.53**) as another example of a sterically flexible ligand (Figure 1.17), a bulkier analogue of IPr (**1.39**).<sup>116,117</sup> When **1.53**

was used as the NHC in one of Organ's signature type precatalysts (Figure 1.17) the synthesis of tetra-*ortho*-substituted biaryls could be attained through Suzuki-Miyaura reactions, however raised temperatures were still needed.

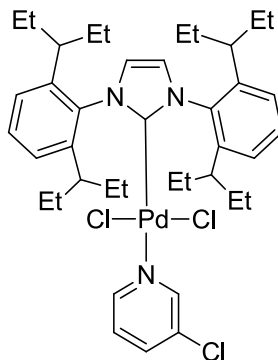


**Figure 1.17** Pd-PEPPSI-IPent precatalyst.

An improvement on this came from an analogue of IPr that is even bulkier, IPr\*(**1.54**). The synthesis of IPr\* was first reported by Markó and co-workers.<sup>118</sup> Subsequently Nolan and co-workers demonstrated that the use of [(IPr\*)Pd(cinnamyl)Cl] (Figure 1.18) could be used for the Suzuki-Miyaura coupling to yield tetra-*ortho*-substituted biaryls, utilising aryl chlorides, at room temperature.<sup>119</sup>

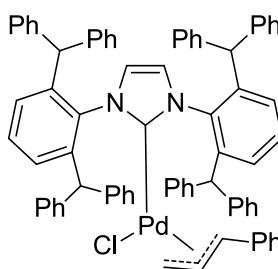
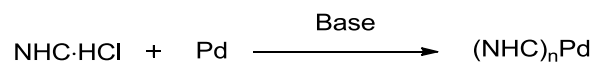


**Figure 1.18** [(IPr\*)Pd(cinnamyl)Cl] precatalyst.

#### 1.4.2.6 Precatalyst designs.

The *in situ* synthesis of an (NHC)-Pd species is a straightforward method to generate the desired catalyst under the reaction conditions without the difficulty of having to isolate the free carbene and perform a ligand substitution. Taking a source of palladium such as Pd(OAc)<sub>2</sub> or Pd<sub>2</sub>(dba)<sub>3</sub> and treating the NHC salt with a base may be practically more simple (Scheme 1.44), but how many NHCs are coordinated to the

metal centre in the resultant complex, or if multiple species have been generated, is difficult to predict with accuracy.



**Scheme 1.44** Typical protocol for the *in situ* formation of NHC palladium complexes.

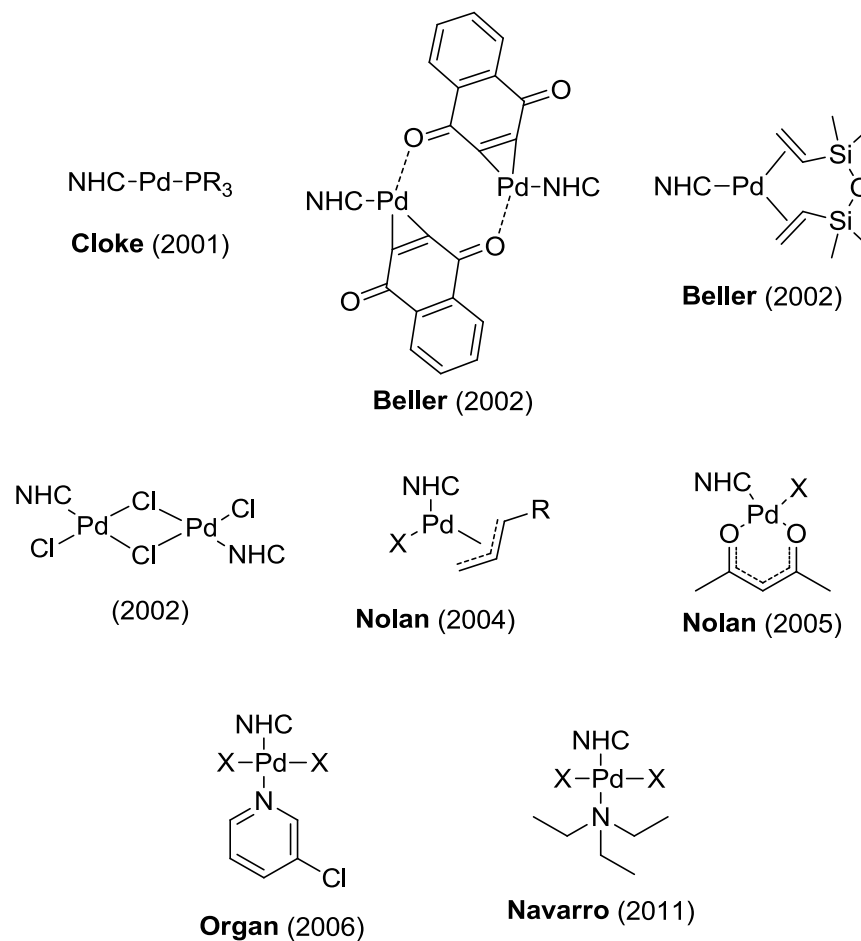
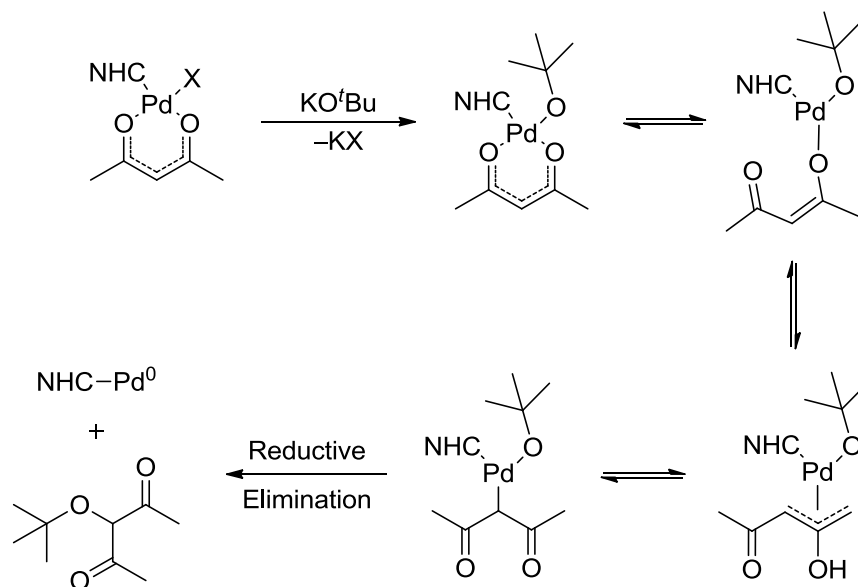


**Figure 1.19** General structures of different (NHC)-Pd precatalysts.

As with phosphines complexes, *in situ* systems have generally been replaced by well-defined (NHC)-Pd complexes, and many developments have been made in this area.<sup>90,91</sup> Figure 1.19 shows a number of (NHC)-Pd(0)<sup>120,121</sup> and (NHC)-Pd(II)<sup>122-125</sup> complexes that have been developed and utilised as precatalysts in cross-coupling reactions. These precatalysts are typically designed to have a well-defined route to a

(NHC)-Pd(0), for example the (NHC)Pd(acac)Cl precatalysts designed by Nolan and co-workers is proposed to be activated as shown in Scheme 1.45.<sup>122</sup>



**Scheme 1.45** Activation of the Pd(II) complex (NHC)PdX(acac) to the (NHC)-Pd(0) species.

Metathesis of the halide anion for the *tert*-butoxide anion, followed by a rearrangement of the acetylacetonate ligand and finally reductive elimination yields the (NHC)-Pd(0) species.

Today a considerable amount of precursor salts and metal complexes of the commonly used NHCs are commercially available. NHCs are no longer seen as a simple phosphine mimics and there are now a vast variety of different (NHC)-metal complexes that have been used for catalysis, beyond the scope of this thesis. Consequently these relevant review articles are gathered here and the reader is encouraged to refer to them for a fuller account if required.<sup>90-94</sup>

### 1.4.3 Palladacycles

Palladacycles are defined by the presence of a C-Pd bond (usually an aryl carbon) accompanied by intramolecular donor interaction, for example from a phosphorus, nitrogen or oxygen atom, forming a cyclopalladated complex. In this section a basic overview of these complexes is presented.

The first palladacycle was reported by Cope in 1965, during his investigation of the reaction between azobenzenes and  $\text{KPtCl}_4$  and  $\text{PdCl}_2$ .<sup>126</sup> He found that when azobenzene were mixed with either of the metal chlorides at room temperature for several weeks a new cyclometalated complex was formed (Figure 1.20).

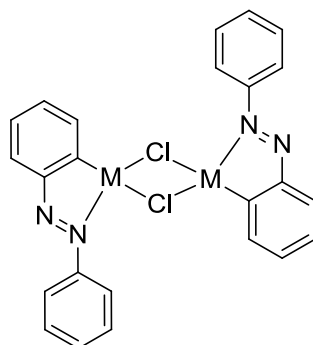
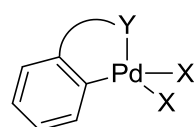
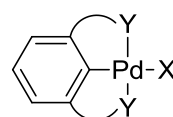


**Figure 1.20** First example of a palladacycle. M = Pt or Pd.

There are two distinct structural classes of palladacycles: CY and YCY (Figure 1.21), where Y is the identity of the donor atom. In CY palladacycles there is one intramolecular donor atom; whereas in YCY palladacycles there are two donor atoms, these are more commonly known as pincer complexes.<sup>127</sup>



CY Palladacycle



YCY Palladacycle

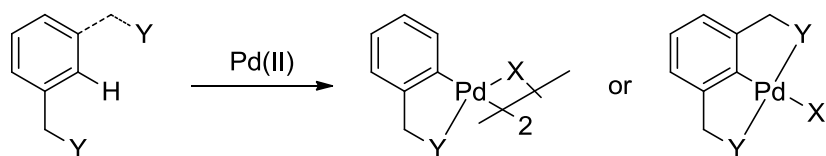
**Figure 1.21** Structural classes of palladacycles.

There are several different types of CY palladacycles:<sup>128</sup> (1) a neutral dimer where the X ligands are bridging between two dimers, as in Cope's first palladacycle; (2) A neutral complex that is bis-cyclometalated, *i.e.* one metal centre with two metalacycles; (3) A neutral complex where one of the X ligands is a neutral donor and the other is an anionic donor; (4) An anionic complex where both X ligands are anionic donors; (5) a cationic complex where both X ligands are neutral donors. In the case of the anionic and cationic complexes, they are associated with the appropriate counter-ions. There is less

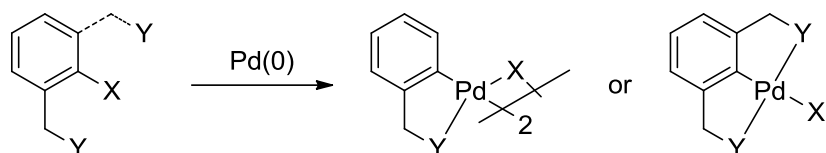
ambiguity for the general structure of the YCY palladacycles, and are typically symmetrical, in the case where they are not they are usually referred to as YCZ palladacycles.

The synthesis of palladacycles can be achieved in a number of ways (Scheme 1.46). C-H activation can be used to yield palladacycles, by treating the desired ligand with a cyclometalating palladium(II) reagent such as  $\text{Li}_2\text{PdCl}_4$ . This is generally thought to occur by initial coordination of the donor part of the ligand (Y) followed by a coordination of the aromatic ring, which can then undergo an electrophilic aromatic substitution to give the cyclometalated product (which then dimerises in the case of CY palladacycles).<sup>128</sup> Oxidative addition of the appropriate ligand to palladium(0) species can also give a direct route to palladacycles.

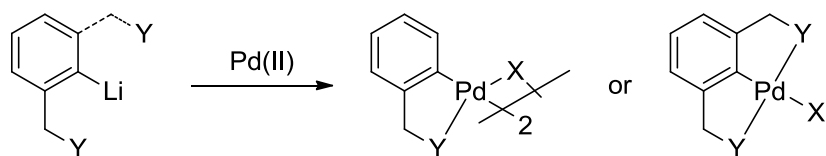




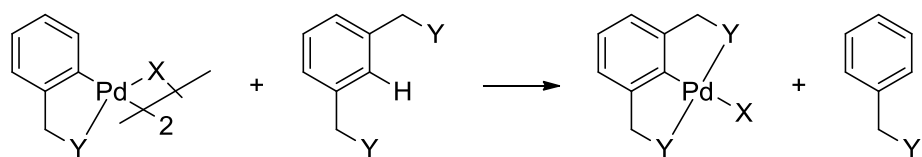
C-H Activation



Oxidative Addition



Transmetalation



Transcyclometalation

**Scheme 1.46** General approaches to the synthesis of palladacycles.

If the formation by the oxidative addition pathway is problematic, then transmetalation may be possible. Lithium/halogen exchange can be used to form a more reactive aryl lithium species which can then undergo transmetalation with an appropriate palladium(II) source such as (cod)PdX<sub>2</sub>. Palladacycle complexes can also be synthesised by the method of transcyclometalation. That is, the substitution of a CY palladacycle by another ligand to yield a new cyclometalated product. This method is typically used for the formation of pincer complexes (Scheme 1.46).

The first example of a palladacycle being used in catalysis was reported by Herrmann and co-workers in 1995, with an example of a Mizoroki-Heck reaction

involving aryl chlorides,<sup>129</sup> the details of which will be discussed in Chapter 3. This started the trend of a plethora of palladacyclic complexes being synthesised and being tested for their activity in catalysis. Hence the activation of aryl chlorides by palladacycles in other cross-coupling reactions, such as the Suzuki-Miyaura coupling and aminations, have been reported.<sup>130-132</sup> The following reviews give a good overview of both CY and YCY palladacycles in catalysis,<sup>127,133</sup> and a review by Spencer and Dupont highlight other uses for palladacycles.<sup>128</sup>

#### 1.4.4 Ligand-free systems

In recent years there has been an increase in interest to find ‘greener’ protocols for C-C cross-coupling reactions, one such solution is the development of ligand-free catalysis with particular attention on palladium nanoparticles (Pd-NPs). Their use has been demonstrated in the majority of palladium cross-coupling reactions;<sup>134</sup> additionally Pd-NPs have been implicated as the active species in some examples of molecular catalysis, for example in the case of palladacycles.<sup>135</sup> Pd-NPs for catalysis are usually produced by the *in situ* reduction of a palladium(II) salt, such as Pd(OAc)<sub>2</sub>, or by thermal decomposition of a well-defined precatalyst. A recent report has also shown that commercially obtained samples of Pd<sub>2</sub>(dba)<sub>3</sub>, a ubiquitous precatalyst for many palladium catalysed reactions, may contain up to 40% of Pd-NPs.<sup>56</sup> Reetz and co-workers reported an investigation of the ligand-free Mizoroki-Heck reaction in 2000.<sup>136</sup> The reaction between styrene and bromobenzene was monitored by GC, and TEM was used to determine the amount and size of any Pd-NPs generated in the reaction mixture at certain intervals. First a catalytic system of [PdCl<sub>2</sub>(PhCN)<sub>2</sub>] (1.5%) precatalyst, NaOAc base and *N, N*-dimethylglycine (DMG) was used as the solvent. The authors observed there was an hour induction period before any product was detected; furthermore no Pd-NPs were seen by TEM until after this induction period. This was attributed to the time taken for Pd(OAc)<sub>2</sub> to be formed *in situ* and its subsequent thermal decomposition to form Pd-NPs. Hence it was clear that the catalysis did not start until the NPs had been formed. When the Mizoroki-Heck reaction of

ethylacrylate and iodobenzene, catalysed by  $\text{Pd}(\text{OAc})_2$  with TBAB as an additive and NaOAc as the base, was tested in a similar manner no induction period was noted and Pd-NPs were detected almost immediately, further confirming TBABs ability to stabilise colloidal palladium. In this case, it was not clear if Pd-NP formation was a requisite for catalysis, if so the NPs should be able to undergo oxidative addition with the iodobenzene. When iodobenzene was subjected to the reaction conditions without the presence of the alkene, the authors observed that the reaction mixture turned from the typical 'palladium black' to a deep red. UV/Vis spectroscopy was used to confirm the presence of a new species and the  $^{13}\text{C}$  NMR spectroscopy was consistent with that of an aromatic ring bound to palladium. Hence the oxidative addition of iodobenzene to the Pd-NPs had occurred. Further evidence for this was obtained when addition of styrene and base to the deep red solution gave the desired cross-coupled product. These studies were among the first to show that Pd-NPs can be implicated as the active species in ligand-free systems.

Several features about Pd-NPs make them an attractive for use in industrial catalysis; one is the obvious saving on the cost of ligands and elaborate specialist precatalysts. Another is that Pd-NPs can be added to the reaction using simple palladium sources such as  $\text{Pd}(\text{OAc})_2$  or  $\text{PdCl}_2$ . For example, a report by Saijiki and co-workers has demonstrated that palladium on charcoal (Pd/C), a common heterogeneous reagent, can be used to affect the Hiyama cross-coupling.<sup>137</sup> Presumably, the active catalyst is just small amounts of soluble Pd-NPs that have leached into solution. This protocol has the practical advantage of simply filtering off the solid-supported catalyst, making its removal from the products straightforward. Along these lines, Plucinski and co-workers have reported that Pd-NPs adsorbed onto a magnetic Fe-NPs can catalyse the Mizoroki-Heck reaction.<sup>138</sup> A magnet can be used to easily separate the catalyst, which the authors showed retained its activity and could be recycled. The reuse of catalysts is a highly desirable feature in any industrial process.

There are many more examples of Pd-NPs supported on different materials and their use in cross-coupling reactions than can be discussed in this short summary of ligand-free systems. The following reviews give an overview of this rapidly developing field.<sup>134,139</sup>

## 1.5 References

- (1) Corbet, J.-P.; Mignani, G. *Chem. Rev.* **2006**, *106*, 2651–2710.
- (2) Johansson Seechurn, C. C. C.; Kitching, M. O.; Colacot, T. J.; Snieckus, V. *Angew. Chem. Int. Ed.* **2012**, *51*, 5062–5085.
- (3) Kiso, Y.; Yamamoto, K.; Tamao, K.; Kumada, M. *J. Am. Chem. Soc.* **1972**, *94*, 4373–4374.
- (4) Corriu, R. J. P.; Masse, J. P. *Chem. Comm.* **1972**, 144a–144a.
- (5) Murahashi, S.-I. *J. Organomet. Chem.* **2002**, *653*, 27–33.
- (6) Huang, J.; Nolan, S. P. *J. Am. Chem. Soc.* **1999**, *121*, 9889–9890.
- (7) Liu, P.; Jacobsen, E. N. *J. Am. Chem. Soc.* **2001**, *123*, 10772–10773.
- (8) Miyaura, N.; Yamada, K.; Suzuki, A. *Tetrahedron Lett.* **1979**, *20*, 3437–3440.
- (9) Miyaura, N.; Suzuki, A. *Chem. Rev.* **1995**, *95*, 2457–2483.
- (10) Ishiyama, T.; Murata, M.; Miyaura, N. *J. Org. Chem.* **1995**, *60*, 7508–7510.
- (11) Watanabe, T.; Shakadou, M.; Uemura, M. *Synlett* **2000**, *2000*, 1141–1144.
- (12) Molander, G. A.; Bernardi, C. R. *J. Org. Chem.* **2002**, *67*, 8424–8429.
- (13) Molander, G. A.; Dehmel, F. *J. Am. Chem. Soc.* **2004**, *126*, 10313–10318.
- (14) King, A. O.; Okukado, N.; Negishi, E.-I. *Chem. Comm.* **1977**, 683–684.
- (15) Negishi, E.-I. *J. Organomet. Chem.* **2002**, *653*, 34–40.
- (16) Zeng, F.; Negishi, E.-I. *Org. Lett.* **2001**, *3*, 719–722.
- (17) Milstein, D.; Stille, J. K. *J. Am. Chem. Soc.* **1978**, *100*, 3636–3638.
- (18) Milstein, D.; Stille, J. K. *J. Am. Chem. Soc.* **1979**, *101*, 4992–4998.
- (19) Merrifield, J. H.; Godschalx, J. P.; Stille, J. K. *Organometallics* **1984**, *3*, 1108–1112.
- (20) Echavarren, A. M.; Stille, J. K. *J. Am. Chem. Soc.* **1988**, *110*, 1557–1565.
- (21) Knight, S. D.; Overman, L. E.; Pairaudeau, G. *J. Am. Chem. Soc.* **1993**, *115*, 9293–9294.
- (22) Hatanaka, Y.; Hiyama, T. *J. Org. Chem.* **1988**, *53*, 918–920.
- (23) Hatanaka, Y.; Hiyama, T. *Synlett* **1991**, *1991*, 845–853.

- (24) Hagiwara, E.; Gouda, K.-I.; Hatanaka, Y.; Hiyama, T. *Tetrahedron Lett.* **1997**, *38*, 439–442.
- (25) Denmark, S. E.; Sweis, R. F. *J. Am. Chem. Soc.* **2001**, *123*, 6439–6440.
- (26) Denmark, S. E.; Regens, C. S.; Kobayashi, T. *J. Am. Chem. Soc.* **2007**, *129*, 2774–2776.
- (27) Kumada, M. *Pure and Applied Chemistry* **1980**, *52*, 669–679.
- (28) Phapale, V. B.; Cárdenas, D. J. *Chem. Soc. Rev.* **2009**, *38*, 1598–1607.
- (29) Zhou, J. S.; Fu, G. C. *J. Am. Chem. Soc.* **2004**, *126*, 1340–1341.
- (30) Powell, D. A.; Fu, G. C. *J. Am. Chem. Soc.* **2004**, *126*, 7788–7789.
- (31) Strotman, N. A.; Sommer, S.; Fu, G. C. *Angew. Chem. Int. Ed.* **2007**, *46*, 3556–3558.
- (32) Powell, D. A.; Maki, T.; Fu, G. C. *J. Am. Chem. Soc.* **2005**, *127*, 510–511.
- (33) Leowanawat, P.; Zhang, N.; Resmerita, A.-M.; Rosen, B. M.; Percec, V. *J. Org. Chem.* **2011**, *76*, 9946–9955.
- (34) Glaser, C. *Ber. Dtsch. Chem. Ges.* **1869**, *2*, 422–424.
- (35) Hay, A. S. *J. Org. Chem.* **1962**, *27*, 3320–3321.
- (36) Stephens, R. D.; Castro, C. E. *J. Org. Chem.* **1963**, *28*, 3313–3315.
- (37) Inamoto, K.; Asano, N.; Kobayashi, K.; Yonemoto, M.; Kondo, Y. *Org. Biomol. Chem.* **2012**, *10*, 1514.
- (38) Chu, L.; Qing, F.-L. *Org. Lett.* **2010**, *12*, 5060–5063.
- (39) Tamura, M.; Kochi, J. K. *J. Am. Chem. Soc.* **1971**, *93*, 1487–1489.
- (40) Cahiez, G.; Avedissian, H. *Synthesis* **1998**, *1998*, 1199–1205.
- (41) Dohle, W.; Kopp, F.; Cahiez, G.; Knochel, P. *Synlett* **2001**, *2001*, 1901–1904.
- (42) Fürstner, A.; Leitner, A.; Méndez, M.; Krause, H. *J. Am. Chem. Soc.* **2002**, *124*, 13856–13863.
- (43) Sherry, B. D.; Fürstner, A. *Acc. Chem. Res.* **2008**, *41*, 1500–1511.
- (44) Hatakeyama, T.; Hashimoto, T.; Kondo, Y.; Fujiwara, Y.; Seike, H.; Takaya, H.; Tamada, Y.; Ono, T.; Nakamura, M. *J. Am. Chem. Soc.* **2010**, *132*, 10674–10676.
- (45) Bedford, R. B.; Brenner, P. B.; Carter, E.; Carvell, T. W.; Cogswell, P. M.; Gallagher, T.; Harvey, J. N.; Murphy, D. M.; Neeve, E. C.; Nunn, J.; Pye, D. *R. Chem. Eur. J.* **2014**, *20*, 7935–7938.
- (46) Adams, C. J.; Bedford, R. B.; Carter, E.; Gower, N. J.; Haddow, M. F.; Harvey, J. N.; Huwe, M.; Cartes, M. Á.; Mansell, S. M.; Mendoza, C.;

- Murphy, D. M.; Neeve, E. C.; Nunn, J. *J. Am. Chem. Soc.* **2012**, *134*, 10333–10336.
- (47) Kharasch, M. S.; Fields, E. K. *J. Am. Chem. Soc.* **1941**, *63*, 2316–2320.
- (48) Amatore, M.; Gosmini, C.; Périchon, J. *Eur. J. Org. Chem.* **2005**, *2005*, 989–992.
- (49) Branchaud, B. P.; Detlefsen, W. D. *Tetrahedron Lett.* **1991**, *32*, 6273–6276.
- (50) Ikeda, Y.; Nakamura, T.; Yorimitsu, H.; Oshima, K. *J. Am. Chem. Soc.* **2002**, *124*, 6514–6515.
- (51) Cahiez, G.; Moyeux, A. *Chem. Rev.* **2010**, *110*, 1435–1462.
- (52) Pucheault, M.; Darses, S.; Genêt, J.-P. *J. Am. Chem. Soc.* **2004**, *126*, 15356–15357.
- (53) Kita, Y.; Tobisu, M.; Chatani, N. *Org. Lett.* **2010**, *12*, 1864–1867.
- (54) Amatore, C.; Jutand, A.; Meyer, G.; Atmani, H.; Khalil, F.; Chahdi, F. O. *Organometallics* **1998**, *17*, 2958–2964.
- (55) Amatore, C.; Jutand, A.; Khalil, F.; M'Barki, M. A.; Mottier, L. *Organometallics* **1993**, *12*, 3168–3178.
- (56) Zaleskiy, S. S.; Ananikov, V. P. *Organometallics* **2012**, *31*, 2302–2309.
- (57) Dewar, M. J. S. *Bull. Chim. Soc. Fr.* **1951**, C79.
- (58) Chatt, J.; Duncanson, L. A.; Venanzi, L. M. *J. Chem. Soc.* **1955**, 4456.
- (59) Chatt, J.; Duncanson, L. A. *J. Chem. Soc.* **1953**, 2939–2947.
- (60) Tolman, C. A. *Chem. Rev.* **1977**, *77*, 313–348.
- (61) Henderson, W. A., Jr; Streuli, C. A. *J. Am. Chem. Soc.* **1960**, *82*, 5794–5800.
- (62) Amatore, C.; Jutand, A.; M'Barki, M. A. *Organometallics* **1992**, *11*, 3009–3013.
- (63) Li, H.; Johansson Seechurn, C. C. C.; Colacot, T. J. *ACS Catal.* **2012**, *2*, 1147–1164.
- (64) Old, D. W.; Wolfe, J. P.; Buchwald, S. L. *J. Am. Chem. Soc.* **1998**, *120*, 9722–9723.
- (65) Christmann, U.; Vilar, R. N. *Angew. Chem. Int. Ed.* **2005**, *44*, 366–374.
- (66) Surry, D. S.; Buchwald, S. L. *Angew. Chem. Int. Ed.* **2008**, *47*, 6338–6361.
- (67) Martin, R.; Buchwald, S. L. *Acc. Chem. Res.* **2008**, *41*, 1461–1473.
- (68) Kaye, S.; Fox, J. M.; Hicks, F. A.; Buchwald, S. L. *Adv. Synth. Catal.* **2001**, *343*, 789–794.
- (69) Gudmundsson, K. S.; Johns, B. A. *Org. Lett.* **2003**, *5*, 1369–1372.

- (70) Mauger, C. C.; Mignani, G. A. *Org. Process Res. Dev.* **2004**, *8*, 1065–1071.
- (71) Zhou, Q.-L. **2011**.
- (72) Kozlowski, M. C.; Walsh, P. J. *Fundamentals of Asymmetric Catalysis*; University Science Books, 2009.
- (73) Miyashita, A.; Yasuda, A.; Takaya, H.; Toriumi, K.; Ito, T.; Souchi, T.; Noyori, R. *J. Am. Chem. Soc.* **1980**, *102*, 7932–7934.
- (74) Noyori, R.; Takaya, H. *Acc. Chem. Res.* **1990**, *23*, 345–350.
- (75) Noyori, R.; Ohta, M.; Hsiao, Y.; Kitamura, M.; Ohta, T.; Takaya, H. *J. Am. Chem. Soc.* **1986**, *108*, 7117–7119.
- (76) Ohta, T.; Takaya, H.; Kitamura, M.; Nagai, K.; Noyori, R. *J. Org. Chem.* **1987**, *52*, 3174–3176.
- (77) Kitamura, M.; Tokunaga, M.; Ohkuma, T.; Noyori, R. *Tetrahedron Lett.* **1991**, *32*, 4163–4166.
- (78) McCarthy, M.; Guiry, P. J. *Tetrahedron* **2001**, *57*, 3809–3844.
- (79) Shimizu, H.; Nagasaki, I.; Matsumura, K.; Sayo, N.; Saito, T. *Acc. Chem. Res.* **2007**, *40*, 1385–1393.
- (80) Otsuka, S.; Tani, K. *Synthesis* **1991**, *1991*, 665–680.
- (81) Takaya, H.; Mashima, K.; Koyano, K.; Yagi, M.; Kumobayashi, H.; Taketomi, T.; Akutagawa, S.; Noyori, R. *J. Org. Chem.* **1986**, *51*, 629–635.
- (82) Cai, D.; Payack, J. F.; Bender, D. R.; Hughes, D. L.; Verhoeven, T. R.; Reider, P. J. *J. Org. Chem.* **1994**, *59*, 7180–7181.
- (83) Ager, D. J.; Laneman, S. A. *Chem. Comm.* **1997**, 2359–2360.
- (84) Enev, V. S.; Felzmann, W.; Gromov, A.; Marchart, S.; Mulzer, J. *Chem. Eur. J.* **2012**, *18*, 9651–9668.
- (85) Fürstner, A.; Dierkes, T.; Thiel, O. R.; Blanda, G. *Chem. Eur. J.* **2001**, *7*, 5286–5298.
- (86) Dounay, A. B.; Overman, L. E. *Chem. Rev.* **2003**, *103*, 2945–2964.
- (87) Ohshima, T.; Kagechika, K.; Adachi, M.; Sodeoka, M.; Shibasaki, M. *J. Am. Chem. Soc.* **1996**, *118*, 7108–7116.
- (88) Maddaford, S. P.; Andersen, N. G.; Cristofoli, W. A.; Keay, B. A. *J. Am. Chem. Soc.* **1996**, *118*, 10766–10773.
- (89) Enders, D.; Niemeier, O.; Henseler, A. *Chem. Rev.* **2007**, *107*, 5606–5655.
- (90) Marion, N.; Nolan, S. P. *Acc. Chem. Res.* **2008**, *41*, 1440–1449.
- (91) Valente, C.; Calimsiz, S.; Hoi, K. H.; Mallik, D.; Sayah, M.; Organ, M. G.

- Angew. Chem. Int. Ed.* **2012**, *51*, 3314–3332.
- (92) Fortman, G. C.; Nolan, S. P. *Chem. Soc. Rev.* **2011**, *40*, 5151.
- (93) Díez-González, S.; Marion, N.; Nolan, S. P. *Chem. Rev.* **2009**, *109*, 3612–3676.
- (94) Hopkinson, M. N.; Richter, C.; Schedler, M.; Glorius, F. *Nature* **2014**, *510*, 485–496.
- (95) Wanzlick, H. W. *Angew. Chem. Int. Ed.* **1962**, *1*, 75–80.
- (96) Cardin, D. J.; Cetinkaya, B.; Lappert, M. F. *Chem. Rev.* **1972**, *72*, 545–574.
- (97) Hitchcock, P. B.; Lappert, M. F.; Pye, P. L. *J Chem Soc Dalton* **1977**, 2160–2172.
- (98) Arduengo, A. J.; Harlow, R. L.; Kline, M. J. *Am. Chem. Soc.* **1991**, *113*, 361–363.
- (99) Arduengo, A. J.; Dias, H. V. R.; Harlow, R. L.; Kline, M. J. *Am. Chem. Soc.* **1992**, *114*, 5530–5534.
- (100) Bourissou, D.; Guerret, O.; Gabbai, F. P.; Bertrand, G. *Chem. Rev.* **2000**, *100*, 39–92.
- (101) Herrmann, W. A.; Köcher, C. *Angew. Chem. Int. Ed.* **1997**, *36*, 2162–2187.
- (102) Arduengo, A. J.; Goerlich, J. R.; Marshall, W. J. *J. Am. Chem. Soc.* **1995**, *117*, 11027–11028.
- (103) Díez-González, S.; Nolan, S. P. *Coord. Chem. Rev.* **2007**, *251*, 874–883.
- (104) Dorta, R.; Stevens, E. D.; Hoff, C. D.; Nolan, S. P. *J. Am. Chem. Soc.* **2003**, *125*, 10490–10491.
- (105) Dorta, R.; Stevens, E. D.; Scott, N. M.; Costabile, C.; Cavallo, L.; Hoff, C. D.; Nolan, S. P. *J. Am. Chem. Soc.* **2005**, *127*, 2485–2495.
- (106) Nelson, D. J.; Nolan, S. P. *Chem. Soc. Rev.* **2013**, *42*, 6723–6753.
- (107) Jacobsen, H.; Correa, A.; Poater, A.; Costabile, C.; Cavallo, L. *Coord. Chem. Rev.* **2009**, *253*, 687–703.
- (108) Hillier, A. C.; Sommer, W. J.; Yong, B. S.; Petersen, J. L.; Cavallo, L.; Nolan, S. P. *Organometallics* **2003**, *22*, 4322–4326.
- (109) Clavier, H.; Nolan, S. P. *Chem. Commun.* **2010**, *46*, 841–861.
- (110) Benhamou, L.; Chardon, E.; Lavigne, G.; Bellemin-Laponnaz, S.; César, V. *Chem. Rev.* **2011**, *111*, 2705–2733.
- (111) Fürstner, A.; Alcarazo, M.; Cesar, V.; Lehmann, C. W. *Chem. Commun.* **2006**, 2176–2178.



- (112) Bon, R. S.; de Kanter, F. J. J.; Lutz, M.; Spek, A. L.; Jahnke, M. C.; Hahn, F. E.; Groen, M. B.; Orru, R. V. A. *Organometallics* **2007**, *26*, 3639–3650.
- (113) Herrmann, W. A.; Elison, M.; Fischer, J.; Koecher, C.; Artus, G. R. *Angew. Chem. Int. Ed.* **1995**, *34*, 2371–2374.
- (114) Altenhoff, G.; Goddard, R.; Lehmann, C. W.; Glorius, F. *Angew. Chem. Int. Ed.* **2003**, *42*, 3690–3693.
- (115) Würtz, S.; Glorius, F. *Acc. Chem. Res.* **2008**, *41*, 1523–1533.
- (116) Organ, M. G.; Calimsiz, S.; Sayah, M.; Hoi, K. H.; Lough, A. J. *Angew. Chem. Int. Ed.* **2009**, *48*, 2383–2387.
- (117) Collado, A.; Balogh, J.; Meiries, S.; Slawin, A. M. Z.; Falivene, L.; Cavallo, L.; Nolan, S. P. *Organometallics* **2013**, *32*, 3249–3252.
- (118) Berthon-Gelloz, G.; Siegler, M. A.; Spek, A. L.; Tinant, B.; Reek, J. N. H.; Markó, I. E. *Dalton Trans.* **2010**, *39*, 1444–1446.
- (119) Chartoire, A.; Lesieur, M.; Falivene, L.; Slawin, A. M. Z.; Cavallo, L.; Cazin, C. S. J.; Nolan, S. P. *Chem. Eur. J.* **2012**, *18*, 4517–4521.
- (120) Titcomb, L. R.; Caddick, S.; Cloke, F. G. N.; Wilson, D. J.; McKerrecher, D. *Chem. Comm.* **2001**, 1388–1389.
- (121) Selvakumar, K.; Zapf, A.; Beller, M. *Org. Lett.* **2002**, *4*, 3031–3033.
- (122) Navarro, O.; Marion, N.; Scott, N. M.; González, J.; Amoroso, D.; Bell, A.; Nolan, S. P. *Tetrahedron* **2005**, *61*, 9716–9722.
- (123) Viciu, M. S.; Navarro, O.; Germaneau, R. F.; Kelly, R. A.; Sommer, W.; Marion, N.; Stevens, E. D.; Cavallo, L.; Nolan, S. P. *Organometallics* **2004**, *23*, 1629–1635.
- (124) Tessin, U. I.; Bantreil, X.; Songis, O.; Cazin, C. S. J. *Eur. J. Inorg. Chem.* **2013**, *2013*, 2007–2010.
- (125) Organ, M. G.; Avola, S.; Dubovyk, I.; Hadei, N.; Kantchev, E. A. B.; O'Brien, C. J.; Valente, C. *Chem. Eur. J.* **2006**, *12*, 4749–4755.
- (126) Cope, A. C.; Siekman, R. W. *J. Am. Chem. Soc.* **1965**, *87*, 3272–3273.
- (127) Selander, N.; J Szabó, K. *Chem. Rev.* **2011**, *111*, 2048–2076.
- (128) Dupont, J.; Consorti, C. S.; Spencer, J. *Chem. Rev.* **2005**, *105*, 2527–2572.
- (129) Beller, M.; Fischer, H.; Herrmann, W. A.; Öfele, K.; Brossmer, C. *Angew. Chem. Int. Ed.* **1995**, *34*, 1848–1849.
- (130) Bedford, R. B.; Hazelwood, S. L.; Limmert, M. E. *Chem. Commun.* **2002**, 2610.

- (131) Bedford, R. B.; Cazin, C. S. J.; Coles, S. J.; Gelbrich, T.; Horton, P. N.; Hursthouse, M. B.; Light, M. E. *Organometallics* **2003**, 22, 987–999.
- (132) Navarro, O.; Kelly, R. A.; Nolan, S. P. *J. Am. Chem. Soc.* **2003**, 125, 16194–16195.
- (133) Beletskaya, I. P.; Cheprakov, A. V. *J. Organomet. Chem.* **2004**, 689, 4055–4082.
- (134) Balanta, A.; Godard, C.; Claver, C. *Chem. Soc. Rev.* **2011**, 40, 4973–4985.
- (135) de Vries, J. G. *Dalton Trans.* **2006**, 421–429.
- (136) Reetz, M. T.; Westermann, E. *Angew. Chem. Int. Ed.* **2000**, 39, 165–168.
- (137) Yanase, T.; Monguchi, Y.; Sajiki, H. *RSC Adv.* **2011**, 2, 590–594.
- (138) Laska, U.; Frost, C. G.; Price, G. J.; Plucinski, P. K. *Journal of Catalysis* **2009**, 268, 318–328.
- (139) Deraedt, C.; Astruc, D. *Acc. Chem. Res.* **2014**, 47, 494–503.

## CHAPTER 2

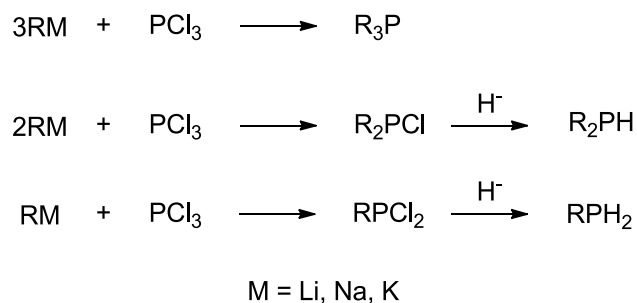
## 2. Investigation into the Reductive Cleavage of BINAP

### 2.1 Background

This chapter provides a background on the reductive lithiation of phosphines, followed by an account of our investigation into the reductive cleavage of BINAP.<sup>1</sup>

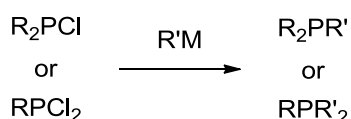
#### 2.1.1 Synthesis of Phosphines

There are numerous approaches to the synthesis of phosphines, where for the purpose of this introduction a phosphine is defined as a phosphorus atom with at least one carbon group bonded to it (examples of P-O and P-N functionalisation are also possible). Conceptually, there are two methods that can be used: one where the organic group is the nucleophile and the phosphorus reagent is an electrophile; or conversely where the phosphorus reagent is nucleophilic and the organic group is the electrophile. The first scenario (Scheme 2.1) represents the synthesis that is used on an industrial scale to produce  $\text{PPh}_3$ , where three equivalents of phenylmagnesium bromide are reacted with trichlorophosphine.<sup>2</sup> If fewer equivalents of Grignard reagent are used, there is the possibility of isolating  $\text{R}_2\text{PCl}$  and  $\text{RPCl}_2$ , however careful addition of the Grignard reagent would be necessary to obtain these halophosphines.



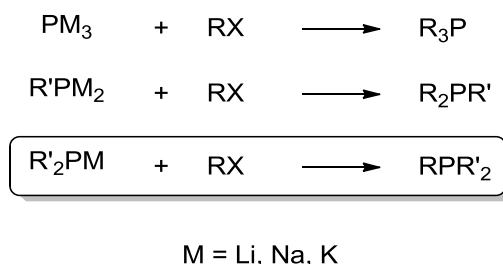
**Scheme 2.1** Phosphine synthesis where the phosphorus reagent is the electrophile.

Halophosphines are an important class of phosphorus compounds and serve as access to other important types of phosphines such as primary and secondary phosphines by reduction with a hydride source (Scheme 2.1), or to phosphines with mixed functionality by reaction with a different organometallic reagent (Scheme 2.2).



**Scheme 2.2** Reaction of halophosphines to give mixed phosphines.

The second scenario represents the use of a phosphide species, such as lithium or sodium phosphide as the nucleophile and an organic (*pseudo*)halide as a electrophile (Scheme 2.3). This method of synthesis tends to be used more commonly when only one group is to be substituted, rather than three or two.



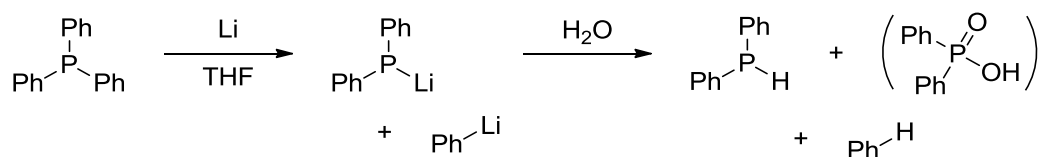
**Scheme 2.3** Phosphine synthesis where the phosphorus reagent is the nucleophile.

The phosphide species can be formed in a number of ways, by deprotonation of the secondary phosphine, or metal-halogen exchange from the appropriate chlorophosphine.

The other convenient method of forming phosphides is by reductive cleavage by an alkali metal.

#### 2.1.1.1 Reductive Cleavage of Phosphines

In 1958, Gilman and Wittenberg were the first to report that treatment of  $\text{PPh}_3$  with lithium metal lead to the reductive cleavage of one of the phenyl groups (Scheme 2.4) resulting in the diphenylphosphide and phenyllithium.<sup>3</sup> The reactions had to be carried out in dry THF under an atmosphere of dry nitrogen, and the authors also reported that the lithiation reactions had a characteristic deep red/brown colour. When the lithiated reaction mixture was quenched with water the secondary phosphine, diphenylphosphine, was obtained along with a small amount of the oxidised diphenylphosphinic acid and benzene.



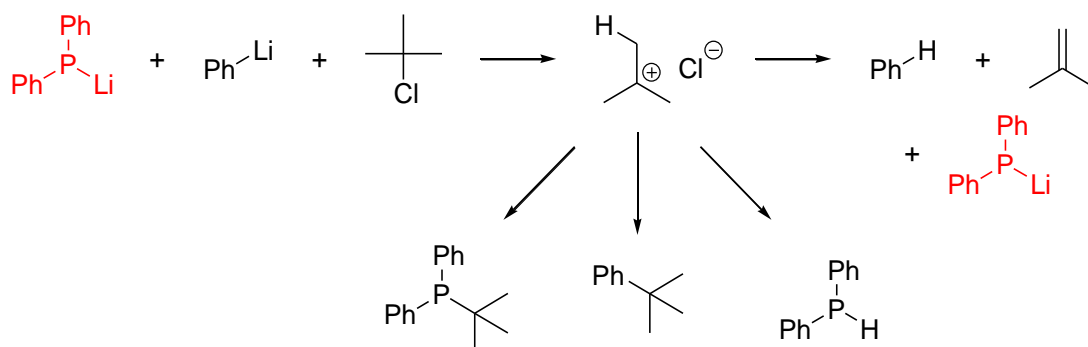
**Scheme 2.4** Reductive lithiation of  $\text{PPh}_3$ .

The alternative preparations of  $\text{LiPPh}_2$ , as previously noted, are to treat chlorodiphenylphosphine ( $\text{ClPPh}_2$ ) or diphenylphosphine ( $\text{HPPh}_2$ ) with *n*-butyl lithium. Chlorophosphines are corrosive, harmful liquids and require special handling;  $\text{HPPh}_2$  is a volatile liquid with a pungent odour that is highly flammable and considered pyrophoric. In comparison,  $\text{PPh}_3$  is much easier to handle due to its stability and solid form.

The mechanism of the Ar-P bond cleavage is considered to be the donation of an electron to the  $\pi^*$  molecular orbital of the aromatic system, given that trialkyl phosphines are not reduced, by the alkali metal.<sup>4</sup> This electron can be transferred to the  $\sigma^*$  orbital of the C-P bond and consequently the bond can cleave. There are two ways in which this bond can break, either to form a carbon based radical and phosphorus based anion or *vice versa*. Regardless of which way this occurs, treatment with another

equivalent of alkali metal yields two anions. Another study of the lithiation of  $\text{PPh}_3$  in THF has revealed that there is a second reduction process that is possible.<sup>5</sup> First the reductive cleavage of the C-P bond by lithium to yield diphenylphospholide occurred and was visible as a yellow-green solution. This was then followed by the reduction of the  $\text{LiPPh}_2$  anion by further lithium metal to give the corresponding radical anion, whose presence was confirmed by ESR spectroscopy. This radical anion formed an orange-red coloured solution in THF. Lithium and sodium were shown to form comparatively less stable radical anions than the potassium analogue in this reaction. Although they note the presence of these radical anions is possible, in their hands, the cleavage reaction still gave the expected products when treated with aqueous acid.

Aguiar and co-workers extended this work,<sup>6</sup> and made progress towards a more synthetically useful reductive lithiation protocol. They first observed that treating the lithiated reaction mixture with benzyl chloride followed by addition of  $\text{H}_2\text{O}_2$  gave the expected benzyldiphenylphosphine oxide in good yield. However as phenyllithium is released during the reductive cleavage, diphenylmethane is also obtained as a side product. In order to make this protocol more practical, the group set out to find a way of selectively quenching the phenyllithium; *t*-BuCl, a hindered alkyl chloride, was found to be able to achieve this, where it can readily lose a chloride ion to form a tertiary carbocation, which is too bulky to undergo addition with either diphenylphosphide or phenyllithium. Phenyllithium is more basic than diphenylphosphide and can remove a proton from the resultant carbocation, releasing isobutene as a gas (Scheme 2.5), hence it can be selectively quenched providing the right number of equivalents are added. Only the diphenylphosphide remains as a reactive species in solution after this quench, so addition of one equivalent of alkyl halide reacts solely with the phosphide anion.



**Scheme 2.5** Selective quench of phenyl lithium using *t*-BuCl.

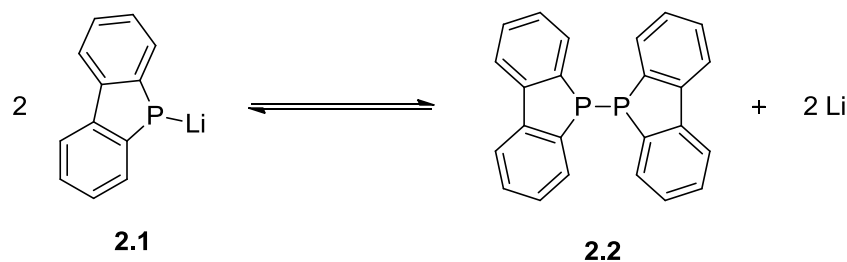
After these studies, the treatment of other phosphines with alkali metals began to be explored. Phenylbiphenylenephosphine (PBP), a phosphine closely related to  $\text{PPh}_3$ , was treated with lithium by Kaiser and Britt.<sup>7</sup> PBP is different to  $\text{PPh}_3$  in that there are two different P-C bonds that can be reductively cleaved: either the P-phenyl bond or the P-biphenylene bond. It was demonstrated that the P-phenyl bond is the one that is selectively cleaved. The reason for this selectivity can be explained using the equilibria detailed in Scheme 2.6. The addition of one electron from lithium yields the radical anion. If one of the P-biphenylene bonds is broken the resulting anion and radical are held close to each other, where they can recombine to reform the original radical anion. This intramolecular recombination is kinetically favoured over the intermolecular heterogeneous reduction by further lithium; hence this cleavage product is not observed.

If the P-phenyl bond is broken, a discrete anion and radical are formed, where they can be removed from close proximity with one another by dilution in the solvent.

This means that recombination is an intermolecular process, which is less dominant over the irreversible reduction of the remaining radical to form the phospholide anion. This reduction shifts the equilibrium along the observed cleavage pathway and hence it is favoured. Similar equilibrium processes have been used to explain the product distribution in the reductive lithiation of dppe.<sup>8</sup>

The resultant phosphide of PBP (**2.1**) was also observed to be able to undergo a dimerisation process to yield **2.2** (Scheme 2.7), this equilibrium is reported to be more favoured towards the dimer as the metal is changed from  $\text{Li} < \text{Na} < \text{K} < \text{Cs}$ .<sup>7</sup> Again, ESR was used to determine the presence of a radical anion which results from the reduction of **2.1** with further metal.





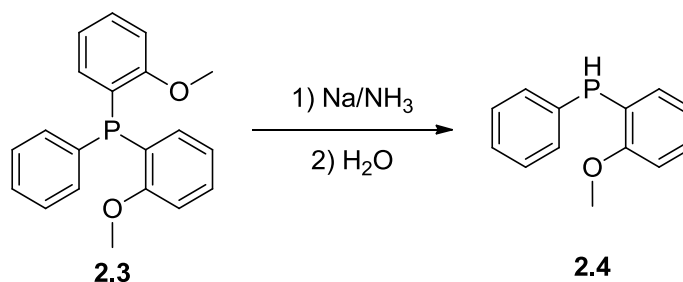
**Scheme 2.7** Equilibrium between free phosphide and dimer.

Van Door and co-workers have published a series of papers that document the effect that various functionalities of triarylphosphines, including those with mixed functionalities, have on the selectivity of the cleavage with either a Na/NH<sub>3</sub> system or a Li/THF system.<sup>4,9,10</sup> This was achieved by performing the reductions, quenching with water or NH<sub>4</sub>Cl and analysing which secondary (or primary) phosphines were present in the resultant reaction mixture by NMR.

Firstly, the group examined triarylphosphines (Ar<sub>3</sub>P) where all of the aryl groups were the same.<sup>4</sup> In general, aryl groups that contained any halogen atoms did not give the expected secondary phosphine Ar<sub>2</sub>PH. Instead the halides were removed from the aryl groups through metal halogen exchange. In the case of reduction by Na/NH<sub>3</sub>, NH<sub>3</sub> can act as a proton source, and in the case of some phosphines, the Birch-reduced product was the major one. Birch reduction was not observed under the Li/THF aprotic system. For example, when the authors treated tri(*o*-tolyl)phosphine with Na/NH<sub>3</sub>, approximately 60% of the expected (*o*-tolyl)<sub>2</sub>PH is obtained along with 40% of the Birch-reduced product. Switching to Li/THF, the desired product (*o*-tolyl)<sub>2</sub>PH could be obtained in a 93% yield. This was not the only difference that the two different alkali metal systems showed; when (*o*-Me<sub>2</sub>N-C<sub>6</sub>H<sub>4</sub>)<sub>3</sub>P was treated under Na/NH<sub>3</sub> conditions, the primary phosphine ArPH<sub>2</sub> is the predominant product, whereas when Li/THF was used the secondary phosphine could be obtained almost quantitatively. A similar situation was found for the *meta*-isomer of this phosphine however, the *para*-isomer gave a mixture of products when reacted with either metal. Alkoxy groups were tolerated well with *ortho*- and *meta*-isomers of (RO-C<sub>6</sub>H<sub>4</sub>)<sub>3</sub>P giving good yields of the

corresponding secondary phosphines, however, as with the dimethylamine analogues, the *para* isomer only provided poor yields.

The group also reported a similar investigation, except the cleavage of mixed triaryl phosphines of the type  $\text{Ph}_2\text{ArP}$  and  $\text{PhAr}_2\text{P}$  were examined.<sup>9</sup> The most significant finding of this study was that if the aryl group contained an *ortho*-substituent that was electron donating (Me,  $\text{NMe}_2$ , or  $\text{OMe}$ ) then this was the aryl group that was cleaved from the phosphine. This gave good access to mixed secondary phosphines, which after oxidation can be elaborated to *P*-chiral phosphines.<sup>11</sup> For example treatment of  $(o\text{-MeO-C}_6\text{H}_4)_2\text{PPh}$  led to the mixed secondary phosphine **2.4** in high yield and selectivity (Scheme 2.8).

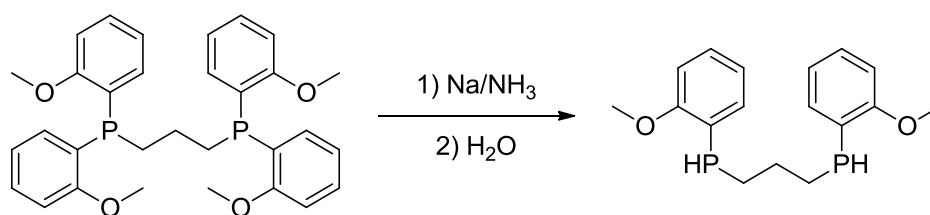


**Scheme 2.8** Synthesis of a mixed secondary phosphine.

This selectivity could be reversed if free  $\text{-OH}$  groups were present on the aryl groups, which under the reaction conditions are deprotonated to form phenoxide anions. In this case the unsubstituted phenyl group is selectively cleaved. Birch reduction by-products were noted to be a problem only when the reductive cleavage reaction was comparatively slow. Regardless of the electronic nature of the functionality, *para*-substituted phosphines proved problematic and gave a mixture of products.

In their third and final paper the group investigated the cleavage of mixed aryl-alkyl phosphines  $\text{R}_2\text{PPh}$  and  $\text{Ph}_2\text{PR}$ .<sup>10</sup> When the alkyl group used was an *n*-butyl or *i*-propyl group, no selectivity in the cleavage was observed for either type of mixed phosphine (dialkyl or diaryl). The cleavage of  $\text{Ph}_2\text{P}t\text{-Bu}$  was shown to provide a high yield of the diphenylphosphine, where the *t*-butyl group had been cleaved. Benzyl and

allyl groups showed a similar trend, although a simpler route to the products of all these reactions is the straightforward cleavage of  $\text{PPh}_3$ . In keeping with their previous report, the group found that *o*-methoxyphenyl groups could be selectively cleaved from  $\text{ArPhPR}$  or  $\text{Ar}_2\text{PR}$  to give the mixed secondary phosphines  $\text{PhP(H)R}$  and  $\text{ArP(H)R}$ . The group also reported the reductive cleavage of bisphosphine ligands similar to  $\text{dppp}$ , where the phenyl groups have an *o*-substituent. In this case the bisphosphine can be symmetrically cleaved to remove two aryl groups, one from either end, resulting in the symmetrical secondary diphosphine (Scheme 2.9).

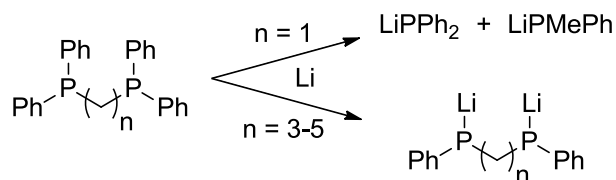


**Scheme 2.9** Selective symmetrical cleavage of diphosphine by  $\text{Na/NH}_3$ .

This series of papers demonstrated that the reductive cleavage of various types of phosphine can provide a valuable synthetic route to important classes of secondary phosphine, particularly those with two differently functionalised aryl groups. It also shows, however, that whilst there is some amount of predictability of these reactions more often than not trial and error followed by optimisation is needed in the case of more highly functionalised phosphines. The merits of the  $\text{Li/THF}$  system have been highlighted, in that Birch-reduced products cannot be obtained under these conditions, although the authors showcase the majority of examples using the  $\text{Na/NH}_3$  protocol. For example, the reductive cleavage of diphosphines using a  $\text{Li/THF}$  reductive system was not examined.

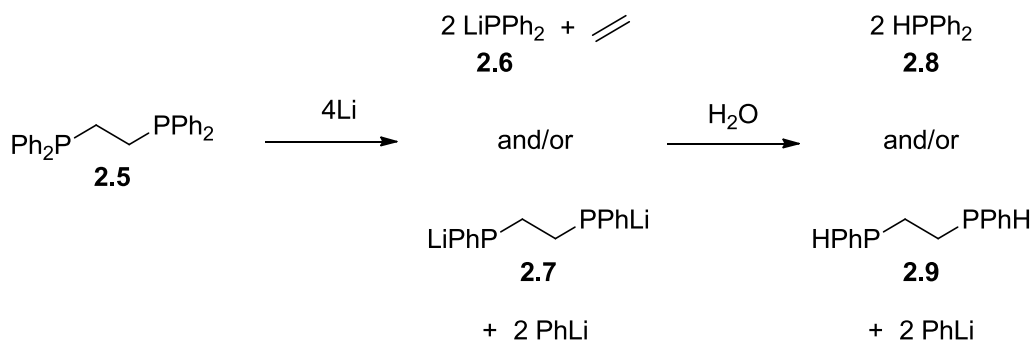
The reductive cleavage of  $\text{dppe}$  has been previously reported with lithium metal,<sup>12</sup> however these reports do not include detailed mechanistic insights. More often than not these syntheses show that low temperatures and long reactions times (7 days) are necessary to obtain the desired secondary diphosphines. Furthermore, in order to get

clean conversion to the secondary diphosphine it is usually necessary to crystallise the lithium diphosphide THF adduct before quenching.<sup>13,14</sup> A more recent report by Swiegers and co-workers has detailed the reductive lithiation of various bisphosphine ligands, where the size of the alkyl linker was varied (Scheme 2.10).<sup>8</sup>



**Scheme 2.10** Dependence of cleavage pattern on the alkyl linker size in diphosphines.

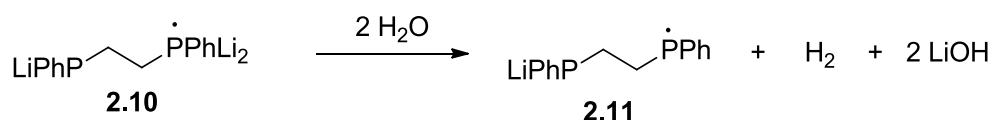
When the alkyl linker was a single CH<sub>2</sub> moiety, the reductive cleavage was selective and LiPPh<sub>2</sub> and LiPMePh were released as the products. Similarly, selective cleavage was observed when the carbon linker was between 3 and 5 CH<sub>2</sub> units in length, with the loss of two phenyl groups, one from both ends of the diphosphine resulting in the symmetrical lithiation product. A carbon linker of two CH<sub>2</sub> units resulted in a mixture of products resulting from the two cleavage pathways (Scheme 2.11), which prompted the group to carry out a detailed investigation into the mechanism of this reaction. One pathway involves the breaking of a P-phenyl bond and the other the breaking of a P-alkyl bond.



**Scheme 2.11** Cleavage pathways observed for dppe, when the linker contains two CH<sub>2</sub> units.

The authors found that the lithiation reaction was temperature dependent. At room temperature after 3 days of reaction, various mixtures of **2.6** and **2.7** were obtained, with

no consistent ratios being observed upon repetition. Performing the reaction at 40 °C lead to a slightly increased amount of **2.6**. The slow addition of a solution of **2.5** to a stirred suspension of Li in THF at 0 °C, followed by heating to 40 °C allowed for the selective formation of **2.7**. Despite obtaining a solution of which **2.7** was the only phosphorus containing species, the hydrolysis of such a solution did not lead to smooth conversion with **2.9** as the exclusive product. Remarkably, dropwise addition of water to a solution of **2.7** at room temperature gave various ratios of the hydrolysis products **2.8** and **2.9**. This observation prompted the authors to find an explanation for the redistribution of products upon hydrolysis. Using ESR and UV/Vis spectroscopy, the radical trianion **2.10** Scheme 2.12 was confirmed to be present in the reaction mixture, which is the product of the reaction of **2.7** with further lithium. When the hydrolysis of a solution of **2.7**, which had been purified by recrystallisation, was carried out in the absence of radical anion **2.10**, only **2.9** was obtained regardless of the temperature. However, carrying out the hydrolysis in the presence of the radical anion **2.10**, the amount of **2.8** is increased at 40 °C, whereas at 0 °C, **2.9** is the sole product. This temperature dependence mirrors the distributions observed in the original lithiation reactions. Hence the authors concluded that when the lithiation reaction occurs, it does so through a set of equilibria whose positions are determined by the temperature of the reaction. When the hydrolysis is attempted in the presence of radical anion **2.10**, it can react with water to yield the radical **2.11**, hydrogen gas and lithium hydroxide (Scheme 2.12).



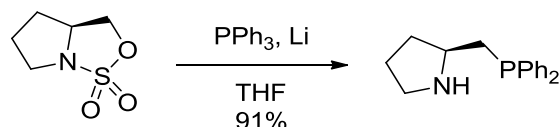
**Scheme 2.12** Quenching of radical anion **2.9** with H<sub>2</sub>O.

The radical **2.11** is postulated to be present in the initial lithiation equilibria, thus it is able to reestablish the distribution of **2.6** and **2.7**. Therefore the position of the cleavage

equilibria is rapidly changed according to the temperature at which the quench is performed. The reaction with further water afterwards gives the hydrolysed products in a distribution dictated by the above process. This investigation highlights that the mechanism of these reductive cleavage reactions is not always straightforward. In order to make the reductive lithiation a viable route for ligand synthesis, the mechanism must be investigated for individual phosphine.

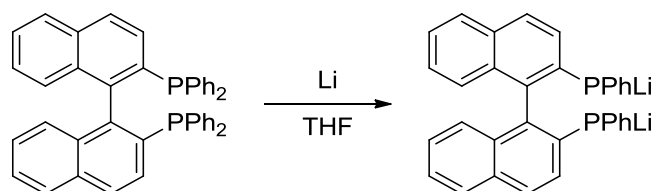
### 2.1.2 Investigation Aim and Initial Studies

The use of lithium phosphides is a valuable strategy for the installation of phosphine functionality on a ligand. Such a strategy was used by the Viseux group, for the synthesis of amino acid based ligands and their corresponding complexes with gold(I) (Scheme 2.13).<sup>15</sup>



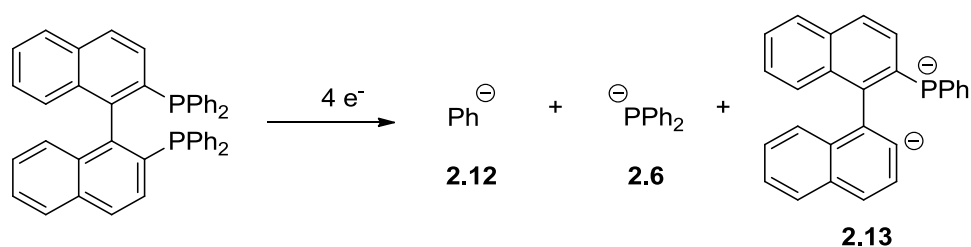
**Scheme 2.13** Bobin's use of reductive lithiation for the installation of a diphenylphosphine moiety.

During this investigation a similar reductive cleavage and displacement sequence was envisaged by Bobin, using BINAP instead of PPh<sub>3</sub> (Scheme 2.14). This however, was found to be unsuccessful. When BINAP was treated with lithium and the reaction mixture analysed by <sup>31</sup>P{<sup>1</sup>H} NMR spectroscopy, two new phosphorus signals were observed, signifying that the cleavage could not have occurred symmetrically as shown in Scheme 2.14. The cleavage product(s) of BINAP appeared to be more air sensitive than that of PPh<sub>3</sub>, so a simple workup and isolation was unable to determine the nature of the cleavage.



**Scheme 2.14** Bobin's predicted fragmentation of BINAP upon reductive elimination.

Preliminary DFT calculations, performed by Viseux (unpublished), predicted that upon addition of four electrons to the BINAP framework the fragmentation would occur as shown in Scheme 2.15.



**Scheme 2.15** Predicted fragmentation of BINAP upon addition of four electrons. Calculation performed by E.M.E. Viseux, singlet state, (HF/6-31G/Opt+Freq).

Despite that some commonly used bidentate phosphine ligands (dppe for example) having been investigated for their participation in reductive cleavage reactions by alkali metals, the bidentate phosphine BINAP has not. The aim of this investigation was to identify the phosphorus containing species formed when BINAP is reductively cleaved with lithium metal, including a consideration of the mechanistic aspects where possible. This work was carried out with the view of utilising such a reaction for ligand synthesis.

## 2.2 Results and Discussion

### 2.2.1 Lithiation

The reaction of BINAP with lithium had to be performed in a glove box as this cleavage reaction proved particularly sensitive to air and moisture, in comparison to that of PPh<sub>3</sub>. All of the reactions were monitored with the use of <sup>31</sup>P{<sup>1</sup>H} NMR

spectroscopy. A sealed capillary tube containing  $\text{OPPh}_3$  in  $\text{d}_6$ -benzene was used as an internal standard ( $\delta_{\text{P}} = 25$  ppm) which avoided the need for  $\text{d}_8$ -THF as only  $^{31}\text{P}$  NMR signals were being observed. This methodology allowed for convenient reaction monitoring by adding a small portion of the reaction mixture to a Young's NMR tube containing the standard, and also allowed for the easy removal of the internal standard without contamination of the sample. Due to the poor solubility of BINAP, solutions of BINAP in THF were prepared with a concentration of 0.01 M. The initiation times for the reaction were sometimes found to be erratic and unpredictable; a similar behaviour has been observed by Swiegers and co-workers for the lithiation of  $\text{dppe}$ .<sup>8</sup> We found that careful preparation of the surface of the lithium metal aided with achieving a more consistent initiation time. By cutting the lithium metal into pieces as small as practical and cleaning the surface of the metal with a fine sand paper the reaction would generally initiate instantly, if not within a space of one minute. Upon initial addition of the lithium metal to the reaction mixture, the solution turned from colourless to yellow. Over the course of 24 hours the reaction mixture darkened to a deep red colour. Hence, the reaction of BINAP with four equivalents of lithium metal in THF resulted in a dark red solution; and complete lithium consumption was typically observed by 48 hours. The resultant reaction mixture showed two signals in the  $^{31}\text{P}\{^1\text{H}\}$  NMR spectrum at +50 and -22 ppm (Table 2.1, entry 2). The signal at -22 ppm could be identified as  $\text{LiPPh}_2$  (**2.6**); treatment of  $\text{PPh}_3$  with lithium metal gave a deep red solution which showed a resonance at -22 ppm in the  $^{31}\text{P}\{^1\text{H}\}$  NMR spectrum (Table 2.1, entry 3), which when combined in a 1 : 1 ratio with the lithiated BINAP solution still showed only one peak in this region of the spectrum (Table 2.1, entry 4). The influence of the number of equivalents of lithium on the reaction was also investigated. A sub-stoichiometric amount (two eq.) led to the partial lithiation of BINAP, whereby there was unreacted BINAP present in the reaction mixture and the two previously observed species. An excess (six and eight equivalents) did not show any significant differences to when four equivalents of lithium were used. It should be noted that Birch-reduced



products were not observed, regardless of the amount of lithium used, as reported by Meijboom in his investigation on other triarylphosphines;<sup>4</sup> reduction with lithium in an aprotic solvent inhibits Birch reduction.

Entry	Compound	Lithium (eq.)	<sup>31</sup> P{ <sup>1</sup> H} Chemical Shifts (ppm)
1	BINAP	0	−14.89 (s)
2	BINAP	4	50.25 (s), −21.67 (s)
3	PPh <sub>3</sub>	2	−21.61 (s)
4	BINAP + PPh <sub>3</sub>	4 (BINAP), 2 (PPh <sub>3</sub> )	50.33 (s), −21.76 (s)

**Table 2.1** <sup>31</sup>P NMR data for the lithiation of triarylphosphines in THF. Multiplicities are indicated in parentheses.

The lithiated solution were found to be reasonably stable over an extended period of time (two months at room temperature under argon), with the appearance of trace signals at −15.9 ppm. The signal at −15.9 ppm was attributed to a small amount of dimerisation of **2.6** to P<sub>2</sub>Ph<sub>4</sub>.<sup>7</sup>

Although the identification of the phosphorus containing species with a <sup>31</sup>P NMR signal of −22 ppm was identified as LiPPh<sub>2</sub>, the identity of the phosphorus containing compound with a signal at 50 ppm was not immediately identifiable. Lithium phosphides are typically characterised by a negative chemical shift in their <sup>31</sup>P NMR spectra, however the signal at 50 ppm is contrary to this. In order to determine if the reactivity of the unknown species fitted that of a lithium phosphide, several quenching studies were carried out.

### 2.2.2 Protonation

Comparative experiments were carried out between the hydrolysis of reaction mixtures of lithiated BINAP and  $\text{PPh}_3$ . The quenching of lithiated BINAP solution with water resulted in the disappearance of the singlets at  $-21.6$  ppm and  $50$  ppm and the appearance of a doublet at  $-40.6$  ppm ( $J = 216.2$  Hz) in the proton-coupled  $^{31}\text{P}$  NMR spectrum (Table 2.2, entry 1). The treatment of a solution of lithiated  $\text{PPh}_3$  with water gave a doublet at  $-40.5$  ppm ( $J = 218.7$  Hz) which is known to be the secondary diphenylphosphine  $\text{HPPH}_2$  (Table 2.2, entry 2).  $^{31}\text{P}$  NMR of a combination of the two solutions revealed that  $\text{HPPH}_2$  appears to be the only hydrolysis product present (Table 2.2, entry 3). The species at  $50$  ppm was no longer present, and therefore no hydrolysis product resulting from it. As discussed above, the hydrolysis of diphosphides are often found to involve complex equilibria,<sup>8</sup> specifically that the presence of a phosphorus based radical dianion could affect the outcome of the hydrolysis by the reestablishment of the initial cleavage equilibria before subsequent hydrolysis. The deep red colour of the lithiated BINAP reaction mixture may indicate the presence of phosphorus based radical anions,<sup>5,8</sup> hence similar equilibria processes could be responsible for  $\text{HPPH}_2$  being the only apparent product of hydrolysis of the lithiated BINAP mixture with water.

Entry	Lithiated Phosphine	$^{31}\text{P}\{^1\text{H}\}$ Chemical Shift (ppm)	$^{31}\text{P}$ Chemical Shift (ppm)
1	BINAP + 4 Li	−40.59 (s), 48.76 (s, trace)	−40.60 (d, $J = 216.2$ Hz), 48.76 (s, trace)
2	$\text{PPh}_3 + 2 \text{Li}$	−40.52 (s)	−40.51 (d, $J = 218.7$ Hz)
3	{BINAP + 4 Li} + { $\text{PPh}_3 + 2 \text{Li}$ }	−40.48 (s)	−40.48 (d, $J = 217.7$ Hz)

**Table 2.2**  $^{31}\text{P}$  NMR and  $^{31}\text{P}\{^1\text{H}\}$  NMR of lithiated phosphine after hydrolysis with water.

Multiplicity and  $J$  values indicated in parentheses.

Protolysis with the weaker acid  $t\text{-BuCl}$  gave different results depending on the quantity used. Addition of two equivalents of  $t\text{-BuCl}$  to the lithiated BINAP mixture rapidly protonated the aryl lithium species; no change in the  $^{31}\text{P}$  NMR spectrum confirmed that neither phosphorus containing species had been protonated. Upon addition of another equivalent of  $t\text{-BuCl}$  the protonation of  $\text{LiPPh}_2$  was possible, but found to be much slower (typically 6 hours at room temperature); there was negligible colour change and the solution retained a deep red colour.  $^{31}\text{P}\{^1\text{H}\}$  NMR spectroscopy showed the disappearance of signal at −22 ppm and the appearance of a signal at −40.5 ppm, corresponding to  $\text{HPPh}_2$ . Interestingly after addition of another 1.5 equivalent of  $t\text{-BuCl}$ , the species at 50 ppm persisted and did not react with a small excess of  $t\text{-BuCl}$ , even when left for over 30 days at room temperature. With a large excess (12 equivalents), however, the signal at 50 ppm disappeared and again the peak for  $\text{HPPh}_2$  (−40.5 ppm) was the only hydrolysis product that was detected. It should be noted that in these studies no nucleophilic substitution was ever observed between the lithium phosphides and  $t\text{-BuCl}$  unlike previously reported by Swiegers.<sup>8</sup>

Use of a strong acid gave a very different outcome to the previous proton sources. For example when methanesulfonic acid was used in excess (5 equivalents) clean protonation of both phosphorus containing species was possible. In addition to the singlet observed in the  $^{31}\text{P}\{^1\text{H}\}$  NMR spectrum at  $-40.5$  ppm for  $\text{HPPH}_2$ , a new signal was noted. The new singlet at  $-62$  ppm was tentatively assigned as a protonated phosphine that originated from the  $50$  ppm signal found in the original lithiated reaction mixture. The proton-coupled  $^{31}\text{P}$  NMR spectrum confirmed the presence of a P-H bond as the signal at  $-62$  ppm was observed as a doublet with a coupling constant of  $198.5$  Hz, which is consistent with a  $^1J_{\text{PH}}$  coupling. Hence, at this point we could conclude that the unknown phosphorus species can be protonated, but is significantly less basic than  $\text{LiPPh}_2$ .

### 2.2.3 Silylation

Earlier attempts in the group to trap the lithiated species as boron adducts were unsuccessful. The reason for attempting this was to introduce another NMR active nucleus to the phosphorus containing species, and therefore gain an additional handle to aid in identifying the unknown species. Addition of a silicon-based group would allow analysis by  $^{29}\text{Si}$  NMR spectroscopy. Quenching of the lithiated BINAP reaction mixture was first attempted using  $\text{TMSOTf}$ , and  $\text{TMSCl}$  gave similar results. Two singlets were observed by  $^{31}\text{P}\{^1\text{H}\}$  NMR at  $-58.53$  and  $-58.69$  ppm (Table 2.3, entry 1). The  $^{31}\text{P}\{^1\text{H}\}$  NMR of  $\text{TMSPPH}_2$  was found to be  $-58.60$  ppm (Table 2.3, entry 2). Mixing of these two solutions showed that one of the two peaks can be assigned to  $\text{TMSPPH}_2$  and the other to the TMS adduct of the unknown phosphorus species. In this case the phosphorus chemical shifts are so close to one another, a difference of only  $0.2$  ppm, it was not easy to conclude which signal belongs to which species.

Entry	Lithiated Phosphine	TMSOTf (eq.)	$^{31}\text{P}\{^1\text{H}\}$ Chemical Shifts (ppm)
1	BINAP + 4 Li	4	-58.53 (s), -58.69 (s)
2	PPh <sub>3</sub> + 2 Li	2	-58.60 (s)
3	{BINAP + 4 Li} + {PPh <sub>3</sub> + 2 Li}	4 {BINAP}, 2 {PPh <sub>3</sub> }	-58.54 (s), -58.69 (s)

**Table 2.3**  $^{31}\text{P}\{^1\text{H}\}$  data for the trapping of lithiated phosphines with TMSOTf. Multiplicity indicated in parentheses.

When the lithiated reaction mixtures were derivitised with the more sterically hindered TBS group, there was a more significant difference in the chemical shifts, allowing their assignment. The lithiated BINAP reaction mixture yielded singlets at -61.9 ppm and at -57.1 ppm after treatment with TBSOTf (Table 2.4, entry 1). A small amount of the secondary phosphine HPPH<sub>2</sub> was also observed at -40.5 ppm, likely due to a trace amount of trifluoromethanesulfonic acid. The peak at -61.9 was identified as TBSPPH<sub>2</sub> (Table 2.4, entry 2). Consequently the signal at -57.1 ppm could be assigned as the TBS derivative of the unknown phosphorus species.

Entry	Compound	TBSOTf (eq.)	$^{31}\text{P}\{^1\text{H}\}$ Chemical Shifts (ppm)
1	BINAP + 4 Li	4	-40.45 (s) trace, -57.06 (s), -61.86 (s)
2	PPh <sub>3</sub> + 2 Li	2	-40.44 (s) trace, -61.87 (s)
3	{BINAP + 4 Li} + {PPh <sub>3</sub> + 2 Li}	4 {BINAP}, 2 {PPh <sub>3</sub> }	-40.53 (s) trace, -57.15 (s), -61.95 (s)

**Table 2.4**  $^{31}\text{P}\{^1\text{H}\}$  data for the trapping of lithiated phosphines with TBSOTf. Multiplicity indicated in parentheses.

The difference in reactivity between the two lithium phosphide species was explored by using the less reactive TBSCl, as the reaction with TBSOTf was found to be rapid at room temperature. The conversion of LiPPh<sub>2</sub> to TBSPPH<sub>2</sub> was observed to be completed within one hour, whereas the conversion of the unknown lithium phosphide to its TBS analogue was notably slower in comparison (typically 12 hours). Treatment of these TBS derivatives with water resulted in the hydrolysis of the P-Si bond as <sup>31</sup>P{<sup>1</sup>H} NMR of the resultant reaction mixture showed two signals at -40.5 ppm (HPPh<sub>2</sub>) and -62 ppm.

Three signals were observed in a <sup>1</sup>H/<sup>29</sup>Si HMBC NMR experiment of the silylated BINAP reaction mixture, signifying three different silicon environments, which does not support the predicted fragmentation shown in Scheme 2.15. Whilst we had established that the unknown phosphorus species has reactivity that is indicative of a lithium phosphide, we were still unsure of the structural details which were still to be confirmed.

#### 2.2.4 <sup>31</sup>P NMR Calculations

As the <sup>31</sup>P NMR signal for the unknown species is significantly downfield (50 ppm) of where a phosphide is expected to appear, it was reasoned that using DFT calculations to predict the <sup>31</sup>P NMR chemical shift of plausible structures for the unknown species would be a suitable approach to aid in its identification.

The computational approach was based upon the report of Zipse and Maryasin,<sup>16</sup> in which the authors examined various basis sets and solvation models to predict the <sup>31</sup>P NMR chemical shifts of various phosphines in solution. Hence for the GIAO NMR calculations 6-311++G(2d, 2p) was chosen as the basis set, in combination with MPW1K functional which had given satisfactory results for Zipse. The direct result of GIAO NMR calculations are values for the isotropic shielding tensors ( $\sigma$ ) of the atom in question, where these values on their own are non relatable to the chemical shift. They can be converted to chemical shift values ( $\delta$ ) using Equation 2.1, where  $\sigma_{\text{ref}}$  must be calculated also. A similar process is used in experimental NMR spectroscopy where, for

example, TMS is the reference for  $^1\text{H}$  NMR ( $\delta_{\text{H}} = 0$  ppm) and  $\text{H}_3\text{PO}_4$  is the zero point for  $^{31}\text{P}$  NMR.

$$\delta_{\text{calc}} = \sigma_{\text{ref}} - \sigma_{\text{calc}}$$

**Equation 2.1** Equation describing how isotropic shielding tensors are converted to chemical shifts.

Therefore, in principle, the simplest way to determine  $\sigma_{\text{ref}}$  would be to calculate  $\sigma$  for an appropriate reference compound; however this approach does not always give the best results. A study by Sarotti and Pellegrinet showed that for the calculation of  $^{13}\text{C}$  chemical shifts using the GIAO methodology, using multiple compounds as reference compounds (the multi-standard approach) gave superior results than that of a single standard approach.<sup>17</sup> For example, by using benzene as  $\sigma_{\text{ref}}$  for the  $\text{sp}$  and  $\text{sp}^2$  carbon atoms and methanol as  $\sigma_{\text{ref}}$  for the  $\text{sp}^3$  carbons more accurate  $\delta_{\text{C}}$  predictions could be made than when just TMS was used for  $\sigma_{\text{ref}}$ . An alternate method for calculating  $\sigma_{\text{ref}}$  is to use a linear regression approach,<sup>18</sup> where multiple compounds that are similar to those of interest can be used to minimize the error for the predicted chemical shifts. In the case outlined in this chapter, known species from the investigation were chosen, where experimentally obtained  $^{31}\text{P}$  chemical shifts were acquired for  $\text{LiPPh}_2$ ,  $\text{HPPh}_2$ ,  $\text{OPPh}_3$ ,  $\text{PPh}_3$  and BINAP. When the known  $^{31}\text{P}$  chemical shifts for these five phosphorus containing compounds were plotted against their  $\sigma_{\text{calc}}$  values in the gas phase (Figure 2.1), there was a poor correlation between the two (green,  $R^2 = 0.51$ ). This was expected as solvent effects are known to influence the chemical shifts in  $^{31}\text{P}$  NMR experiments.<sup>16</sup> In order to obtain a better correlation two implicit solvation models that were used in Zipse's study were compared, namely an integral equation formalism polarisable continuum model (IEFPCM) and conductor polarisable continuum model (CPCM). These models treat the solvent as a polarisable continuum, with a given dielectric constant, in which the molecule of interest sits within a cavity.<sup>19</sup> The use of explicit solvent molecules was discarded as computationally cheap calculations were the main aim, whilst maintaining a level of accuracy high enough for

the identification of the unknown species. Using both of these solvation models proved to give more satisfactory correlations with R-squared values of 0.94 for IEFPCM (red, Figure 2.1 and 0.98 for CPCM (blue, Figure 2.1); hence CPCM was used for the purpose of this study.

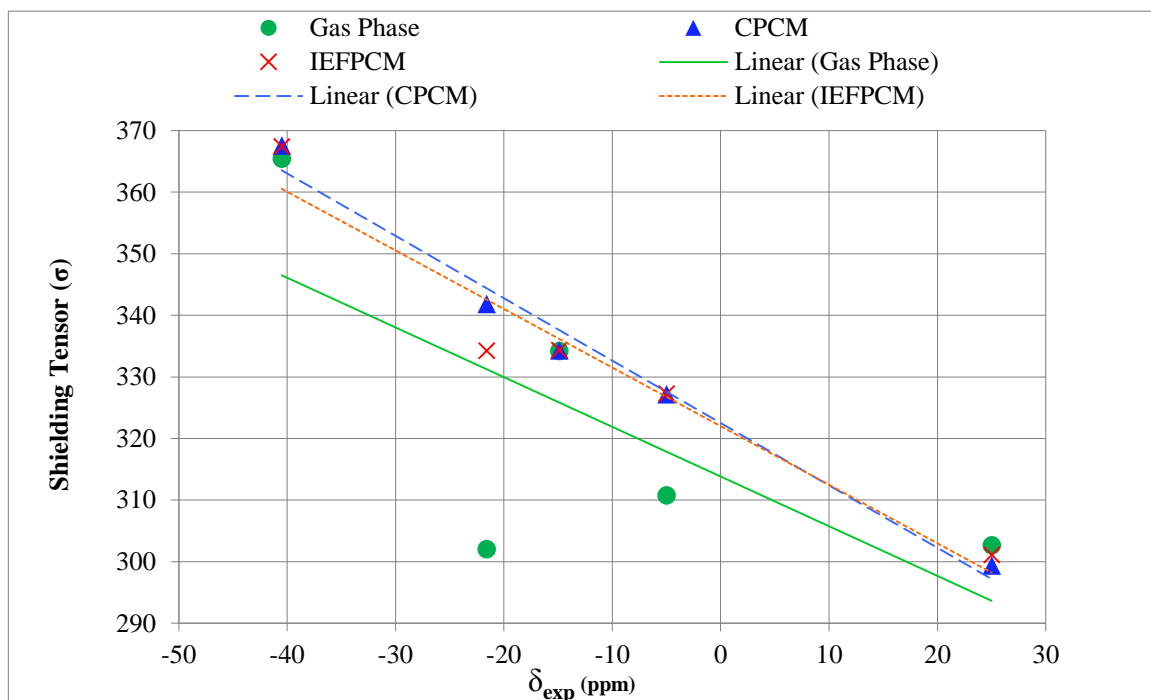


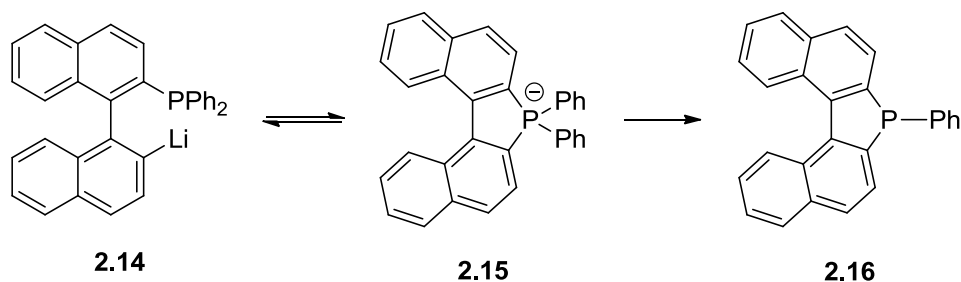
**Figure 2.1** Linear regression of the calculated shielding tensors vs. experimental chemical shifts. Regression and R-squared values: i) Gas Phase  $y = -0.8069x + 313.81$ ,  $R^2 = 0.51743$ ; ii) IEFPCM  $y = -0.9519x + 322.01$ ,  $R^2 = 0.94281$ ; iii) CPCM  $y = -1.0136x + 322.5$ ,  $R^2 = 0.98416$ .

The intercept of the CPCM regression line with the y-axis gives the value of the isotropic shielding tensor that corresponds to 0 ppm, hence 322.5 was used as  $\sigma_{\text{ref}}$  for the determination of the calculated chemical shifts as given by Equation 2.1. The  $^{31}\text{P}$  NMR shifts of postulated species and intermediates of the lithiation of BINAP were calculated using this methodology.

Compound **2.13**, which initial calculations predicted was the structure of the unknown species, was calculated to have a  $\delta_{\text{P}}$  of  $-14.8$  ppm and so was discarded as a possible structure. A study into the synthesis of monodentate analogues of BINAP by Hayashi and co-workers had detailed an observation that organolithium species **2.14**

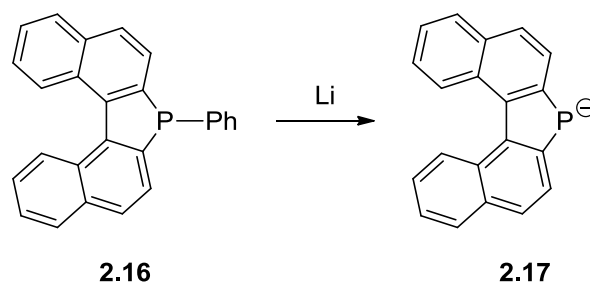


could form dinaphthylphosphole **2.16** *via* the postulated phosphoranide intermediate **2.15** when treated with TMSCl (Scheme 2.16).<sup>20</sup>



**Scheme 2.16** Equilibrium proposed by Hayashi for the conversion of **2.14** to **2.16**.

The authors reported the  $\delta_P$  of **2.16** to be  $-4.2$  ppm, so this potential species could be ruled out. The  $\delta_P$  of **2.15** was calculated (through the DFT method outlined) to be  $-97$  ppm, discounting this as the structure of the unknown species. As **2.14** could be a potential intermediate in the lithiation of BINAP, the formation of **2.16** *via* this intermediate aroused intrigue. A search of the literature revealed that Gladiali and co-workers had synthesised **2.16** by an alternate route: the lithiation of the dibromide and subsequent reaction with  $\text{Cl}_2\text{PPh}$ .<sup>21</sup> In the same publication the authors disclosed a route from **2.16** to other alkylated dinaphthophospholes, by the reductive cleavage of the P-phenyl bond with lithium to form the dinaphthylphospholide anion **2.17** (Scheme 2.17). The authors only reported the  $\delta_P$  of the alkylated phospholes and not of the anion **2.17** before alkylation. When the  $\delta_P$  for **2.17** was calculated a chemical shift of  $49$  ppm was obtained, which was not only in the right region of the spectrum but is also extremely close (with regards to phosphorus chemical shifts) to the unknown species signal at  $50$  ppm.



**Scheme 2.17** Reductive cleavage of phenyldinaphthophosphole.

Furthermore, a study by Mathey and co-workers has reported that the  $^{31}\text{P}$  chemical shifts of various phospholide anions were within the region of 59 to 99 ppm.<sup>22</sup> Whilst the unknown species signal at 50 ppm doesn't directly fall into this range, it is close to this region such that this signal was assigned to dinaphthylphospholide **2.17**.

### 2.2.5 Alkylation

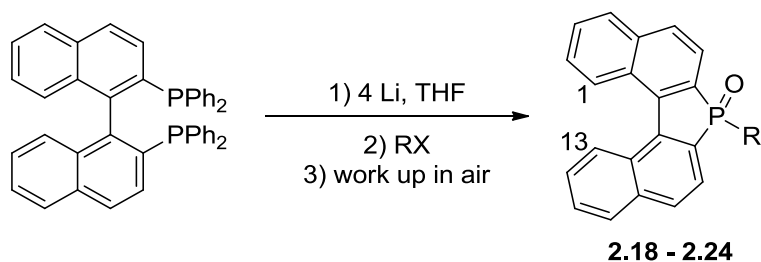
Gladiali reported a route to various alkylated dinaphthylphospholes by the reductive cleavage of **2.16**, which was synthesised by nucleophilic substitutions on highly toxic and pyrophoric phenyldichlorophosphines.<sup>21</sup> The access to phospholides subsequently requires an additional reductive step with lithium to cleave the C-P bond to form **2.17** (Scheme 2.17), which can then react with the appropriate alkylhalide.

It was envisaged by us that the direct treatment of BINAP with lithium could give convenient one-pot access to alkylated dinaphthophospholes, without the use of a multistep process involving the undesirable chlorophosphine reagent. Furthermore, the synthesis and isolation of alkylated dinaphthophospholes would provide further evidence that the  $\delta_{\text{P}}$  signal at 50 ppm belongs to the dinaphthylphospholide **2.17**.

The reaction was first trialled using benzyl bromide as the alkylating agent. Lithiated BINAP solution was treated with 4 equivalents of *t*-BuCl to quench the phenyl lithium and  $\text{LiPPh}_2$  present in solution.  $^{31}\text{P}$  NMR confirmed that  $\text{LiPPh}_2$  had been quenched as the signal at -22 ppm disappeared and was replaced by the signal for  $\text{HPPH}_2$  at -40.5 ppm. The peak at 50 ppm confirmed that the dinaphthylphospholide **2.17** was still present in solution and had not been quenched. Upon the addition of

benzyl bromide to this solution, the  $^{31}\text{P}$  NMR showed a mixture of the benzylated dinaphthophosphole,  $\text{BnPPh}_2$  and  $\text{HPPh}_2$ , suggesting that  $\text{HPPh}_2$  is capable of reacting with benzyl bromide to form  $\text{BnPPh}_2$ . Hence, the reaction was repeated avoiding the *t*-BuCl quench, addition of benzyl bromide directly to the lithiated BINAP solution at room temperature giving clean conversion to the two benzylated phosphines. Although Gladiali isolated the phosphines *via* work up in air, when our reaction mixture was subject to aqueous work up in air, both of the phosphines were converted to their corresponding phosphine oxides, as observed by  $^{31}\text{P}$  NMR. Column chromatography was used to separate the desired benzyldinaphthylphosphole oxide **2.18** from the unwanted  $\text{Bn(O)PPh}_2$  and diphenylmethane. Recrystallisation from toluene gave the dinaphthophosphole oxide **2.18** as a crystalline solid, suitable to confirm this structure by X-ray crystallography. This allowed the unequivocal assignment of the  $\delta_{\text{P}}$  at 50 ppm to the dinaphthylphospholide species **2.17**. Following on, further experiments for the alkylation of the dinaphthylphospholide were performed (Table 2.5); the reactions were monitored by  $^{31}\text{P}$  NMR spectroscopy and the signals for the alkylated phospholes were observed between  $-17$  to  $8$  ppm. The colour change of the solution proved useful as an indicator for reaction progress; upon addition of the alkyl halide the solution changed from dark red for the lithiated species to pale yellow for the alkylated products. The rate of the colour change was dependant on the halide used and the nature of the electrophile, as it is expected that alkyl bromides react faster than alkyl chlorides. For example, the alkylation with benzyl bromide was essentially instantaneous at room temperature, whereas the same reaction with benzyl chloride took several hours to complete. The addition of tertiary halide *t*-BuCl did not yield the corresponding alkylated phosphole under any of the conditions examined. After work up in air the corresponding oxides, with  $^{31}\text{P}$  NMR signals ranging from  $30$  to  $50$  ppm, were obtained. Of note, the cyclobutylphosphole **2.22** required extended vigorous stirring in air to effect full conversion to its corresponding oxide. This synthetic route has the advantage of ease of operation in comparison to the multistep syntheses reported thus far, although

the desired alkylated phosphole oxides are only obtained in modest to poor yields, it allows rapid access to these compounds from commercially available *rac*-BINAP.



**Scheme 2.18** One pot synthesis of alkylated dinaphthophosphole oxides from *rac*-BINAP.

Entry	Product	R	Yield (%)
1	<b>2.18</b>		36
2	<b>2.19</b>		56
3	<b>2.20</b>		40
4	<b>2.21</b>		42
5	<b>2.22</b>		40
6	<b>2.23</b>		37
7	<b>2.24</b>		19

**Table 2.5** One pot synthesis of alkylated dinaphthophosphole oxides from *rac*-BINAP.

$^{13}\text{C}\{^1\text{H}\}$  NMR of the alkylated dinaphthylphosphole oxides gave indications of the dynamic conformer changes of the binaphthyl moiety. Broad signals for carbon atoms C1 and C13 (Scheme 2.18) are consistently observed for all the alkylated dinaphthophosphole oxides. A  $^{13}\text{C}\{^{31}\text{P}\}$  experiment was carried out in order to rule out

poorly resolved  $^{13}\text{C}$ - $^{31}\text{P}$  coupling as the source of the broadening of the signals; this was found not to be the case as no enhanced resolution of the coupled signals was observed. The broadening is instead attributed to the dynamic exchange between the conformers of the binaphthyl moiety. This behaviour is most obvious when examining the  $^{13}\text{C}$  and  $^1\text{H}$  NMR spectra of oxide **2.18**. The  $\alpha$ - and  $\gamma$ -aliphatic carbon atoms (with respect to the phosphorus atom) appear as doublets in the  $^{13}\text{C}$  NMR spectrum, with the splitting being larger for the  $\alpha$ -carbon than for the  $\gamma$ -carbon (Figure 2.2, top trace). This splitting is absent in the  $^{13}\text{C}\{^{31}\text{P}\}$  experiment, hence the splitting is down to the coupling between the carbon and phosphorus atoms (Figure 2.2).

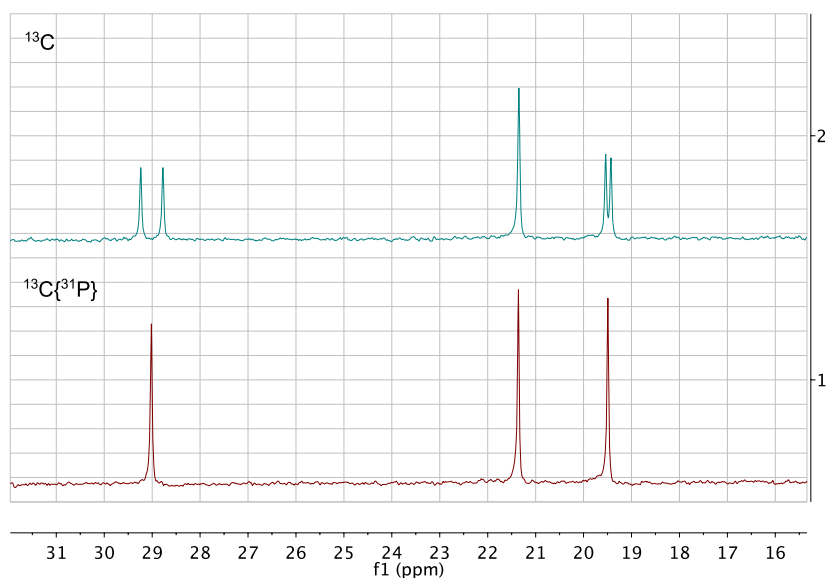


**Figure 2.2** Comparison of the aliphatic region of the  $^{13}\text{C}$  and  $^{13}\text{C}\{^{31}\text{P}\}$  NMR spectra in  $\text{CDCl}_3$  for oxide **2.19**.

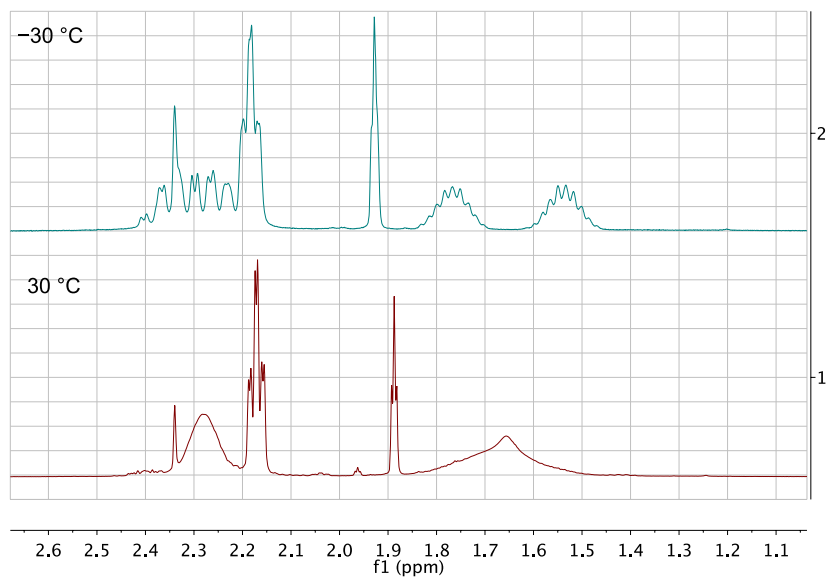


**Figure 2.3** Comparison of  $^1\text{H}$  NMR spectra of **2.19** in  $\text{CDCl}_3$  at variable temperatures, with toluene used as internal standard ( $\delta_{\text{H}} = 2.34$  ppm).

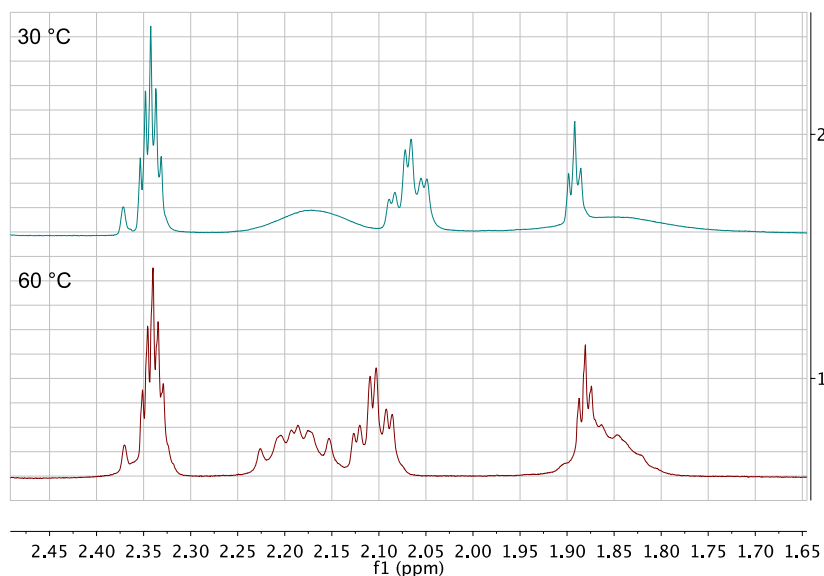


**Figure 2.4** Comparison of  $^1\text{H}$  NMR spectra of **2.18** in toluene- $\text{d}_6$  ( $\delta_{\text{H}} = 2.34$  ppm) at variable temperatures.

At 30 °C (in  $\text{CDCl}_3$ ) the aliphatic region of the  $^1\text{H}$  NMR spectrum of **2.19** shows two broad signals for the  $\alpha$ -protons at 2.2-2.35 ppm and the  $\beta$ -protons at 1.5-1.84 ppm (Figure 2.3, top trace). These signal for the  $\beta$ -protons split and form two resolved signals when the temperature is lowered to  $-30$  °C (Figure 2.3, bottom trace), which is

indicative of the existence of two distinct atropisomers. The signals of the  $\alpha$ -protons (multiplet between 2.2-2.45) are also resolved at low temperature but appear to overlap for both conformers. At a higher temperature (Figure 2.4), the peaks narrow and the coupling begins to resolve as exchange between the two atropisomers is more rapid and comparable to the NMR timescale. All these observations are consistent with exchange between the atropisomers of the binaphthyl backbone. Gladiali also observed this change in conformation in his studies of diastereomeric equilibration of a *P*-alkyl dinaphthophospholes.<sup>21</sup> Additionally, it should be noted that studies by Wild and co-workers have also observed the fluxional nature of dinaphthophospholes and dinaphthoarsoles, including their use as a ligand in iron complexes in which dinaphthophospholes still show fluxional behaviour at room temperature.<sup>24</sup> Therefore, unlike BINAP, dinaphthylphospholes and their oxides are not suitable as ligands for enantioselective catalysis.

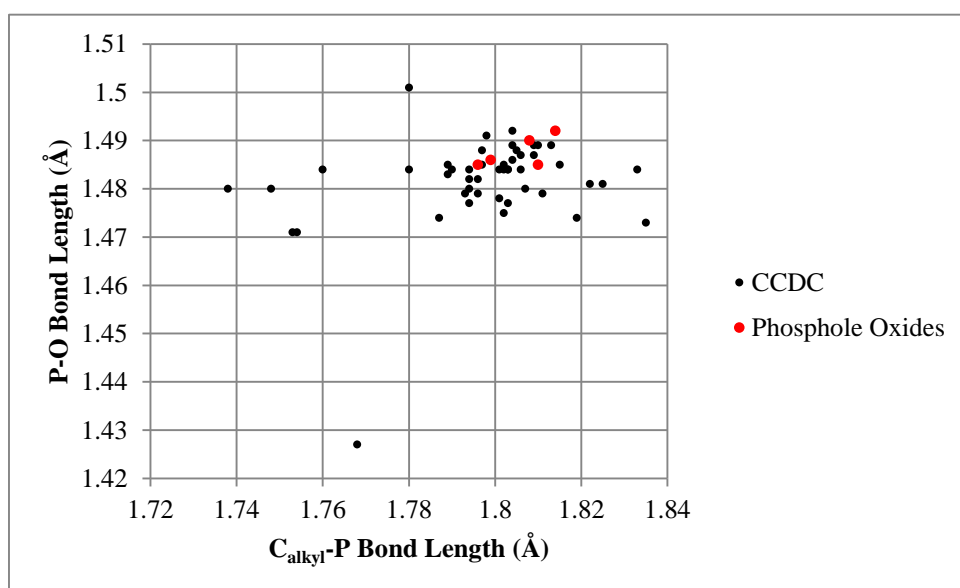


**Figure 2.5** Comparison of P-O bond length and C<sub>alkyl</sub>-P bond length in the crystal structures of phosphole oxides.

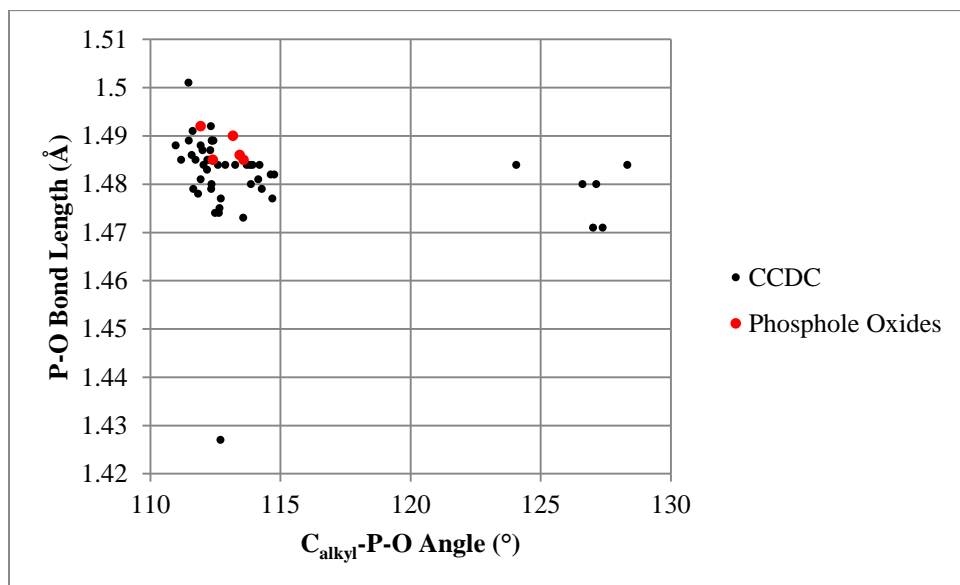


**Figure 2.6** Comparison of P-O bond length and C<sub>alkyl</sub>-P-O bond angle in the crystal structures of phosphole oxides.

Oxides **2.18-2.24** yielded crystals that were suitable for X-ray diffraction studies (see appendix A3). Inspection of the CCDC showed that in comparison to the 48 structures that contained phosphole oxides, oxides **2.18-2.24** had P-O and P-C bond distances and C-P-O bond angles consistent with those not coordinated to a metal centre (Figure 2.5 and Figure 2.6). The structures show that the formation of the 5-membered ring causes a distortion in the outer naphthyl rings, which in turn causes a decrease in steric clash between H13 and H8 (Figure 2.7). This reduces the energy barrier for the flipping of the naphthyl rings, compared to BINAP; hence the exchange process between the two atropoisomers is observed at 30 °C.



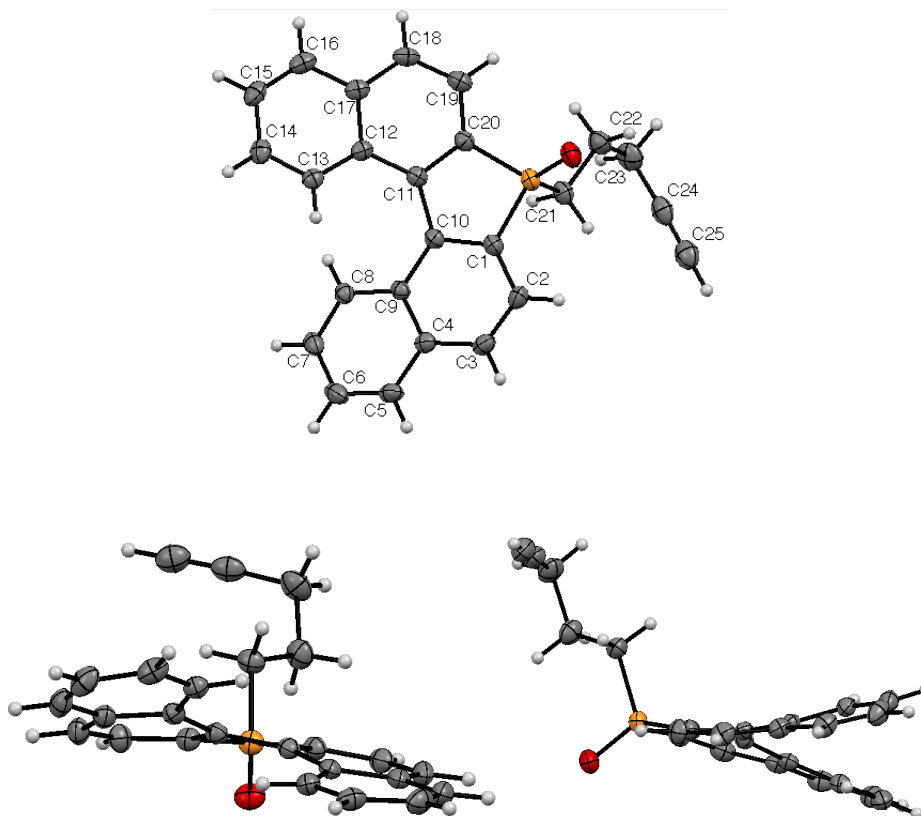
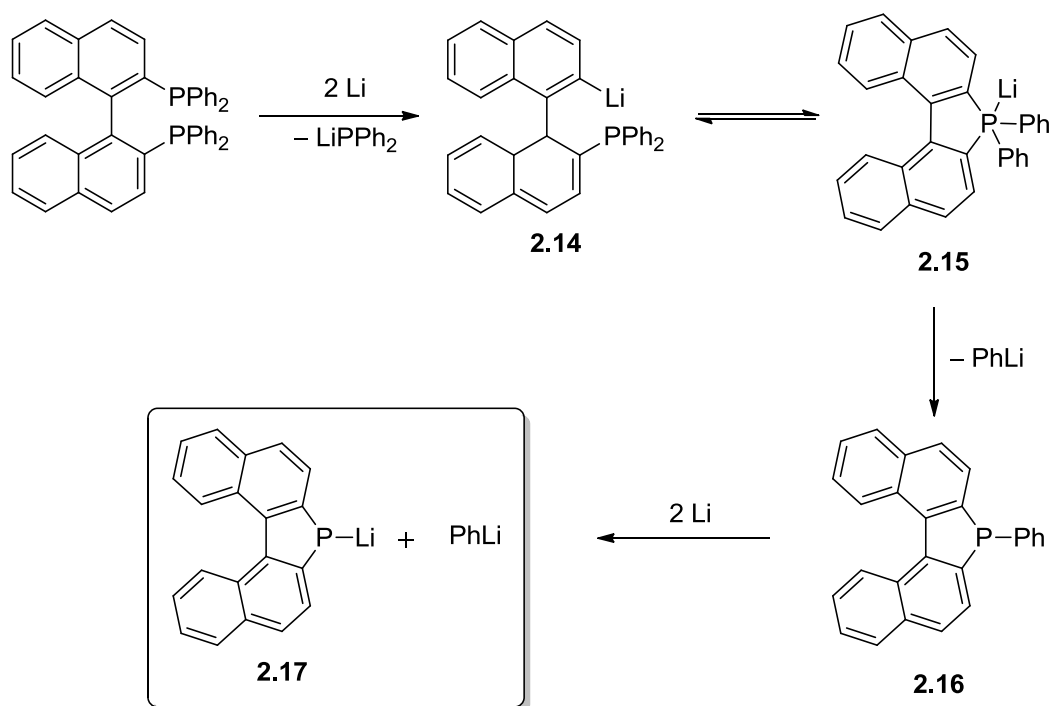


**Figure 2.7** Solid state structure of **2.18** from different angles.<sup>1</sup>

### 2.2.6 Mechanistic Insights

Based on the observations throughout this investigation, and from observations in the literature, we began to piece together a mechanism for the reductive cleavage of BINAP. The first step is the reductive cleavage of the phosphorus- $C_{\text{naphthyl}}$  bond by two equivalents of lithium to yield the corresponding lithiated aromatic species **2.14** and  $\text{LiPPh}_2$  as a by-product (Scheme 2.19).



**Scheme 2.19** Proposed mechanism for the reductive cleavage of BINAP by lithium.

This cleavage pattern is logical as the binaphthyl anion is more stable than the alternative phenyl anion. During the DFT investigations an attempt to perform a geometry optimisation on **2.14** was carried out, the result of which was a structure that corresponded to the tetravalent phosphoranide **2.15**. This internal lithiation and formation of **2.15** was originally postulated by Hayashi in 2001.<sup>20</sup> To further validate **2.15** as the lowest energy structure, a relaxed potential energy surface (PES) scan was performed, where the dihedral angle was varied through 360° in 1° increments (Figure 2.8). The initial dihedral angle used for intermediate **2.14** was assumed to be approximately the same as that of BINAP (87°).<sup>24</sup> The results of the scan confirmed intermediate **2.15** (dihedral angle of -32°) has the lowest energy of all the possible structures. Although the PES scan was performed without additional diffuse functions, a geometry optimization and frequency calculation of **2.14** at the B3LYP/6-31++G(d) level of theory also confirmed that the structure pertaining to intermediate **2.15** had the lowest energy (See appendix A2).

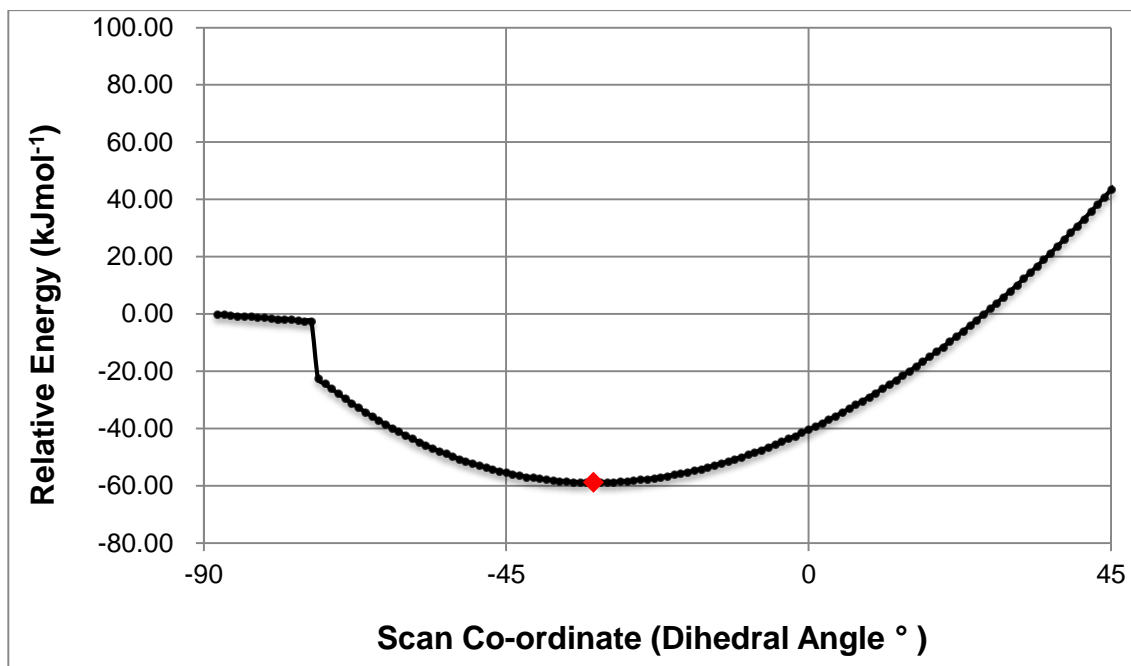


**Figure 2.8** Plot of the relaxed PES scan of **2.14**, carried out at the B3LYP/6-31G(d) level of theory, by varying the dihedral angle. Full scan can be found in Appendix A2.

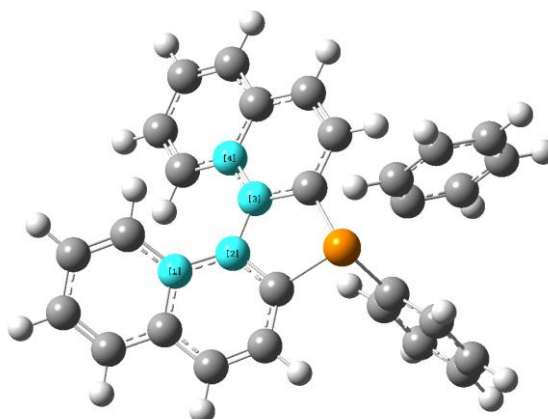


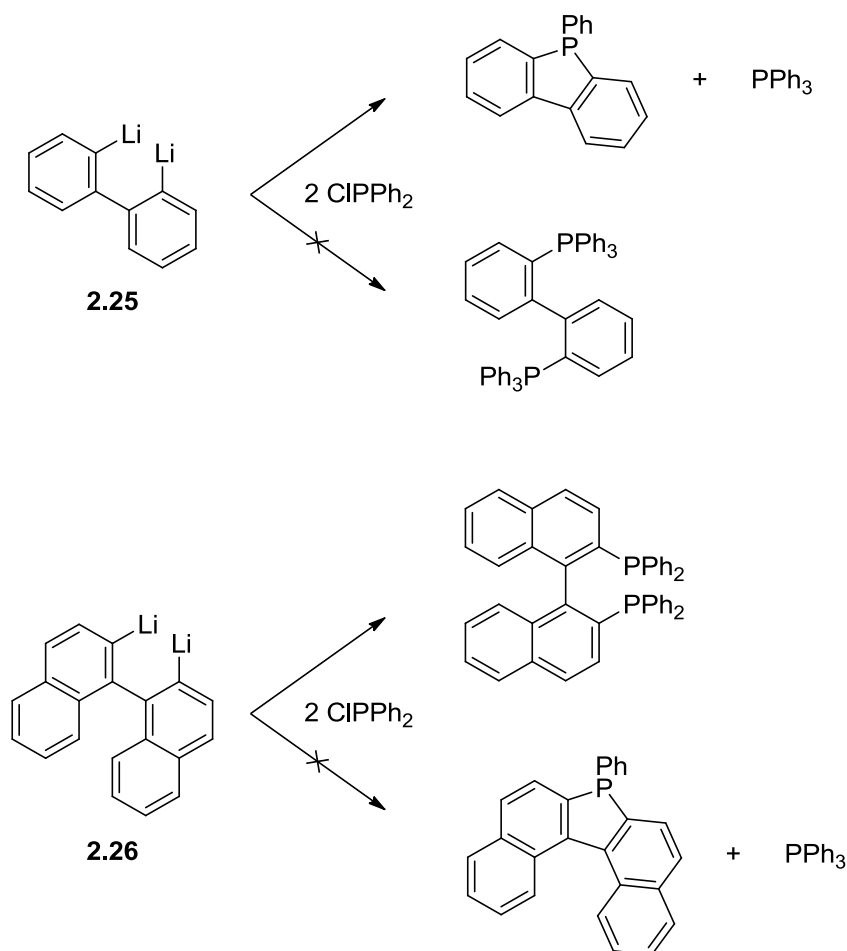
**Figure 2.9** The lowest energy structure (marked with a red diamond in Figure 2.8) corresponding to structure **2.15**. Structures were modeled as anions without explicit Li atoms.

The steric hindrance imparted by the diphenylphosphine groups is relieved upon cleavage of the first diphenylphosphine group and allows free rotation of C-C bond between the naphthyl rings. During rotation of this bond internal lithiation can occur and the electron rich phosphorane **2.15** is formed. **2.15** can then undergo an irreversible elimination of phenyllithium to yield dinaphthophosphole **2.16**. Phosphole

**2.16** can then react with a further 2 equivalents of lithium to yield the dinaphthylphospholide anion **2.17** as reported by Gladiali.<sup>21</sup> Phosphole **2.16** was never observed with <sup>31</sup>P NMR, even when substoichiometric amounts of lithium metal were used. Although the mechanism depicted in Scheme 2.19 invokes anions as the reactive species, a similar mechanism that occurs *via* a radical pathway, as highlighted in previous studies into the reductive cleavage of aryl phosphines,<sup>25</sup> cannot be ruled out.

On a related note, a study by Schlosser and Desponds<sup>26</sup> highlights that the internal lithiation of **2.14** to yield **2.15** is not always favoured over intermolecular trapping with a suitable electrophile. The authors have shown that in the reaction of 2,2'-dilithiobiphenyl **2.25** and two equivalents of ClPPh<sub>2</sub> always results in the formation of the cyclic phosphole (Scheme 2.20). Yet, the reaction of 2,2'-dilithiobinaphthyl **2.26** under the same conditions, results in BINAP as the product and not dinaphthophosphole **2.16**. For the cyclisation to occur, after the addition of the first diphenylphosphine moiety (for example as in **2.14**), the rings must be approximately in the same plane as one another, which is achieved by rotation of the rings. The biphenyl system can rotate more freely in comparison to the binaphthyl system, so the intramolecular lithiation is kinetically favoured over the intermolecular substitution reaction with ClPPh<sub>2</sub>. The binaphthyl backbone must have a comparatively higher energy of rotation, hence in the presence of a suitably reactive external electrophile the ring closure is disfavoured and BINAP is product of the reaction. Nevertheless this is not always the case, as reported by Hayashi and co-workers (Scheme 2.16).<sup>20</sup> When **2.14** was treated with the electrophile TMSCl, the expected substitution reaction did not occur, instead the dinaphthylphosphole **2.16** was formed. The authors suggested that addition of TMSCl shifts the equilibrium towards the phosphole **2.14** by reacting with, and removing, the phenyllithium by-product. In the case of our mechanism presented in Scheme 2.19 there is no external electrophile, so the only likely competing pathway is an intermolecular and heterogeneous process where the remaining PPh<sub>2</sub> is cleaved from **2.14** by further lithium metal. The results obtained in our study, however, have shown that this process

must be surpassed by the intramolecular lithiation to yield the cyclic phosphole **2.16** *via* phosphoranide **2.15**.



**Scheme 2.20** Comparison of the reactivity of **2.25** and **2.26** with  $\text{ClPPh}_2$ .

### 2.3 Conclusions

The aim of this investigation was to identify the unknown species produced when the diphosphine BINAP undergoes reductive cleavage with lithium metal. We have shown that when BINAP is treated with lithium metal it undergoes an initial reductive cleavage of one of the diphenylphosphine groups, followed by a cyclisation to the phenyldinaphthylphosphole **2.16**. Subsequently, a second reductive elimination can occur which yields the dinaphthylphospholide anion **2.17**. One-pot access to this anion facilitates a straightforward and convenient synthesis of alkylated dinaphthophosphole oxides. This study has also highlighted the convenience of GIAO DFT calculations for

predicting chemical shifts, in this case for  $^{31}\text{P}$  NMR, which can aid in the identification of unknown species that synthetic chemists can encounter in their investigations. The calculations were straightforward and computationally cheap to perform, demonstrating that these types of theoretical studies are no longer confined to the expertise of computational chemists and have an important place in the synthetic research laboratory.

## 2.4 References

- (1) Gallop, C. W. D.; Bobin, M.; Hourani, P.; Dwyer, J.; Roe, S. M.; Viseux, E. M. E. *J. Org. Chem.* **2013**, 6522–6528.
- (2) McCleverty, J. A.; Meyer, T. J. *Comprehensive coordination chemistry II*; Elsevier, 2004.
- (3) Wittenberg, D.; Gilman, H. *J. Org. Chem.* **1958**, 23, 1063–1065.
- (4) Budzelaar, P.; Vandoorn, J.; Meijboom, N. *Recl Trav Chim Pay B* **1991**, 110, 420–432.
- (5) Britt, A. D.; Kaiser, E. T. *Chem. Rev.* **1965**, 69, 2775–2779.
- (6) Aguiar, A. M.; Beisler, J.; Mills, A. *J. Org. Chem.* **1962**, 27, 1001–1005.
- (7) Britt, A. D.; Kaiser, E. T. *J. Org. Chem.* **1966**, 31, 112–114.
- (8) Dogan, J.; Schulte, J. B.; Swiegers, G. F.; Wild, S. B. *J. Org. Chem.* **2000**, 65, 951–957.
- (9) Vandoorn, J.; Frijns, J.; Meijboom, N. *Recl Trav Chim Pay B* **1991**, 110, 441–449.
- (10) Vandoorn, J.; Meijboom, N. *Recl Trav Chim Pay B* **1992**, 111, 170–177.
- (11) Pietrusiewicz, K. M.; Zablocka, M. *Chem. Rev.* **1994**, 94, 1375–1411.
- (12) Airey, A. L.; Swiegers, G. F.; Willis, A. C.; Wild, S. B. *Inorg. Chem.* **1997**, 36, 1588–1597.
- (13) Anderson, D. M.; Hitchcock, P. B.; Lappert, M. F.; moss, I. *Inorganica Chimica Acta* **1988**, 141, 157–159.
- (14) Brooks, P.; Craig, D.; Gallagher, M.; Rae, A.; Sarroff, A. *J. Organomet. Chem.* **1987**, 323, C1–C4.
- (15) Bobin, M.; Day, I. J.; Roe, S. M.; Viseux, E. M. E. *Dalton Trans.* **2013**, 42, 6592–6602.
- (16) Maryasin, B.; Zipse, H. *Phys. Chem. Chem. Phys.* **2011**, 13, 5150–5158.

- (17) Sarotti, A. M.; Pellegrinet, S. C. *J. Org. Chem.* **2009**, *74*, 7254–7260.
- (18) Lodewyk, M. W.; Siebert, M. R.; Tantillo, D. J. *Chem. Rev.* **2012**, *112*, 1839–1862.
- (19) NSCCS Applied Computational Chemistry Workshop for Synthetic Organic Chemists. April 2012.
- (20) Shimada, T.; Kurushima, H.; Cho, Y.-H.; Hayashi, T. *J. Org. Chem.* **2001**, *66*, 8854–8858.
- (21) Gladiali, S.; Dore, A.; Fabbri, D.; De Lucchi, O.; Valle, G. *J. Org. Chem.* **1994**, *59*, 6363–6371.
- (22) Charrier, C.; Bonnard, H.; De Lauzon, G.; Mathey, F. *J. Am. Chem. Soc.* **1983**, *105*, 6871–6877.
- (23) Watson, A. A.; Willis, A. C.; Wild, S. B. *J. Organomet. Chem.* **1993**, *445*, 71–78.
- (24) Raghunath, M.; Zhang, X. *Tetrahedron Lett.* **2005**, *46*, 8213–8216.
- (25) Britt, A. D.; Kaiser, E. T. *Chem. Rev.* **1965**, *69*, 2775–2779.
- (26) Desponds, O.; Schlosser, M. *J. Organomet. Chem.* **1996**, *507*, 257–261.

## CHAPTER 3

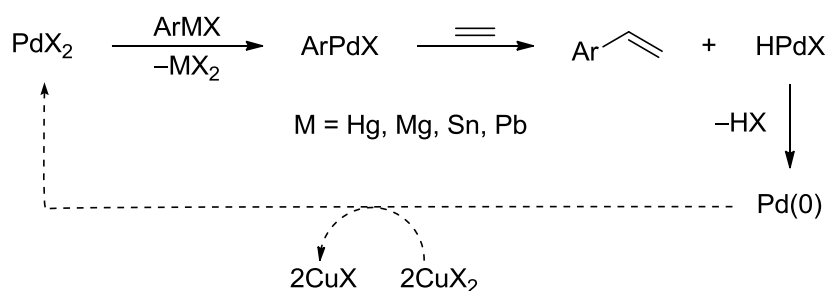
### 3. (NHC)PdCl<sub>2</sub>(TEA) catalysts for the Mizoroki-Heck Reaction

#### Reaction

#### 3.1 Background

##### 3.1.1 Discovery of the Mizoroki-Heck Reaction

The groundwork for the modern day Mizoroki-Heck reaction was disclosed in several reports by Heck's group in 1968. Initially they reported that aryl palladium halides, formed by the transmetalation of a palladium(II) salt with an arylmercury, -magnesium, -lead or -tin compound (ArMX), could be coupled with a range of olefins (Scheme 3.1).<sup>1-3</sup>

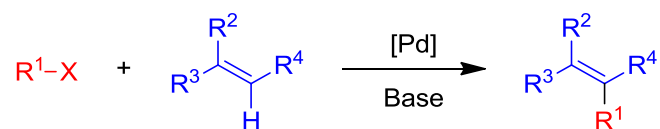


**Scheme 3.1.** Heck's stoichiometric and catalytic coupling of arylmetallic reagents and olefins.

Even though this method presented a convenient route to arylated alkenes it still had two major downfalls, the first being that the reaction was stoichiometric in palladium. Heck amended this by using a copper(II) salt as a stoichiometric oxidant to effect the oxidation of palladium(0) back to the active palladium(II) species (represented in Scheme 3.1 by the dashed arrow).<sup>4,5</sup> The second issue was that the majority of the couplings were still being carried out with toxic and undesirable arylmercury reagents. Work by Fitton and co-workers had shown that a palladium(0) complex, Pd(PPh<sub>3</sub>)<sub>4</sub>, would undergo oxidative addition with chloroolefins, alkylhalides and arylhalides.<sup>6,7</sup> The catalytic cycle could be simplified, and the need for the ArHgX reagent eradicated, by



the oxidative addition of ArX directly to a palladium(0) species. This development was reported independently by Mizoroki in 1971<sup>8</sup> and Heck shortly after in 1972.<sup>9</sup> Therefore, treatment of an olefin with an arylhalide in the presence of a palladium(0) catalyst afforded a convenient route to arylated olefins; known today as the Mizoroki-Heck reaction.



$\text{R}^1$  = alkenyl, aryl, benzyl.  $\text{X}$  = OTf, OTs, Cl, Br, I.  $\text{R}^{3-4}$  = Alkyl, alkenyl, aryl.

**Scheme 3.2.** General Scheme for a Mizoroki-Heck reaction.

### 3.1.2 Mechanism

The first step of the Mizoroki-Heck reaction is oxidative addition of a organic halide to the palladium(0) species. This is followed by an alkene insertion and  $\beta$ -hydride elimination step to release the desired product (Figure 3.1).<sup>10</sup>

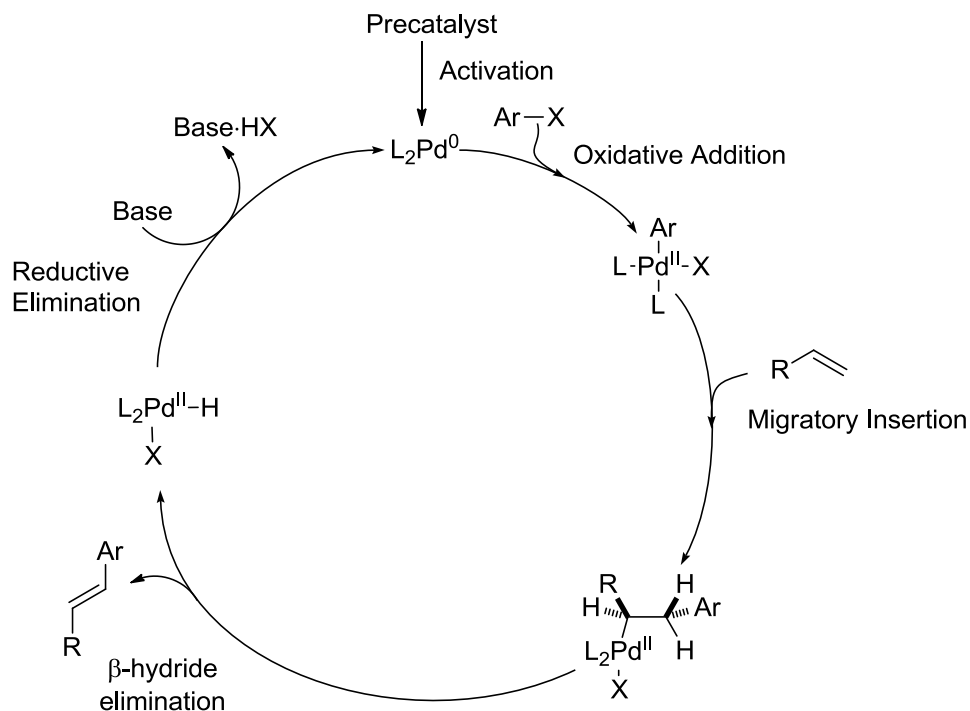


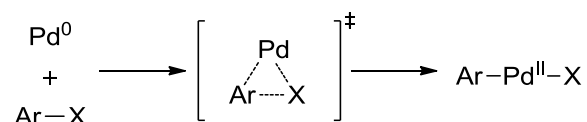
**Figure 3.1.** Catalytic cycle for a Mizoroki-Heck reaction.

### 3.1.2.1 Catalyst activation

The Mizoroki-Heck, like most cross-coupling reactions, requires a palladium(0) catalyst. This catalyst is generated from a palladium(II) precatalyst or less commonly a palladium(0) precatalyst. In either case the precatalyst needs to be activated in some way, usually by a process with a net loss of ligands (accompanied by reductive elimination in the case of palladium(II) complexes) to open up the coordination sphere of the active species. Phosphines are known to reduce palladium(II) to palladium(0) and in the absence of phosphine ligands, amines, olefins and quaternary ammonium and phosphonium salts are also thought to be able to affect this reduction.<sup>11</sup> Well-defined catalysts are often designed to facilitate an activation pathway in order to reduce the induction time often associated with palladium-catalysed cross-couplings.

### 3.1.2.2 Oxidative addition

The oxidative addition of aryl halides is generally accepted to be a concerted process, with the breaking of the C-X bond and formation of the Pd-X and Ar-Pd bonds are synchronised (Scheme 3.3).<sup>11</sup>



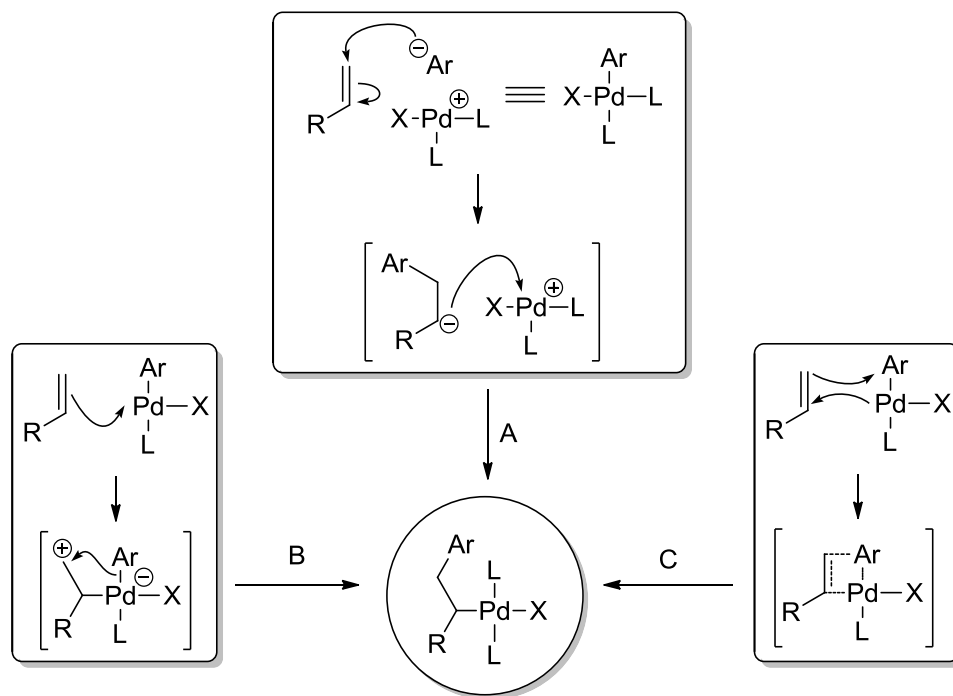
**Scheme 3.3** Concerted nature of oxidative addition.

The efficiency of the catalytic cycle, as with most cross-coupling reactions, is normally dependent on the strength of the C-X bond (where X is a halide or *pseudohalide*) as well as how active the palladium(0) species to undergo the oxidative addition is. The difficulty of oxidative addition increases from  $\text{I} \ll \text{OTf} < \text{Br} \ll \text{Cl}$ ,<sup>12</sup> due the relative strengths of the C-X bond. Due to this, chlorides have long been seen as the target for performing cross-coupling reactions, as they are the most challenging to activate and are cheaper than their other halogen analogues.<sup>13</sup> It should be noted that when discussing cross-couplings that follow this general catalytic cycle, the aryl halides are sometimes

distinguished as activated or unactivated. These terms refer to their activity towards the initial oxidative addition step: an activated aryl halide is one that contains an electron withdrawing groups (like an acetyl or nitro group) and an unactivated aryl halide contains electron donating groups (like alkyl or alkoxy groups).

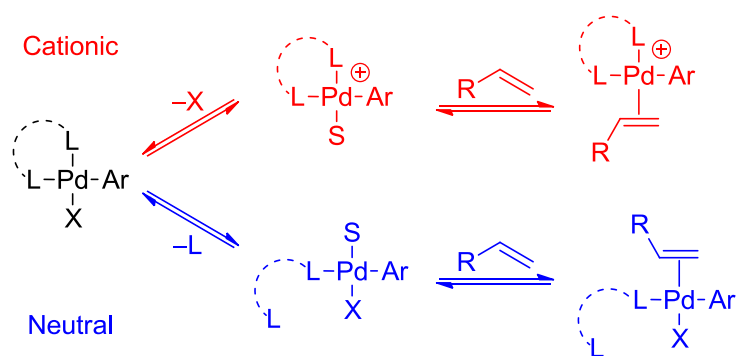
### 3.1.2.3 Migratory insertion

The migratory insertion step is the most significant step of the reaction as it is the step in which the new C-C bond is formed. Furthermore, during this step the regiochemistry and stereochemistry of the product is determined. There are three possible ways that the insertion of the alkene into the Ar-Pd bond can be represented.<sup>11</sup> Firstly by considering the organopalladium species as the nucleophile, where the organic moiety is a carbanion with an accompanying metal-based cation (Scheme 3.4, path A). Secondly, the reverse situation where the alkene is seen as the nucleophile, which can attack the electrophilic Pd species (path B). The last mechanism is the more realistic middle ground between these two extremes and involves a four centre concerted process in which the bond breaking and bond forming processes are synchronous (path C). The electronic adaptability that a concerted transition state invokes results in the accommodation of varying electronics for both the alkene and Pd species, as such steric factors are suggested to be the primary source of selectivity in this mechanism.



**Scheme 3.4** Possible pathways for the migratory insertion of the alkene.

Before the migratory insertion can take place the alkene must be coordinated to the palladium centre. For this to be possible, a ligand must be lost from the  $L_2ArPd^{II}X$  species to open up a coordination site. Depending on which ligand is lost there are two pathways that can be followed, a cationic or a neutral pathway (Scheme 3.5).<sup>14</sup> If an X ligand is dissociated then a cationic palladium(II) alkene complex is ultimately formed. The neutral pathway arises when a neutral ligand (L) is dissociated from the complex. By choosing a suitable catalyst system and additives the reaction can be directed towards one pathway over the other. The neutral pathway is dominant when monodentate L ligands are used; especially when significantly bulky L ligands are used, as they can favour the loss of the L ligand. The cationic pathway can be favoured either by using a halide-abstracting reagent, such as a silver salt, or by replacing the aryl halide with the more labile aryl triflate. Bidentate ligands generally suppress the neutral pathway. However, if the ligand has a sufficiently large bite angle or a spacer unit that is large and flexible enough, as with dppp for example, then the neutral pathway is possible.



**Scheme 3.5** Cationic and neutral pathways for the coordination of the alkene coupling partner.

The regioselectivity of the Mizoroki-Heck reaction is also largely controlled at this step, and varies depending on the substrate choice and which of the above mechanistic pathways are taken. Figure 3.2 depicts the regioselectivity of a variety of different alkenes when operating under the two different mechanisms.<sup>14</sup> For the neutral mechanism selectivity is generally under steric control. Alkenes with a  $\pi$ -acceptor group (or unactivated alkenes) result in selectivity towards the  $\beta$ -position. Electron-rich alkenes substituted with  $\pi$ -donor groups (heteroatoms) shifts the selectivity back towards electronic control and reaction at the  $\alpha$ -position, this means that a mixture of regioisomers are often obtained. For the cationic mechanism the selectivity is dominated by electronic control, as coordination of the alkene to the cationic Pd complex polarises the C=C bond to some extent.

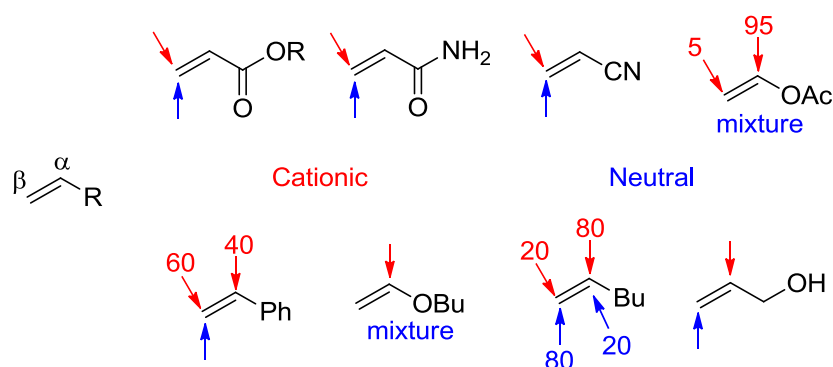
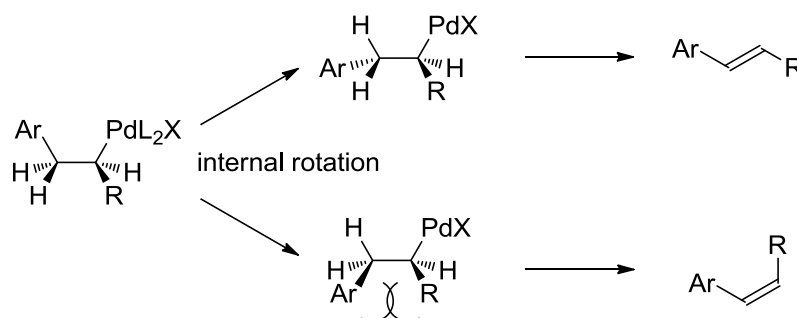


**Figure 3.2** Regioselectivities of various alkenes used in the Mizoroki-Heck reaction. Cationic pathway indicated in red. Neutral pathway in blue.

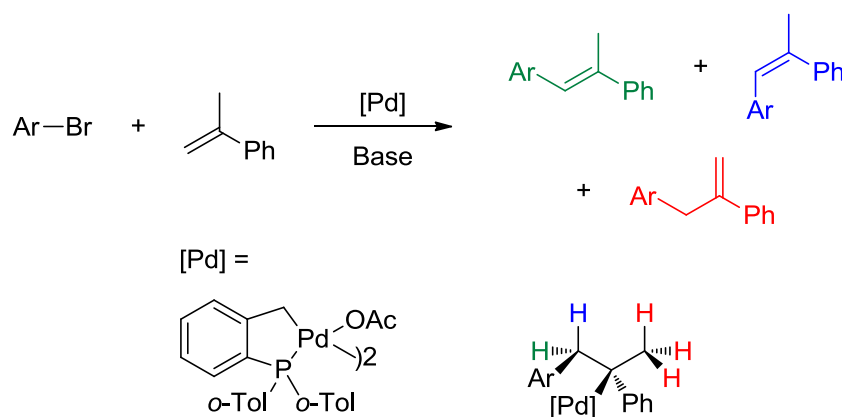
### 3.1.2.4 $\beta$ -hydride elimination

In order to release the product by  $\beta$ -hydride elimination there must be a  $\beta$ -hydrogen *syn* to the palladium. Internal rotation of the  $\sigma$ -bond means that there are two possible conformers that the *syn*-elimination can occur in leading to the (*E*) and (*Z*) products. However, the conformer leading to the (*Z*)-alkene is higher in energy due to the steric clash between the R and aryl groups (Scheme 3.6). This is the source of the Mizoroki-Heck's high stereoselectivity for (*E*)-alkenes.



**Scheme 3.6** Control of (*E*) and (*Z*) selectivity at the  $\beta$ -hydride elimination step.

When 1,1 disubstituted alkenes are used, the situation becomes more complex and the selectivity of the reaction is non-trivial to predict. A study by Beller and Riermeier in 1998 showed an apparent E2 type elimination if a suitable base was chosen for the reaction (Scheme 3.7).<sup>15</sup>



**Scheme 3.7** Beller's palladacycle-catalysed Mizoroki-Heck reaction.

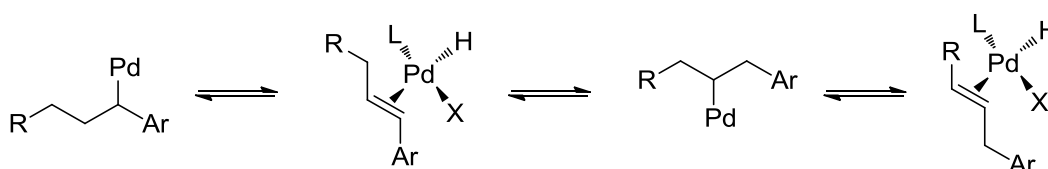
Base	Yield (%)	Internal/Terminal (%)	E/Z
NaOAc	94	39/61	17
Na <sub>2</sub> CO <sub>3</sub>	97	43/57	12
DIPEA	65	95/5	2.5

**Table 3.1** Selectivity for the various products as a result of changing the base.

When inorganic bases, such as NaOAc and Na<sub>2</sub>CO<sub>3</sub>, were used there was little selectivity between the internal and terminal products (Table 3.1). If an organic base was used, such as *N,N*-diisopropylethylamine (DIPEA), the formation of the internal alkenes were favoured, albeit with a decrease in overall yield and *E/Z* selectivity. The authors explained the selectivity for internal alkene formation by the amine base assisting elimination of the more acidic benzylic protons (relative to the terminal protons); this may also explain the poor *E/Z* selectivity, as both benzylic protons effectively have the same *pK<sub>A</sub>*.

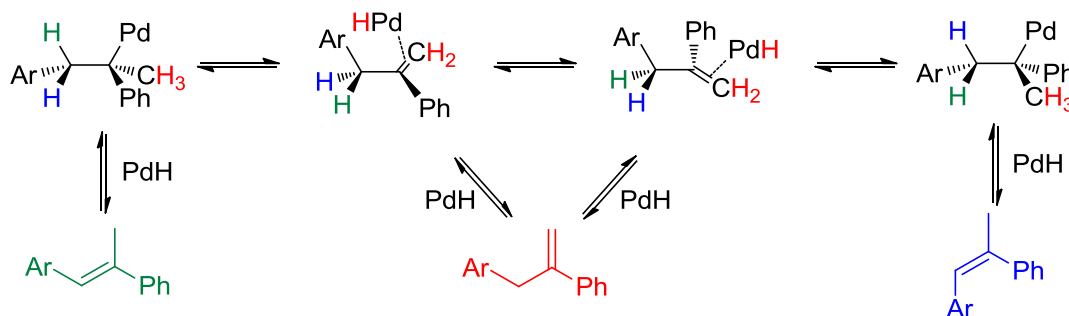
### 3.1.2.5 Reductive elimination

After the  $\beta$ -hydride elimination step the alkene is still coordinated to the Pd centre in an  $\eta^2$  fashion. If the Pd-H species does not rapidly undergo reductive elimination then the readdition of Pd-H to the alkene can occur resulting in the isomerisation of either the product (Scheme 3.8) or the starting alkene, ultimately leading to a different isomer.



**Scheme 3.8** Isomerisation of the Mizoroki-Heck product.

The main role of the base in the Mizoroki-Heck reaction is to encourage the  $\beta$ -hydride elimination by sequestering the HX that is generated. Halide scavengers can also have a similar effect and both help to prevent alkene isomerisation by Pd-H. Beletskaya and Cheprakov have reasoned that the isomerisation of alkenes by Pd-H could explain the selectivity for internal alkenes when DIPEA is used,<sup>11</sup> rather than an E2 type elimination.<sup>15</sup> They suggested that the hindered DIPEA is less efficient at assisting the reductive elimination of Pd-H, thus giving sufficient time to equilibrate to the most stable internal olefin products (Scheme 3.9).



**Scheme 3.9** PdH induced isomerisation used to explain the regio- and stereoselectivity of Beller's Mizoroki-Heck reaction.

### 3.1.3 Use of Aryl Chlorides in the Mizoroki-Heck Reaction

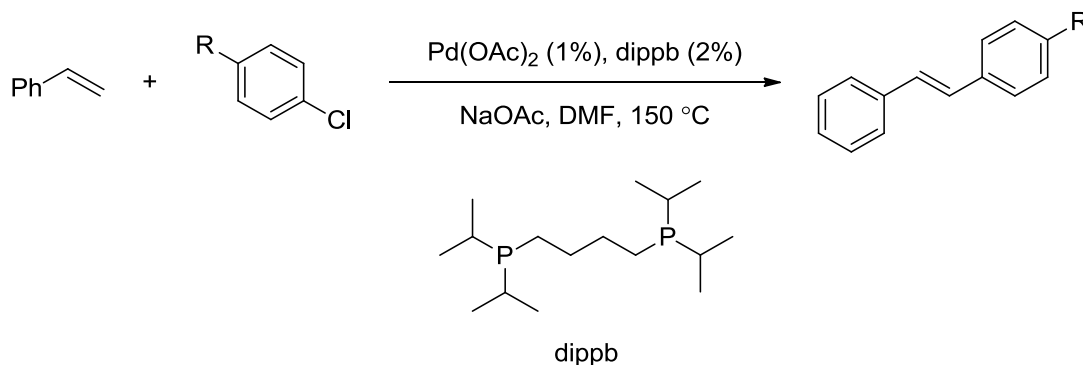
As mentioned in Chapter 1, the use of aryl chlorides in the majority of cross-coupling reactions is not facile due to the strength of the carbon-chlorine bond.<sup>16</sup> Despite this there are several examples of different palladium catalysts that are able to activate these difficult substrates.<sup>17-42</sup>

#### 3.1.3.1 Palladium Phosphine Complexes

In the case of phosphines, the first example of an electron-rich trialkyl phosphine being able to activate aryl chlorides towards Mizoroki-Heck couplings was reported by Milstein and co-workers in 1992 (Scheme 3.10).<sup>17</sup> The authors utilised a chelating bisphosphine, dippb, and were able to achieve good yields for the coupling of



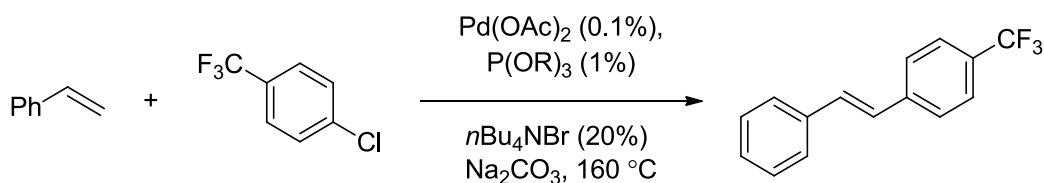
styrene with activated and neutral aryl chlorides and reasonable yields with unactivated aryl chlorides.



**Scheme 3.10.** Milstein's use of the electron rich chelating biphosphine dippb.

Compared to similar bisphosphines and monophosphines, dippb clearly showed an enhanced activity when coupling styrene and chlorobenzene. When a shorter alkyl linker was used (dippe, dippp) no conversion was recorded, and bisphosphine dppe afforded only a small conversion of 17%. The monophosphines *i*Pr<sub>3</sub>P and *i*Pr<sub>2</sub>P<sup>n</sup>Bu also gave poor yields of 26% and 15% respectively.

Beller and co-workers showed, that bulky phosphites could be used for the coupling of activated aryl chlorides (Scheme 3.11).<sup>21</sup>

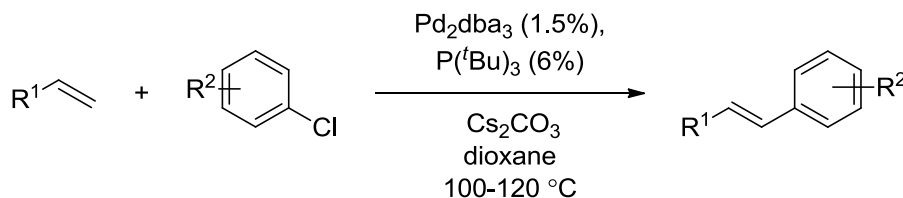


**Scheme 3.11** First phosphite ligands used for a Mizoroki-Heck reaction of an activated aryl chloride. R = 2,4-'Bu<sub>2</sub>C<sub>6</sub>H<sub>3</sub>.

This is somewhat counterintuitive as phosphites are generally less electron donating than their phosphine analogues, this results in more metal to ligand backbonding and a net loss of electron density on the palladium centre. Nevertheless, this system showed that the use of an electron rich palladium(0) centre may not always be necessary to

activate and insert into the carbon-chlorine bond, although a high ratio of phosphite and *n*-Bu<sub>4</sub>NBr to palladium were necessary in order to stabilise the active species and achieve good yields.

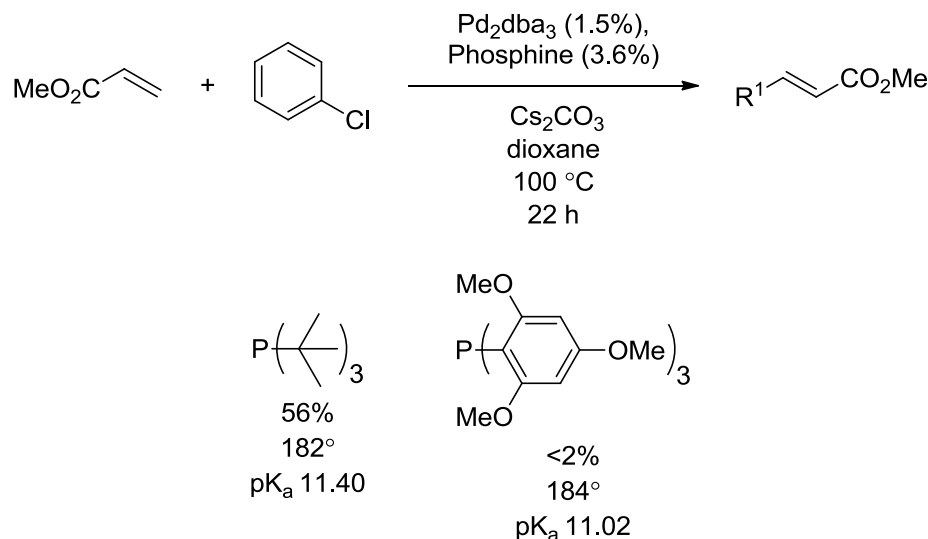
The real breakthrough for phosphine-based systems was the high activity of palladium(0) ligated with the electron rich alkyl phosphine P(*t*-Bu)<sub>3</sub> for the activation of aryl halides under mild conditions. This was independently accomplished in 1999 by the groups of Hartwig and Fu. Hartwig and co-workers used a clever fluorescence-based assay to screen 40 separate phosphine ligands and test their ability to promote the Mizoroki-Heck reaction of aryl chlorides, where P(*t*-Bu)<sub>3</sub> gave the best results.<sup>22</sup> Based on their studies of the Suzuki coupling with P(*t*-Bu)<sub>3</sub>, Fu and Littke revealed this ligand allowed the coupling of aryl chlorides in good yields (70-84%, 6 examples, Scheme 3.12).<sup>23</sup> The system showed the best generality towards both the alkene (styrene or acrylate) and aryl chloride at that point in time; aryl chlorides could be not only electron rich (4-chloroanisole) but also sterically hindered (2-chlorotoluene).



**Scheme 3.12** Fu and Littke's initial conditions utilizing the bulky phosphine P(*t*-Bu)<sub>3</sub>.

Inspired by results published by Buchwald's group,<sup>43</sup> Fu and Littke reported a significant improvement to their original conditions by replacing the inorganic caesium base with tertiary amine Cy<sub>2</sub>NMe.<sup>30</sup> This alteration led to several improvements: (1) there was better tolerance to wider range of alkenes; (2) aryl bromides and activated aryl chlorides could be coupled with alkenes at room temperature; (3) hindered and deactivated aryl chlorides could be coupled with alkenes at elevated temperatures (comparable or less than those typically reported). When the ratio of ligand: Pd was changed from 1:1 to 2:1, in the coupling of 4'-chloroacetophenone and styrene, a

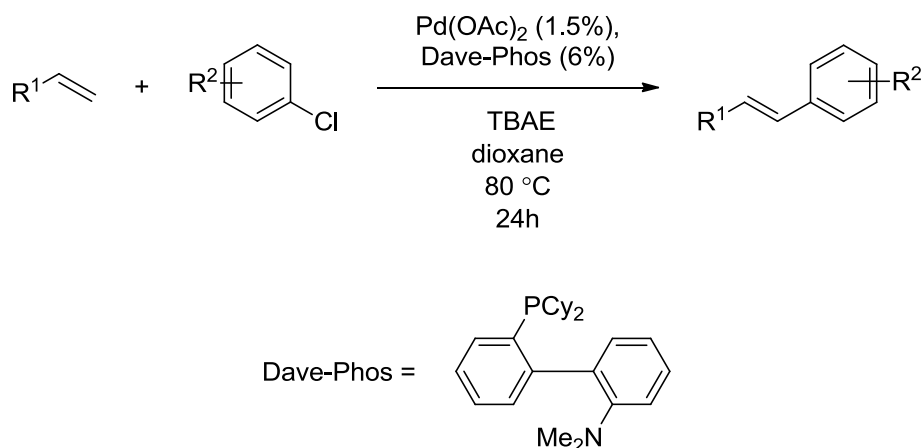
dramatic decrease in reaction rate was observed. This led the authors to suggest that the reactive mono-ligated  $\text{PdP}(t\text{-Bu})_3$  species can be formed under the reaction conditions. The ability of the  $\text{P}(t\text{-Bu})_3$  to shield the reactive metal centre favours the formation of the mono-ligated palladium(0) species, resulting in high activity of this catalytic system in cross-coupling reactions. The large steric environment and electron rich characteristics of these phosphines are often used to explain the stabilisation of the mono-ligated  $\text{LPd}(0)$  species. However, Fu has noted that a phosphine ( $\text{P}(1,3,5\text{-methoxy-C}_6\text{H}_2)_3$ ) with similar steric and electronic properties as  $\text{P}(t\text{-Bu})_3$  showed almost no activity in a Mizoroki-Heck reaction that were effectively catalysed when  $\text{P}(t\text{-Bu})_3$  was used (Scheme 3.13).<sup>23</sup>



**Scheme 3.13** Fu's demonstration that a ligand with similar electronic and steric properties to that of  $\text{P}(t\text{-Bu})_3$  is ineffective in a Mizoroki-Heck reaction.

This further highlights that predicting a ligands performance is not always straightforward and bulky, electron-rich ligands do not always guarantee good catalytic activity towards aryl chlorides.

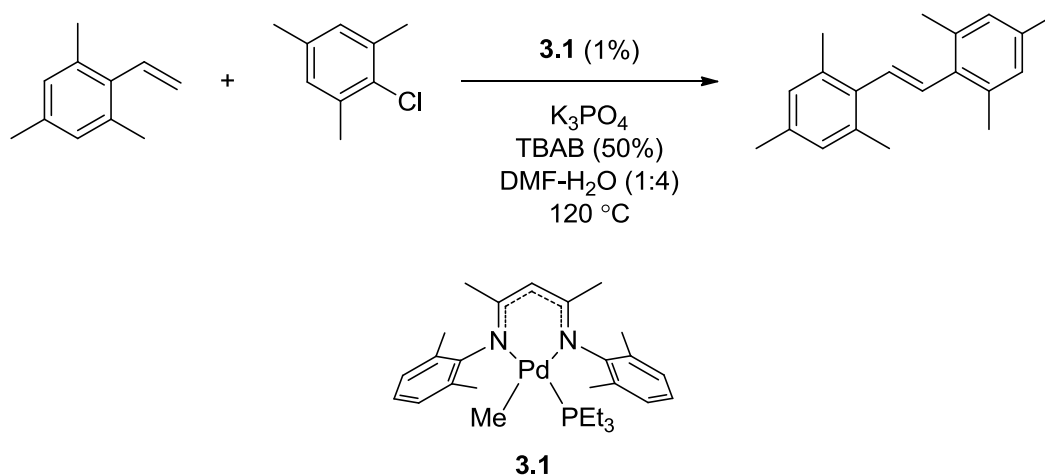
Dialkylbiaryl phosphines have also been used to promote the coupling of aryl chlorides, and in a recent report Zhou and co-workers combined the use of these ligands with an ionic base  $n\text{-Bu}_4\text{NOAc}$  (TBAE).<sup>36</sup>



**Scheme 3.14** Zhou's application of bulky dialkylbiaryl phosphines.

This catalytic system allowed for the use of milder temperatures (80 °C rather than the usual 120-140 °C) and tolerated both activated and non-activated aryl chlorides, giving good to excellent yields when coupled with styrenes (Scheme 3.14). Only one *ortho*-substituted chloride was tested (2-chlorobenzaldehyde), and in order to obtain a high yield the reaction time had to be doubled and the temperature raised. Finally, the authors showed that the coupling with 4-chlorobenzaldehyde a range of substituted styrenes and acrylates could be achieved.

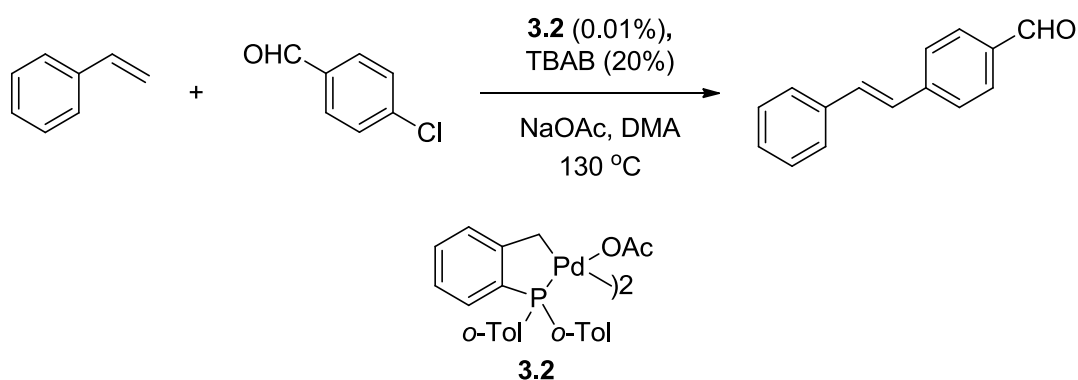
Jin and co-workers demonstrated that palladium(II) complex **3.1**, furnished with a  $\beta$ -diketiminato (BDI) and a phosphine ligand, could facilitate the coupling of a wide variety of electron rich and hindered aryl chlorides with different olefins, a particularly challenging example is shown in Scheme 3.15. This Mizoroki-Heck protocol, along with Fu's discussed above, represent the most general protocols for the coupling aryl chlorides to date.



**Scheme 3.15** - Jin's BDI based catalyst for the Mizoroki-Heck coupling of challenging aryl chlorides.

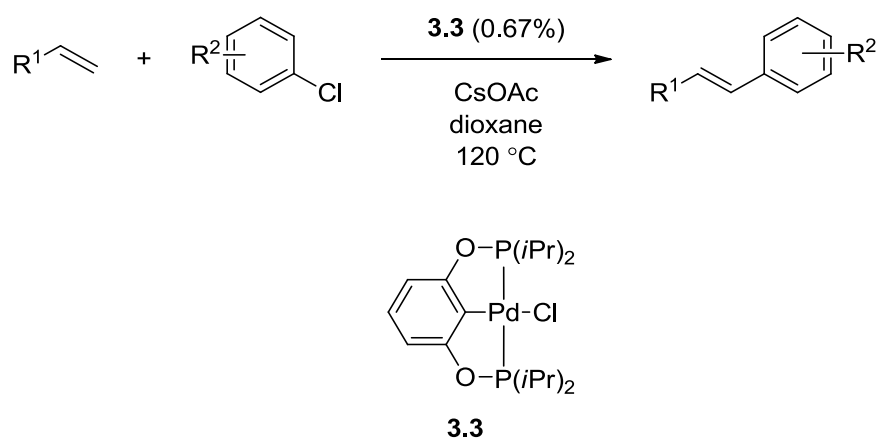
### 3.1.3.2 Palladacycles

The use of palladacycles as precatalysts for Mizoroki-Heck reactions of aryl chlorides was first reported by Herrmann and co-workers in 1995.<sup>19</sup> The authors noted that P-Pd bond cleavage was observed at temperatures higher than 120 °C when using catalysts formed from Pd(OAc)<sub>2</sub> and triaryl phosphines, assuming that this deactivated the catalyst by the formation of palladium black. PC-palladacycle **3.2** showed better stability than typical phosphine-palladium systems, however in coupling of 4-chlorobenzaldehyde the addition of tetrabutylammonium bromide (TBAB) was necessary to stabilise the catalyst and achieve high turnovers (Scheme 3.16).



**Scheme 3.16** Herrmann and Beller's palladacycle for the Mizoroki-Heck reaction of activated aryl chlorides.

Developments were made to these catalytic systems including the incorporation of NHCs into their precatalyst complexes,<sup>44</sup> although the substrate scope was still fairly limited and could not be extended past activated aryl chlorides. A different class of palladacycles, incorporating a PCP pincer ligand, was reported by Jensen and co-workers in 2000.<sup>25</sup> Although these complexes were successful in activating electron neutral and electron rich aryl chlorides towards coupling with styrene (Scheme 3.17), the reactions took a long time (5 days at 120 °C or 24 h at 180 °C). The authors propose that the catalyst is stable at high temperatures and that complex **3.3** itself is the active species, suggesting a Pd(II)/Pd(IV) catalytic cycle was operating. However, a more recent study of four different PCP pincer palladium(II) complexes (including Jensen's) has shown that these complexes are likely to just be precursors to metallic palladium(0), which may be the active species.<sup>45</sup> This could explain why **3.3** is more active, simply because it can decompose more easily releasing the active palladium(0) species.



**Scheme 3.17** PCP pincer complex used by Jensen and co-workers to couple styrene and aryl chlorides.

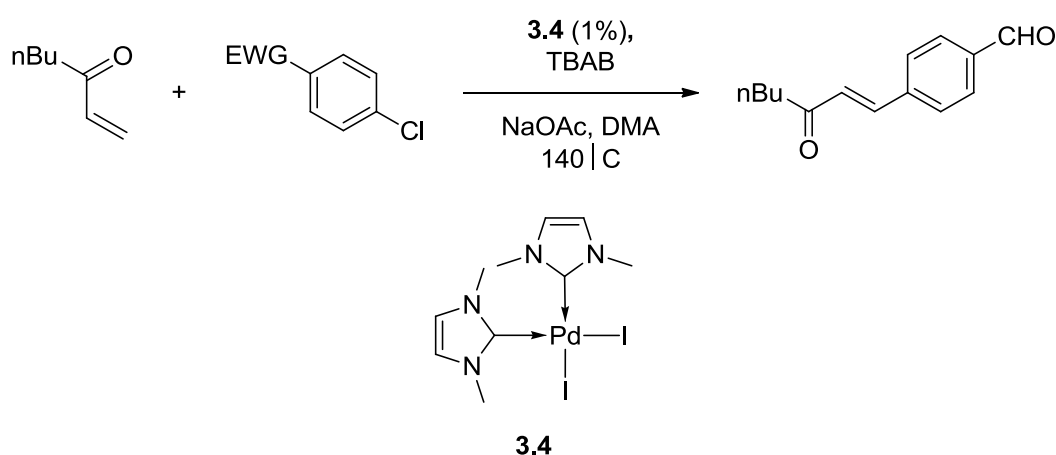
### 3.1.3.3 Ligand-free Pd systems

Ligandless systems have been developed to perform catalytic transformations. These systems typically involve the reduction of a palladium(II) precursor *in situ* to form catalytically active palladium(0) nanoparticles (NPs).<sup>46</sup> It is important to note that Pd-NPs may be formed unintentionally, to some amount, by catalyst decomposition at

high temperatures in the homogeneous catalytic systems mentioned above.<sup>47</sup> This is supported by the observation first made by Jeffery<sup>48</sup> that tetrabutylammonium salts have a positive effect on the outcome of Mizoroki-Heck reactions. The numerous roles tetrabutylammonium salts can play to achieve this effect have been nicely summarised by Beletskaya;<sup>11</sup> chief among which were their ability to stabilise underligated palladium(0)-NPs and their well known role as a phase transfer catalyst (more important when inorganic bases are used). As a result many protocols include an ammonium or phosphonium salts in their Mizoroki-Heck conditions. Most examples in which Pd-NPs are explicitly used as the catalyst for Mizoroki-Heck reactions involve coupling aryl bromides and iodides, there are fewer examples for aryl chlorides, particularly electron rich aryl chlorides.<sup>49</sup>

#### 3.1.3.4 NHC Palladium Complexes

The Mizoroki-Heck cross-coupling was the first reaction in which NHCs were utilised as modulating ligands.<sup>50</sup> Biscarbene complex **3.4** was successful in coupling butyl acrylate with the activated aryl chlorides 4-chloroacetophenone and 1-chloro-4-nitrobenzene (Scheme 3.18); although TBAB was needed as a co-catalyst in order to obtain good conversions.



**Scheme 3.18** The first NHC complex used for catalysis, an example of the Mizoroki-Heck reaction of activated chlorides.

The use of tetrabutylammonium salts is a recurring theme in the activation of aryl chlorides using NHC containing palladium precatalysts that was instigated by this seminal report.

Beller and co-workers demonstrated that (NHC)-Pd(0) complexes **3.5**, **3.6** and **3.7** are successful in the Mizoroki-Heck coupling of aryl chlorides (Figure 3.3).<sup>32</sup> In theory, the only activation step required for these precatalysts is the decoordination of one or more of the ancillary ligands. Rather than using TBAB as just an additive to the reaction, the authors used TBAB as a cheap and readily available ionic liquid in which to perform the cross-couplings at 140 °C (melting point 102 - 106 °C). Sodium acetate was chosen as an appropriate base and the catalyst loading was found to be effective at the low level of 0.5 mol%. Complexes **3.6** and **3.7** were found to be superior to **3.5**, which only gave a poor yield of the coupled product between chlorobenzene and styrene (17%), whereas both **3.6** and **3.7** afforded a 62% yield of stilbene.

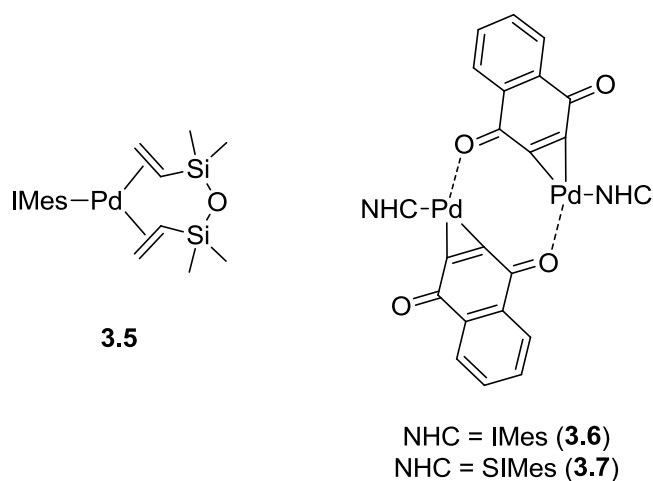


**Figure 3.3** Beller and co-workers' (NHC)-Pd(0) complexes used for Mizoroki-Heck reactions.

Under these conditions, with either complex **3.6** or **3.7**, electron-deficient aryl chlorides were coupled with styrene providing good to excellent yields of the expected products (84-97%). A low yield of 39% was obtained when 4-chlorotoluene was coupled with styrene using complex **3.7**, which was improved to 62% by raising the reaction temperature to 160 °C. Excellent yields could be obtained when 2-ethylhexyl acrylate



was coupled with electron-deficient aryl chlorides. Yet, when using this alkene, poor yields persisted for unactivated aryl chlorides even when doubling the catalyst loading to 1%. The complexes showed good activity towards aryl chlorides but their synthesis was not as straightforward as other (NHC)-Pd complexes, specifically these (NHC)-Pd(0) complexes require more careful handling than (NHC)-Pd(II) complexes.

Hermann and co-workers made an effort to improve upon the activity of phosphapallacyclic complexes by incorporating an NHC ligand into this structural class of precatalysts.<sup>44</sup> Several different complexes were trialed; those most effective at catalysing the Mizoroki-Heck reaction are shown in Figure 3.4.

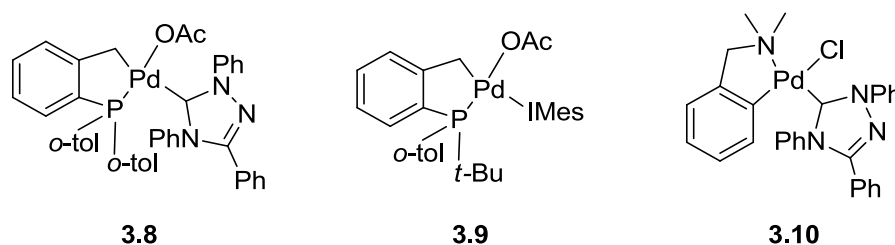


**Figure 3.4** Palladacycles incorporating an NHC ligand.

These complexes (**3.8 - 3.10**) proved to be extremely active catalysts, meaning catalyst loadings as low as  $10^{-3}$  mol% could be used. However, this is only applicable to the activated chloride 4-chloroacetophenone and activated bromides and electron-neutral bromobenzene. Therefore, despite their high activity, this class of NHC-bearing catalyst do not represent an extension in scope for the use of aryl chlorides in the Mizoroki-Heck reaction.

Amide-functionalised (NHC)-Pd(0) and palladium(II) complexes have also been shown to be competent catalysts for the coupling of activated and deactivated aryl chlorides and also electron rich chlorides in the Mizoroki-Heck reaction.<sup>51</sup>

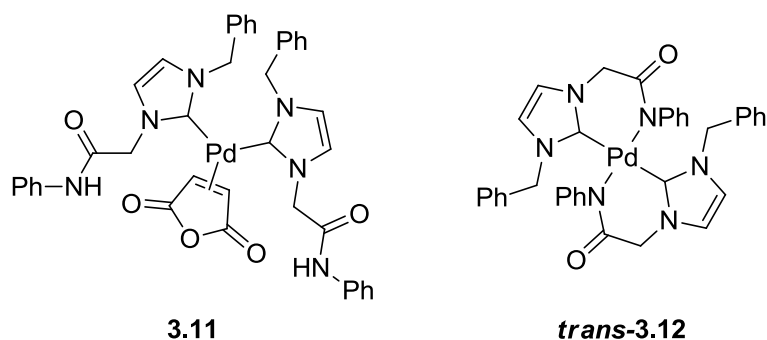
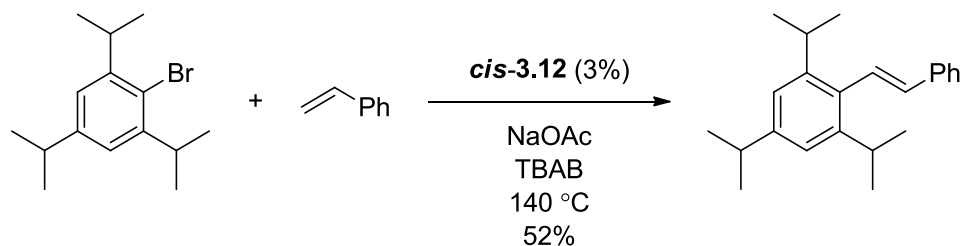


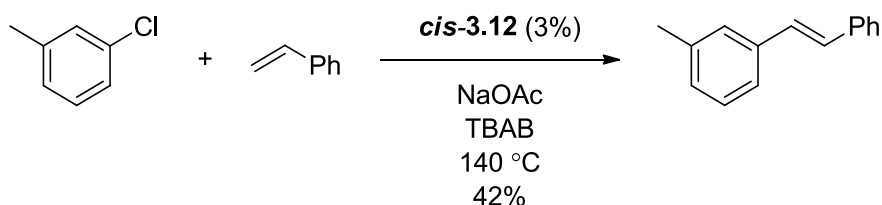
**Figure 3.5** Amide functionalised (NHC)-Pd complexes used for the Mizoroki-Heck reaction.

The authors initially synthesised palladium(0) complex **3.11** (Figure 3.5), which like most palladium(0) complexes was found to degrade when in solution and exposed to air. The main degradation product was shown to be the *trans* isomer of palladium(II) complex **3.12**. When applied to the Mizoroki-Heck reaction between 4'-chloroacetophenone and styrene with a catalyst loading of 0.5 mol%, complex **3.11** was found to be an effective catalyst at 120 °C; however, neither isomer of **3.12** showed good activity at this temperature. This was attributed to the need for the activation of the palladium(II) complex to an active palladium(0) species before catalysis could occur. Indeed, increasing the temperature to 140 °C aided this activation and both isomers of **3.12** were efficient catalysts under these conditions. A comparison of the two catalysts under these conditions revealed that there is an induction period for the palladium(II) precatalysts of an hour before the reaction begins, whereas there was no appreciable activation time for the palladium(0) precatalyst. In general the palladium(0) complex **3.11** provided higher yields than palladium(II) complex *cis*-**3.12**. No difference in activity between the two isomers of **3.12** was observed, both giving similar yields of products. However, the authors preferentially used the *cis* isomer as they had previously reported its synthesis.<sup>52</sup> When the group progressed to using more challenging substrates such as bulky electron-rich aryl bromides and chlorides, palladium(II) complex **3.12** was found to be the superior precatalyst over **3.11**. Using 3 mol% of *cis*-**3.12** allowed the coupling of some challenging aryl bromides with either styrene or *n*-butylacrylate in moderate to good yields (Scheme 3.19).



**Scheme 3.19** Example of a Mizoroki-Heck reaction of a sterically hindered aryl bromide with styrene.

Similarly, higher catalyst loadings were also necessary when utilising electron-neutral/rich aryl chlorides, the coupling products of which could be obtained in moderate to good yields (Scheme 3.20).



**Scheme 3.20** Example of a Mizoroki-Heck reaction of an electron rich aryl chloride with styrene.

Although these (NHC)-Pd complexes did allow for a degree of expansion of the scope of aryl chlorides they required relatively high catalyst loadings in comparison to typical systems (1 mol%).

In 2006 Organ introduced a new class of (NHC)-Pd precatalysts which he dubbed PEPPSI (Pyridine-Enhanced Precatalyst Preparation, Stabilisation and Initiation).<sup>53</sup> Organ set out to form a palladium(II) precatalyst that could be synthesised in air, be bench stable and easily activated to yield the active palladium(0) species.<sup>54</sup> They reasoned that the precatalyst should contain one NHC ligand, two anionic halides (Cl or Br) and then a final 'throw-away' ligand. The 'throw-away' ligand had to be sufficiently coordinating in order to stabilise the palladium(II) species, but also labile enough to facilitate activation to the palladium(0) species. Inspired by Grubbs use of pyridine ligands in a (NHC)-ruthenium complex, Organ's group showed that complexes

with general structure (NHC)PdX<sub>2</sub>(3-chloropyridine) (Figure 3.6) are efficient catalysts for numerous cross-coupling reactions.<sup>55</sup>

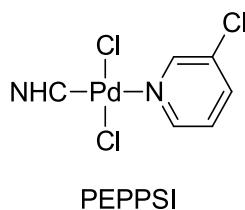


**Figure 3.6** General structure of a PEPPSI precatalyst.

The Organ group have not reported the use of their PEPPSI complexes in the Mizoroki-Heck reaction, although in recent years other groups have adopted this structural template for their own PEPPSI-themed (NHC)-palladium complexes for the Mizoroki-Heck cross-coupling reaction.

Liu and Lin showed that PEPPSI-themed (NHC)-palladium precatalysts can activate aryl chlorides for coupling in the Mizoroki-Heck reaction.<sup>41</sup> The group tested a series of imidazole and benzimidazole derived NHC ligands (Figure 3.7, R = Me, Et, *n*Bu). In general, benzimidazole based complexes **3.13** were found to be more active than the corresponding imidazole complexes **3.14**. With DMF as a solvent, TBAB as an additive and K<sub>2</sub>CO<sub>3</sub> as base, these precatalysts were sufficiently active enough for the coupling of activated aryl chlorides at 140 °C, giving good to excellent yields of the coupled products. However, only moderate to good yields were obtained when chlorobenzene was used, and poor yields were achieved with the comparatively more electron-rich chlorotoluene. It should be noted that there is evidence that palladium nanoparticles can also be generated from these PEPPSI-type complexes under the reaction conditions.<sup>41,56</sup>

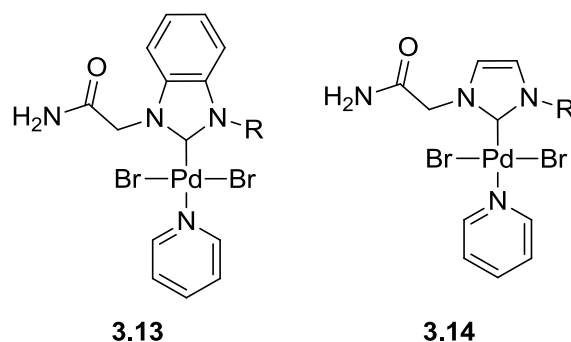


**Figure 3.7** Amide functionalised imidazole and benzimidazole derived (NHC)-Pd complexes based on the PEPPSI framework.

An interesting study by Lee and co-workers used a PEPPSI themed complex to investigate the difference in activity between normal and abnormal carbene complexes **3.15** and **3.16** in the Mizoroki-Heck reaction (Figure 3.8).<sup>42</sup>

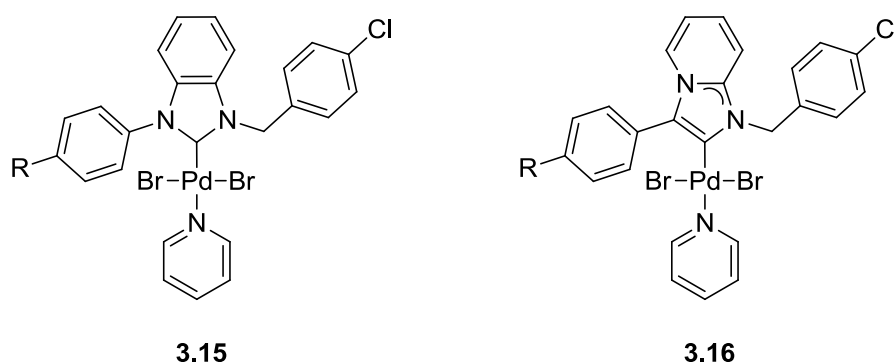


**Figure 3.8** General structures of normal and abnormal (NHC)-Pd complexes synthesised by Lee. R = H, OMe or F.

The authors calculated the %  $V_{\text{bur}}$  of the complexes, which revealed only minor steric differences between the isomeric pair of ligands, and reasoned that any difference in reactivity would likely be due to electronic and not steric factors. When tested for the Mizoroki-Heck reaction between 4-chloroanisole and styrene, with TBAB as the solvent and NaOAc as the base, the normal carbene complexes **3.15** only gave poor yields of the desired product (16-32%) whereas as the more electron donating abnormal carbene complexes allowed the synthesis of the same products in moderate yields (52-54%). As

they expected, complex **3.16** where R is an electron-donating methoxy group was the most active catalyst, giving the highest yields of cross-coupled products.

Shao and co-workers exchanged the pyridine based ligand for 1-methylimidazole and found that complex **3.17** was an effective catalyst for the Mizoroki-Heck reaction (Figure 3.9).<sup>40</sup>

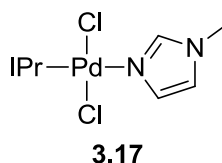


**Figure 3.9** Shao and co-workers PEPPSI-themed (NHC)-Pd complex.

Using the typical conditions found in the literature ( $\text{Cs}_2\text{CO}_3$  as the base, TBAB as an ionic liquid) the authors showed the complex **3.13** had a significantly broader substrate scope when coupling aryl chlorides and styrenes. A variety of functionalisation, both electron rich and electron poor groups, on the styrene coupling partner could be tolerated in the Mizoroki-Heck reaction with chlorobenzene. Notably, the yields of the coupling product of electron-rich aryl chlorides were as high as those of activated aryl chlorides (71-94%).

Currently, these PEPPSI-themed complexes represent some of the most efficient (NHC)-palladium based precatalysts for the Mizoroki-Heck reaction. Although (NHC)-palladium complexes are currently inferior to some of the phosphine based systems examined above, the performance gap between (NHC)- and phosphine-palladium complexes is getting narrower.

### 3.1.4 Investigation Aim

The Navarro group have recently synthesised a novel selection of (NHC)-Pd(II) complexes similar to the PEPPSI structure, but where the 'throw-away' pyridine ligand has been replaced by triethylamine. These complexes, with general formula  $(\text{NHC})\text{PdCl}_2(\text{TEA})$  (referred to henceforth as TEA-complexes) have been successfully

applied to Suzuki-Miyaura cross-couplings, Buchwald-Hartwig aminations and polymerisation reactions.<sup>57-59</sup> Furthermore, studies from our group have revealed that for both the Suzuki-Miyaura and Buchwald-Hartwig aminations, (NHC)-Pd complexes using TEA as the 'throw-away' ligand exhibit higher activity over other typical 'throw-away' ligands such as 3-chloropyridine, acetylacetonate and cinnamyl groups. Encouraged by the high activity of the TEA-complexes in other cross-coupling reactions, we set out to investigate the activity of the TEA-complexes in the Mizoroki-Heck reaction of aryl chlorides.

### 3.2 Results and Discussion

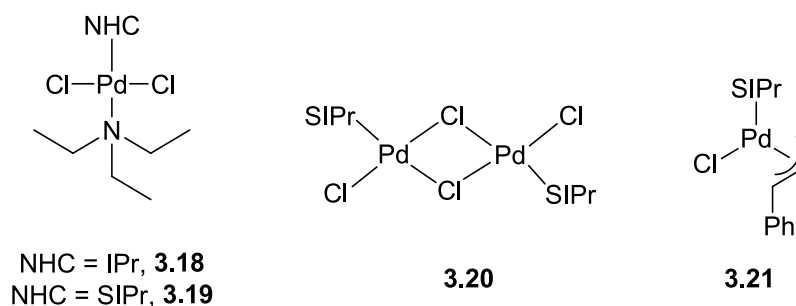
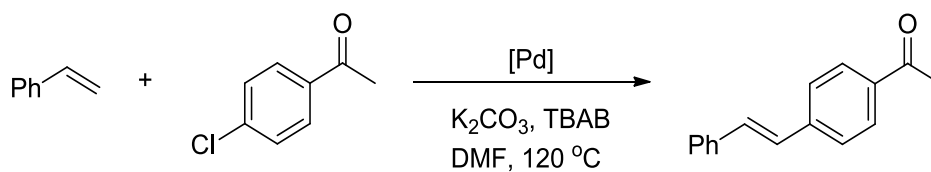


**Figure 3.10** (NHC)-Pd(II) complexes that were trialed for the Mizoroki-Heck reaction of 4-chloroacetophenone and styrene.

The investigation began by optimising the coupling between 4-chloroacetophenone and styrene, employing the successful reaction conditions reported by Liu and Lin as a starting point.<sup>41</sup> Hence anhydrous DMF (2mL) was used as a solvent, TBAB as an additive,  $\text{K}_2\text{CO}_3$  was employed as the base and the reaction conducted under an inert atmosphere. TEA-complexes **3.19** and **3.20** (Figure 3.10) were synthesised as was reported in the literature,<sup>57</sup> by the straightforward treatment of the appropriate dimer (which are commercially available, or easily synthesised) with triethylamine in THF at room temperature. Our initial trial showed that the reaction of 1 equivalent of 4-chloroacetophenone with 1.5 equivalents of styrene, catalysed by 1 mol% of **3.18** in the presence of 1.5 equivalents of TBAB at 120 °C could yield the

desired product in high yield, albeit in a non optimised reaction time of 9 h (Table 3.2, Entry 1).



**Scheme 3.21** Optimisation of the Mizoroki-Heck reaction between 4-chloroacetophenone and styrene.

Entry	[Pd] (mol%)	Time (h)	Yield (%) <sup>a</sup>
1	<b>3.18</b> (1)	9	94
2 <sup>b</sup>	<b>3.18</b> (1)	18	9
3 <sup>c</sup>	<b>3.18</b> (0.5)	6	94
4 <sup>c, d</sup>	<b>3.18</b> (0.5)	6	91
5 <sup>c, e</sup>	<b>3.18</b> (0.5)	6	51
6 <sup>c, d, f</sup>	<b>3.18</b> (0.125)	5	82
7 <sup>c, d, f</sup>	<b>3.19</b> (0.125)	5	97
8 <sup>c, d, f, g</sup>	<b>3.19</b> (0.125)	6	85
9 <sup>c, d, f, g</sup>	<b>3.20</b> (0.0625)	6	52
10 <sup>c, d, f, g</sup>	<b>3.21</b> (0.125)	5	62

**Table 3.2** Optimisation of the Mizoroki-Heck reaction between 4-chloroacetophenone and styrene

<sup>a</sup>Isolated yield of product, average of two runs. <sup>b</sup>No TBAB. <sup>c</sup>Styrene (1.1 equivalents) <sup>d</sup>TBAB (1 equivalent) <sup>e</sup>TBAB (0.5 equivalent) <sup>f</sup>DMF (1 mL). <sup>g</sup>In air, anhydrous solvent.

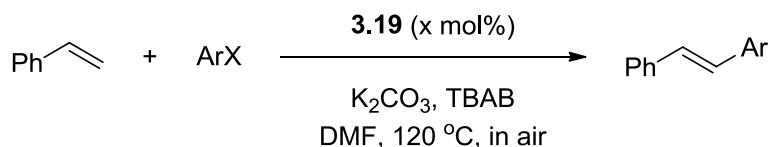
Unsurprisingly, using the same reaction conditions in the absence of the TBAB additive the reaction did not proceed smoothly, despite having doubled the reaction



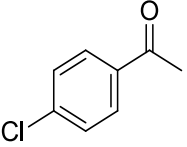
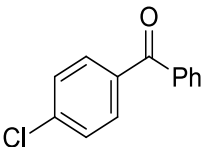
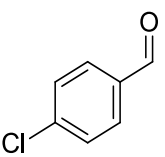
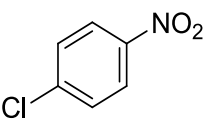
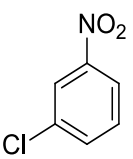
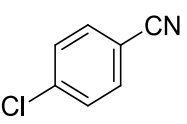
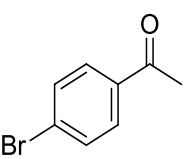
time, a poor yield of coupled stilbene was obtained (Table 3.2, entry 2). In order to make the reaction more economical, we next explored whether the catalyst loading could be successfully decreased, along with the equivalents of reagents used, without having a detrimental effect on the reaction. Decreasing the catalyst loading to 0.5 mol% and reduction of the excess of styrene to 1.1 equivalents still allowed the stilbene product to be obtained in a high yield (Table 3.2, Entry 3), and the reduction of the equivalents of TBAB from 1.5 to 1 showed no significant detriment to the product yield (Table 3.2, Entry 4). This was not the case when the amount of TBAB was further lowered to 0.5 equivalents, as reflected by the decrease in yield from 91% to 51% (Table 3.2, entry 5). Increasing the concentration of the reaction mixture by lowering the volume of DMF to 1 ml allowed for a further reduction of the catalyst loading of **3.18** to 0.125 mol% whilst maintaining a respectable, albeit decreased yield of 82% (Table 3.2, entry 6). Using a different NHC, SIPr, (complex **3.19**) under the same conditions the yield was vastly improved to 97% (Table 3.2, entry 7). We also investigated the possibility of performing the reactions in air, since reactions that do not require inert atmosphere or rigorously anhydrous conditions are more convenient to conduct on either a laboratory or an industrial scale. Only a 12% decrease in yield was observed when the reaction was carried out in air, providing a good yield of 85%. It should be noted that once complete the reaction mixtures were black in colour, which is characteristic of Pd-NPs. However, when the reaction (Table, 3.2, Entry 8) was followed by GC at time intervals of thirty minutes, it was apparent that most conversion was occurring before the generation of Pd-NPs (in the first 3 hours). This suggests that there is a NHC-Pd molecular catalyst operating before the Pd-NPs are generated, which may or may not aid in completing the conversion. We also carried out a comparison with parent dimer **3.20**, recently reported by Cazin and co-workers as a highly active catalyst for Mizoroki-Heck reactions using exceptionally low catalyst loadings (100-200 ppm).<sup>60</sup> The authors only examined activated and deactivated aryl bromides as substrates, with no attempts made to activate aryl chlorides in the Mizoroki-Heck

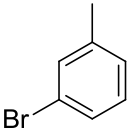
reactions. The coupling of 4-chloroacetophenone with styrene under our reaction conditions catalysed by **3.20** afforded only 52% of the desired stilbene product (Table 3.2, entry 9), showing that the dimer **3.20** is capable of facilitating the coupling of electron-poor aryl chlorides, but is not as active as the corresponding TEA-complex **3.19**. (NHC)-palladium complexes that use a cinnamyl group as the ‘throw-away’ ligand have been shown to have high activity in other cross-coupling reactions and anaerobic oxidation reactions.<sup>61,62</sup> However, only a moderate yield was obtained when (SIPr)Pd(cinnamyl)Cl **3.21** was utilised as the precatalyst under our reaction conditions (Table 3.2, entry 10). Throughout the reactions performed during the optimisation, only the (*E*) isomer was isolated, the (*Z*) isomer was not observed by <sup>1</sup>H NMR or GC.

The application of these optimised conditions to the aryl chlorides activated with an electron-withdrawing ketone group in the *para*-position, 4-chloroacetophenone and 4-chlorobenzophenone, provided good yields of the desired coupling products in reasonable reaction times of 6 hours (Table 3.3, entry 1 and 2). Unfortunately, when other activated aryl chlorides with different electron-withdrawing groups were subject to the reaction conditions, it was evident that the reactions were not proceeding as smoothly as anticipated. The reaction of 4-chlorobenzaldehyde with styrene provided a reasonable GC conversion of 75%, albeit after a considerably longer reaction time, 18 h (Table 3.3, Entry 3).



**Scheme 3.22** Application of optimised conditions to the Mizoroki-Heck reactions of styrene and various aryl halides.

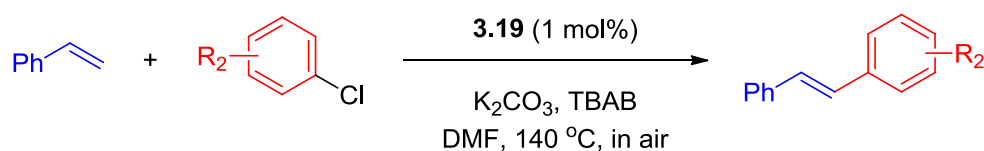
Entry	Time (h)	Catalyst Loading (mol%)	Aryl Halide	GC Conversion (%)	Isolated Yield (%) <sup>a</sup>
1	6	0.125		>99	85
2	6	0.25		>99	93
3	18	0.25		75	n.d.
4	22	0.25		28	n.d.
5	18	0.25		52	n.d.
6	22	0.25		7	n.d.
7	2	0.125		>99	97

8	18	0.125		<5	n.d.
---	----	-------	---	----	------

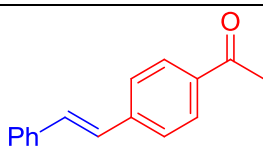
**Table 3.3** Application of optimised conditions to the Mizoroki-Heck reactions of styrene and various aryl halides. <sup>a</sup>Average of two runs.

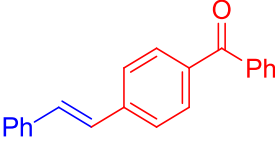
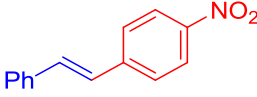
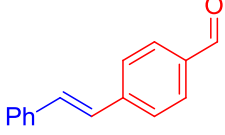
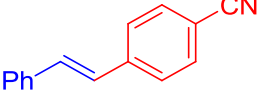
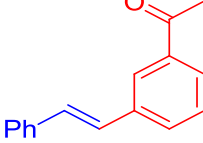
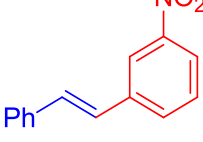
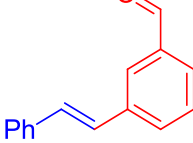
Similarly disappointing results were obtained with nitro- and cyano-substituted aryl chlorides (Table 3.3, entries 4 - 6). Whilst the coupling of 4-bromoacetophenone with styrene was successful in 2 h (97%), the coupling of 3-bromotoluene showed less than 5% conversion by GC even after 18 h (Table 3.3, entries 7 and 8).

In order to develop a general protocol that could be set up and carried out in air, we brought our conditions back in line with what is typically found in the literature, the temperature was increased to 140 °C and the catalyst loading of **3.19** was raised to 1 mol%. These new conditions allowed for successful couplings of aryl chlorides bearing a variety of electron-withdrawing groups that had proven problematic under our original optimised conditions (Scheme 3.22).



**Scheme 3.23** Revised Mizoroki-Heck reactions of styrene with activated aryl chlorides.

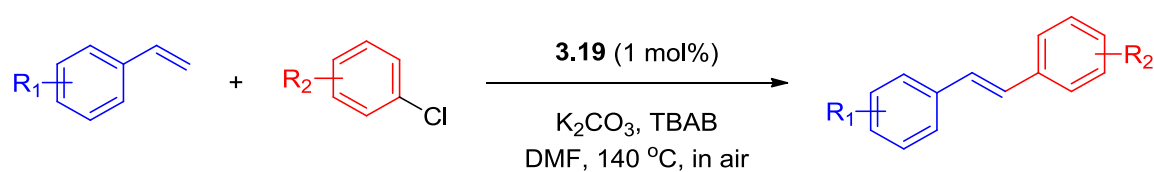
Entry	Time (h)	Product	Isolated Yield (%) <sup>a</sup>
1	1	 <b>3.22</b>	95

2	2	 <b>3.23</b>	96
3	2	 <b>3.24</b>	91
4	4	 <b>3.25</b>	81
5	6	 <b>3.26</b>	57
6	4	 <b>3.27</b>	64
7	2	 <b>3.28</b>	82
8	21	 <b>3.29</b>	56

**Table 3.4** Revised Mizoroki-Heck reactions of styrene with various activated aryl chlorides.

<sup>a</sup>Average of two runs.

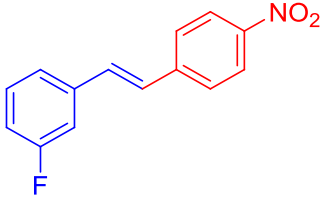
Aryl chlorides containing a *para* electron-withdrawing group gave good to excellent yields (Table 3.4, Entries 1 - 4, 82-96%) with the exception of 1-chloro-4-cyanobenzene which only gave a moderate yield (Table 3.4, Entry 5). *Meta*-substituted chlorides all gave decreased yields compared to their *para* isomers (Table 3.4, Entries 6 - 8), with 3-chlorobenzaldehyde taking a significantly longer reaction time than any other substrate tested, providing the lowest yield of 56%.



**Scheme 3.24** Revised Mizoroki-Heck reactions of substituted styrenes with activated aryl chlorides.

Entry	Time (h)	Product	Isolated Yield (%) <sup>a</sup>
1	4	<p style="text-align: center;"><b>3.30</b></p>	97
2	4	<p style="text-align: center;"><b>3.31</b></p>	90
3	4	<p style="text-align: center;"><b>3.32</b></p>	91

---

5	5		74
<b>3.33</b>			

---

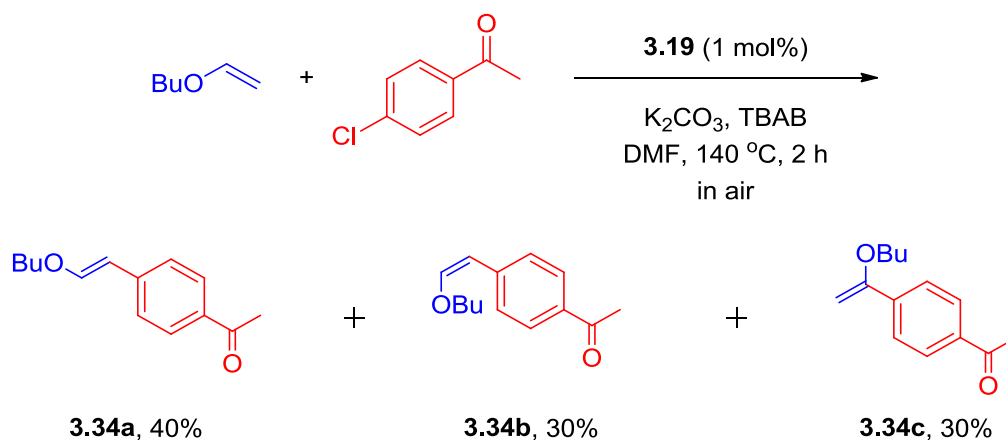
**Table 3.5** Revised Mizoroki-Heck reactions of substituted styrenes with activated aryl chlorides.

<sup>a</sup>Average of two runs. 0.5mmol of aryl halide.

Different functionalised styrenes were also tolerated, with electron-donating methyl and methoxy-substituted styrenes providing good yields of the corresponding coupling products **3.30** and **3.31** with 4'-chloroacetophenone (Table 3.5, Entries 1 and 2). An electron-withdrawing fluoride substituent on the styrene partner could also be tolerated with no detriment to the yield (Table 3.5, Entry 3). Compound **3.33** posed as an interesting synthetic target, as it has been shown to be a precursor to a  $\beta$ -amyloid aggregation inhibitor.<sup>63</sup> Hence a larger-scale reaction (2 mmol) was conducted and afforded an 83% yield of this intermediate in 7 hours.

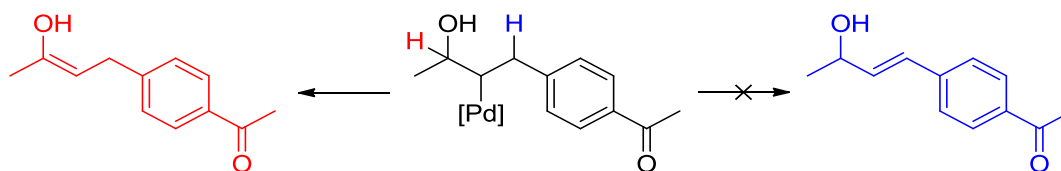
Having successfully involved numerous styrenes in the Mizoroki-Heck coupling with aryl chlorides, we turned our attention to other alkenes commonly employed in this reaction. Unfortunately electron-poor alkenes ethyl acrylate and methylvinylketone did not show any conversion to products using our reaction conditions. However, coupling 4'-chloroacetophenone with electron-rich *n*-butyl-vinyl ether was possible and gave a mixture of  $\alpha$ - and  $\beta$ -substituted products (Scheme 3.25, **3.34a-c**) as expected (see section 3.1.2.3). Changing the catalyst from the SIPr-bearing **3.19** to IPr-bearing **3.18** had no appreciable effect on the distribution of isomeric products. Of note, the (*E*) and (*Z*) products such as **3.34a** and **3.34b** are typically reported in the literature as a mixture, presumably due to problematic separation, and <sup>1</sup>H NMR is used to determine the ratio between them.<sup>30,64</sup> In our hands, however, all three isomers could be separated by column chromatography. Vinyl ethers **3.34b** and **3.34c** were notably unstable in CDCl<sub>3</sub>

as decomposition was observed by  $^{13}\text{C}$  NMR during long data collections. The same behaviour was not exhibited by the (*E*) isomer **3.34a**.



**Scheme 3.25** Mizoroki-Heck reaction of 4-chloroacetophenone with butylvinylether. Yields depicted are of isolated product after flash chromatography, average of 2 runs.

Encouraged by Gaviño and Cárdenas' study on the Mizoroki-Heck reaction of allylic alcohols with aryl bromides,<sup>65</sup> we tested this variety of alkene under our reaction conditions with 4'-chloroacetophenone. Allyl alcohol gave no conversion, however secondary allylic alcohol but-3-en-2-ol provided the corresponding ketone product **3.37** in a moderate yield (Table 3.6, Entry 3). The ketone originates from the  $\beta$ -hydride elimination step, where the enol is evidently formed in preference to the allylic alcohol (Scheme 3.26). The enol can then tautomerise to the more stable ketone form **3.37**.

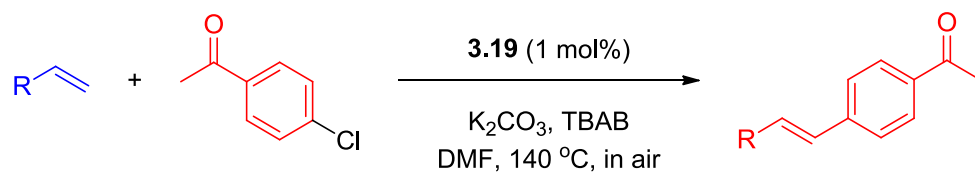


**Scheme 3.26** Possible pathways for  $\beta$ -hydrogen elimination.

Tertiary allylic alcohol 2-methylbut-3-en-2-ol afforded the coupled product **3.36** in a moderate yield (Table 3.6, Entry 2). The absence of a  $\beta$ -hydrogen precluded the formation of the corresponding ketone. Simple chain alkenes could also be employed in



the reaction, but less efficiently than with styrenes. For example, hex-1-ene gave an inferior yield (Table 3.6, Entry 1) than for styrene and its derivatives.



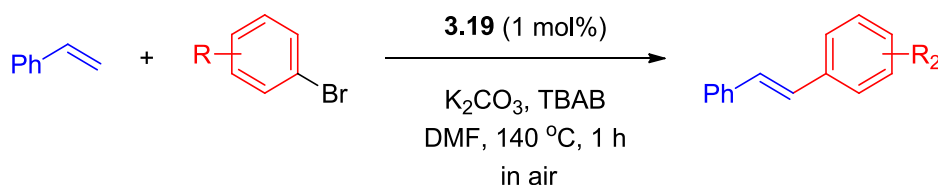
**Scheme 3.27** Mizoroki-Heck reactions of various alkenes and 4'-chloroacetophenone.

Entry	Time (h)	Product	Isolated Yield (%) <sup>a</sup>
1	2	<p style="text-align: center;"><b>3.35</b></p>	64
2	2	<p style="text-align: center;"><b>3.36</b></p>	54
3	2	<p style="text-align: center;"><b>3.37</b></p>	65

**Table 3.6** Mizoroki-Heck reactions of various alkenes and 4'-chloroacetophenone. <sup>a</sup>Average of two runs.

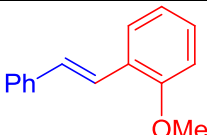
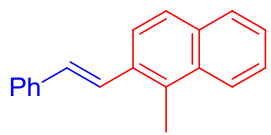
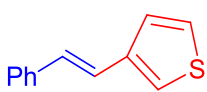
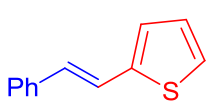
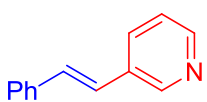
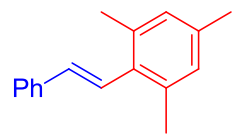
The reactivity of catalysts **3.18** and **3.19** towards aryl chlorides was limited to activated substrates. Attempts to couple styrene with unactivated chlorides such as chlorobenzene or 4-chlorotoluene were unsuccessful and only traces (< 5% by GC) of the desired products were observed, despite extended reaction times, larger catalyst loadings and

higher temperatures. In order to have access to electron-rich aryl groups, as well as heteroaromatic groups, we turned our focus towards the coupling of unactivated aryl bromides. Under the same reaction conditions as for the aryl chlorides, a variety of aryl and heteroaryl bromides could be coupled with styrene in good yields and generally much shorter times than those required for aryl chlorides (Scheme 3.28).



**Scheme 3.28** Mizoroki-Heck reactions of aryl bromides with styrene catalysed by **3.19** in air.

Entry	Product	Isolated Yield (%) <sup>a</sup>
1	 <b>3.38</b>	90
2	 <b>3.39</b>	83
3	 <b>3.40</b>	81
4	 <b>3.41</b>	92

5	 <b>3.42</b>	81 <sup>b</sup>
6	 <b>3.43</b>	94
7	 <b>3.44</b>	84
8	 <b>3.45</b>	88
9	 <b>3.46</b>	83
10	 <b>3.47</b>	21 <sup>c</sup>

**Table 3.7** Mizoroki-Heck reactions of aryl bromides with styrene catalysed by **3.19** in air. <sup>a</sup>Average of two runs. <sup>b</sup>Reaction time was 4 h. <sup>c</sup>Reaction time was 23 h.

The isomers of bromotoluene showed the expected trend, with *p*-bromotoluene having the highest yield of 90% (Table 3.7, entry 1) and hindered *o*-bromotoluene providing a lower, but reasonable yield of 81% (Table 3.7, entry 3). *o*-Substituted 1-bromo-2-methylnaphthalene also gave the expected coupled product in excellent yield (Table 3.7, entry 6). When the more electron-donating methoxy group was incorporated, *p*-bromoanisole was coupled with styrene in an excellent yield of 92% (Table 3.7, entry

4). The more challenging *o*-bromoanisole still provided a good yield of 81% (Table 3.7, entry 5), although it required a reaction time four times longer than the majority of the other substrates. For heteroaromatic bromides, both thiophene- and pyridine-derived bromides could be successfully coupled with styrene to afford the corresponding products in good yields (Table 3.7, entries 7 - 9); we noted that 3-bromopyridine could be used in the coupling reaction, although this was not the case for the isomeric 2-bromopyridine. The limit of our catalytic system for aryl bromides was seemingly found in the di-*ortho* substituted mesityl bromide, which provided only a poor yield of 21% in a much longer reaction time of 23 hours.

The means by which the TEA-complexes **3.18** and **3.19** catalyse the Mizoroki-Heck is assumed to be in line with the accepted mechanism, whereby the reaction is catalysed by an (NHC)-Pd(0) species that is generated *in situ* from the TEA-palladium(II) complexes. In the absence of a phosphine ligand to reduce the palladium(II) complex to palladium(0) other reducing agents are often implicated, including: quaternary ammonium salts, the alkene coupling partner or amines.<sup>11</sup> Upon completion of our Mizoroki-Heck reactions a peak corresponding to tributylamine was always observed in the gas chromatogram. The same peak was not evident when the reaction mixture was stirred overnight at room temperature. We deduced the origin of the tributylamine to be as a result of thermal decomposition of TBAB under the reaction conditions, this may provide enough tertiary amine to affect the oxidation of the palladium(II) precatalyst to the presumed palladium(0) active species. Also, we cannot rule out potential assistance from palladium nanoparticles that may be eventually generated under the reaction conditions. The darkening of the reaction mixture was observed for the majority of the Mizoroki-Heck couplings, typically after 2-3 hours, and could be an indication that Pd-NPs had been formed. Although some conversion to product was observed by GC in all cases before the reaction mixture darkened.

### 3.3 Conclusions

The aim of this chapter was to explore the activity of the TEA-complexes towards the coupling of the aryl chlorides. We have successfully developed a general protocol for the Mirozoki-Heck coupling of activated aryl chlorides and a variety of styrenes. One highlight of which is that they are operationally simple and can be set up and carried out in air. Although this protocol could not be extended to electron-rich aryl chlorides, the coupling of a variety of challenging electron-rich bromides with alkenes could be achieved, in comparatively short reaction times with good to excellent yields of the desired products.

### 3.4 References

- (1) Heck, R. F. *J. Am. Chem. Soc.* **1968**, *90*, 5518–5526.
- (2) Heck, R. F. *J. Am. Chem. Soc.* **1968**, *90*, 5526–5531.
- (3) Heck, R. F. *J. Am. Chem. Soc.* **1968**, *90*, 5531–5534.
- (4) Heck, R. F. *J. Am. Chem. Soc.* **1968**, *90*, 5535–5538.
- (5) Heck, R. F. *J. Am. Chem. Soc.* **1968**, *90*, 5538–5542.
- (6) Fitton, P.; McKeon, J. E. *Chem. Commun. (London)* **1968**, 4–6.
- (7) Fitton, P.; Johnson, M. P.; McKeon, J. E. *Chem. Commun. (London)* **1968**, 6.
- (8) Mizoroki, T.; Mori, K.; Ozaki, A. *Bull. Chem. Soc. Jpn.* **1971**, *44*, 581–581.
- (9) Heck, R. F.; Nolley, J. P. *J. Org. Chem.* **1972**, *37*, 2320–2322.
- (10) de Meijere, A.; Meyer, F. E. *Angew. Chem. Int. Ed.* **1995**, *33*, 2379–2411.
- (11) Beletskaya, I. P.; Cheprakov, A. V. *Chem. Rev.* **2000**, *100*, 3009–3066.
- (12) Miyaura, N.; Suzuki, A. *Chem. Rev.* **1995**, *95*, 2457–2483.
- (13) Slagt, V. F.; de Vries, A. H. M.; de Vries, J. G.; Kellogg, R. M. *Org. Process Res. Dev.* **2010**, *14*, 30–47.
- (14) Cabri, W.; Candiani, I. *Acc. Chem. Res.* **1995**, *28*, 2–7.
- (15) Beller, M.; Riermeier, T. H. *Eur. J. Inorg. Chem.* **1998**, *1998*, 29–35.
- (16) Littke, A. F.; Fu, G. C. *Angew. Chem. Int. Ed.* **2002**, *41*, 4176–4211.
- (17) Ben-David, Y.; Portnoy, M.; Gozin, M.; Milstein, D. *Organometallics* **1992**, *11*, 1995–1996.
- (18) Portnoy, M.; Ben-David, Y.; Milstein, D. *Organometallics* **1993**, *12*, 4734–4735.

- (19) Herrmann, W. A.; Brossmer, C.; Öfele, K.; Reisinger, C.-P.; Priermeier, T.; Beller, M.; Fischer, H. *Angew. Chem. Int. Ed.* **1995**, *34*, 1844–1848.
- (20) Herrmann, W. A.; Brossmer, C.; Reisinger, C.-P.; Riermeier, T. H.; Öfele, K.; Beller, M. *Chem. Eur. J.* **1997**, *3*, 1357–1364.
- (21) Beller, M.; Zapf, A. *Synlett* **1998**, 1998, 792–793.
- (22) Shaughnessy, K. H.; Kim, P.; Hartwig, J. F. *J. Am. Chem. Soc.* **1999**, *121*, 2123–2132.
- (23) Littke, A. F.; Fu, G. C. *J. Org. Chem.* **1999**, *64*, 10–11.
- (24) Iyer, S.; Ramesh, C. *Tetrahedron Lett.* **2000**, *41*, 8981–8984.
- (25) Morales-Morales, D.; Redón, R.; Yung, C.; Jensen, C. M. *Chem. Comm.* **2000**, 1619–1620.
- (26) Reetz, M. T.; Westermann, E. *Angew. Chem. Int. Ed.* **2000**, *39*, 165–168.
- (27) McGuinness, D. S.; Cavell, K. J. *Organometallics* **2000**, *19*, 741–748.
- (28) Gruber, A. S.; Zim, D.; Ebeling, G.; Monteiro, A. L.; Dupont, J. *Org. Lett.* **2000**, *2*, 1287–1290.
- (29) Peris, E.; Mata, J.; Loch, J. A.; Crabtree, R. H. *Chem. Comm.* **2001**, 201–202.
- (30) Littke, A. F.; Fu, G. C. *J. Am. Chem. Soc.* **2001**, *123*, 6989–7000.
- (31) Böhm, V. P. W.; Herrmann, W. A. *Chem. Eur. J.* **2001**, *7*, 4191–4197.
- (32) Selvakumar, K.; Zapf, A.; Beller, M. *Org. Lett.* **2002**, *4*, 3031–3033.
- (33) Bedford, R. B. *Chem. Commun.* **2003**, 1787.
- (34) Ruan, J.; Iggo, J. A.; Berry, N. G.; Xiao, J. *J. Am. Chem. Soc.* **2010**, *132*, 16689–16699.
- (35) Chandrasekhar, V.; Narayanan, R. S. *Tetrahedron Lett.* **2011**, *52*, 3527–3531.
- (36) Xu, H.-J.; Zhao, Y.-Q.; Zhou, X.-F. *J. Org. Chem.* **2011**, *76*, 8036–8041.
- (37) Lee, D.-H.; Taher, A.; Hossain, S.; Jin, M.-J. *Org. Lett.* **2011**, *13*, 5540–5543.
- (38) Heshmatpour, F.; Abazari, R.; Balalaie, S. *Tetrahedron* **2012**, *68*, 3001–3011.
- (39) Wang, W.; Yang, Q.; Zhou, R.; Fu, H.-Y.; Li, R.-X.; Chen, H.; Li, X.-J. *J. Organomet. Chem.* **2012**, *697*, 1–5.
- (40) Gao, T.-T.; Jin, A.-P.; Shao, L.-X. *Beilstein J. Org. Chem.* **2012**, *8*, 1916–1919.
- (41) Lin, Y.-C.; Hsueh, H.-H.; Kanne, S.; Chang, L.-K.; Liu, F.-C.; Lin, I. J. B.; Lee, G.-H.; Peng, S.-M. *Organometallics* **2013**, *32*, 3859–3869.
- (42) Ke, C.-H.; Kuo, B.-C.; Nandi, D.; Lee, H. M. *Organometallics* **2013**, *32*, 4775–4784.
- (43) Gürtler, C.; Buchwald, S. L. *Chem. Eur. J.* **1999**, *5*, 3107–3112.

- (44) Frey, G. D.; Schütz, J.; Herdtweck, E.; Herrmann, W. A. *Organometallics* **2005**, *24*, 4416–4426.
- (45) Eberhard, M. R. *Org. Lett.* **2004**, *6*, 2125–2128.
- (46) Balanta, A.; Godard, C.; Claver, C. *Chem. Soc. Rev.* **2011**, *40*, 4973–4985.
- (47) de Vries, J. G. *Dalton Trans.* **2006**, 421–429.
- (48) Jeffery, T. *Chem. Comm.* **1984**, 1287–1289.
- (49) Astruc, D. *Inorg. Chem.* **2007**, *46*, 1884–1894.
- (50) Herrmann, W. A.; Elison, M.; Fischer, J.; Koecher, C.; Artus, G. R. *Angew. Chem. Int. Ed.* **1995**, *34*, 2371–2374.
- (51) Lee, J.-Y.; Cheng, P.-Y.; Tsai, Y.-H.; Lin, G.-R.; Liu, S.-P.; Sie, M.-H.; Lee, H. M. *Organometallics* **2010**, *29*, 3901–3911.
- (52) Liao, C.-Y.; Chan, K.-T.; Zeng, J. Y.; Hu, C.-H.; Tu, C.-Y.; Lee, H. M. *Organometallics* **2007**, *26*, 1692–1702.
- (53) O'Brien, C. J.; Kantchev, E. A. B.; Valente, C.; Hadei, N.; Chass, G. A.; Lough, A.; Hopkinson, A. C.; Organ, M. G. *Chem. Eur. J.* **2006**, *12*, 4743–4748.
- (54) Organ, M.; Chass, G.; Fang, D.-C.; Hopkinson, A.; Valente, C. *Synthesis* **2008**, 2008, 2776–2797.
- (55) Valente, C.; Calimsiz, S.; Hoi, K. H.; Mallik, D.; Sayah, M.; Organ, M. G. *Angew. Chem. Int. Ed.* **2012**, *51*, 3314–3332.
- (56) Keske, E. C.; Zenkina, O. V.; Wang, R.; Crudden, C. M. *Organometallics* **2012**, *31*, 6215–6221.
- (57) Chen, M.-T.; Vicic, D. A.; Chain, W. J.; Turner, M. L.; Navarro, O. *Organometallics* **2011**, *30*, 6770–6773.
- (58) Guest, D.; Chen, M.-T.; Tizzard, G. J.; Coles, S. J.; Turner, M. L.; Navarro, O. *Eur. J. Inorg. Chem.* **2014**, 2014, 2200–2203.
- (59) Sprick, R. S.; Hoyos, M.; Chen, M.-T.; Turner, M. L.; Navarro, O. *J. Polym. Sci. Part A: Polym. Chem.* **2013**, *51*, 4904–4911.
- (60) Tessin, U. I.; Bantreil, X.; Songis, O.; Cazin, C. S. J. *Eur. J. Inorg. Chem.* **2013**, 2013, 2007–2010.
- (61) Landers, B.; Berini, C.; Wang, C.; Navarro, O. *J. Org. Chem.* **2011**, *76*, 1390–1397.
- (62) Marion, N.; Navarro, O.; Mei, J.; Stevens, E. D.; Scott, N. M.; Nolan, S. P. *J. Am. Chem. Soc.* **2006**, *128*, 4101–4111.
- (63) Simons, L. J.; Caprathe, B. W.; Callahan, M.; Graham, J. M.; Kimura, T.; Lai,

- Y.; LeVine, H., III; Lipinski, W.; Sakkab, A. T.; Tasaki, Y.; Walker, L. C.; Yasunaga, T.; Ye, Y.; Zhuang, N.; Augelli-Szafran, C. E. *Bioorg. Med. Chem. Lett.* **2009**, *19*, 654–657.
- (64) Datta, G. K.; Schenck, von, H.; Hallberg, A.; Larhed, M. *J. Org. Chem.* **2006**, *71*, 3896–3903.
- (65) Sauza, A.; Morales-Serna, J.; García-Molina, M.; Gaviño, R.; Cárdenas, J. *Synthesis* **2011**, *2012*, 272–282.



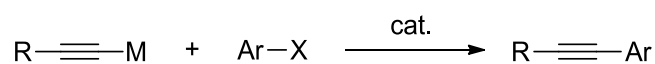
## CHAPTER 4

## 4. Sonogashira Couplings Catalysed by Collaborative (NHC)-Copper and -Palladium Complexes

### 4.1 Background

#### 4.1.1 Discovery of the Sonogashira Reaction

A seminal study by Castro and Stephens in 1963 demonstrated that aryl iodides could effectively be coupled with preformed cuprous acetylides as a convenient preparation of arylated alkynes (Scheme 4.1).<sup>1</sup> Over ten years later the groups of Heck and Cassar independently accomplished this C(sp)-C(sp<sup>2</sup>) bond formation from alkynes and aryl iodides in the presence of a palladium catalyst.<sup>2,3</sup> Sonogashira and co-worker's breakthrough was to realise that this coupling could be enhanced by forming the copper acetylide *in situ* by the addition of CuI to the system.<sup>4</sup> This allowed the coupling to be carried out under much milder conditions, i.e. at room temperature.



Castro-Stephens: M = [Cu]  
 Heck-Cassar: M = H, cat. = [Pd]  
 Sonogashira: M = H, cat. = [Pd], [Cu]

**Scheme 4.1** Early protocols for C(sp)-C(sp<sup>2</sup>) coupling reactions.

The Sonogashira coupling is generally used today as a global term to describe the coupling of an aromatic halide to a terminal alkyne to gain access to arylated alkynes by means of a transition metal catalyst.<sup>5-7</sup>

### 4.1.2 Mechanism

There is little in-depth mechanistic detail about the Sonogashira reaction in the literature. The currently accepted mechanism is similar to that which was proposed in the original publication:<sup>4</sup> two catalytic cycles, one for palladium and one for copper, acting in tandem (Figure 4.1). The palladium cycle follows the general mechanism for cross-coupling reactions. The first two steps of the palladium cycle are omitted from the following discussion, as they are much the same as the Mirozoki-Heck reaction described in section 3.1.2.

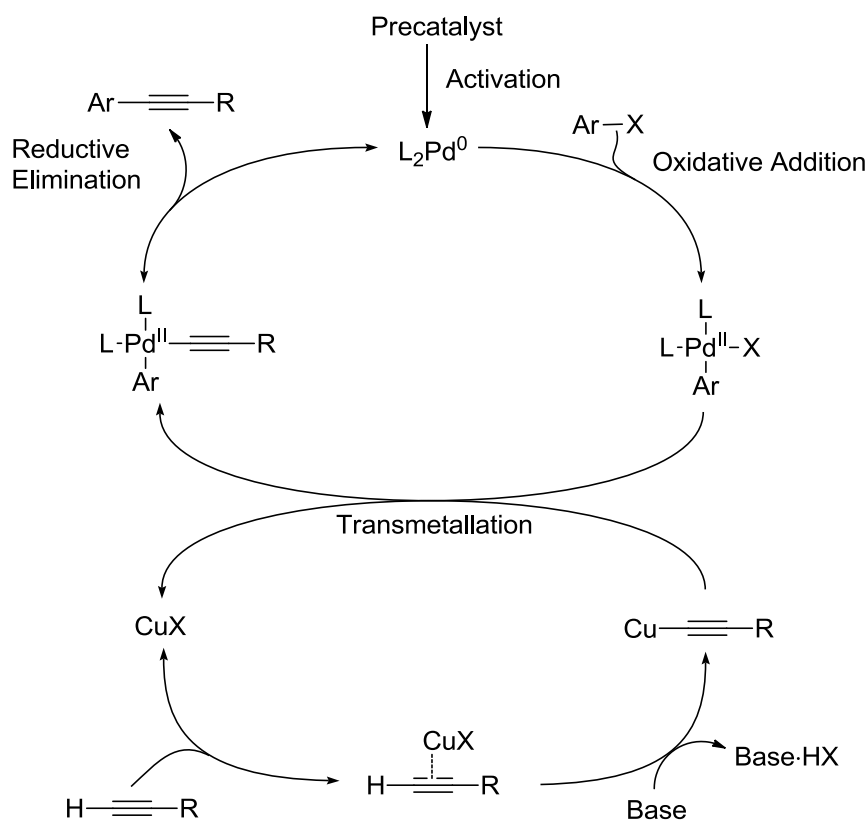


**Figure 4.1** Classic catalytic cycle for the Sonogashira reaction.

While the 14-electron palladium(0) species has been generated and undergoes oxidative addition with the aryl halide, the copper cycle forms the acetylide to undergo transmetalation. The copper cycle of the Sonogashira reaction is still not well known. The most accepted hypothesis is that the terminal proton of the alkyne is deprotonated in the presence of a copper(I) salt to form the copper acetylide.<sup>5</sup> Typical bases used for

the Sonogashira reaction are amines such as TEA, or inorganic bases such as  $\text{K}_2\text{CO}_3$ . As the  $\text{pK}_a$  of phenyl acetylene ( $\text{PhCCH}$ ), for example, is 23 and the  $\text{pK}_a$  of TEA and  $\text{K}_2\text{CO}_3$  are approximately 11 and 10, respectively, it is clear that these bases are not strong enough to deprotonate the alkyne directly. To account for this it is assumed that, in a similar manner to the formation of silver acetylides,<sup>8</sup> the alkyne forms a  $\pi$ -complex with the copper(I) which then enhances the acidity of the proton so that deprotonation can occur. The transmetalation can then take place followed by reductive elimination, yielding the desired product and the starting catalytic palladium(0) species.

### 4.1.3 Development of Alternative Sonogashira Protocols

#### 4.1.3.1 Palladium-Only Systems

Sonogashira's addition of copper(I) salt to Heck and Cassar's original conditions had the advantage of being more active and required milder conditions, although it did mean that the reaction was rendered air sensitive. In the presence of oxygen, copper(I) salts couple acetylenes to form diacetylenes, in what is known as the Glaser-Hay coupling.<sup>9-11</sup> This potential side reaction in the Sonogashira conditions is avoided by using an inert atmosphere, but can also be omitted by removal of the copper(I) salt altogether. General advancements in the design of bulky electron-rich ligands resulting in the increased activity of palladium complexes have made this possible. Consequently, the copper-free Sonogashira reaction (sometimes known as Heck alkynylation) has received renewed interest and there are now numerous examples of such reactions in the literature.<sup>12-23</sup>

Before examining the catalytic systems that made these advancements possible, the mechanism of the copper-free transformation will be examined.

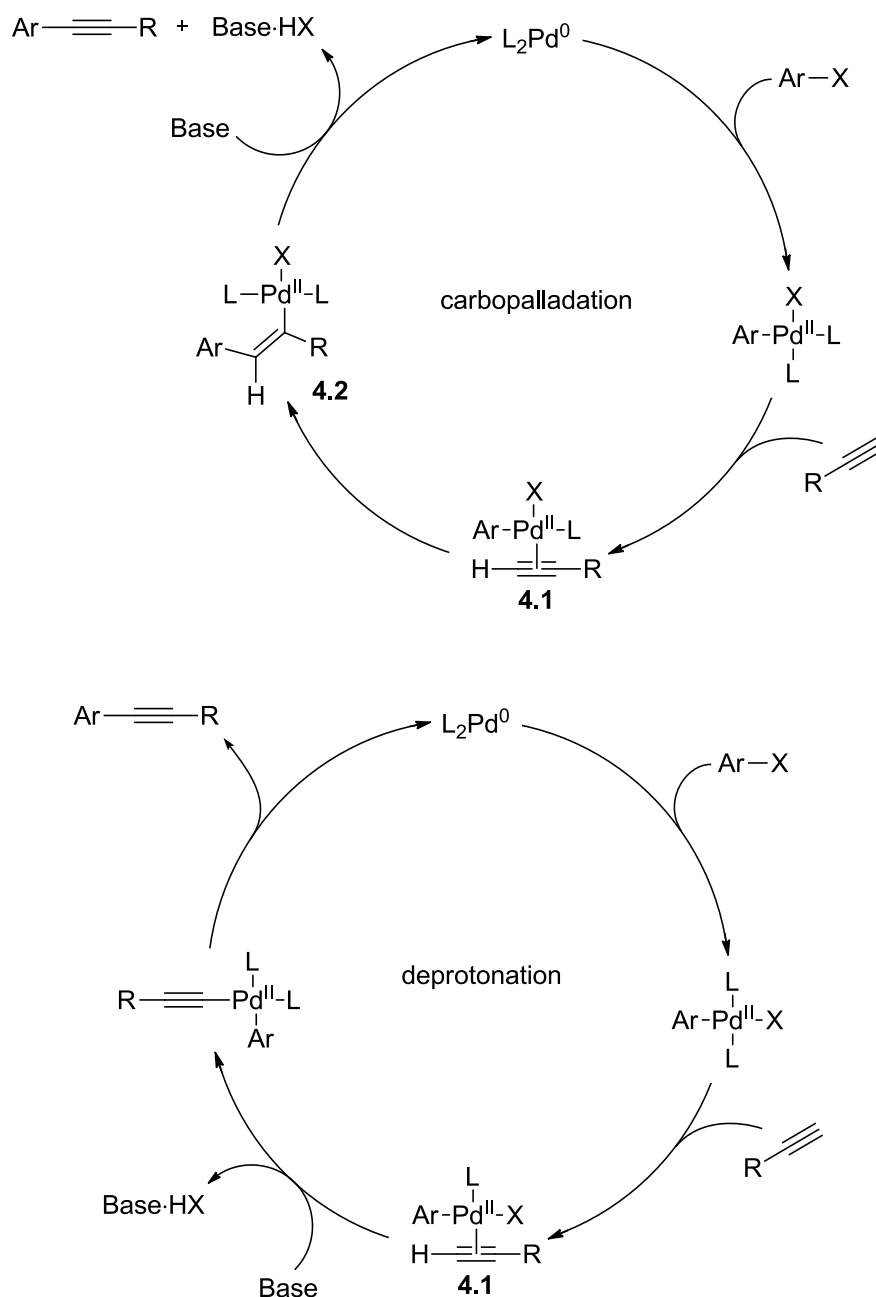
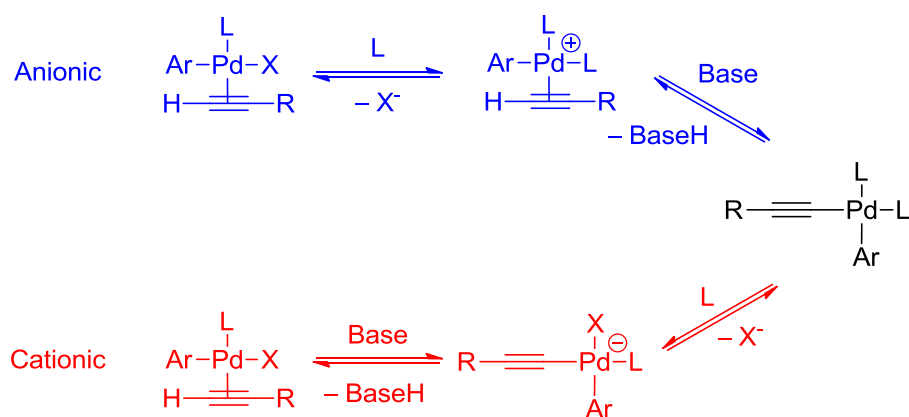


**Figure 4.2** Carbopalladation and deprotonation, two possible mechanism for the copper-free Sonogashira reaction.

The palladium-only mechanism has received more direct studies than its copper-co-catalysed counterpart, likely due to the simpler investigation of a single metal system. Two catalytic cycles have been proposed (Figure 4.2), one occurring by deprotonation<sup>21</sup> and the other by a carbopalladation route.<sup>3</sup> Both pathways involve the oxidative addition of an aryl halide followed by the formation of a side-bound  $\pi$ -

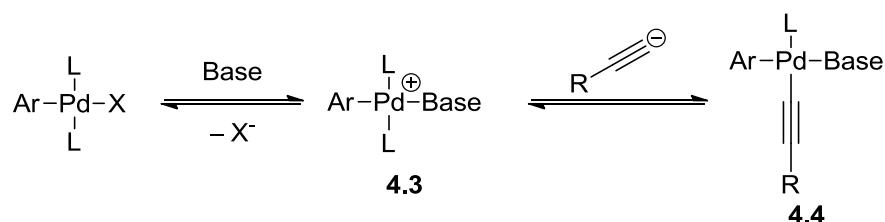
complex with the alkyne (**4.1**, Figure 4.2). The deprotonation pathway, as its name suggests, invokes the intervention of the base to remove the proton to form the end-on palladium acetylide complex, then reductive elimination directly forms the product. The carbopalladation pathway differs in that the Ar-Pd bond is added across the carbon-carbon triple bond of the alkyne and  $\beta$ -hydride elimination yields the cross-coupled product.

Reports by Amatore and Jutland revealed that alkynes can impede the oxidative addition to  $L_2Pd(0)$  by forming an  $[(\eta^2\text{-PhCCH})PdL_2]$  complex, which is unreactive.<sup>24</sup> The same group also published details about the additional role of amines when they are chosen as bases for these reactions.<sup>25</sup> Firstly, if a sufficiently donating amine is used they can form  $[(\text{amine})PdL]$  type complexes which show an enhanced activity towards oxidative additions. Secondly, they can compete for the Pd centre with one of L ligands from the *trans*- $[IPd(Ph)L_2]$  complex, opening the way for an amine-ligated catalytic cycle. In 2008 Mårtenson and co-workers showed, importantly, that the carbopalladation route can be discarded under typical Sonogashira reaction conditions.<sup>26</sup> They demonstrated this fact by synthesising several examples of the intermediate complex **4.2** by the oxidative addition of halostilbenes to  $PdL_2$ . No  $\beta$ -hydride elimination from this complex was detected, even after addition of excess base, and hence the expected arylated alkyne was not synthesised.



**Scheme 4.2** Cationic and anionic pathways for the deprotonation mechanism.

It was proposed, in the same work, that there are two possible pathways that can operate for the deprotonation mechanism, named as *cationic* and *anionic* by the authors. The difference between the two depending on which step comes first, the halide displacement or deprotonation (Scheme 4.2). Selectivity of these pathways is determined by the electronic nature of the *para*-substituted phenylacetylene being used. Electron-donating groups were suggested to favour the cationic pathway, while electron-withdrawing groups should favour the anionic pathway. Further experimental and theoretical investigation of these findings was conducted in 2012 by Ujaque and co-workers.<sup>27</sup> Calculations of the Gibbs energy profiles for the different mechanisms by DFT were performed. The results showed that, in agreement with Mårtensson's findings, the energy barrier for the carbopalladation mechanism is sufficiently high enough that it can be discounted. Furthermore, preference for the anionic and cationic pathways can indeed be predicted to some extent by the functionalisation of the alkyne. The author's theoretical approach also suggested that an alternative mechanism (Scheme 4.3), dubbed *ionic*, may also be plausible and in competition with the anionic and cationic pathways.



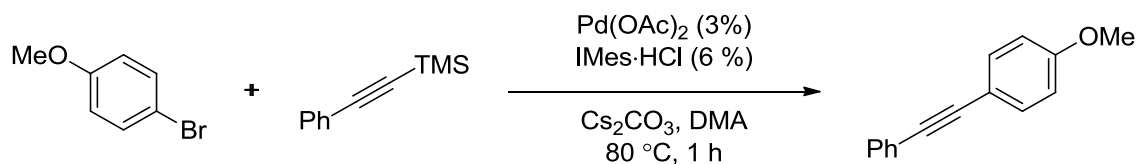
**Scheme 4.3.** Theoretical *ionic* mechanism proposed by Ujaque and co-workers. Base = pyrrolidine.

The difference between the ionic and deprotonation pathways (Scheme 4.3) is that the base substitutes the halide (X) before the coordination of the alkyne to form a  $\pi$ -complex. This gives intermediate **4.3** which, according to the calculated required energies for formation, is at least 5 kcal mol<sup>-1</sup> less than for the formation of alkyne  $\pi$ -complex **4.1**. Calculations showed that intermediate **4.3** can undergo exchange of an L ligand (phosphine) with phenylacetylide in an essentially barrier free process to give

**4.4**, which, after reductive elimination, would yield the product and the [(base)PdL] complex. The issue with this mechanism stems from the author's assumption that the use of excess base might mean the phenylacetylide anion is present in solution. As mentioned earlier the  $pK_a$  of terminal acetylene protons is such that they are unable to be directly deprotonated by amine bases. Even if an equilibrium was possible between the alkyne and acetylide, it would be significantly in favour of the alkyne. Therefore the reaction would, kinetically, be more likely to proceed by one of the deprotonation pathways, despite the higher energy barrier for the formation of the required alkyne  $\pi$ -complex.

As can be seen from some of the select examples that follow, the Cu-free Sonogashira reaction has followed a similar route to that of the Mizoroki-Heck reaction, in which bulky, electron-rich ligands have been used to activate aryl chlorides towards coupling.

Nolan and co-workers reported a Sonogashira protocol that makes use of an (NHC)-Pd complex.<sup>28</sup> After initial studies using phenylacetylene proved problematic due to the dimerisation of the alkyne, 1-phenyl-2-TMS-acetylene (TMS = trimethylsilyl) was used to suppress this side reaction. A screening of several NHCs, in their efficiency of coupling 4-bromoanisole and 1-phenyl-2-TMS-acetylene, established IMes to be the NHC of choice providing a yield of 87% (Scheme 4.4). Unfortunately only 4 examples of aryl bromides were coupled under Cu-free conditions. The other examples all required the addition of CuI to accelerate the reaction.



**Scheme 4.4** Nolan's (NHC)-Pd catalysed Sonogashira reaction.

Andrus and co-workers reported a palladium-only catalytic system containing an exceptionally bulky NHC ligand,<sup>22</sup> able to couple aryl bromides with different types of

alkynes (alkyl and aryl). They also reported good tolerance to the type of aryl bromide that could be used: electron-rich, *ortho* substituted, heteroaryl and alkenyl bromide examples were given. The downside of this catalytic system stems from its *in situ* formation from  $\text{Pd}(\text{PPh}_3)_2\text{Cl}_2$ : *t*-BuOK has to be used in conjunction with the additive 18-crown-6 in order to deprotonate the imidazolidium salt and generate the free carbene. *t*-BuOK is also very likely to be responsible for the reducing the palladium(II) complex to  $(\text{PPh}_3)_2\text{Pd}(0)$ . The carbene presumably then displaces one of the  $\text{PPh}_3$  ligands to form  $(\text{NHC})\text{Pd}(\text{PPh}_3)_n$ , but there is certainly ambiguity as to the exact nature of the active species. For example, the active species could be  $(\text{NHC})\text{Pd}(\text{PPh}_3)$  or  $(\text{NHC})\text{Pd}$ . It is likely that the NHC used (Figure 4.3) is sufficiently bulky to stabilise the reactive monoligated  $(\text{NHC})\text{Pd}$  species.

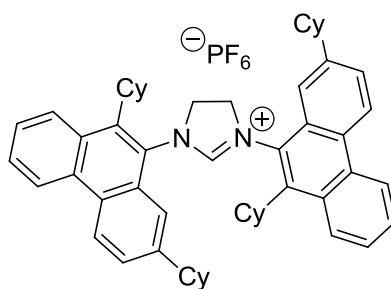


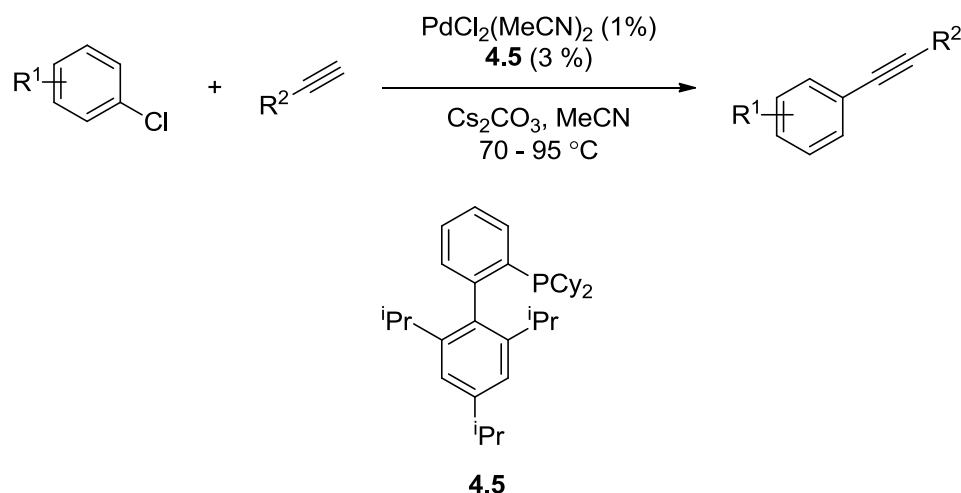
**Figure 4.3** Bulky NHC utilized by Andrus and co-workers for copper-free Sonogashira reactions.

The bulky electron-rich phosphine  $\text{P}(t\text{-Bu})_3$  has also been investigated for its activity in the Cu-free Sonogashira reaction. Hermann and Bölm screened 58 potential ligands for the coupling of an aryl bromide with phenylacetylene and TEA as the solvent and base, discovering that  $\text{P}(t\text{-Bu})_3$  gave the best outcome.<sup>23</sup> Soheili and co-workers at Merck found that in combination with  $[(\text{allyl})\text{PdCl}_2]_2$ , piperidine or DABCO in acetonitrile,  $\text{P}(t\text{-Bu})_3$  was able to affect the coupling of alkynes and aryl, alkenyl and heteroaryl bromides at room temperature in good to excellent yields. Of note was the coupling of 4'-chloroacetophenone with phenylacetylene in a moderate yield,<sup>21</sup> although raised temperatures were required. More recently Liu and co-workers used microwave heating to develop a rapid Sonogashira protocol capable of coupling



challenging aryl and heteroaryl chlorides with alkynes, with a Pd catalytic system involving  $P(t\text{-Bu})_3$ .<sup>18</sup> Although the high activity of these catalytic systems is certainly an advantage, one distinct disadvantage is the air sensitivity of  $P(t\text{-Bu})_3$  and the palladium(0) complexes that it forms.

Buchwald and co-workers have also applied the biaryldialkyl phosphine ligands developed by his group to the classical Sonogashira reaction of aryl chlorides and aryl tosylates (Scheme 4.5).<sup>29</sup> However, contrary to the usual effect that the addition of copper(I) salts have, it was found that including CuI in the catalytic system was detrimental to product formation; hence the system ended up as an example of a Cu-free Sonogashira protocol.



**Scheme 4.5** Buchwald phosphine-palladium complex for copper-free Sonogashira reactions.

Finally, Colacot and co-workers have reported their findings on the Cu-free Sonogashira reactions catalysed by well-defined palladium(II) and palladium(0) complexes of  $t\text{-Bu}_2(p\text{-NMe}_2\text{C}_6\text{H}_4)\text{P}$  (Figure 4.4).<sup>13</sup>

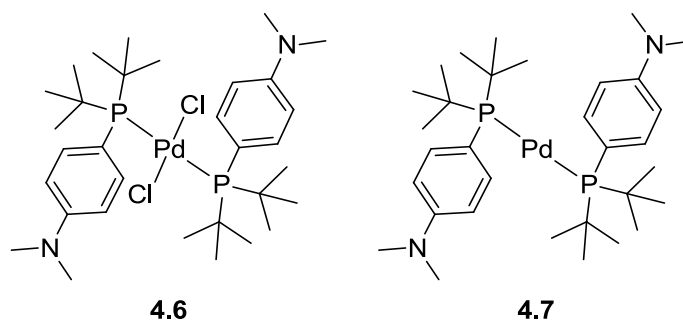


**Figure 4.4** Pd(II) and Pd(0) complexes, incorporating a bulky phosphine ligand, used by Colacot for copper-free Sonogashira reactions.

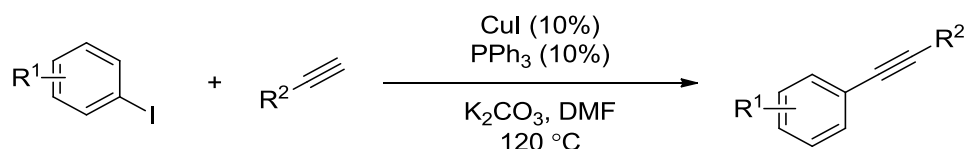
The group reported that the results obtained using either of these complexes was dependant on the aryl halide to be coupled. Air-stable palladium(II) complex **4.6** could be used effectively to couple a variety of different aryl and heteroaryl bromides or aryl chlorides; the use of the less stable, but more reactive, palladium(0) complex **4.7** was necessary in order to be able to couple heteroaryl chlorides. The authors found good tolerance of alkyl and alkenyl substituted acetylenes, but the use of non-*ortho* substituted phenylacetylenes in a one-pot fashion led to oligomerisation side products, therefore slow addition of the acetylene was necessary to obtain the desired yields. A comparison of P-Pd-P bond angle and the activity of similarly bulky phosphine  $L_2Pd(0)$  complexes revealed that where typical complexes of this type have a P-Pd-P bond angle of  $180^\circ$ , complex **4.7** has a smaller angle of  $175^\circ$ . The least active complexes were found to be those with larger P-Pd-P angles, such as in  $Pd(P(t-Bu)_3)_2$  ( $180^\circ$ ). Hence the authors proposed that, based on their structure-activity relationship study, the enhanced activity of palladium(0) complex **4.7** may be due to the smaller P-Pd-P angle.

#### 4.1.3.2 Copper-Only Systems

The desire to remove the relatively expensive palladium component from the catalytic Sonogashira protocol has driven the development of cheaper copper-only catalytic systems, which is commercially more appealing to industrial processes. The seminal work in this area, by Castro and Stephens,<sup>1</sup> demonstrated that copper acetylides can couple  $sp^2$  halides with acetylenes, albeit in a stoichiometric fashion. However,

these systems have to overcome the shortcomings that copper brings to this coupling reaction, primarily the air sensitive nature of the copper acetylide. Presented in this section are some select examples of such catalytic systems and is by no means exhaustive. A very recent mini-review provides a less in depth, but wider variety of copper catalysed Sonogashira reactions.<sup>30</sup>

In 1992 Miura and co-workers reported one of the earliest cases of a copper-catalysed Sonogashira reaction in a short communication.<sup>31</sup> The following year the group published a more detailed report on the scope of the reaction conditions, which utilised a catalytic system of a copper(I) salt and PPh<sub>3</sub> (Scheme 4.6).<sup>32</sup> During the optimisation reaction of coupling phenylacetylene and iodobenzene, CuI, CuBr and CuCl all proved to be suitable copper sources, whereas Cu(OAc)<sub>2</sub> and Cu<sub>2</sub>O were not. The ratio of PPh<sub>3</sub> to CuI was also noted to be important with little to no product being obtained when no phosphine was added; more than a twofold excess of phosphine also proved detrimental to the reaction. The optimal base was found to be K<sub>2</sub>CO<sub>3</sub> and organic bases suppressed product formation. With regard to the substrates, the reaction was found to tolerate a wide variety of functionalised acetylenes when being coupled with iodobenzene. Similarly, good yields were obtained when phenylacetylene was coupled with activated aryl iodides. The catalytic system struggled when electron-rich or *ortho*-substituted substrates were used, and products were generally only obtained in poor yields. Furthermore, the scope of the halide was found to be limited to iodides; using bromobenzene gave only a 5% yield of the coupled product. The authors demonstrated, however, that vinyl iodides could also be coupled under these conditions.



**Scheme 4.6** Miura and co-workers conditions for a copper-only Sonogashira reaction.

The authors postulated that the mechanism follows the catalytic cycle shown in Figure 4.5. Complex **4.8** is formed by coordination of the ligand added ( $\text{PPh}_3$ ) or by solvent, then acetylide complex **4.9** can be formed presumably by initial  $\pi$ -coordination and then subsequent deprotonation.

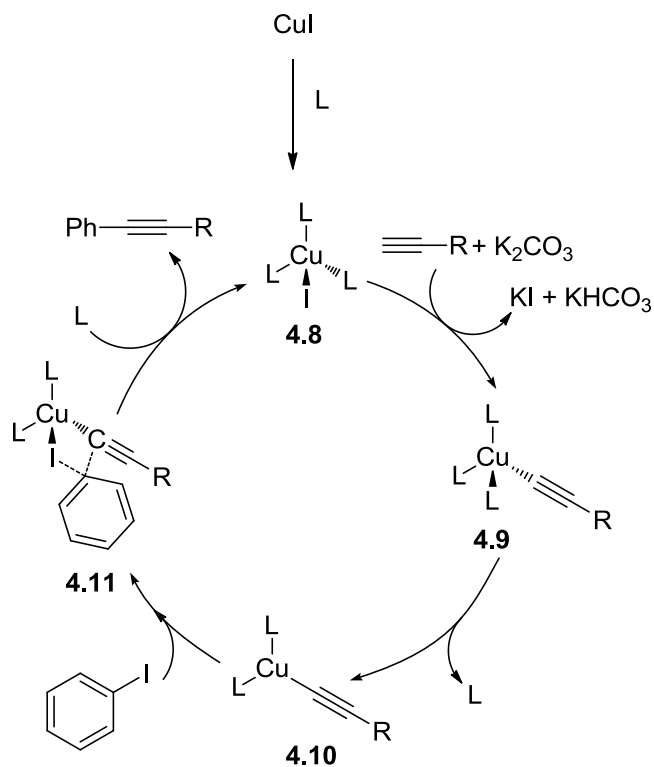
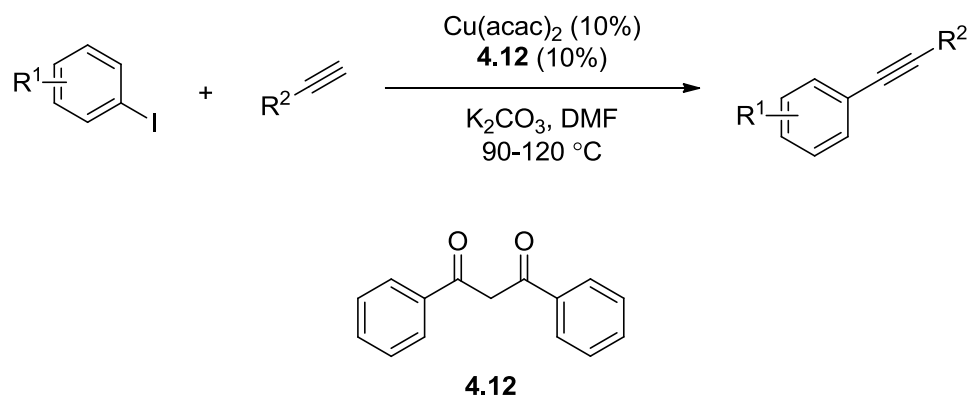


**Figure 4.5** Catalytic cycle proposed by Miura for the copper-only Sonogashira reaction.

It was deduced that coordinatively unsaturated complex **4.10** was a significant intermediate that must be formed for the reaction to proceed, for two reasons: increasing the phosphine: $\text{Cu}$  ratio past 2:1 and the use of more electron-donating phosphines than  $\text{PPh}_3$  both hindered the reaction. The C-C bond formation is then achieved in a concerted fashion by means of a 4-centered transition state (**4.11**). This was one of the most in-depth studies and convenient systems for the copper only Sonogashira reaction at the time.

An example of a copper-only Sonogashira protocol involving oxygen-containing ligands was reported by Taillefer and co-workers in 2008.<sup>33</sup> After screening a range of O and N-donor ligands with different copper sources the combination of  $\text{Cu}(\text{acac})_2$

(10%) and the  $\beta$ -diketone ligand **4.12** (30%) was established to give optimal activity (Scheme 4.7). Activated aryl iodides could then be coupled with phenyl and alkyl acetylenes at lower temperatures (90 °C) whereas both electron-neutral and -rich iodides required higher temperatures (120 °C).



**Scheme 4.7** Protocol for Taillefer's copper-only Sonogashira reaction using  $\beta$ -diketone ligand **4.12**.

The authors presented a different mechanism for their catalytic cycle than that proposed by Miura. The key difference is that the C-C bond formation is achieved by oxidative addition of the aryl iodide and then reductive elimination of the product (Figure 4.6), as opposed to the 4-centre concerted bond formation invoked by Miura. Taillefer's proposed cycle begins with complex **4.13** followed by the generation of the acetylide species **4.14** in the presence of a base. The next step is the oxidative addition of the PhI and can lead to either a cationic (**4.15**) or a neutral (**4.16**) copper(III). Reductive elimination from the copper(III) species releases the product and **4.13**, which starts the catalytic cycle again.

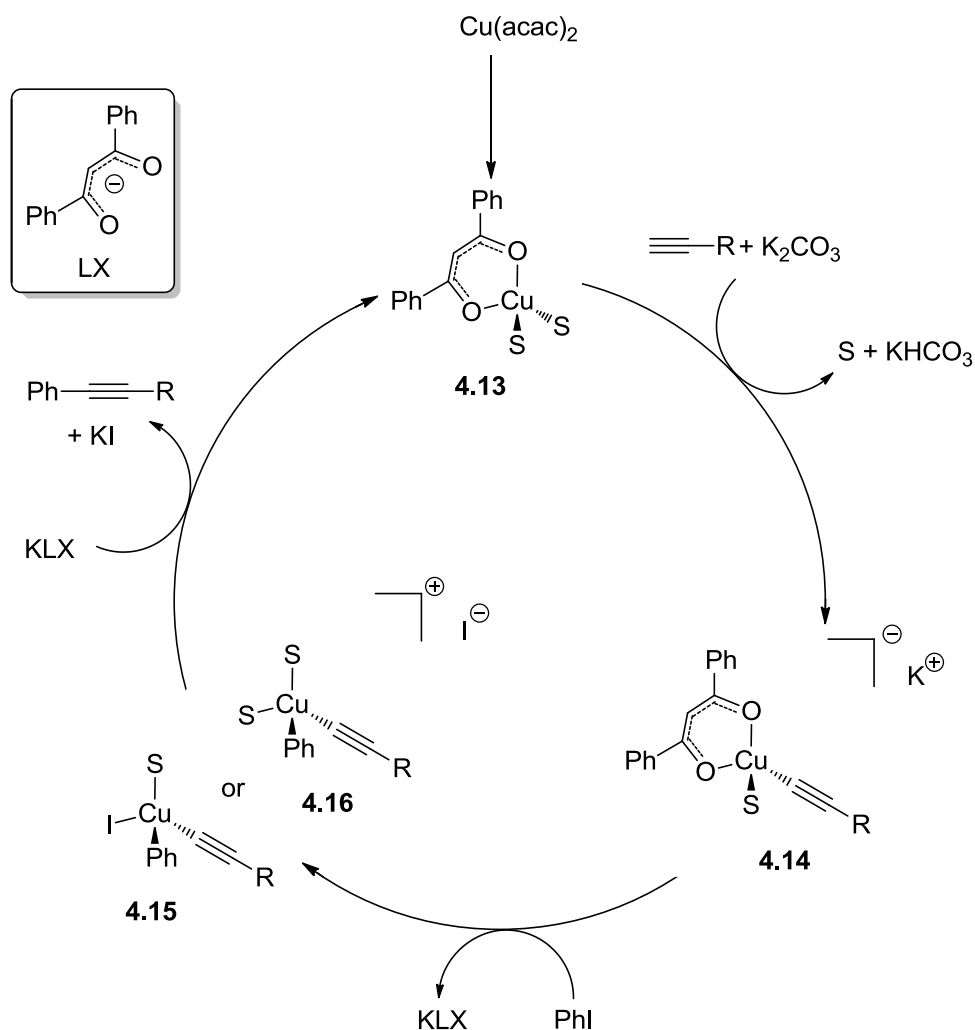


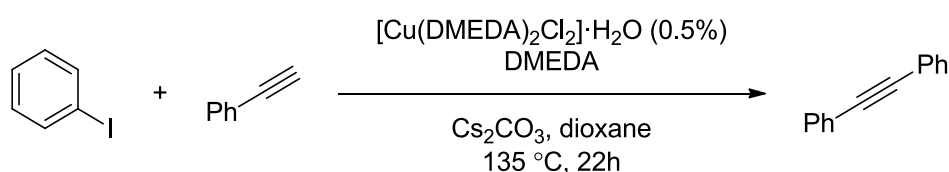
**Figure 4.6** Catalytic cycle proposed by Taillefer for the copper-only Sonogashira reaction.

$\text{S}$  = solvent.

Li and co-workers provided a protocol where the tricyclic diamine DABCO is employed as the ligand for  $\text{CuI}$ .<sup>34</sup> Unlike the previous system discussed, Li's catalytic system was able to couple phenylacetylene with unactivated aryl bromides (such as 4-bromoanisole), and could even be extended to the activated 4-chloroacetophenone although it was necessary for the addition of TBAB to enable good yields. Despite the improvement in the scope of substrates that could be used, the catalytic loading is still high, with 10% of  $\text{CuI}$  and 20% of DABCO being necessary. Combining this with the high temperatures (135-140 °C) and the need for the reaction to be conducted under an inert atmosphere still left significant room for improvement. These harsh conditions are

fairly common for the examples given so far, particularly the undesirably high catalyst loadings necessary to affect these copper-only Sonogashira reactions.

In 2010 a report by Lee and co-workers demonstrated that it was possible to carry out these reactions with much more reasonable catalyst loadings, without the need for an excess of ligand.<sup>35</sup> The use of the bisphosphine ligand Xantphos (1-2.5%) in combination with Cu<sub>2</sub>O (1-2.5%) in a 1:1 ratio, with Cs<sub>2</sub>CO<sub>3</sub> as the base, gave good to excellent yields for the coupling of aryl and alkyl acetylenes with a good range of aryl iodides.



**Scheme 4.8** Bolm's sub mol% copper-catalysed Sonogashira reaction.

DMEDA (%)	Yield [%] (GC)	
	3 h	22 h
0	3	14
30	48	>99
10,000 <sup>a</sup>	>99	>99

**Table 4.1** Table showing GC conversion of various ligand and catalyst ratios. <sup>a</sup>DMEDA as solvent.

In the same year Bolm and Zuidema took this further and presented the significant finding that sub-mol% levels of [Cu(DMEDA)<sub>2</sub>]Cl<sub>2</sub>·H<sub>2</sub>O could be used to catalyse the coupling of phenylacetylenes and aryl iodides (Scheme 4.8).<sup>36</sup> Table 4.1 shows how the excess of the diamine used (DMEDA) is important to obtain good conversions. When no excess DMEDA is added the reaction gives a poor yield, addition of 30% of DMEDA allows the reaction to go to completion in 22 h and when the

reaction is carried out in DMEDA as the solvent (10,000% excess) the reaction is completed in just 3 h. This increase in reaction rate with the increase of ligand excess is known as ligand accelerated catalysis.<sup>37</sup> From kinetic studies, the authors hypothesised that the resting state of the catalyst could be some polymeric complex. They further investigated the nature of the resting state by carrying out reactions systematically omitting components from the reaction mixture. When  $[\text{Cu}(\text{DMEDA})_2]\text{Cl}_2 \cdot \text{H}_2\text{O}$  was mixed with an excess of phenylacetylene in the presence of  $\text{Cs}_2\text{CO}_3$  and heated, a yellow precipitate was formed. Elemental analysis of the precipitate revealed that no nitrogen was present; hence there could be no DMEDA present in the complex. The carbon and hydrogen quantities suggested the yellow solid was a polymeric copper-acetylide cluster. From this information, the group proposed the mechanism shown in Figure 4.7. The  $[\text{Cu}(\text{DMEDA})_2]\text{Cl}_2 \cdot \text{H}_2\text{O}$  copper(II) precatalyst is reduced by DMEDA to form the copper(I) complex **4.17**. The monomeric copper acetylide species **4.18** is formed but is in equilibrium with the non-active polymeric species **4.19**. Addition of the diamine DMEDA shifts the equilibrium towards the monomeric acetylide species **4.18**, which can then go forward and react with the aryl halide, releasing the product and restarting the cycle. This highlights the importance of having a large Cu:ligand ratio (in this case 30 mol% DMEDA is 1:60) in order to break up the inactive Cu-acetylide polymeric species.



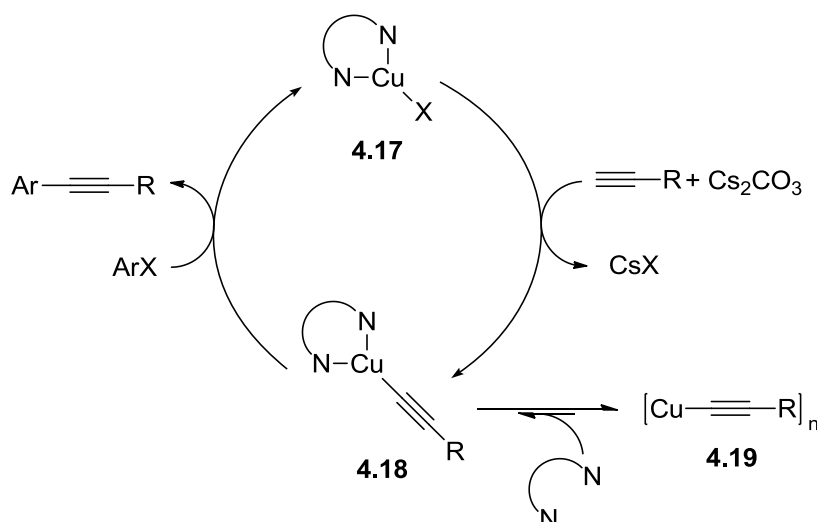


**Figure 4.7** Mechanism proposed by Bolm for the sub-mol% copper-catalysed Sonogashira reaction.

In a subsequent publication Bolm's group explored the substrate scope of the reaction and found that a variety of aryl and heteroaromatic iodides could be coupled with phenylacetylene in reasonable to excellent yields.<sup>38</sup> The group also performed DFT calculations to further probe the mechanism of the C-C bond-forming step. This was conducted by carrying out a potential energy surface scan of the reaction between phenyl iodide and [(DMEDA)Cu(CCPh)]. Besides two other transition states that were not viable due to no pathway being found for the forward reaction, a third transition state was found and showed good agreement with the experimentally determined activation energy. The transition state corresponded to the concerted breaking of the carbon-iodine bond and formation of the new C(sp)-C(sp<sup>2</sup>) bond. Furthermore, calculations for electronically modified aryl iodides, i.e. with electron donating or electron withdrawing groups, also correlated excellently with their experimental activation energies, *via* similar transition states.

Whilst the use of NHC ligands has been extensively explored for the palladium-only Sonogashira reaction, the same cannot be said for the copper-only variant. There are only three different (NHC)-Cu complexes that are reported to catalyse the Sonogashira reaction without palladium. All three are based on complex tripodal

NHCs.<sup>39,40</sup> Biffis and co-workers reported the synthesis and characterisation of tripodal (NHC)-Cu complex **4.20** in 2009 (Figure 4.8).<sup>39</sup>

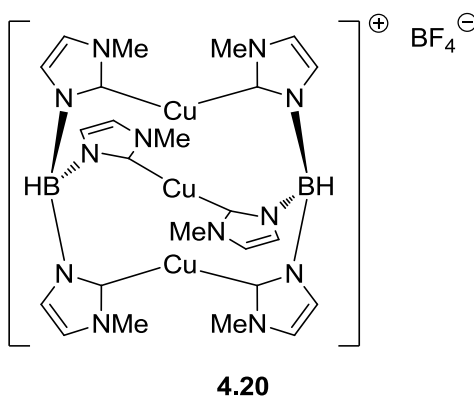


**Figure 4.8** First (NHC)-Cu complex to be utilised for copper-only Sonogashira reactions.

When the authors trialled complex **4.20** they found that 3 mol% (9 mol% Cu) was sufficient to catalyse the coupling of phenylacetylene and a variety of aryl iodides, from electron poor 4'-iodoacetophenone to electron rich 4-iodoanisole, in DMSO with Cs<sub>2</sub>CO<sub>3</sub> as the base at 110 °C. In these cases, good to excellent yields were obtained but under the same reaction conditions the mononuclear (NHC)-Cu complex, (IPr)CuCl, did not afford the desired coupled product. When the scope of the aryl halide was extended to 4'-bromoacetophenone only a poor yield of 10% was obtained. Similarly, the protocol was limited when it came to varying the alkyne and attempts to couple 4'-iodoacetophenone with oct-1-yne or ethyl acetylenecarboxylate provided the corresponding products in only 41% and 37% yield, respectively. Despite having limitations in substrate scope, this is the first example of an (NHC)-Cu catalysed Sonogashira reaction. The following year Pascu and Whittlesey also reported the synthesis of two novel tripodal (NHC)-Cu complexes **4.21** (Figure 4.9).<sup>39</sup>

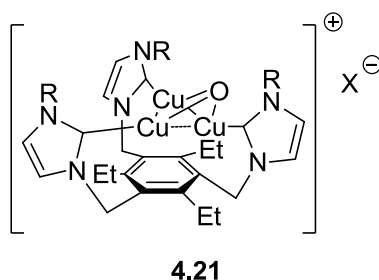


**Figure 4.9** Pascu and Whittlesey's tripodal (NHC)-Cu complex. **4.21a** : R = dipp. **4.21b** R = *t*-Bu.

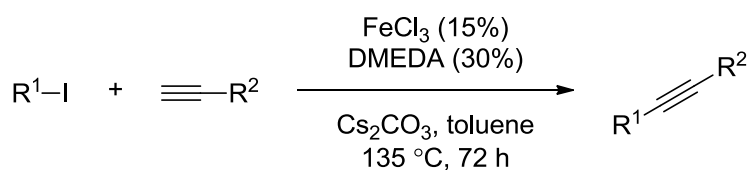
The authors employed the same condition used by Biffis and co-workers and found that complexes **4.21** could both be used to catalyse Sonogashira reactions. These complexes were shown to be a minor improvement over complex **4.20**. For example, **4.21a** was able to successfully catalyse the coupling of 4'-bromoacetophenone and phenylacetylene with an 83% yield, although the reaction temperature had to be increased to 120 °C.

Real advances have been made in the copper-only Sonogashira coupling, chief among which has been the reduction of copper loadings typically as high as 10% reduced to just 0.5%. Although a good range of aryl bromides have been shown to be amenable to these coupling reactions, aryl chlorides have yet to be incorporated with as much success, currently only activated aryl chlorides have been used. Despite the advantage of not needing the expensive palladium co-catalyst, these couplings still require high temperatures, careful handling and inert atmospheres in order to turn out good yields.

#### 4.1.3.3 Other Transition Metals

The range of different metals, with and without a copper co-catalyst, that have been reported to catalyse the Sonogashira coupling is remarkable. The main examples that will be briefly examined in this section are that of silver,<sup>41</sup> nickel,<sup>42,43</sup> iron<sup>44</sup> and gold;<sup>45</sup> although there are other instances including those catalysed by indium,<sup>46</sup> cobalt<sup>47</sup> and ruthenium.<sup>48</sup>

The lone example of a silver-only catalysed Sonogashira reaction was reported in 2006 by Wang and Li.<sup>41</sup> The catalytic protocol included 10% of silver iodide and 30% of triphenylphosphine in DMF at 100 °C with K<sub>2</sub>CO<sub>3</sub> as the base. Using these conditions the authors demonstrated that phenylacetylene and alkylacetylenes could both be coupled with a range of electronically diverse aryl iodides, and in some cases also with aryl bromides. Although the authors did not propose a mechanism, they indicate that it is likely that a silver acetylide (akin to complex **4.9**, Figure 4.5) is being generated under the reaction conditions. There is precedence in the literature for silver acetylide formation.<sup>8,49</sup> Therefore, it is possible that the silver-catalysed Sonogashira reaction is completed by a catalytic cycle similar to that shown in Figure 4.5. Other than its novelty, this catalytic system shows no advantage over the copper-only systems discussed earlier. The catalyst loading required is high at 10% and the use of a more expensive metal does not seem justified with any real increase in activity, this perhaps explains why it is the only example of such a Sonogashira protocol. On the contrary, the remarkable report of an iron based Sonogashira protocol by Bolm and co-workers<sup>44</sup> would seem more relevant. The group reported that aromatic and triethylsilyl-protected acetylenes can be effectively coupled with aryl and heteroaromatic iodides in reasonable to excellent yields, using the conditions shown in Scheme 4.9.



**Scheme 4.9** The first iron-catalysed Sonogashira reaction reported by the group of Bolm.

R<sup>1</sup> = aryl, heteroaromatic. R<sup>2</sup> = Ph, SiEt<sub>3</sub>.

The mechanistic details of the role of the iron were not fully discussed, though the authors hypothesise that the Lewis acidity of FeCl<sub>3</sub> has a role in activating the C-I bond and increasing its electrophilicity. Plenio has highlighted that Sonogashira-type

reactions can be enhanced by the addition of Lewis acids,<sup>50</sup> and the Lewis acid  $\text{InCl}_3$  has also been shown to catalyse a Sonogashira coupling.<sup>46</sup>

Liu's group have reported a bis(oxazoline) nickel complex with a copper(I) co-catalyst system that is capable of performing the Sonogashira coupling between alkynes and primary/secondary alkyl bromides/iodides.<sup>42</sup> The functional group tolerance of the coupling includes many groups: amines, alcohols, amides, ethers, fluorides, ketals, sulfonamides, esters, nitriles, boronates and carbamates; making the coupling protocol synthetically relevant for organic transformations.

A report by Corma and co-workers revealed that gold supported on a microcrystalline cerium oxide support ( $\text{Au/CeO}_2$ ) was able to catalyse the Sonogashira coupling of iodobenzene and phenylacetylene,<sup>45</sup> although homocoupling of both the acetylene and the aryl iodide were observed. As the solid catalyst was shown by X-ray photoelectron spectroscopy to contain gold(0), gold(I) and gold(III) species the group decided to further investigate which species was responsible for which reactivity pattern. Colloidal gold(0) particles showed poor activity for any of the transformations with only 6% consumption of the starting materials. A gold(I) complex supported by a Schiff base ligand showed good conversion for the desired cross-coupling reaction, whereas a similar gold(III) complex displayed selectivity for the alkyne homocoupling reaction. The authors gave no explanation for the selectivity of gold(I) for the cross-coupling, but do highlight that " $\text{Au}^{\text{I}}$  has the same  $d^{10}$  electronic structure",<sup>45</sup> i.e the same  $d^{10}$  electronic structure of palladium(0), thus suggesting parallels between the role of palladium(0) and gold(I).<sup>45</sup> Echavarren's group set out to investigate the mechanism of this gold(I) catalysed coupling reaction.<sup>51</sup>

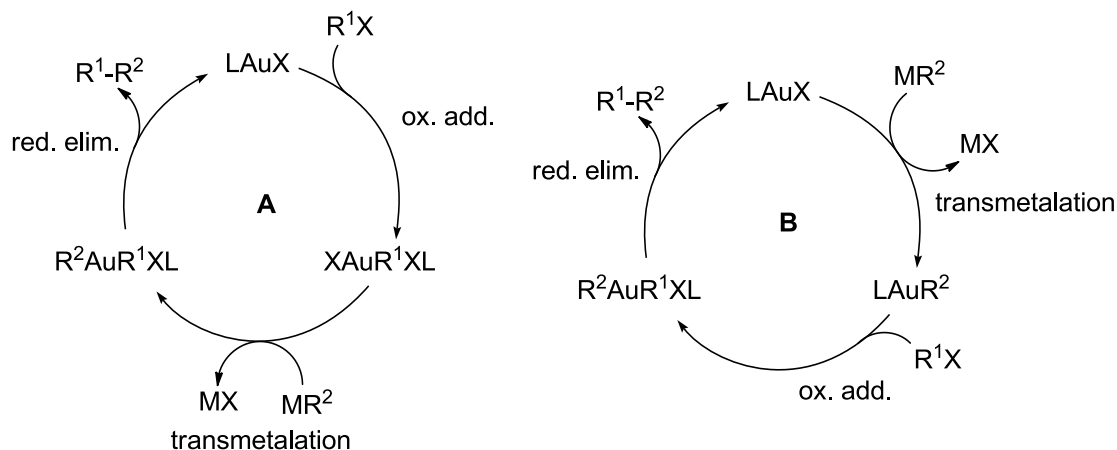
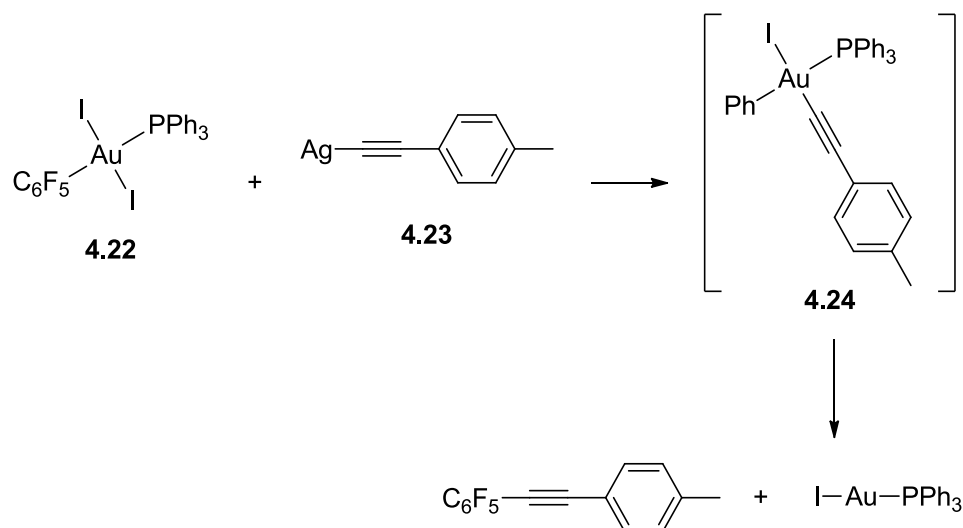


**Figure 4.10** The two catalytic cycles proposed by Echavarren to affect the gold catalysed cross-coupling reaction.  $\text{R}^1$  = aryl.  $\text{R}^2$  = alkynyl.

They initially proposed that two different catalytic cycles (Figure 4.10) could be plausible based on a gold(I)/gold(III) mechanism, analogous to the palladium(0)/palladium(II) redox couple that is widely accepted for palladium catalysed couplings. The principle difference between the cycles is the order in which the oxidative addition and transmetalation steps occur, but both cycles have the reductive elimination from a gold(III) species in common. To test the feasibility of this step, the authors set out to prepare a gold(III) complex of the type that immediately precedes the reductive elimination. They anticipated that mixing gold(III) complex **4.22** and silver acetylide **4.23** would yield the desired complex **4.24** (Scheme 4.10). Instead, the cross coupled product was obtained, suggesting that the reductive elimination step from intermediate **4.24** is possible.



**Scheme 4.10** Proof of concept for the reductive elimination from Au(III) species **4.24**.

The group also examined the oxidative addition step of the mechanism for both of the cycles. In the case of cycle A, the oxidative addition of  $\text{ArX}$  to  $\text{LAuX}$  must give the complex  $\text{LAuX}_2\text{Ar}$ . They report that this type of complex is known when the aryl group is perhalogenated (as with complex **4.22**), but there are no known examples of an oxidative additions of a regular  $\text{ArX}$  to  $\text{LAuX}$ . Indeed, their attempts to achieve such a reaction between a variety of aryl halides and  $\text{Ph}_3\text{PAuCl}$  only lead to the recovery of starting materials, hence cycle A was discounted as a possible mechanism. Cycle B requires the oxidative addition of  $\text{ArX}$  to occur with  $\text{LAu(alkyne)}$ , complexes of this type are well known and can be easily formed, for example, by transmetalation of a silver acetylide with  $\text{Ph}_3\text{PAuCl}$ , and the group synthesised  $[\text{Ph}_3\text{PAu}(\text{C}\equiv\text{CPh})]$  to test for its susceptibility towards oxidative additions. If the oxidative addition of  $\text{ArX}$  did occur, resulting in a complex similar to **4.24**, this should be followed by reductive elimination and isolation of the desired coupled product. All such attempts were unsuccessful and no product was obtained, hence the authors concluded that cycle B is not a valid mechanism. However, when 1.4 mol% of  $(\text{Ph}_3\text{P})_2\text{PdCl}_2$  and  $i\text{-Pr}_2\text{NH}$  were included in the reaction, the product was obtained in a quantitative yield. Echavarren therefore concluded that the Sonogashira reaction is not catalysed by a gold(I) complex as reported by Corma,<sup>45</sup> but in fact was likely being catalysed by palladium impurities,

with the gold(I) complex playing the role of the copper(I) salt in the tradition Sonogashira protocol.<sup>51</sup> Since then, there have been reports that provide evidence of gold nanoparticles/clusters (which are likely to be formed to some extent in homogeneous catalysis) activating aryl iodides in the absence of palladium.<sup>52,53</sup>

The paradigm of a gold-catalysed Sonogashira reaction highlights two complexities that can befall homogeneous catalysis: (1) the presence of other metals as trace impurities that could be playing a role in the catalysis;<sup>54</sup> and (2) that there may be some heterogeneous components of the catalytic system that are generated under the reaction conditions contributing to the reaction in some way.<sup>55</sup> The latter is much harder to observe, whereas the presence of trace impurities can usually be accounted for from the beginning. For example: catalysts can be synthesised from the purest metal precursors possible and metal content measured by ICP-MS. A thorough and systematic optimisation process can show that impurities from the reagents, substrates, catalysts and solvent are insignificant if product is not obtained in the absence of each component.

With these things in mind then, it might seem trivial to devise new coupling protocols using non-traditional metals (such as seen in this section), but much harder to unequivocally prove what species the reaction is being catalysed by and how the transformation is achieved. Knowledge of the specific active species is important if deliberate advances in catalysis are to be made. Of course there is weight in the argument that if a protocol is synthetically useful and reliably repeatable, the mechanistic details are not of paramount importance, providing that the end result is the desired product (in good yield). This is exemplified, to some extent, by the fact that in spite of all the developments of the Sonogashira reaction, the application of the coupling in organic synthesis in the literature favours the use of simple catalyst systems such as  $[(PPh_3)_2PdCl_2]$  or  $[(PPh_3)_4Pd]$  with CuI as a co-catalyst and aryl iodides as substrates.<sup>50</sup>



## 4.2 Investigation Aims

The use of (NHC)-Cu complexes in the Sonogashira reaction is, to the best of our knowledge, very limited. Whilst the current trend seems to be the use of (NHC)-Pd complexes for copper-free protocols, there are only a handful of examples of (NHC)-Cu complexes that have been for used for copper-only couplings. Furthermore, there are no examples of classic Pd/Cu-co-catalysed Sonogashira protocols which make use of an (NHC)-Cu complex. When used in synthesis, these catalytic systems tend to use (relatively) large amount of copper, generally ranging from 10 to 50 mol% of a copper salt.<sup>56</sup> The development of the classic protocol has essentially only involved the modification of the palladium ligand set, with the nature of copper generally being a simple copper(I) salt such as CuI. We were first inspired by Hierso's report from 2010, in which the authors disclose the synthesis of a phosphine-CuI adduct **4.25**, which is based on a polydentate ferrocenyl phosphine (Figure 4.11).<sup>57</sup>

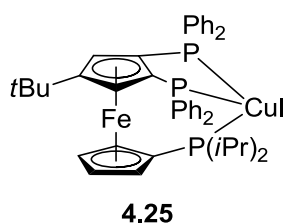
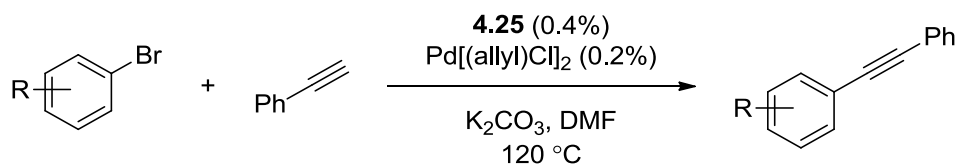


**Figure 4.11** Polydentate ferrocenyl phosphine-CuI adduct.

Using these adducts Sonogashira reactions could be performed between phenylacetylene and aryl bromides with sub-mol% catalyst loadings, but despite **4.25** being an air stable solid the couplings had to be carried out under argon (Scheme 4.11).



**Scheme 4.11** Sonogashira protocol for coupling aryl bromides using sub mol% of [Cu] and [Pd].

Secondly, recent studies in our group have shown that (NHC)CuX complexes can be used as efficient catalysts for the  $A^3$  coupling of an amine, aldehyde and alkyne to form propargylamines under mild conditions and in air.<sup>58</sup> The role of the NHC ligand in this case is to enhance the nucleophilicity of the copper acetylide species towards the imine electrophile that is formed *in situ*. Furthermore, our group has recently reported a convenient one pot microwave synthesis of (NHC)MX complexes (M = Cu, Ag or Au), which gives rapid access to the desired (NHC)-Cu complexes.<sup>59</sup> Based on these studies, the aim of this investigation was to examine the incorporation of a simple (NHC)-Cu(I) complex into the Sonogashira protocol, which should ideally be carried out without the need for dry solvents and inert atmospheres, as well as readily available catalysts. In relation to the Sonogashira reaction, the incorporation of an (NHC)-Cu complex should enhance of the nucleophilicity of the copper acetylide and therefore facilitate the transmetalation step of the catalytic cycle.

### 4.3 Results and Discussion

(NHC)CuCl complexes **4.26-4.29** (Figure 4.12) were first synthesised using the one pot microwave synthesis developed in our group,<sup>59</sup> ensuring that the CuCl used for the synthesis was of high purity (99.999% metal basis). We reasoned that as palladium TEA-complexes, **4.32** and **4.33**, have previously shown good activity in other cross-coupling reactions,<sup>60-62</sup> including the Mizoroki-Heck reaction (Chapter 3), they would be a suitable palladium source for these Sonogashira couplings. Our initial studies started with the facile coupling between iodobenzene and phenylacetylene, with technical grade DMSO as the solvent and  $K_2CO_3$  as a cheap and readily available base (Scheme 4.12).

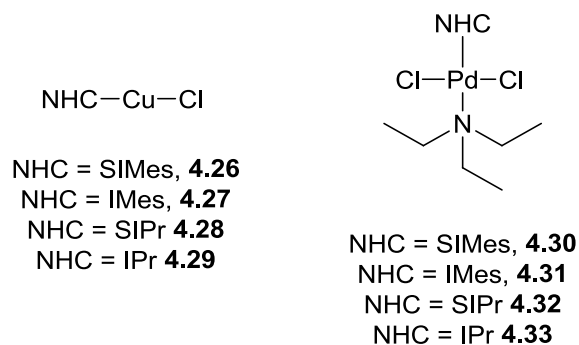
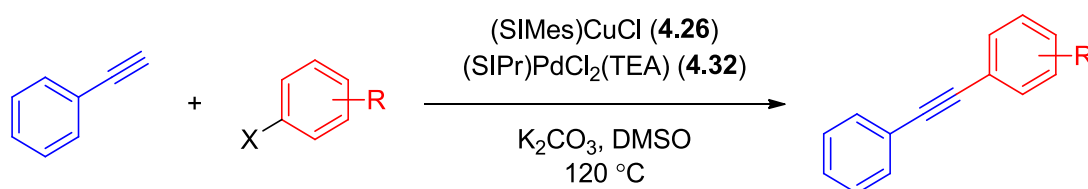


**Figure 4.12** (NHC)-Cu and (NHC)-Pd complexes used in the Sonogashira couplings.

The initial results proved positive and 1 mol% of (NHC)CuCl complex **4.26** used in combination with 0.01% of (NHC)-Pd(II) complex **4.32** afforded the coupled product in 99% yield within a short reaction time of just 30 minutes (Table 4.2, entry 1). When either metal complex was used individually a diminished product yield was obtained. Using the copper complex **4.26** on its own, a respectable yield of 72% could be achieved despite requiring a significantly increased reaction time of 21 h (Table 4.2, entry 2). This apparent activity of the copper complex alone could be the consequence of trace amounts of palladium present in the reaction mixture, as it has recently been shown as little as ppb amounts of palladium can catalyse these couplings.<sup>63</sup> Regardless of this fact, the coupling is still performed significantly quicker and in higher yields when the palladium complex **4.32** is used in tandem with (NHC)CuCl. The sole use of 0.01% of palladium complex **4.32** gave a poor yield of 31% and shows that the palladium complex alone is not an efficient catalyst for this coupling even with aryl iodides (Table 4.2, entry 3). In light of the sensitivity of the coupling to trace amounts of palladium, and in an effort to ensure any trace amounts of palladium brought to the reaction by the equipment were kept consistent, all couplings carried out from this point forward were conducted in new glass vials with magnetic stir bars that had been rigorously cleaned in aqua regia.



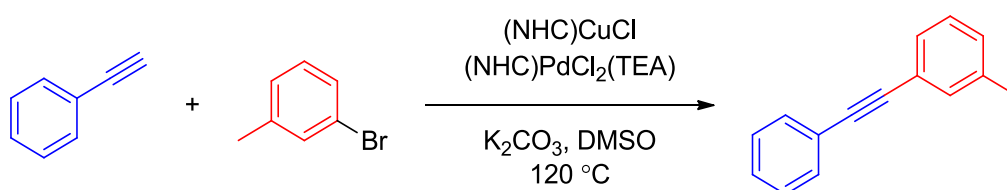
**Scheme 4.12** Initial Sonogashira couplings catalysed by collaborative (NHC)-Cu and (NHC)-Pd complexes.

Entry	R	X	[Cu] <b>4.26</b> (mol%)	[Pd] <b>4.32</b> (mol%)	t (h)	Isolated Yield (%) <sup>a</sup>
<b>1</b>	H	I	1	0.01	0.5	99
<b>2</b>	H	I	1	0	21	72
<b>3</b>	H	I	0	0.01	4	31
<b>4</b>	H	Br	1	0.01	21	91
<b>5</b>	MeCO	Cl	1	1	24	n.d.

**Table 4.2** Initial Sonogashira couplings catalysed by collaborative (NHC)-Cu and (NHC)-Pd complexes. <sup>a</sup>Average of two runs.

Attempts to extend the substrate scope to aryl bromides proved possible and bromobenzene could be coupled with phenylacetylene under the dual-metal conditions in a 91% yield (Table 4.2, entry 4). However, aryl chlorides could not be coupled using this protocol: efforts to couple activated aryl chloride 4'-chloroacetophenone proved to be ineffective even when the loading of the palladium component was increased 100 fold (Table 4.2, entry 5). It is worth noting that less than 5% of the Glaser homocoupled product was observed (by GC) in all of these experiments, which is significant given the high reaction temperatures and lack of an inert atmosphere. As greater emphasis is being placed on reducing the environmental impact of chemical processes<sup>64</sup> we made efforts to adapt the protocol to accommodate 'green' solvents. A perspective published by Pfizer medicinal chemists in 2008 provides guidelines for solvents that are

environmentally preferred and those that should be avoided.<sup>65</sup> Unfortunately, attempts to couple iodobenzene and phenylacetylene in approved solvents such as *n*-butanol and cyclopentyl methyl ether<sup>66</sup> were unsuccessful, likely due to the poor solubility of the (NHC)-Pd in these solvents. Our original solvent choice, DMSO, is not among the preferred green solvents, but neither is it in the undesirable category. Under Pfizer guidelines DMSO is a useable solvent, so we set about the optimisation of the Sonogashira coupling of phenylacetylene and 3-bromotoluene with DMSO as an acceptably green solvent (Scheme 4.13, Table 4.3).



**Scheme 4.13** Optimisation of the Sonogashira reaction between phenylacetylene and 3-bromotoluene.

Entry	[Cu] (mol%)	[Pd] (mol%)	Time (h)	Isolated Yield (%) <sup>a</sup>
1	4.26 SIMes (1)	4.32 SIPr (0.01)	24	67
2	4.27 IMes (1)	4.32 SIPr (0.01)	24	34
3	4.28 SIPr (1)	4.32 SIPr (0.01)	24	94
4	4.29 IPr (1)	4.32 SIPr (0.01)	24	16
5	4.28 SIPr (1)	4.30 SIMes (0.005)	24	64
6	4.28 SIPr (1)	4.31 IMes (0.005)	24	52
7	4.28 SIPr (1)	4.32 SIPr (0.005)	24	93
8	4.28 SIPr (1)	4.33 IPr (0.005)	24	79

<b>9</b>	<b>4.28</b> SIPr (1)	0	24	5
<b>10</b>	0	<b>4.32</b> SIPr (0.005)	24	14
<b>11</b>	0	<b>4.32</b> SIPr (0.1)	24	27
<b>12</b>	<b>4.28</b> SIPr (0.5)	<b>4.32</b> SIPr (0.005)	24	83
<b>13</b>	<b>4.28</b> SIPr (1)	<b>4.32</b> SIPr (0.005)	16	78
<b>14</b>	<b>4.28</b> SIPr (1)	<b>4.32</b> SIPr (0.1)	6	86
<b>15</b>	CuCl (1)	<b>4.32</b> SIPr (0.005)	24	51 <sup>b</sup>
<b>16</b>	<b>4.28</b> SIPr (1)	Pd(OAc) <sub>2</sub> (0.005)	24	56

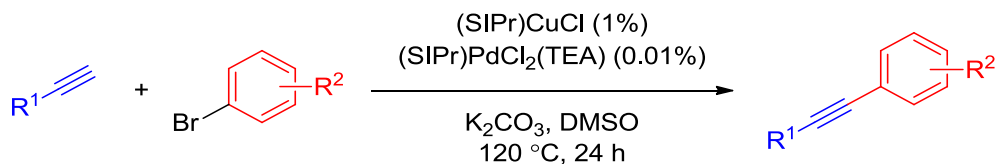
**Table 4.3** Optimisation of the Sonogashira reaction between phenylacetylene and 3-bromotoluene.

<sup>a</sup>Average of two runs. <sup>b</sup>12% of Glaser-homocoupled product observed by GC.

We began the optimisation process by investigating which NHC ligand performed best when bound to the copper complex (Table 4.3, entries 1-4), fixing SIPr as the NHC on palladium(**4.32**). We found that SIPr gave the best yield of coupled product of 94% whereas the similarly saturated NHC SIMes gave an inferior yield of 67%. Significantly, both the unsaturated analogues, IMes and IPr, proved to be worse catalysts giving 34% and 16% yields respectively. Next, we examined the effect of changing the NHC ligand on the palladium complex (Table 4.3, entries 5-9), and SIPr bearing **4.28** was chosen as the copper component due to its superior activity. The first trial of this comparison showed that at 0.01 mol% loading of (NHC)-Pd complex, the difference between NHCs was negligible (as judged by GC conversions). Hence, as a means of accentuating the difference in activity of the different NHC ligands, the catalyst loading of the (NHC)-Pd complex was decreased to 0.005%. Under these conditions both mesityl bearing (NHC)-Pd complexes **4.30** and **4.31** only gave moderate yields of 64% and 52% respectively (Table 4.3, entries 5 and 6), whereas

complexes **4.32** and **4.33** gave superior yields (Table 4.3, entries 7 and 8). SIPr-bearing complex **4.32** still gave an excellent yield of 93%. Again, both of the unsaturated NHCs were outperformed by their saturated analogues. Having determined the optimal catalysts for this coupling reaction to be **4.28** for the (NHC)-Cu component and **4.32** for the (NHC)-Pd component, we again carried out single metal reactions to ensure that the successful coupling was a result of the collaboration of the two NHC-metal complexes. Use of only the (NHC)-Cu component **4.28** (1 mol%) or the palladium component **4.32** (0.005%) resulted in poor yields of the desired product, 5% and 14% respectively (Table 4.3, entries 9 and 10). Even increasing the loading of the (NHC)-Pd complex **4.32** to 0.1 mol% (10 times the original catalyst loading) could only increase the yield to 27%. Therefore, we were confident that in this case of coupling an aryl bromide with phenylacetylene, the palladium potentially present from reagent contamination does not provide a significant contribution to the catalysis. Whilst we had found that halving the amount of (NHC)-Pd component **4.32** still allowed for an excellent yield of product to be obtained, this was not the case for the (NHC)-Cu component: when the amount of **4.28** was lowered to 0.5 mol% it proved to be detrimental to the amount of product isolated (Table 4.3, entry 12). In our efforts to optimise the reaction time, we found that performing the reaction in less than 24 h gave good but inferior isolated yields, even with an increased loading of the (NHC)-Pd complex (Table 4.3, entries 13 and 14). Finally, we examined whether it was necessary for both metal components to contain NHC ligands to achieve good activity with this catalytic system. To this end, the use of 1 mol% of CuCl in tandem with (NHC)-Pd complex **4.32** afforded an inferior yield of the desired product, with a concomitant increase in the amount of Glaser by-product (Table 4.3, entry 15). Likewise, when the (NHC)-Pd complex was switched for Pd(OAc)<sub>2</sub> and used in tandem with (NHC)-Cu complex **4.28**, this catalytic system failed to perform as adequately as our collaborative (NHC)-metal catalytic system (Table 4.3, entry 16).

With the optimized conditions in hand, various aryl bromides were coupled with arylacetylenes (Scheme 4.14). Surprisingly, when comparing the yields obtained from coupling the isomers of electron rich bromotoluene, the *ortho* substituted bromotoluene gave superior yields to the *para* substituted isomer, 89% and 64% respectively (Table 4.4, entry 2 and 3). A similar trend was noted with *p*-bromoanisole and *o*-bromoanisole, both gave reasonable yields of 63 and 66% respectively (Table 4.4, entries 4 and 5), with the *ortho* substituted analogue giving a slightly superior yield. As expected, the coupling of electron-poor aryl bromides could be accomplished in a significantly shorter reaction time of 3 hours. 4'-Bromoacetophenone and 4-bromobenzaldehyde gave excellent yields of 93 and 92% respectively (Table 4.4, entries 6 and 7).

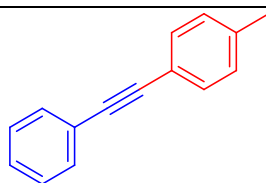


**Scheme 4.14** Sonogashira couplings of arylacetylenes and aryl bromides catalysed in tandem by (NHC)-Cu complex **4.28** and (NHC)-Pd complex **4.32**.

Entry	Product	Isolated Yield (%) <sup>a</sup>
1	 <b>4.34</b>	93 <sup>b</sup>
2	 <b>4.35</b>	89



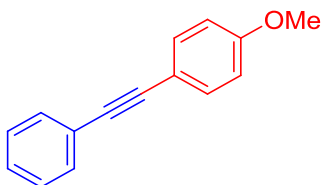
3



64

4.36

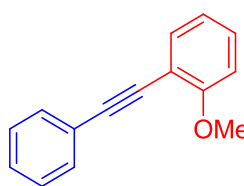
4



63

4.37

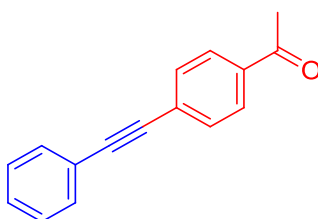
5



66

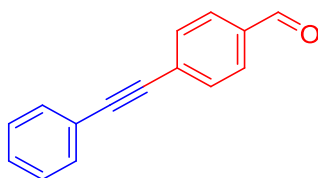
4.38

6

93<sup>b, c</sup>

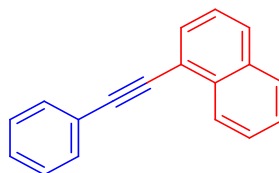
4.39

7

92<sup>c</sup>

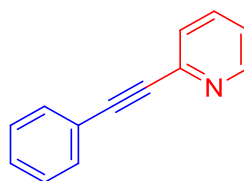
4.40

8

95<sup>b</sup>

4.41

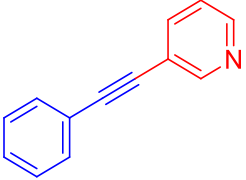
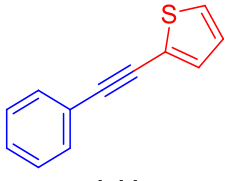
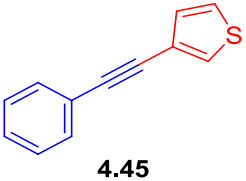
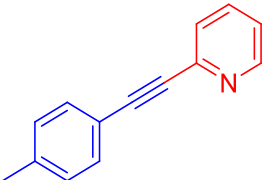
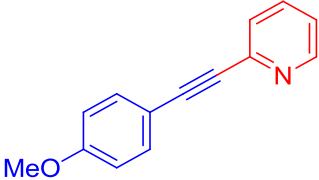
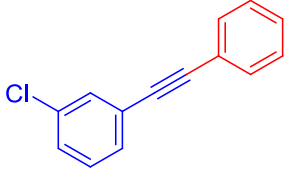
9



93

4.42

---

10	 <b>4.43</b>	78 <sup>b</sup>
11	 <b>4.44</b>	81 <sup>b</sup>
12	 <b>4.45</b>	49
13	 <b>4.46</b>	98
14	 <b>4.47</b>	94
15	 <b>4.48</b>	64

---

**Table 4.4** Sonogashira couplings of arylacetylenes and aryl bromides catalysed in tandem by (NHC)-Cu complex **4.28** and (NHC)-Pd complex **4.32**. <sup>a</sup>Average of two runs. <sup>b</sup>0.005 mol% of **4.32**.

<sup>c</sup>reaction time of 3 h.

Due to the pharmaceutical importance of heteroaromatic systems, we turned our attention to coupling of bromopyridines and bromothiophenes. In contrast to what was observed earlier in the Mizoroki-Heck reactions (Chapter 3), 2-bromopyridine gave an excellent yield of 93 (Table 4.4, entry 9), whereas 3-bromopyridine only gave a good yield of 78% (Table 4.4, entry 10). The catalytic system also gave good to moderate yields when bromothiophenes were coupled with phenylacetylene (Table 4.4, entries 11 and 12). Next we examined the effect of different substituents on the aryl ring of the acetylene coupling partner. Electron-donating groups, such as *p*-methyl and *p*-methoxy groups, favoured the coupling with 2-bromopyridine (Table 4.4, entries 13 and 14), and greater yields were obtained than with unsubstituted phenylacetylene. Aromatic acetylene substituted with an electron-withdrawing chloride atom proved to be detrimental to the reaction, as the coupled product was only obtained in a moderate yield (Table 4.4, entry 15). Attempts to extend the scope of the alkyne coupling partner to alkyl alkynes were unsuccessful, neither dec-1-yne or but-3-yn-1-ylbenzene would participate in the coupling with bromobenzene under our reaction conditions. Also, heteroarylacetylenes 2-ethynylpyridine and 2-ethynylthiophene did not show any activity.

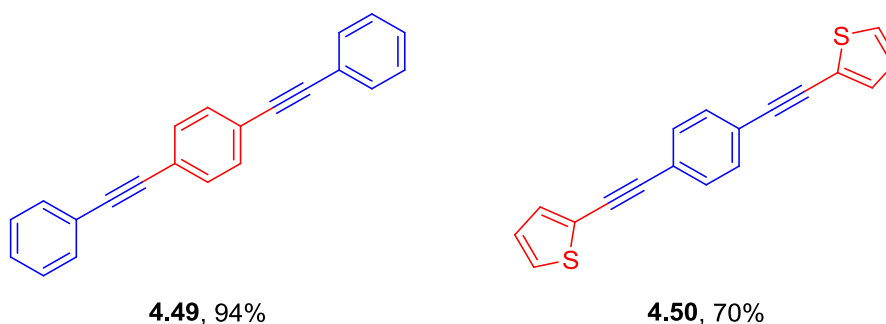


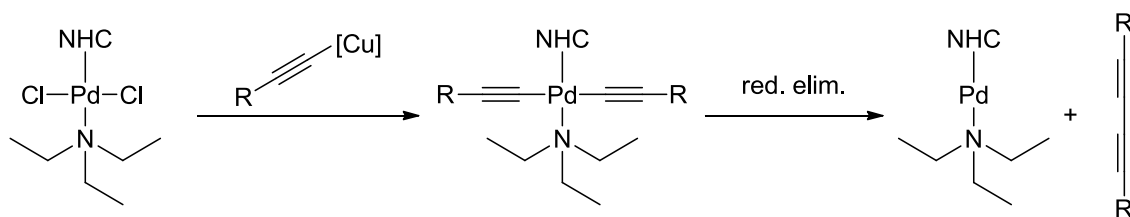
**Figure 4.13** Synthesis of polyaromatic conjugated molecules that can be applied in electron transport.

Molecular electronics have become more prominent in recent years, and highly conjugated molecules, such as those obtained from Sonogashira couplings, have been shown to be important single molecule conductors.<sup>67,68</sup> To this end, we decided to test

the potential of our protocol for the synthesis of these highly conjugated polymers. Our first approach showed that it was possible to couple 1,4-dibromobenzene with 2.1 equivalents of phenylacetylene to give **4.49** in an excellent yield (Figure 4.13). In an alternate approach we employed a dialkyne, 1,4-diethynylbenzene, in the coupling with 2-bromothiophene which gave the desired product **4.50** in good yield (Figure 4.13).

In order to be able to accurately add 0.01mol% of the (NHC)-Pd complex it was necessary to make up a stock solution of **4.32** in DMSO and perform serial dilutions of until an appropriate concentration had been reached (for more details see section 5.3.2). During our first coupling attempts, we ensured that the (NHC)-Pd catalyst solution was freshly prepared and not used after 24 h. However, we later noted that the catalyst solutions of **4.32** were still catalytically viable, and showed no sign of palladium black formation, after storage over a period of 28 days. For example, repeating the coupling of phenylacetylene with 3-bromotoluene using the month old stock solution still afforded the expected product **4.34** with no significant decrease in yield (91%). Consequently, this makes our protocol highly convenient for the Sonogashira coupling of aryl bromides as the protocol operates without the need for dry solvents, in the presence of air and the same stock solution of the (NHC)-Pd complex can be used up to a month without any detriment to the yield.

The use of both copper(I) and palladium(II) complexes for these Sonogashira reactions suggests that the mechanism follows the classic mechanism (Figure 4.1) where two catalytic cycles operate in tandem. The first cycle is a typical Pd(0)/Pd(II) oxidative addition, transmetalation and reductive elimination cycle. The second is the reaction of the (NHC)CuCl catalyst with the terminal alkyne, (NHC)Cu(acetylide) is formed and the acetylide transmetalated to the palladium cycle and the (NHC)-Cu complex is regenerated. The activation of the (NHC)PdCl<sub>2</sub>(TEA) complexes is assumed to be analogous with that of the PEPPSI complexes, which are suggested to be activated by a double transmetalation followed by reductive elimination (Scheme 4.15).<sup>69</sup>



**Scheme 4.15** Activation of the TEA-complexes by a double transmetalation/reductive elimination process.

#### 4.4 Conclusions

The aim of this investigation was to incorporate a simple (NHC)-Cu(I) complex into the Sonogashira protocol, with the view that this should enhance the transmetalation step. We have successfully developed the first Sonogashira protocol in which (NHC)-Cu and (NHC)-Pd complexes work in tandem to furnish the coupled products. This protocol is one of very few examples which makes use of low copper and palladium catalyst loadings; although the catalyst loadings are not the lowest that have been utilised,<sup>57</sup> our protocol has the significant advantage of being operationally simple. That is, the reactions can be carried out in air, in technical grade solvent with no need to exclude moisture from the system. The (NHC)-Cu and (NHC)-Pd complexes utilised are readily accessible in just a one-step synthesis from commercially available compounds. Moreover, the (NHC)PdCl<sub>2</sub>(TEA) complexes show good stability in solution (DMSO) allowing the catalyst stock solutions to be conveniently kept and reused for periods of up to one month.

#### 4.5 References

- (1) Stephens, R. D.; Castro, C. E. *J. Org. Chem.* **1963**, 28, 3313–3315.
- (2) Cassar, L. *J. Organomet. Chem.* **1975**, 93, 253–257.
- (3) Dieck, H. A.; Heck, F. R. *J. Organomet. Chem.* **1975**, 93, 259–263.
- (4) Sonogashira, K.; Tohda, Y.; Hagihara, N. *Tetrahedron Lett.* **1975**, 16, 4467–4470.
- (5) Chinchilla, R.; Nájera, C. *Chem. Soc. Rev.* **2011**, 40, 5084–5121.
- (6) Chinchilla, R.; Nájera, C. *Chem. Rev.* **2007**, 107, 874–922.
- (7) Doucet, H.; Hierso, J.-C. *Angew. Chem. Int. Ed.* **2007**, 46, 834–871.

- (8) Halbes-Letinois, U.; Weibel, J.-M.; Pale, P. *Chem. Soc. Rev.* **2007**, *36*, 759–769.
- (9) Hay, A. S. *J. Org. Chem.* **1962**, *27*, 3320–3321.
- (10) Glaser, C. *Ann. Chem. Pharm.* **1870**, *154*, 137–171.
- (11) Glaser, C. *Ber. Dtsch. Chem. Ges.* **1869**, *2*, 422–424.
- (12) Savicheva, E. A.; Kurandina, D. V.; Nikiforov, V. A. *Tetrahedron* **2014**.
- (13) Pu, X.; Li, H.; Colacot, T. J. *J. Org. Chem.* **2013**, *78*, 568–581.
- (14) Zhong, H.; Wang, J.; Li, L.; Wang, R. *Dalton Trans.* **2013**, *43*, 2098.
- (15) Yang, L.; Guan, P.; He, P.; Chen, Q.; Cao, C.; Peng, Y.; Shi, Z.; Pang, G.; Shi, Y. *Dalton Trans.* **2012**, *41*, 5020–5025.
- (16) Samantaray, M. K.; Shaikh, M. M.; Ghosh, P. *J. Organomet. Chem.* **2009**, *694*, 3477–3486.
- (17) Torborg, C.; Huang, J.; Schulz, T.; Schäffner, B.; Zapf, A.; Spannenberg, A.; Börner, A.; Beller, M. *Chem. Eur. J.* **2009**, *15*, 1329–1336.
- (18) Huang, H.; Liu, H.; Jiang, H.; Chen, K. *J. Org. Chem.* **2008**, *73*, 6037–6040.
- (19) Lipshutz, B. H.; Chung, D. W.; Rich, B. *Org. Lett.* **2008**, *10*, 3793–3796.
- (20) Yi, C.; Hua, R. *J. Org. Chem.* **2006**, *71*, 2535–2537.
- (21) Soheili, A.; Albaneze-Walker, J.; Murry, J. A.; Dormer, P. G.; Hughes, D. L. *Org. Lett.* **2003**, *5*, 4191–4194.
- (22) Ma, Y.; Song, C.; Jiang, W.; Wu, Q.; Wang, Y.; Liu, X.; Andrus, M. B. *Org. Lett.* **2003**, *5*, 3317–3319.
- (23) Böhm, V. P. W.; Herrmann, W. A. *Eur. J. Org. Chem.* **2000**, *2000*, 3679–3681.
- (24) Amatore, C.; Bensalem, S.; Ghalem, S.; Jutand, A.; Medjour, Y. *Eur. J. Org. Chem.* **2004**, *2004*, 366–371.
- (25) Tougeri, A.; Negri, S.; Jutand, A. *Chem. Eur. J.* **2007**, *13*, 666–676.
- (26) Ljungdahl, T.; Bennur, T.; Dallas, A.; Emtenäs, H.; Mårtensson, J. *Organometallics* **2008**, *27*, 2490–2498.
- (27) García-Melchor, M.; Pacheco, M. C.; Nájera, C.; Lledos, A.; Ujaque, G. *ACS Catal.* **2012**, *2*, 135–144.
- (28) Yang, C.; Nolan, S. P. *Organometallics* **2002**, *21*, 1020–1022.
- (29) Gelman, D.; Buchwald, S. L. *Angew. Chem. Int. Ed.* **2003**, *42*, 5993–5996.
- (30) Thomas, A. M.; Sujatha, A.; Anilkumar, G. *RSC Adv.* **2014**, *4*, 21688–21698.
- (31) Okuro, K.; Furuune, M.; Miura, M.; Nomura, M. *Tetrahedron Lett.* **1992**, *33*, 5363–5364.

- (32) Okuro, K.; Furuune, M.; Enna, M.; Miura, M.; Nomura, M. *J. Org. Chem.* **1993**, *58*, 4716–4721.
- (33) Monnier, F.; Turtaut, F.; Duroure, L.; Taillefer, M. *Org. Lett.* **2008**, *10*, 3203–3206.
- (34) Li, J.-H.; Li, J.-L.; Wang, D.-P.; Pi, S.-F.; Xie, Y.-X.; Zhang, M.-B.; Hu, X.-C. *J. Org. Chem.* **2007**, *72*, 2053–2057.
- (35) Lin, C.-H.; Wang, Y.-J.; Lee, C.-F. *Eur. J. Org. Chem.* **2010**, 4368.
- (36) Zuidema, E.; Bolm, C. *Chem. Eur. J.* **2010**, *16*, 4181–4185.
- (37) Berrisford, D. J.; Bolm, C.; Sharpless, K. B. *Angew. Chem. Int. Ed.* **1995**, *34*, 1059–1070.
- (38) Zou, L. H.; Johansson, A. J.; Zuidema, E.; Bolm, C. *Chem. Eur. J.* **2013**, *19*, 8144–8152.
- (39) Biffis, A.; Tubaro, C.; Scattolin, E.; Basato, M.; Papini, G.; Santini, C.; Alvarez, E.; Conejero, S. *Dalton Trans.* **2009**, 7223.
- (40) Ellul, C. E.; Reed, G.; Mahon, M. F.; Pascu, S. I.; Whittlesey, M. K. *Organometallics* **2010**, *29*, 4097–4104.
- (41) Li, P.; Wang, L. *Synlett* **2006**, *2006*, 2261–2265.
- (42) Yi, J.; Lu, X.; Sun, Y.-Y.; Xiao, B.; Liu, L. *Angew. Chem. Int. Ed.* **2013**, *52*, 12409–12413.
- (43) Wang, L.; Li, P.; Zhang, Y. *Chem. Commun.* **2004**, 514.
- (44) Carril, M.; Correa, A.; Bolm, C. *Angew. Chem. Int. Ed.* **2008**, *47*, 4862–4865.
- (45) González-Arellano, C.; Abad, A.; Corma, A.; García, H.; Iglesias, M.; Sánchez, F. *Angew. Chem. Int. Ed.* **2007**, *46*, 1536–1538.
- (46) Borah, H. N.; Prajapati, D.; Boruah, R. C. *Synlett* **2005**, 2823–2825.
- (47) Feng, L.; Liu, F.; Sun, P.; Bao, J. *Synlett* **2008**, *2008*, 1415–1417.
- (48) Park, S.; Kim, M.; Koo, D. H.; Chang, S. *Adv. Synth. Catal.* **2004**, *346*, 1638–1640.
- (49) Chen, M.-T.; Landers, B.; Navarro, O. *Org. Biomol. Chem.* **2012**, *10*, 2206–2208.
- (50) Plenio, H. *Angew. Chem. Int. Ed.* **2008**, *47*, 6954–6956.
- (51) Lauterbach, T.; Livendahl, M.; Rosellón, A.; Espinet, P.; Echavarren, A. M. *Org. Lett.* **2010**, *12*, 3006–3009.
- (52) Corma, A.; Juárez, R.; Boronat, M.; Sánchez, F.; Iglesias, M.; García, H. *Chem. Commun.* **2011**, *47*, 1446.

- (53) Robinson, P. S. D.; Khairallah, G. N.; da Silva, G.; Lioe, H.; O'Hair, R. A. J. *Angew. Chem. Int. Ed.* **2012**, *51*, 3812–3817.
- (54) Thomé, I.; Nijs, A.; Bolm, C. *Chem. Soc. Rev.* **2012**, *41*, 979–987.
- (55) Crabtree, R. H. *Chem. Rev.* **2012**, *112*, 1536–1554.
- (56) Nicolaou, K. C.; Bulger, P. G.; Sarlah, D. *Angew. Chem. Int. Ed.* **2005**, *44*, 4442–4489.
- (57) Beaupérin, M.; Job, A.; Cattey, H.; Royer, S.; Meunier, P.; Hierso, J.-C. *Organometallics* **2010**, *29*, 2815–2822.
- (58) Chen, M.-T.; Navarro, O. *Synlett* **2013**, *24*, 1190–1192.
- (59) Landers, B.; Navarro, O. *Eur. J. Inorg. Chem.* **2012**, *2012*, 2980–2982.
- (60) Chen, M.-T.; Vicic, D. A.; Chain, W. J.; Turner, M. L.; Navarro, O. *Organometallics* **2011**, *30*, 6770–6773.
- (61) Guest, D.; Chen, M.-T.; Tizzard, G. J.; Coles, S. J.; Turner, M. L.; Navarro, O. *Eur. J. Inorg. Chem.* **2014**, *2014*, 2200–2203.
- (62) Sprick, R. S.; Hoyos, M.; Chen, M.-T.; Turner, M. L.; Navarro, O. *J. Polym. Sci. Part A: Polym. Chem.* **2013**, *51*, 4904–4911.
- (63) Wang, R.; Mo, S.; Lu, Y.; Shen, Z. *Adv. Synth. Catal.* **2011**, *353*, 713–718.
- (64) Sheldon, R. A. *Chem. Soc. Rev.* **2012**, *41*, 1437–1451.
- (65) Alfonsi, K.; Colberg, J.; Dunn, P. J.; Fevig, T.; Jennings, S.; Johnson, T. A.; Kleine, H. P.; Knight, C.; Nagy, M. A.; Perry, D. A. *Green. Chem.* **2008**, *10*, 31–36.
- (66) Watanabe, K.; Yamagiwa, N.; Torisawa, Y. *Org. Process Res. Dev.* **2007**, *11*, 251–258.
- (67) Arroyo, C. R.; Tarkuc, S.; Frisenda, R.; Seldenthuis, J. S.; Woerde, C. H. M.; Eelkema, R.; Grozema, F. C.; van der Zant, H. S. J. *Angew. Chem. Int. Ed.* **2013**, *52*, 3152–3155.
- (68) Aradhya, S. V.; Venkataraman, L. *Nature Nanotech* **2013**, *8*, 399–410.
- (69) Organ, M.; Chass, G.; Fang, D.-C.; Hopkinson, A.; Valente, C. *Synthesis* **2008**, *2008*, 2776–2797.



## CHAPTER 5

## 5. Experimental Details

### 5.1 Investigation into the Reductive Cleavage of BINAP

#### 5.1.1 General Remarks

Starting materials and reagents were purchased from commercial sources and were used without any prior purification unless otherwise noted. Both TMS triflate and TBS triflate were purified by distillation under an inert atmosphere. All solvents were dried and distilled using standard methods.  $^1\text{H}$  NMR and  $^{13}\text{C}$  NMR spectra were collected at 30 °C in  $\text{CDCl}_3$  at 500 MHz and 125 MHz respectively, and referenced using the residual solvent signal ( $\delta_{\text{H}} = 7.27$ ,  $\delta_{\text{C}} = 77$ ).  $^{13}\text{C}\{^{31}\text{P}\}$  NMR Spectra were recorded at 150.81 MHz. The majority of  $^{31}\text{P}$  NMR spectra were carried out in THF with a sealed capillary tube containing  $\text{OPPh}_3$  in  $\text{D}_6$ -benzene as an internal standard ( $\delta_{\text{P}} = 25$ ).  $^{31}\text{P}$  NMR of the phosphole oxides was carried out in  $\text{CDCl}_3$  and referenced to 85% aqueous solution of  $\text{H}_3\text{PO}_4$  ( $\delta_{\text{P}} = 0$ ). All  $^{31}\text{P}$  NMR spectra were collected at 30 °C, with exception of the variable temperature experiments, at 161.72 MHz. The IR spectra were recorded using a FT-IR spectrometer equipped with an ATR accessory with a diamond top plate. High resolution mass spectra were obtained using ESI in either positive or negative mode. Unless stated otherwise, all reactions were carried out in a glove-box or on a Schlenk line.

#### 5.1.2 Computational Methods

##### 5.1.2.1 $^{31}\text{P}$ NMR Calculations

Gas phase geometry optimisations were performed using Gaussian 09 using B3LYP/6-31G(d) level of theory (unless stated otherwise); all geometries were confirmed as minima by the absence of imaginary frequencies. The NMR single point calculations

were performed using GIAO-MPW1K/6-311G++(2d,2p) in the gas phase, and using both a CPCM and IEF-PCM solvent model to obtain the  $^{31}\text{P}$  isotropic shielding tensors.

#### **5.1.2.2 Potential Energy Surface Scan**

The potential energy surface surrounding the potential intermediate species **2.15** was explored using a relaxed PES scan at the B3LYP/6-31G(d) level of theory. The dihedral angle between the binaphthyl rings was rotated around a total of  $360^\circ$  in increments of  $1^\circ$ . It should be noted this calculation was carried out without the use of a diffuse functional due to restrictions of computational resources.

#### **5.1.3 General Procedure for the Lithiation of Phosphines**

The lithiations were carried out on 0.01 M solution of the desired phosphine in a Young's ampoule equipped with a glass stirrer bar. The appropriate amount of lithium was weighed and cut into small pieces and cleaned with fine glass paper. Upon addition the reaction mixture changed from colourless to yellow, typically within 30 seconds of addition. The reaction mixtures were stirred vigorously for 2-7 days, until no lithium metal was visible and the solution was burgundy in colour.

#### **5.1.4 General Procedure for the Trapping of the Lithiated Solutions**

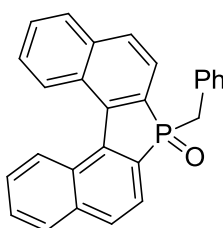
The required amount of the lithiated solution was syringed into an ampoule or a glass vial and the necessary trapping reagent added. Most quenching agents were handled and added in the glove box, or alternatively by standard Schlenk techniques.

#### **5.1.5 General Procedure for the Alkylation of Binaphthylphospholes**

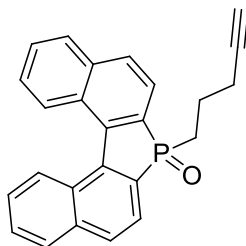
A solution of lithiated BINAP (0.16 mmol) was syringed into an ampoule or a glass vial and the requisite alkyl halide (0.64 mmol) was added in one portion. The solution was left at room temperature until  $^{31}\text{P}$  NMR showed the disappearance of the peaks at 50 and  $-22$  ppm and the appearance of two new peaks between 0 and  $-15$  ppm. The resultant solution was then removed from the glove box, quenched with saturated

ammonium chloride solution and extracted with dichloromethane. The combined organic layers were washed with water and brine, dried over sodium sulfate, filtered and evaporated under reduced pressure to yield a yellow oil. The phosphine oxides were separated by flash chromatography<sup>31</sup> using a gradient solvent system (80 to 100% EtOAc in hexanes) to give a yellow waxy solid, which was further purified by recrystallization from toluene and hexanes.

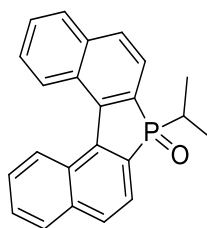
**7-benzyl-7H-benzo[e]naphtho[2,1-b]phosphindole 7-oxide (2.17)**



Following the general procedures and reaction with benzyl bromide, the product was obtained as a pale yellow solid (22.4 mg, 36%).  $R_f$  (60:40, EtOAc:Hexanes): 0.32;  $^1\text{H}$  NMR ( $\text{CDCl}_3$ , 500 MHz)  $\delta_{\text{H}}$ : 8.20 - 7.91 (m, 6H), 7.90 - 7.66 (m, 1H), 7.61 (t,  $J = 7.5$  Hz, 2H), 7.48 (t,  $J = 7.7$  Hz, 2H), 6.99 (dt,  $J = 14.7, 7.7$  Hz, 3H), 6.91 - 6.82 (m, 2H), 3.76 - 3.22 (m, 2H);  $^{13}\text{C}$  NMR ( $\text{CDCl}_3$ , 125 MHz)  $\delta_{\text{C}}$ : 137.2 (s), 131.2 (d,  $J = 7.6$  Hz), 129.9 (s, br.), 129.6 (d,  $J = 5.3$ ), 128.6 (s, br.), 128.0 (d,  $J = 3.0$  Hz), 127.9 (s, br.), 127.45 (s), 126.7 (d,  $J = 3.4$  Hz), 125.61 (s, br.), 124.46 (s, br.), 38.2 (d,  $J = 63.9$  Hz);  $^{31}\text{P}\{^1\text{H}\}$  NMR ( $\text{CDCl}_3$ , 162 MHz)  $\delta_{\text{P}}$ : 41.8 (s); IR (neat,  $\nu_{\text{max}}$ ,  $\text{cm}^{-1}$ ): 3039, 2939, 1497, 1334, 1232, 1205, 1175, 1145, 881, 818, 748, 700, 657; HRMS:  $\text{C}_{27}\text{H}_{19}\text{OPNa}$ , Mass calculated: 413.1071, Mass found: 413.1071.

**7-(pent-4-yn-1-yl)-7H-benzo[e]naphtho[2,1-b]phosphindole 7-oxide (2.18)**

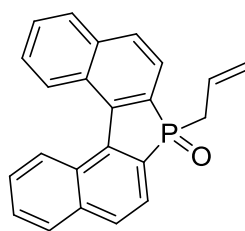
Following the general procedures and reaction with 5-chloropent-1-yne, the product was obtained as a yellow solid (32.7 mg, 56%).  $R_f$  (75:25, EtOAc:Hexanes): 0.29;  $^1\text{H}$  NMR ( $\text{CDCl}_3$ , 500 MHz)  $\delta_{\text{H}}$ : 8.17 (d,  $J = 8.6$  Hz, 2H), 8.05 (dd,  $J = 8.1, 3.4$  Hz, 2H), 7.98 (q,  $J = 8.2$  Hz, 4H), 7.64 (t,  $J = 7.5$  Hz, 2H), 7.53 (dd,  $J = 8.4, 7.0$  Hz, 2H), 2.38 - 2.24 (m, 2H), 2.20 (td,  $J = 6.9, 2.5$  Hz, 2H), 1.91 (t,  $J = 2.7$  Hz, 1H), 1.68 (s br., 2H);  $^{13}\text{C}$  NMR ( $\text{CDCl}_3$ , 125 MHz)  $\delta_{\text{C}}$ : 137.3 (s), 130.3 (s, br.), 128.9 (s), 128.8 (s), 128.0 (s), 127.6 (s), 125.8 (s), 123.9 (s, br.), 82.6 (s), 69.6 (s), 29.1 (d,  $J = 69.9$  Hz), 21.4 (d,  $J = 2.1$  Hz), 19.5 (d,  $J = 16.7$  Hz);  $^{31}\text{P}\{^1\text{H}\}$  NMR ( $\text{CDCl}_3$ , 162 MHz)  $\delta_{\text{P}}$ : 43.7 (s); IR (neat,  $\nu_{\text{max}}$ ,  $\text{cm}^{-1}$ ): 3250, 3043, 2944, 1445, 1338, 1186, 1147, 966, 883, 821, 757, 729, 657; HRMS:  $\text{C}_{25}\text{H}_{20}\text{OP}$ , Mass calculated: 367.1252, Mass found: 367.1248.

**7-isopropyl-7H-benzo[e]naphtho[2,1-b]phosphindole 7-oxide (2.19)**

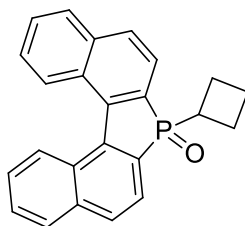
Following the general procedures and reaction with 2-bromopropane, the product was obtained as a pale yellow solid (22.0 mg, 40%).  $R_f$  (80:20, EtOAc:Hexanes): 0.30;  $^1\text{H}$  NMR ( $\text{CDCl}_3$ , 500 MHz)  $\delta_{\text{H}}$ : 8.15 (d,  $J = 8.6$  Hz, 2H), 8.07 - 7.91 (m, 6H), 7.63 (t,  $J = 8.2$ , 2H), 7.52 (t,  $J = 8.4$  Hz, 2H), 2.43 (sept,  $J = 7.3$  Hz, 1H), 1.12 (s, 6H);  $^{13}\text{C}$  NMR ( $\text{CDCl}_3$ , 125 MHz)  $\delta_{\text{C}}$ : 137.12 (s), 129.9 (s, br.), 128.8 (s), 128.7 (s), 128.0 (s), 127.4

(s), 125.7 (s), 124.4 (s, br.), 110.0 (s), 29.0 (d,  $J = 70.5$  Hz), 15.69 (s);  $^{31}\text{P}\{^1\text{H}\}$  NMR ( $\text{CDCl}_3$ , 162 MHz)  $\delta_{\text{P}}$ : 51.3 (s); IR (neat,  $\nu_{\text{max}}$ ,  $\text{cm}^{-1}$ ): 3050, 2965, 2926, 2869, 1662, 1443, 1338, 1257, 1198, 1178, 1133, 1026, 886, 814, 749, 692, 654; HRMS:  $\text{C}_{23}\text{H}_{20}\text{OP}$ , Mass calculated: 343.1252, Mass found: 343.1236.

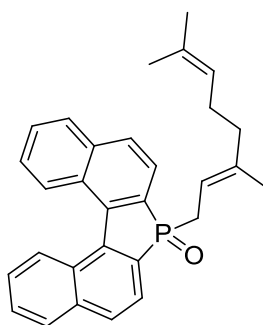
**7-allyl-7H-benzo[e]naphtho[2,1-b]phosphindole 7-oxide (2.20)**



Following the general procedures and reaction with 3-bromopropene, the product was obtained as a yellow solid (23.0 mg, 42%).  $R_f$  (80:20, EtOAc:Hexanes): 0.26;  $^1\text{H}$  NMR ( $\text{CDCl}_3$ , 500 MHz)  $\delta_{\text{H}}$ : 8.16 (d,  $J = 8.6$  Hz, 2H), 8.07 - 7.92 (m, 6H), 7.63 (t,  $J = 7.1$  Hz, 2H), 7.53 (ddd,  $J = 8.3, 6.8, 1.3$  Hz, 2H), 5.64 (ddtd,  $J = 17.5, 10.1, 7.5, 5.4$  Hz, 2H), 5.12 - 4.93 (m, 2H), 3.01 (s br. 2H);  $^{13}\text{C}$  NMR ( $\text{CDCl}_3$ , 125 MHz)  $\delta_{\text{C}}$ : 137.2 (s), 130.1 (s, br.), 128.8 (s), 128.7 (s), 128.7 (s), 128.0 (s), 127.5 (s), 126.7 (d,  $J = 8.9$  Hz), 125.7 (s), 124.2 (s, br.), 120.6 (d,  $J = 12$  Hz), 35.8 (d,  $J = 66.3$  Hz);  $^{31}\text{P}\{^1\text{H}\}$  NMR ( $\text{CDCl}_3$ , 162 MHz)  $\delta_{\text{P}}$ : 40.8 (s); IR (neat,  $\nu_{\text{max}}$ ,  $\text{cm}^{-1}$ ): 3043, 2936, 1444, 1420, 1334, 1221, 1183, 1146, 1027, 985, 915, 882, 818, 774, 749, 663; HRMS:  $\text{C}_{23}\text{H}_{18}\text{OP}$ , Mass calculated: 341.1108, Mass found: 341.1095.

**7-cyclobutyl-7H-benzo[e]naphtho[2,1-b]phosphindole 7-oxide (2.21)**

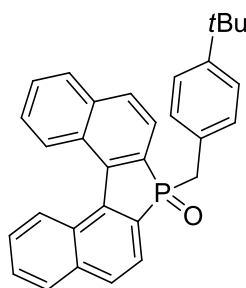
Following the general procedures and reaction with cyclobutyl bromide, the product was obtained as a yellow solid (22.7 mg, 40%).  $R_f$  (80:20, EtOAc:Hexanes): 0.26;  $^1\text{H}$  NMR ( $\text{CDCl}_3$ , 500 MHz)  $\delta_{\text{H}}$ : 8.16 (d,  $J = 8.6$  Hz, 2H), 8.03 - 7.93 (m, 6H), 7.62 (t,  $J = 7.2$  Hz, 2H), 7.52 (d,  $J = 7.0$  Hz, 2H), 2.96 (td,  $J = 8.9, 4.2$  Hz, 1H), 2.76 - 2.02 (m, 4H), 1.96 (dt,  $J = 9.9, 4.4$  Hz, 1H);  $^{13}\text{C}$  NMR ( $\text{CDCl}_3$ , 125 MHz)  $\delta_{\text{C}}$ : 137.2 (s), 130.0 (s, br.), 128.8 (s), 128.7 (s), 128.0 (s), 127.4 (s), 125.6 (s), 124.3 (s, br.), 33.64 (d,  $J = 71.2$  Hz), 22.1 (d,  $J = 5.2$  Hz), 20.4 (d,  $J = 15.7$  Hz);  $^{31}\text{P}\{^1\text{H}\}$  NMR ( $\text{CDCl}_3$ , 162 MHz)  $\delta_{\text{P}}$ : 43.9 (s); IR (neat,  $\nu_{\text{max}}$ ,  $\text{cm}^{-1}$ ): 3045, 2979, 2933, 2858, 1572, 1443, 1339, 1182, 1148, 1003, 907 812, 749; HRMS:  $\text{C}_{24}\text{H}_{20}\text{OP}$ , Mass calculated: 355.1246, Mass found: 355.1252.

**(E)-7-(3,7-dimethylocta-2,6-dien-1-yl)-7H-benzo[e]naphtho[2,1-b]phosphindole 7-oxide (2.22)**

Following the general procedures and reaction with geranyl bromide, the product was obtained as a pale yellow solid (26.4 mg, 37%).  $R_f$  (80:20, EtOAc:Hexanes): 0.33;  $^1\text{H}$  NMR ( $\text{CDCl}_3$ , 500 MHz)  $\delta_{\text{H}}$ : 8.13 (d,  $J = 8.6$  Hz, 2H), 8.06 - 7.89 (m, 6H), 7.60 (t,  $J = 7.5$  Hz, 2H), 7.50 (t,  $J = 7.7$  Hz, 2H), 5.01 - 4.76 (m, 2H), 3.00 (d,  $J = 15.5$  Hz, 2H),

1.78 – 1.59 (m, 4H), 1.57 (s, 3H), 1.40 (s, 3H), 1.27 (d,  $J = 3.9$  Hz, 3H);  $^{13}\text{C}$  NMR ( $\text{CDCl}_3$ , 125 MHz)  $\delta_{\text{C}}$ : 141.2 (d,  $J = 12.5$  Hz), 137.1 (s), 131.5 (s), 130.0 (s, br.), 128.7 (s), 127.9 (s), 127.4 (s), 125.6 (s), 124.1 (s, br.), 123.7 (s), 111.7 (d,  $J = 8.7$  Hz), 39.4 (d,  $J = 2.9$  Hz), 34.1 (s), 30.5 (d,  $J = 67.2$  Hz), 17.5 (s), 16.4 (d,  $J = 2.8$  Hz);  $^{31}\text{P}\{^1\text{H}\}$  NMR ( $\text{CDCl}_3$ , 162 MHz)  $\delta_{\text{P}}$ : 42.6 (s); IR (neat,  $\nu_{\text{max}}$ ,  $\text{cm}^{-1}$ ): 3192, 3050, 2967, 2918, 2850, 1443, 1336, 1178, 1140, 1026, 970, 864, 815, 748, 730; HRMS:  $\text{C}_{30}\text{H}_{30}\text{OP}$ , Mass calculated: 437.2029, Mass found: 437.2040.

**7-(4-(*tert*-butyl)benzyl)-7H-benzo[e]naphtho[2,1-b]phosphindole 7-oxide (2.23)**



Following the general procedures and reaction with 4-*t*-butylbenzyl bromide, the product was obtained as a pale yellow solid (13.5 mg, 19%).  $R_f$  (80:20, EtOAc:Hexanes): 0.24;  $^1\text{H}$  NMR ( $\text{CDCl}_3$ , 500 MHz)  $\delta_{\text{H}}$ : 8.08 – 7.91 (m, 6H), 7.89 – 7.71 (m, 1H), 7.60 (dd,  $J = 8.1, 6.9$  Hz, 2H), 7.53 – 7.39 (m, 2H), 6.95 (d,  $J = 8.0$  Hz, 2H), 6.77 (dd,  $J = 8.2, 2.4$  Hz, 2H), 3.49 (d,  $J = 67.8$  Hz, 2H), 1.12 (s, 9H);  $^{13}\text{C}$  NMR ( $\text{CDCl}_3$ , 125 MHz)  $\delta_{\text{C}}$ : 149.6 (s), 137.1 (s), 129.2 (d,  $J = 5.2$  Hz), 128.6 (s, br.), 127.8 (d,  $J = 7.4$  Hz), 127.4 (s), 125.6 (s, br.), 124.8 (d,  $J = 3.0$  Hz), 124.4 (s, br.), 37.6 (d,  $J = 64.3$  Hz), 34.3 (s), 31.2 (s);  $^{31}\text{P}\{^1\text{H}\}$  NMR ( $\text{CDCl}_3$ , 162 MHz)  $\delta_{\text{P}}$ : 42.5 (s); IR (neat,  $\nu_{\text{max}}$ ,  $\text{cm}^{-1}$ ): 3051, 2960, 2906, 2898, 1507, 1455, 1336, 1206, 1142, 1024, 882, 812, 746, 723; HRMS:  $\text{C}_{31}\text{H}_{27}\text{NaOP}$ , Mass calculated: 469.1692, Mass found: 469.1712.

## 5.2 (NHC)PdCl<sub>2</sub>(TEA) catalysts for the Mizoroki-Heck Reaction

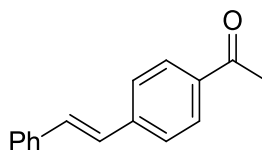
### 5.2.1 General Remarks

All reactions were carried out in screw-capped vials equipped with silicone/ptfe septa. All reagents and solvents were purchased from commercial suppliers and used without further purification unless otherwise noted. Dry DMF was purchased from Sigma-Aldrich and was further dried by 3 successive treatments with activated 4Å molecular sieves. (NHC)-Pd complexes **3.18** and **3.19** were prepared according to procedures in the literature.<sup>1</sup> Chromatography was performed using a Biotage Isolera Prime system with silica gel cartridges (P60, 35-70 µm). NMR spectra were recorded on a Varian 500 Mhz spectrometer or 400 Mhz spectrometer. Chemical shifts are reported in ppm and are referenced to the residual solvent peak or to TMS used as an internal standard. Multiplicities are reported as follows: s (singlet), d (doublet), t (triplet), dt (doublet of triplets), tdd (triplet of doublet of doublets), m (multiplet). High resolution mass spectrometry (HRMS) were recorder in positive EI mode. CHN elemental analyses were sent to London Metropolitan University for analysis.

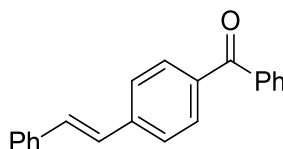
### 5.2.2 General Procedure for the Heck couplings

In a glove box, a 4ml vial was charged with potassium carbonate (1mmol), TBAB (0.5mmol), aryl halide (if solid, 0.5 mmol) and the appropriate amount of catalyst in 1ml of dry DMF. Outside of the glove box, the vial was opened to air and aryl halide (if liquid, 0.5mmol) and the required alkene (0.55mmol) added. The reaction mixture was then heated at 140°C until GC chromatography indicated the reaction was complete or there was no further increase in conversion. After cooling to room temperature the reaction mixture was poured into water (10 ml) and extracted with Et<sub>2</sub>O or EtOAc (3 x 10 ml). The combined organic layers were washed with water (3 x 10 ml) and brine (10 ml), dried over MgSO<sub>4</sub> and filtered. The resultant solution was concentrated onto Celite under reduced pressure for purification by column chromatography. All reported isolated yields are an average of two runs.

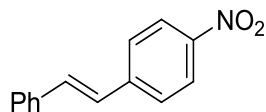


**1-(4-styrylphenyl)ethanone (3.22)<sup>2</sup>**

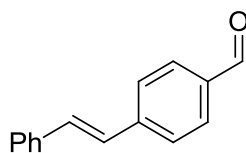
Following the general procedure, the reaction of styrene (0.55 mmol) and 4'-chloroacetophenone (0.5 mmol) gave the desired product as a pale yellow solid (211 mg, 95%). Melting point 135.6 – 138.2 °C. Eluent gradient: 5 : 95 to 20 : 80. Et<sub>2</sub>O : 40/60 petroleum ether. <sup>1</sup>H NMR (500 MHz, CDCl<sub>3</sub>) δ = 7.96 (d, *J* = 8.3 Hz, 2H), 7.60 (d, *J* = 8.2 Hz, 2H), 7.55 (d, *J* = 7.6 Hz, 2H), 7.40 (t, *J* = 7.6 Hz, 2H), 7.32 (t, *J* = 7.3 Hz, 1H), 7.24 (d, *J* = 16.3 Hz, 1H), 7.14 (d, *J* = 16.3 Hz, 1H), 2.62 (s, 3H). <sup>13</sup>C{<sup>1</sup>H} NMR (126 MHz, CDCl<sub>3</sub>) δ = 197.4, 142.0, 136.7, 136.0, 131.5, 128.9, 128.8, 128.3, 127.5, 127.4, 126.8, 126.5, 26.5.

**Phenyl(4-styrylphenyl)methanone (3.23)<sup>3</sup>**

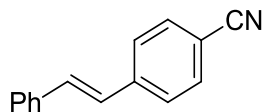
Following the general procedure, the reaction of styrene (0.55 mmol) and 4'-chlorobenzophenone (0.5 mmol) gave the desired product as an off white solid (270 mg, 96%). Melting Point 139.6 – 143.8 °C. Eluent gradient: 5 : 95 to 30 : 70. EtOAc : 40/60 petroleum ether. <sup>1</sup>H NMR (500 MHz, CDCl<sub>3</sub>) δ = 7.82 (t, *J* = 7.0 Hz, 4H), 7.64 – 7.52 (m, 5H), 7.49 (t, *J* = 7.6 Hz, 2H), 7.39 (t, *J* = 7.5 Hz, 2H), 7.34 – 7.21 (m, 2H), 7.16 (d, *J* = 16.3 Hz, 1H). <sup>13</sup>C NMR (126 MHz, CDCl<sub>3</sub>) δ = 196.0, 141.5, 137.9, 136.8, 136.3, 132.3, 131.4, 130.7, 129.9, 128.8, 128.3, 127.5, 126.8, 126.2.

**4-nitrostilbene (3.24)<sup>4</sup>**

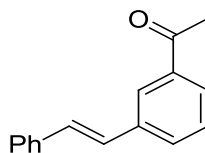
Following the general procedure, the reaction of styrene (0.55 mmol) and 1-chloro-4-nitrobenzene (0.5 mmol) gave the desired product as a yellow solid (193 mg, 91%). Melting point 153.8 – 154.7 °C. Eluent: 99 : 1. 40/60 petroleum ether : Et<sub>2</sub>O. <sup>1</sup>H NMR (500 MHz, CDCl<sub>3</sub>)  $\delta$  = 8.21 (d,  $J$  = 8.4 Hz, 2H), 7.62 (d,  $J$  = 8.4 Hz, 2H), 7.55 (d,  $J$  = 7.6 Hz, 2H), 7.45 – 7.30 (m, 3H), 7.26 (d,  $J$  = 16.3 Hz, 1H), 7.13 (d,  $J$  = 16.3 Hz, 1H). <sup>13</sup>C NMR (126 MHz, CDCl<sub>3</sub>)  $\delta$  = 146.8, 143.8, 136.2, 133.3, 128.9, 128.8, 127.0, 126.8, 126.3, 124.1.

**4-styrylbenzaldehyde (3.25)<sup>5</sup>**

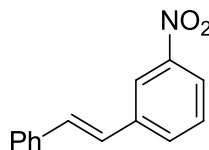
Following the general procedure, the reaction of styrene (0.55 mmol) and 4-chlorobenzaldehyde (0.5 mmol) gave the desired product as a yellow solid (170 mg, 81%). Melting point 112.4 – 114.2 °C. Eluent: 95 : 5. 40/60 petroleum ether : Et<sub>2</sub>O. <sup>1</sup>H NMR (500 MHz, CDCl<sub>3</sub>)  $\delta$  = 10.01 (s, 1H), 7.88 (d,  $J$  = 8.2 Hz, 2H), 7.67 (d,  $J$  = 8.1 Hz, 2H), 7.56 (d,  $J$  = 7.5 Hz, 2H), 7.40 (t,  $J$  = 7.5 Hz, 2H), 7.33 (t,  $J$  = 7.3 Hz, 1H), 7.28 (d,  $J$  = 16.3 Hz, 1H), 7.16 (d,  $J$  = 16.3 Hz, 1H). <sup>13</sup>C NMR (126 MHz, CDCl<sub>3</sub>)  $\delta$  = 191.5, 143.4, 136.6, 135.4, 132.2, 130.2, 128.8, 128.5, 127.3, 126.9, 126.9, 126.9.

**4-cyanostilbene (3.25)<sup>6</sup>**

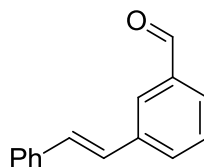
Following the general procedure, the reaction of styrene (0.55 mmol) and 1-chloro-4-cyanobenzene gave the desired product as a white solid (147 mg, 57%). Melting point 113.4 – 115.0 °C. Eluent: 10 : 1. 40/60 petroleum ether : EtOAc. <sup>1</sup>H NMR (500 MHz, CDCl<sub>3</sub>) δ = 7.65 (d, *J* = 8.3 Hz, 2H), 7.60 (d, *J* = 8.4 Hz, 2H), 7.55 (d, *J* = 7.6 Hz, 2H), 7.40 (t, *J* = 7.6 Hz, 2H), 7.33 (t, *J* = 7.3 Hz, 1H), 7.23 (d, *J* = 16.3 Hz, 1H), 7.10 (d, *J* = 16.3 Hz, 1H). <sup>13</sup>C NMR (126 MHz, CDCl<sub>3</sub>) δ = 141.8, 136.3, 132.5, 132.4, 128.8, 128.6, 126.9, 126.8, 126.7, 119.0, 110.6.

**1-(3-styrylphenyl)ethanone (3.27)<sup>7</sup>**

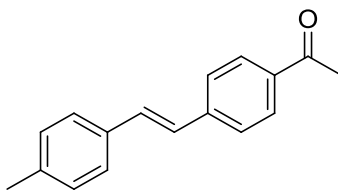
Following the general procedure, the reaction of styrene (0.55 mmol) and 3'-chloroacetophenone (0.5 mmol) gave the desired product as a pale yellow solid (143 mg, 64%). Melting point 78.8 – 80.1 °C. Eluent gradient: 1 : 9 to 35 : 65. Et<sub>2</sub>O : 40/60 petroleum ether. <sup>1</sup>H NMR (500 MHz, CDCl<sub>3</sub>) δ = 8.11 (s, 1H), 7.85 (d, *J* = 7.8 Hz, 1H), 7.72 (d, *J* = 7.8 Hz, 1H), 7.55 (d, *J* = 7.0 Hz, 2H), 7.47 (t, *J* = 7.7 Hz, 1H), 7.39 (t, *J* = 7.7 Hz, 2H), 7.30 (t, *J* = 7.4 Hz, 1H), 7.21 (d, *J* = 16.4 Hz, 1H), 7.15 (d, *J* = 16.3 Hz, 1H), 2.66 (s, 3H). <sup>13</sup>C{<sup>1</sup>H} NMR (126 MHz, CDCl<sub>3</sub>) δ = 198.0, 137.9, 137.6, 136.9, 130.8, 130.1, 128.9, 128.7, 128.0, 127.6, 127.4, 126.6, 126.1, 26.7.

**3-nitrostilbene (3.28)<sup>8</sup>**

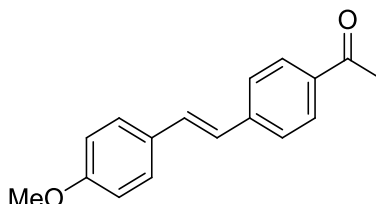
Following the general procedure, the reaction of styrene (0.55 mmol) and 1-chloro-3-nitrobenzene (0.5 mmol) as a pale yellow solid (184 mg, 82%). Melting point 110.2 – 111.2 °C. Eluent: 99 : 1. 40/60 petroleum ether : Et<sub>2</sub>O. <sup>1</sup>H NMR (500 MHz, CDCl<sub>3</sub>)  $\delta$  = 8.38 – 8.34 (m, 1H), 8.09 (d,  $J$  = 8.3 Hz, 1H), 7.79 (d,  $J$  = 8.2 Hz, 1H), 7.57 – 7.49 (m, 3H), 7.39 (t,  $J$  = 7.4 Hz, 2H), 7.32 (t,  $J$  = 7.3 Hz, 1H), 7.23 (d,  $J$  = 16.4 Hz, 1H), 7.13 (d,  $J$  = 16.3 Hz, 1H). <sup>13</sup>C NMR (126 MHz, CDCl<sub>3</sub>)  $\delta$  = 148.7, 139.2, 136.3, 132.2, 131.8, 129.5, 128.8, 128.5, 126.8, 126.1, 122.0, 120.9.

**3-styrylbenzaldehyde (3.29)<sup>5</sup>**

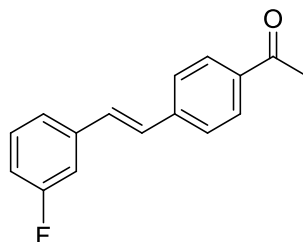
Following the general procedure, the reaction of styrene (0.55 mmol) and 3-chlorobenzaldehyde (0.5 mmol) as a yellow solid (117 mg, 56%). Melting point 98.7 – 100.2 °C. Eluent: 95 : 5. 40/60 petroleum ether : Et<sub>2</sub>O. <sup>1</sup>H NMR (500 MHz, CDCl<sub>3</sub>)  $\delta$  = 10.07 (s, 1H), 8.04 (s, 1H), 7.78 (d,  $J$  = 7.4 Hz, 2H), 7.54 (t,  $J$  = 7.4 Hz, 3H), 7.40 (t,  $J$  = 7.6 Hz, 2H), 7.31 (t,  $J$  = 7.3 Hz, 1H), 7.23 (d,  $J$  = 16.4 Hz, 1H), 7.16 (d,  $J$  = 16.3 Hz, 1H). <sup>13</sup>C NMR (126 MHz, CDCl<sub>3</sub>)  $\delta$  = 192.2, 138.4, 136.9, 136.7, 132.3, 130.6, 129.3, 128.8, 128.8, 128.1, 127.2, 127.1, 126.7.

**1-(4-(4-methylstyryl)phenyl)ethanone (3.30)**<sup>9</sup>

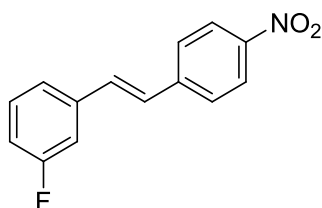
Following the general procedure, the reaction of 1-methyl-4-vinylbenzene (0.55 mmol) and 4'-chloroacetophenone (0.5 mmol) gave the product as a pale yellow solid (231 mg, 97%). Melting point 170.1 – 172.1 °C. Eluent gradient: 5 : 95 to 40 : 60. Et<sub>2</sub>O : 40/60 petroleum ether. <sup>1</sup>H NMR (500 MHz, CDCl<sub>3</sub>) δ = 7.96 (d, *J* = 8.3 Hz, 2H), 7.58 (d, *J* = 8.3 Hz, 2H), 7.45 (d, *J* = 8.0 Hz, 2H), 7.29 – 7.17 (m, 3H), 7.09 (d, *J* = 16.3 Hz, 1H), 2.61 (s, 3H), 2.39 (s, 3H). <sup>13</sup>C NMR (126 MHz, CDCl<sub>3</sub>) δ = 197.4, 142.2, 138.3, 135.8, 133.9, 131.4, 129.5, 128.8, 126.7, 126.5, 126.3, 26.5, 21.3.

**1-(4-(4-methoxystyryl)phenyl)ethanone (3.31)**<sup>9</sup>

Following the general procedure, the reaction of 1-methoxy-4-vinylbenzene (0.55 mmol) and 4'-chloroacetophenone (0.5 mmol) gave the product as a yellow solid (228 mg, 90%). Melting point 168.0 – 170.4 °C. Eluent gradient: 5 : 95 to 20 : 80. EtOAc : 40/60 petroleum ether. <sup>1</sup>H NMR (500 MHz, CDCl<sub>3</sub>) δ = 7.94 (d, *J* = 7.9 Hz, 2H), 7.55 (d, *J* = 8.0 Hz, 2H), 7.48 (d, *J* = 8.3 Hz, 2H), 7.19 (d, *J* = 16.3 Hz, 1H), 7.00 (d, *J* = 16.3 Hz, 1H), 6.92 (d, *J* = 8.2 Hz, 2H), 3.84 (s, 3H), 2.60 (s, 3H). <sup>13</sup>C NMR (126 MHz, CDCl<sub>3</sub>) δ = 197.4, 159.9, 142.4, 135.6, 131.0, 129.5, 128.8, 128.1, 126.2, 125.3, 114.3, 77.3, 77.0, 76.8, 55.3, 26.5.

**1-(4-(3-fluorostyryl)phenyl)ethanone (3.32)**

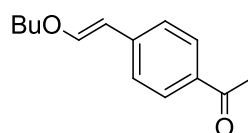
Following the general procedure, the reaction of 1-fluoro-3-vinylbenzene (0.55 mmol) and 4'-chloroacetophenone (0.5 mmol) gave the product as a yellow solid (177 mg, 74%). Melting point 95.4 – 98.4 °C. Eluent gradient: 5 : 95 to 20 : 80. Et<sub>2</sub>O : 40/60 petroleum ether. <sup>1</sup>H NMR (500 MHz, CDCl<sub>3</sub>) δ = 7.97 (d, *J* = 8.4 Hz, 2H), 7.59 (d, *J* = 8.3 Hz, 2H), 7.35 (td, *J* = 7.9, 5.8 Hz, 1H), 7.32 – 7.28 (m, 1H), 7.25 (dt, *J* = 10.1, 2.0 Hz, 1H), 7.19 (d, *J* = 16.3 Hz, 1H), 7.13 (d, *J* = 16.3 Hz, 1H), 7.00 (tdd, *J* = 8.4, 2.5, 1.1 Hz, 1H), 2.62 (s, 3H). <sup>13</sup>C NMR (126 MHz, CDCl<sub>3</sub>) δ = 197.3, 163.2 (d, <sup>1</sup>*J*<sub>FC</sub> = 245.8 Hz), 141.4, 139.1 (d, <sup>3</sup>*J*<sub>FC</sub> = 7.8 Hz), 136.3, 130.2, 130.2, 130.1, 128.9, 128.8, 126.6, 122.8 (d, <sup>4</sup>*J*<sub>FC</sub> = 2.7 Hz), 115.1 (d, <sup>2</sup>*J*<sub>FC</sub> = 21.5 Hz), 113.0 (d, <sup>2</sup>*J*<sub>FC</sub> = 21.9 Hz), 26.5. HRMS C<sub>16</sub>H<sub>14</sub>FO mass calculated 241.1023, mass found 241.1027. E.A. (CHN) %calculated for C<sub>16</sub>H<sub>14</sub>FO: %C 79.98 %H 5.45; %found: %C 79.87 %H 5.58.

**1-fluoro-3-(4-nitrostyryl)benzene (3.33)<sup>4</sup>**

Following the general procedure, the reaction of 1-fluoro-3-vinylbenzene (0.55 mmol) and 1-chloro-4-nitrobenzene (0.5 mmol) gave the product as a yellow solid (222 mg, 91%). A larger scale reaction (2 mmol of aryl chloride) afforded the product Melting point 126.8 – 129.0 °C. Eluent Gradient: 1 : 99 to 20 : 80. Et<sub>2</sub>O : 40/60 petroleum ether. <sup>1</sup>H NMR (500 MHz, CDCl<sub>3</sub>) δ = 8.24 (d, *J* = 8.7 Hz, 2H), 7.65 (d, *J* = 8.7 Hz, 2H), 7.40

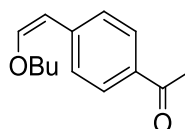
– 7.35 (m, 1H), 7.32 (d,  $J = 7.7$  Hz, 1H), 7.28 – 7.20 (m, 2H), 7.15 (d,  $J = 16.3$  Hz, 1H), 7.07 – 7.01 (m, 1H).  $^{13}\text{C}$  NMR (126 MHz,  $\text{CDCl}_3$ )  $\delta = 163.2$  (d,  $^1J_{\text{FC}} = 246.3$  Hz), 147.1, 143.3, 138.5, 132.0 (d,  $^4J_{\text{FC}} = 2.8$  Hz), 130.4 (d,  $^3J_{\text{FC}} = 8.4$  Hz), 127.6, 127.0, 124.2, 123.0 (d,  $J = 2.9$  Hz), 115.6 (d,  $J = 21.5$  Hz), 113.3 (d,  $^2J_{\text{FC}} = 22.0$  Hz).

**(E)-1-(4-(2-butoxyvinyl)phenyl)ethanone (3.34a)**<sup>10</sup>

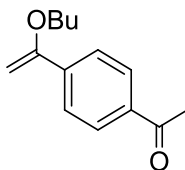


Following the general procedure, the reaction of *n*butylvinyl ether (0.55 mmol) and 4'-chloroacetophenone (0.5 mmol) gave the product as a colourless oil (86 mg, 40%). Eluent Gradient: 1 : 99 to 1 : 9. EtOAc : 40/60 petroleum ether.  $^1\text{H}$  NMR (500 MHz,  $\text{CDCl}_3$ )  $\delta = 7.85$  (d,  $J = 8.4$  Hz, 2H), 7.30 – 7.25 (m, 2H), 7.14 (d,  $J = 12.9$  Hz, 1H), 5.86 (d,  $J = 12.9$  Hz, 1H), 3.88 (t,  $J = 6.5$  Hz, 2H), 2.56 (s, 3H), 1.78 – 1.64 (m, 2H), 1.51 – 1.40 (m, 2H), 0.97 (t,  $J = 7.4$  Hz, 3H).  $^{13}\text{C}$  NMR (100 MHz,  $\text{CDCl}_3$ )  $\delta = 197.3$ , 150.4, 142.0, 134.3, 128.9, 124.6, 105.1, 70.2, 31.3, 26.4, 19.1, 13.7.

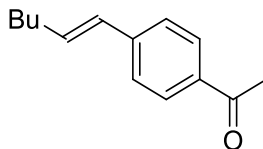
**(Z)-1-(4-(2-butoxyvinyl)phenyl)ethanone (3.34b)**<sup>10</sup>



Following the general procedure, the reaction of *n*butylvinyl ether (0.55 mmol) and 4'-chloroacetophenone (0.5 mmol) gave the product as a colourless oil (66 mg, 30%). Eluent Gradient: 1 : 99 to 1 : 9. EtOAc : 40/60 petroleum ether.  $^1\text{H}$  NMR (500 MHz,  $\text{CDCl}_3$ )  $\delta = 7.89$  (d,  $J = 8.5$  Hz, 2H), 7.65 (d,  $J = 8.5$  Hz, 2H), 6.33 (d,  $J = 7.0$  Hz, 1H), 5.25 (d,  $J = 7.0$  Hz, 1H), 3.98 (t,  $J = 6.5$  Hz, 2H), 2.57 (s, 3H), 1.80 – 1.67 (m, 2H), 1.56 – 1.40 (m, 2H), 0.98 (t,  $J = 7.4$  Hz, 3H).  $^{13}\text{C}$  NMR (126 MHz,  $\text{CDCl}_3$ )  $\delta =$  Clean spectrum unobtainable due to partial product decomposition.

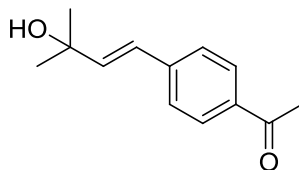
**1-(4-(1-butoxyvinyl)phenyl)ethanone (3.34c)<sup>10</sup>**

Following the general procedure, the reaction of *n*butylvinyl ether (0.55 mmol) and 4'-chloroacetophenone (0.5 mmol) gave the product as a colourless oil (65 mg, 30%). Eluent Gradient: 1 : 99 to 1 : 9. EtOAc : 40/60 petroleum ether. <sup>1</sup>H NMR (500 MHz, CDCl<sub>3</sub>)  $\delta$  = 7.93 (d, *J* = 8.5 Hz, 2H), 7.72 (d, *J* = 8.4 Hz, 2H), 4.77 (d, *J* = 2.8 Hz, 1H), 4.32 (d, *J* = 2.8 Hz, 1H), 3.88 (t, *J* = 6.4 Hz, 2H), 2.60 (s, 3H), 1.85 – 1.77 (m, 2H), 1.59 – 1.48 (m, 2H), 1.01 (t, *J* = 7.4 Hz, 3H). <sup>13</sup>C NMR (126 MHz, CDCl<sub>3</sub>)  $\delta$  = 197.6, 158.9, 141.1, 136.7, 128.2, 125.3, 84.2, 67.7, 31.1, 26.6, 19.5, 13.8.

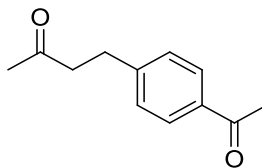
**(E)-1-(4-(hex-1-en-1-yl)phenyl)ethanone (3.35)<sup>11</sup>**

Following the general procedure, the reaction of hex-1-ene (0.55 mmol) and 4'-chloroacetophenone (0.5 mmol) gave the product as a pale yellow oil (127 mg, 64%). Eluent Gradient: 1 : 99 to 1 : 9. EtOAc : 40/60 petroleum ether. <sup>1</sup>H NMR (400 MHz, CDCl<sub>3</sub>)  $\delta$  = 7.86 (d, *J* = 8.4 Hz, 2H), 7.38 (d, *J* = 8.3 Hz, 2H), 6.44 – 6.27 (m, 2H), 2.54 (s, 3H), 2.28 – 2.16 (m, 2H), 1.53 – 1.28 (m, 4H), 0.92 (t, *J* = 7.2 Hz, 3H). <sup>13</sup>C NMR (100 MHz, CDCl<sub>3</sub>)  $\delta$  = 197.3, 142.6, 135.4, 134.4, 128.9, 128.7, 125.9, 32.8, 31.3, 26.4, 22.3, 13.9.

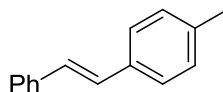


**(E)-1-(4-(3-hydroxy-3-methylbut-1-en-1-yl)phenyl)ethanone (3.36)**<sup>12</sup>

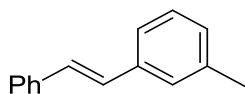
Following the general procedure, the reaction of 2-methylbut-3-en-2-ol (0.55 mmol) and 4'-chloroacetophenone (0.5 mmol) gave the product as a pale yellow oil (110 mg, 54%). Eluent Gradient: 15 : 85 to 1 : 1. EtOAc : 40/60 petroleum ether. <sup>1</sup>H NMR (500 MHz, CDCl<sub>3</sub>)  $\delta$  = 7.88 (d,  $J$  = 8.2 Hz, 2H), 7.43 (d,  $J$  = 8.1 Hz, 2H), 6.63 (d,  $J$  = 16.0 Hz, 1H), 6.47 (d,  $J$  = 16.1 Hz, 1H), 2.57 (s, 3H), 1.43 (s, 6H). <sup>13</sup>C NMR (126 MHz, CDCl<sub>3</sub>)  $\delta$  = 197.6, 141.8, 140.6, 135.9, 128.7, 126.4, 125.4, 71.0, 29.8, 26.5.

**4-(4-acetylphenyl)butan-2-one (3.37)**<sup>13</sup>

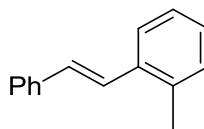
Following the general procedure, the reaction of but-3-en-2-ol (0.55 mmol) and 4'-chloroacetophenone (0.5 mmol) gave the product as a pale yellow oil (123 mg, 65%). Eluent gradient: 1 : 9 to 3 : 7. EtOAc : 40/60 petroleum ether. <sup>1</sup>H NMR (400 MHz, CDCl<sub>3</sub>)  $\delta$  = 7.82 (d,  $J$  = 8.2 Hz, 2H), 7.25 – 7.19 (m, 2H), 2.90 (t,  $J$  = 7.5 Hz, 2H), 2.74 (t,  $J$  = 7.5 Hz, 2H), 2.51 (d,  $J$  = 0.6 Hz, 3H), 2.09 (s, 3H). <sup>13</sup>C NMR (100 MHz, CDCl<sub>3</sub>)  $\delta$  = 207.1, 197.6, 146.8, 135.3, 128.6, 128.5, 44.4, 30.0, 29.5, 26.5.

**(E)-1-methyl-4-styrylbenzene (3.38)<sup>4</sup>**

Following the general procedure, the reaction of styrene (0.55 mmol) and 4-bromotoluene (0.5 mmol) gave the product as a white solid (174 mg, 90%). Melting point 108.8 – 113.1 °C. Eluent: 1 : 99. EtOAc : 40/60 petroleum ether. <sup>1</sup>H NMR (500 MHz, CDCl<sub>3</sub>)  $\delta$  = 7.44 (d,  $J$  = 7.1 Hz, 1H), 7.35 (d,  $J$  = 8.1 Hz, 2H), 7.29 (t,  $J$  = 7.6 Hz, 2H), 7.20 – 7.15 (m, 2H), 7.11 (d,  $J$  = 8.0 Hz, 2H), 7.04 (d,  $J$  = 16.2 Hz, 1H), 7.01 (d,  $J$  = 16.4 Hz, 1H), 2.30 (s, 3H). <sup>13</sup>C NMR (126 MHz, CDCl<sub>3</sub>)  $\delta$  = 137.5, 137.5, 134.5, 129.4, 128.6, 127.7, 127.4, 126.4, 126.4, 21.2.

**(E)-1-methyl-3-styrylbenzene (3.39)<sup>4</sup>**

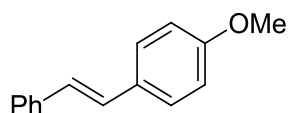
Following the general procedure, the reaction of styrene (0.55 mmol) and 3-bromotoluene (0.5 mmol) gave the product as a white solid (163 mg, 84%). Melting point 44.5 – 47.3 °C Eluent: 40/60 petroleum ether. <sup>1</sup>H NMR (400 MHz, CDCl<sub>3</sub>)  $\delta$  =  $\delta$  7.49 – 7.43 (m, 2H), 7.34 – 7.25 (m, 4H), 7.24 – 7.17 (m, 2H), 7.07 – 7.00 (m, 3H), 2.33 (s, 3H). <sup>13</sup>C NMR (126 MHz, CDCl<sub>3</sub>)  $\delta$  = 138.3, 137.6, 137.4, 128.9, 128.8, 128.7, 128.6, 128.6, 127.6, 127.3, 126.6, 123.8, 21.5.

**(E)-1-methyl-2-styrylbenzene (3.40)<sup>4</sup>**

Following the general procedure, the reaction of styrene (0.55 mmol) and 2-bromotoluene (0.5 mmol) gave the product as a colourless oil (157 mg, 81%). Eluent:

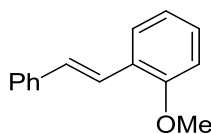
40/60 petroleum ether.  $^1\text{H}$  NMR (500 MHz,  $\text{CDCl}_3$ )  $\delta$  = 7.66 (d,  $J$  = 7.4 Hz, 1H), 7.61 – 7.57 (m, 2H), 7.46 – 7.38 (m, 3H), 7.37 – 7.23 (m, 4H), 7.07 (d,  $J$  = 16.1 Hz, 1H), 2.50 (s, 3H).  $^{13}\text{C}$  NMR (126 MHz,  $\text{CDCl}_3$ )  $\delta$  = 137.8, 136.5, 135.8, 130.4, 130.1, 128.7, 127.6, 127.6, 126.6, 126.6, 126.2, 125.4, 19.9.

**(E)-1-methoxy-4-styrylbenzene (3.41)<sup>4</sup>**

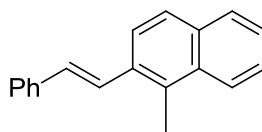


Following the general procedure, the reaction of styrene (0.55 mmol) and 4-bromoanisole (0.5 mmol) gave the product as a white solid (193 mg, 92%). Melting point 132.8 – 134.6 °C. Eluent gradient: 0 : 1 to 2 : 8. 40/60 petroleum ether :  $\text{Et}_2\text{O}$ .  $^1\text{H}$  NMR (400 MHz,  $\text{CDCl}_3$ )  $\delta$  = 7.53 – 7.43 (m, 3H), 7.34 (t,  $J$  = 7.7 Hz, 2H), 7.26 – 7.20 (m, 2H), 7.07 (d,  $J$  = 16.3 Hz, 1H), 6.97 (d,  $J$  = 16.3 Hz, 1H), 6.92 – 6.87 (m, 2H), 3.83 (s, 3H).  $^{13}\text{C}$  NMR (100 MHz,  $\text{CDCl}_3$ )  $\delta$  = 159.3, 137.6, 130.2, 128.6, 128.2, 127.7, 127.2, 126.6, 126.2, 114.1, 55.3.

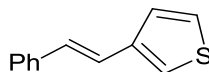
**(E)-1-methoxy-2-styrylbenzene (3.41)<sup>14</sup>**



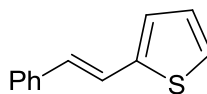
Following the general procedure, the reaction of styrene (0.55 mmol) and 2-bromoanisole (0.5 mmol) gave the product as a colourless oil (163 mg, 78%). Eluent gradient: 0 : 1 to 5 : 95.  $\text{Et}_2\text{O}$  : 40/60 petroleum ether.  $^1\text{H}$  NMR (400 MHz,  $\text{CDCl}_3$ )  $\delta$  = 7.61 (dd,  $J$  = 7.7, 1.7 Hz, 1H), 7.57 – 7.54 (m, 2H), 7.51 (d,  $J$  = 16.4 Hz, 1H), 7.36 (t,  $J$  = 7.7 Hz, 2H), 7.29 – 7.23 (m, 2H), 7.13 (d,  $J$  = 16.5 Hz, 1H), 6.99 (t,  $J$  = 7.5 Hz, 1H), 6.92 (d,  $J$  = 8.3 Hz, 1H), 3.90 (s, 3H).  $^{13}\text{C}$  NMR (100 MHz,  $\text{CDCl}_3$ )  $\delta$  = 156.9, 138.0, 129.1, 128.6, 128.6, 127.3, 126.5, 126.5, 126.4, 123.5, 120.7, 111.0, 55.5.

**(E)-1-methyl-2-styrylnaphthalene (3.43)**<sup>15</sup>

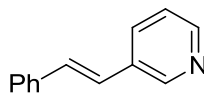
Following the general procedure, the reaction of styrene (0.55 mmol) and 2-bromo-1-methylnaphthalene (0.5 mmol) gave the product as a white solid (230 mg, 94%). Melting point 70.8 – 74.2 °C. Eluent: 40/60 petroleum ether. <sup>1</sup>H NMR (400 MHz, CDCl<sub>3</sub>)  $\delta$  = 8.25 (d,  $J$  = 7.4 Hz, 1H), 7.92 – 7.86 (m, 1H), 7.77 (d,  $J$  = 8.5 Hz, 1H), 7.69 – 7.63 (m, 2H), 7.57 – 7.36 (m, 7H), 6.85 (d,  $J$  = 16.6 Hz, 1H), 2.61 (s, 3H). <sup>13</sup>C NMR (100 MHz, CDCl<sub>3</sub>)  $\delta$  = 137.5, 135.6, 133.8, 133.3, 132.4, 132.3, 129.0, 128.8, 128.2, 127.8, 127.1, 126.5, 126.0, 125.9, 125.4, 124.9, 21.0.

**(E)-3-styrylthiophene (3.44)**<sup>2</sup>

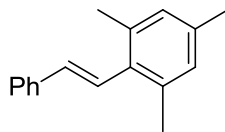
Following the general procedure, the reaction of styrene (0.55 mmol) and 3-bromothiophene (0.5 mmol) gave the product as a pale yellow solid (156 mg, 84%). Melting point 121.8 – 124.4 °C. Eluent gradient: 0 : 1 to 5 : 95 Et<sub>2</sub>O : 40/60 petroleum ether. <sup>1</sup>H NMR (400 MHz, CDCl<sub>3</sub>)  $\delta$  = 7.52 – 7.47 (m, 2H), 7.40 – 7.32 (m, 4H), 7.30 – 7.24 (m, 2H), 7.15 (d,  $J$  = 16.2 Hz, 1H), 6.98 (d,  $J$  = 16.3 Hz, 1H). <sup>13</sup>C NMR (100 MHz, CDCl<sub>3</sub>)  $\delta$  = 140.1, 137.4, 128.7, 128.6, 127.4, 126.3, 126.1, 124.9, 122.9, 122.3.

**(E)-2-styrylthiophene (3.45)<sup>4</sup>**

Following the general procedure, the reaction of styrene (0.55 mmol) and 2-bromothiophene (0.5 mmol) gave the product as a yellow solid (163 mg, 88%). Melting point 101.4 – 104.2 °C. Eluent gradient: 0 : 1 to 5 : 95 Et<sub>2</sub>O : 40/60 petroleum ether. <sup>1</sup>H NMR (400 MHz, CDCl<sub>3</sub>) δ = 7.50 – 7.46 (m, 2H), 7.36 (t, *J* = 7.7 Hz, 2H), 7.29 – 7.18 (m, 3H), 7.09 (d, *J* = 3.5 Hz, 1H), 7.02 (dd, *J* = 5.1, 3.6 Hz, 1H), 6.95 (d, *J* = 16.1 Hz, 1H). <sup>13</sup>C NMR (100 MHz, CDCl<sub>3</sub>) δ = 142.9, 137.0, 128.7, 128.4, 127.6, 126.3, 126.0, 124.3, 121.8.

**(E)-3-styrylpyridine (3.46)<sup>2</sup>**

Following the general procedure, the reaction of styrene (0.55 mmol) and 3-bromopyridine (0.5 mmol) gave the product as a pale yellow solid (150 mg, 83%). Melting point 79.3 – 81.4 °C. Eluent gradient: 5 : 95 to 40 : 60. 40/60 petroleum ether : Et<sub>2</sub>O. <sup>1</sup>H NMR (400 MHz, CDCl<sub>3</sub>) δ = 8.72 (d, *J* = 2.6 Hz, 1H), 8.49 (dd, *J* = 4.8, 1.6 Hz, 1H), 7.85 – 7.76 (m, 1H), 7.55 – 7.50 (m, 2H), 7.38 (t, *J* = 7.6 Hz, 2H), 7.32 – 7.25 (m, 2H), 7.16 (d, *J* = 16.4 Hz, 1H), 7.06 (d, *J* = 16.4 Hz, 1H). <sup>13</sup>C NMR (100 MHz, CDCl<sub>3</sub>) δ = 148.6, 136.6, 133.0, 132.6, 130.8, 128.8, 128.2, 126.6, 124.9, 123.5.

**(E)-1,3,5-trimethyl-2-styrylbenzene (3.47)**<sup>8</sup>

Following the general procedure, the reaction of styrene (0.55 mmol) and 2-bromomesitylene (0.5 mmol) gave the product as a white solid (47 mg, 21%). Melting point 50.8 – 53.6 °C. Eluent gradient: 0 : 1 to 5 : 95 EtOAc : 40/60 petroleum ether. <sup>1</sup>H NMR (400 MHz, CDCl<sub>3</sub>) δ = 7.53 (d, *J* = 7.0 Hz, 2H), 7.40 (d, *J* = 7.6 Hz, 2H), 7.32 – 7.27 (m, 1H), 7.13 (d, *J* = 16.6 Hz, 1H), 6.94 (s, 2H), 6.62 (d, *J* = 16.6 Hz, 1H), 2.38 (s, 6H), 2.32 (s, 3H). <sup>13</sup>C NMR (100 MHz, CDCl<sub>3</sub>) δ = 137.8, 136.3, 136.1, 134.0, 133.7, 128.7, 128.6, 127.4, 127.0, 126.2, 21.0, 21.0.

### 5.3 Sonogashira Couplings Catalysed by Collaborative (NHC)-Copper and -Palladium Complexes

#### 5.3.1 General Remarks

All reagents and solvents were purchased from commercial suppliers and used without further purification unless otherwise noted. (NHC)-Cu complexes **4.26-4.29** were prepared following procedures in the literature.<sup>16</sup> (NHC)-Pd complexes **4.30-4.33** were prepared according to procedures reported in the literature.<sup>1</sup> Chromatography was performed using a Biotage Isolera Prime system with silica gel cartridges (P60, 35-70  $\mu\text{m}$ ). NMR spectra were recorded on a Varian 500 or 400 Mhz spectrometer. Chemical shifts are reported in ppm and are referenced to the residual solvent peak or to a TMS used as an internal standard. Multiplicities are reported as follows: s (singlet), d (doublet), t (triplet), dt (doublet of triplets), dd (doublet of doublets), m (multiplet).

#### 5.3.2 Preparation of Catalyst Stock Solutions

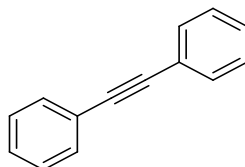
The appropriate amount of (NHC)PdCl<sub>2</sub>(TEA) (5  $\mu\text{mol}$ ) was weighed into a 2 mL vial and dissolved in 1 mL of technical grade DMSO. An aliquot (100  $\mu\text{L}$ ) was taken and diluted to a total volume of 1 mL; 100  $\mu\text{L}$  of the resultant solution is equivalent to 0.01 mol% of [Pd], based on a 0.5 mmol reaction scale (0.005  $\mu\text{mol}$  [Pd]/100  $\mu\text{L}$ ).

#### 5.3.3 General Procedure for the Sonogashira Couplings

A 4 mL screw capped vial, equipped with a magnetic stirrer bar, was charged with potassium carbonate (1 mmol) and the appropriate amount of (NHC)-copper chloride (5  $\mu\text{mol}$ , 1 mol%). The appropriate amount of Pd stock solution was added, and diluted to a total volume of 0.5 mL with technical grade DMSO. Acetylide (0.75 mmol) and aryl halide (0.5 mmol) were added and the reaction heated at 120 °C for the appropriate amount of time; the reactions were monitored by GC. After completion the reaction mixture was poured into brine and extracted with ethyl acetate, dried over magnesium sulfate, filtered and concentrated under reduced pressure. The crude material was

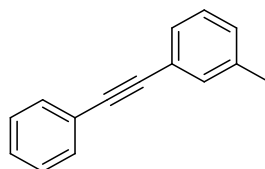
purified on silica gel (petroleum ether/ethyl acetate) to afford the pure product. All reported isolated yields are the average of two runs.

**1,2-diphenylethyne (Table 4.2, entries 1-4)<sup>17</sup>**



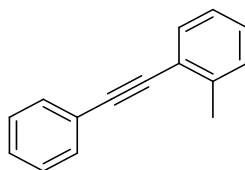
Following the general procedure, the reaction of phenyl acetylene and iodobenzene or bromobenzene using 0.01 mol% of **4.32** gave the desired product as a white solid (176 mg, 99%) after purification on a pad of silica gel (40/60 petroleum ether). Melting point: 57.8 – 61.1 °C. <sup>1</sup>H NMR (400 MHz, CDCl<sub>3</sub>) δ 7.58 – 7.51 (m, 4H), 7.40 – 7.31 (m, 6H). <sup>13</sup>C NMR (100 MHz, CDCl<sub>3</sub>) δ 131.7, 128.4, 128.3, 123.4, 89.5.

**1-methyl-3-(phenylethynyl)benzene (4.34)<sup>17</sup>**

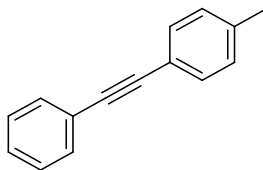


Following the general procedure, the reaction of phenyl acetylene and 3-bromotoluene using 0.005 mol% of **4.32** gave the desired product as a colourless oil (180 mg, 93%) after purification on a pad of silica gel (40/60 petroleum ether). <sup>1</sup>H NMR (400 MHz, CDCl<sub>3</sub>) δ 7.61 – 7.56 (m, 2H), 7.44 – 7.34 (m, 5H), 7.28 (t, *J* = 7.7 Hz, 1H), 7.18 (d, *J* = 7.6 Hz, 1H), 2.39 (s, 3H). <sup>13</sup>C NMR (100 MHz, CDCl<sub>3</sub>) δ 138.0, 132.2, 131.6, 129.2, 128.7, 128.3, 128.3, 128.2, 123.4, 123.1, 89.6, 89.1, 21.2.

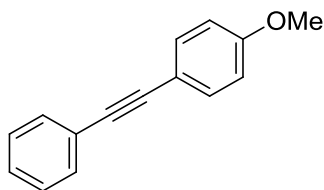


**1-methyl-2-(phenylethynyl)benzene (4.35)**<sup>17</sup>

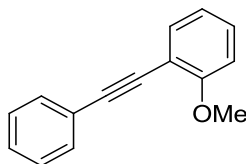
Following the general procedure, the reaction of phenyl acetylene and 2-bromotoluene using 0.01 mol% of **4.32** gave the desired product as a colourless oil (171 mg, 89%) after purification on a pad of silica gel (40/60 petroleum ether). <sup>1</sup>H NMR (400 MHz, CDCl<sub>3</sub>) δ 7.65 – 7.54 (m, 3H), 7.40 (d, *J* = 6.7 Hz, 3H), 7.31 – 7.26 (m, 2H), 7.26 – 7.18 (m, 1H), 2.59 (s, 3H). <sup>13</sup>C NMR (100 MHz, CDCl<sub>3</sub>) δ 140.2, 131.9, 131.6, 129.5, 128.4, 128.3, 128.2, 125.6, 123.6, 123.1, 93.4, 88.4, 20.8.

**1-methyl-4-(phenylethynyl)benzene (4.36)**<sup>17</sup>

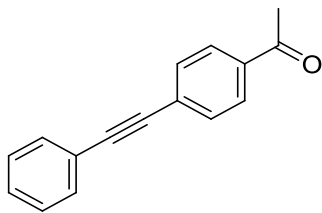
Following the general procedure, the reaction of phenyl acetylene and 4-bromotoluene using 0.01 mol% of **4.32** gave the desired product as a white solid (123 mg, 89%) after purification by flash chromatography on silica (40/60 petroleum ether). Melting point: 69.4 – 70.5 °C. <sup>1</sup>H NMR (400 MHz, Chloroform-*d*) δ 7.59 – 7.54 (m, 2H), 7.47 (d, *J* = 8.1 Hz, 2H), 7.40 – 7.33 (m, 3H), 7.19 (d, *J* = 7.9 Hz, 2H), 2.40 (s, 3H). <sup>13</sup>C NMR (100 MHz, CDCl<sub>3</sub>) δ 138.4, 131.6, 131.5, 131.5, 129.1, 128.3, 128.1, 123.5, 120.3, 89.6, 88.8, 77.4, 77.0, 76.7, 21.

**1-methoxy-4-(phenylethynyl)benzene (4.37)<sup>17</sup>**

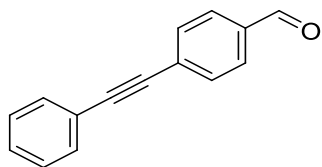
Following the general procedure, the reaction of phenyl acetylene and 4-bromoanisole using 0.01 mol% of **4.32** gave the desired product as a light yellow solid (122 mg, 63%) after purification by flash chromatography on silica. Gradient eluent: 0 : 1 to 1 : 9. EtOAc : 40/60 petroleum ether. Melting point 58.2 - 59.6 °C <sup>1</sup>H NMR (400 MHz, CDCl<sub>3</sub>) δ 7.56 – 7.46 (m, 4H), 7.39 – 7.29 (m, 3H), 6.89 (d, *J* = 8.7 Hz, 2H), 3.83 (s, 3H). <sup>13</sup>C NMR (100 MHz, CDCl<sub>3</sub>) δ 159.6, 133.0, 131.4, 128.3, 127.9, 123.6, 115.4, 114.0, 89.4, 88.1, 55.3.

**1-methoxy-2-(phenylethynyl)benzene (4.38)<sup>17</sup>**

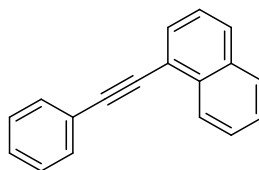
Following the general procedure, the reaction of phenyl acetylene and 2-bromoanisole using 0.01 mol% of **4.32** gave the desired product as a pale brown oil (127 mg, 66%) after purification by flash chromatography on silica. Gradient eluent: 0 : 1 to 1 : 9. EtOAc : 40/60 petroleum ether. <sup>1</sup>H NMR (400 MHz, CDCl<sub>3</sub>) δ 7.63 – 7.58 (m, 2H), 7.54 (dd, *J* = 7.6, 1.7 Hz, 1H), 7.41 – 7.29 (m, 4H), 6.97 (td, *J* = 7.5, 1.1 Hz, 1H), 6.92 (d, *J* = 8.7 Hz, 1H), 3.93 (s, 3H). <sup>13</sup>C NMR (100 MHz, CDCl<sub>3</sub>) δ 160.0, 133.6, 131.7, 129.8, 128.3, 128.1, 123.6, 120.5, 112.5, 110.8, 93.5, 85.8, 55.8.

**1-(4-(phenylethynyl)phenyl)ethanone (4.39)<sup>18</sup>**

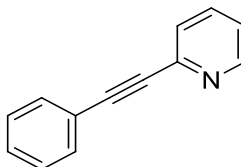
Following the general procedure, the reaction of phenyl acetylene and 4'-bromoacetophenone using 0.005 mol% of **4.32** gave the desired product as a yellow solid (205 mg, 93%) after purification on a pad of silica gel (1 : 10, EtOAc : 40/60 petroleum ether). Melting point 92.4 - 94.5 °C. <sup>1</sup>H NMR (400 MHz, CDCl<sub>3</sub>) δ 7.93 (d, *J* = 8.3 Hz, 2H), 7.61 (d, *J* = 8.4 Hz, 2H), 7.57 – 7.52 (m, 2H), 7.40 – 7.34 (m, 3H), 2.60 (s, 3H). <sup>13</sup>C NMR (100 MHz, CDCl<sub>3</sub>) δ 197.2, 136.2, 132.5, 131.7, 131.7, 128.8, 128.4, 128.2, 128.2, 122.7, 92.7, 88.6, 26.6.

**4-(phenylethynyl)benzaldehyde (4.40)<sup>19</sup>**

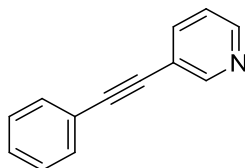
Following the general procedure, the reaction of phenyl acetylene and 4-bromoacetophenone using 0.01 mol% of **4.32** gave the desired product as a yellow solid (189 mg, 92%) after purification on a pad of silica gel (1 : 10, EtOAc : 40/60 petroleum ether). Melting point 86.6 - 89.3 °C. <sup>1</sup>H NMR (400 MHz, CDCl<sub>3</sub>) δ 10.01 (s, 1H), 7.89 – 7.82 (m, 2H), 7.67 (dd, *J* = 8.3, 2.6 Hz, 2H), 7.59 – 7.49 (m, 2H), 7.41 – 7.35 (m, 3H). <sup>13</sup>C NMR (100 MHz, CDCl<sub>3</sub>) δ 191.3, 135.4, 132.5, 132.1, 131.8, 129.5, 128.9, 128.5, 122.5, 93.4, 88.5.

**1-(phenylethynyl)naphthalene (4.41)**<sup>17</sup>

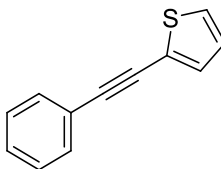
Following the general procedure, the reaction of phenyl acetylene and 1-bromonaphthalene using 0.005 mol% of **4.32** gave the desired product as a yellow oil (216 mg, 95%) after purification on a pad of silica gel (40/60 petroleum ether). <sup>1</sup>H NMR (400 MHz, CDCl<sub>3</sub>) δ 8.47 (d, *J* = 8.8 Hz, 1H), 7.87 (t, *J* = 8.9 Hz, 2H), 7.79 (dd, *J* = 7.2, 1.2 Hz, 1H), 7.67 (dd, *J* = 7.8, 1.8 Hz, 2H), 7.62 (ddd, *J* = 8.4, 6.8, 1.4 Hz, 1H), 7.55 (ddd, *J* = 8.1, 6.8, 1.3 Hz, 1H), 7.47 (dd, *J* = 8.3, 7.2 Hz, 1H), 7.44 – 7.36 (m, 3H). <sup>13</sup>C NMR (100 MHz, CDCl<sub>3</sub>) δ 133.3, 133.2, 131.7, 130.4, 128.7, 128.4, 128.4, 128.3, 126.8, 126.4, 126.2, 125.3, 123.4, 120.9, 94.3, 87.5.

**2-(phenylethynyl)pyridine (4.42)**<sup>20</sup>

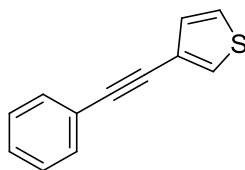
Following the general procedure, the reaction of phenyl acetylene and 1-bromonaphthalene using 0.01 mol% of **4.32** gave the desired product as a brown oil (167 mg, 93%) after purification on a pad of silica gel (2 : 10, EtOAc : 40/60 petroleum ether). <sup>1</sup>H NMR (400 MHz, CDCl<sub>3</sub>) δ 8.61 (s, 1H), 7.65 (td, *J* = 7.7, 1.7 Hz, 1H), 7.60 (dd, *J* = 6.7, 3.0 Hz, 2H), 7.51 (d, *J* = 8.0 Hz, 1H), 7.38 – 7.30 (m, 3H), 7.24 – 7.19 (m, 1H). <sup>13</sup>C NMR (100 MHz, CDCl<sub>3</sub>) δ 150.0, 143.5, 136.1, 132.0, 128.9, 128.4, 127.1, 122.7, 122.3, 89.2, 88.7.

**3-(phenylethynyl)pyridine (4.43)<sup>19</sup>**

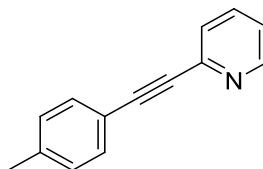
Following the general procedure, the reaction of phenyl acetylene and 1-bromonaphthalene using 0.005 mol% of **4.32** gave the desired product as a brown solid (140 mg, 78%) after purification on a pad of silica gel (2 : 10, EtOAc : 40/60 petroleum ether). <sup>1</sup>H NMR (500 MHz, CDCl<sub>3</sub>) δ 8.82 (s, 1H), 8.58 (s, 1H), 7.80 (d, *J* = 7.9 Hz, 1H), 7.59 – 7.51 (m, 2H), 7.40 – 7.33 (m, 3H), 7.32 – 7.24 (m, 1H). <sup>13</sup>C NMR (126 MHz, CDCl<sub>3</sub>) δ 152.2, 148.5, 138.3, 131.7, 128.8, 128.4, 122.5, 92.7, 86.0.

**2-(phenylethynyl)thiophene (4.44)<sup>19</sup>**

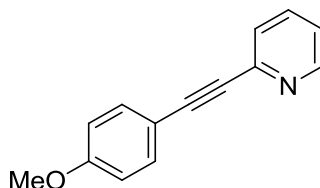
Following the general procedure, the reaction of phenyl acetylene and 2-bromothiophene using 0.005 mol% of **4.32** gave the desired product as a white solid (149 mg, 81%) after purification on a pad of silica gel (40/60 petroleum ether). Melting point: 45.3 - 48.2 °C. <sup>1</sup>H NMR (500 MHz, CDCl<sub>3</sub>) δ 7.58 – 7.50 (m, 2H), 7.37 (dt, *J* = 5.2, 2.6 Hz, 3H), 7.33 – 7.29 (m, 2H), 7.04 (dd, *J* = 5.1, 3.7 Hz, 1H). <sup>13</sup>C NMR (126 MHz, CDCl<sub>3</sub>) δ 131.9, 131.4, 128.4, 128.4, 127.2, 127.1, 123.4, 123.0, 93.1, 82.6.

**3-(phenylethynyl)thiophene (4.45)<sup>21</sup>**

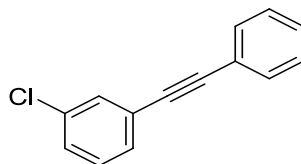
Following the general procedure, the reaction of phenyl acetylene and 3-bromothiophene using 0.01 mol% of **4.32** gave the desired product as a white solid (91 mg, 49%) after purification by flash chromatography on silica (40/60 petroleum ether). Melting point: 44.4 - 46.8 °C. <sup>1</sup>H NMR (400 MHz, CDCl<sub>3</sub>) δ 7.57 – 7.51 (m, 3H), 7.40 – 7.33 (m, 3H), 7.31 (dd, *J* = 5.0, 3.0 Hz, 1H), 7.22 (dd, *J* = 5.0, 1.2 Hz, 1H). <sup>13</sup>C NMR (100 MHz, CDCl<sub>3</sub>) δ 131.5, 129.9, 128.6, 128.3, 128.2, 125.3, 123.2, 122.3, 88.9, 84.5.

**2-(*p*-tolylethynyl)pyridine (4.46)<sup>22</sup>**

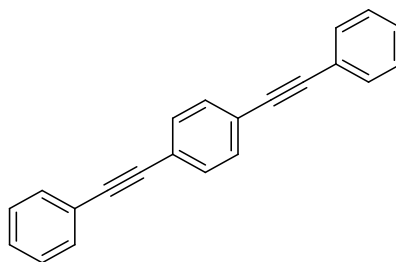
Following the general procedure, the reaction of 4-ethynyltoluene and 2-bromopyridine using 0.01 mol% of **4.32** gave the desired product as a brown oil (190 mg, 98%) after purification by flash chromatography on silica. Gradient eluent: 5 : 95 to 1 : 3. EtOAc : 40/60 petroleum ether. <sup>1</sup>H NMR (400 MHz, CDCl<sub>3</sub>) δ 8.59 (d, *J* = 4.2 Hz, 1H), 7.63 (td, *J* = 7.7, 1.8 Hz, 1H), 7.48 (d, *J* = 8.1 Hz, 3H), 7.21 – 7.12 (m, 3H), 2.34 (s, 3H). <sup>13</sup>C NMR (100 MHz, CDCl<sub>3</sub>) δ 150.0, 143.6, 139.2, 136.0, 131.9, 129.1, 127.0, 122.5, 119.2, 89.5, 88.1, 21.5.

**2-((4-methoxyphenyl)ethynyl)pyridine (4.47)<sup>22</sup>**

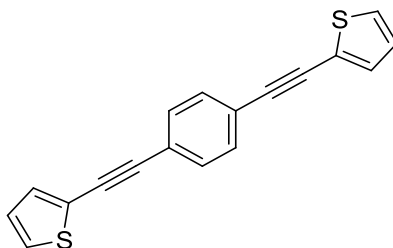
Following the general procedure, the reaction of 4-ethynylanisole and 2-bromopyridine using 0.01 mol% of **4.32** gave the desired product as a yellow oil (195 mg, 94%) after purification by flash chromatography on silica. Gradient eluent: 15 : 85 to 3 : 7. EtOAc : 40/60 petroleum ether. <sup>1</sup>H NMR (400 MHz, CDCl<sub>3</sub>) δ 8.55 (s, 1H), 7.59 (td, *J* = 7.7, 1.8 Hz, 1H), 7.49 (d, *J* = 8.8 Hz, 2H), 7.46 – 7.41 (m, 1H), 7.14 (ddd, *J* = 7.7, 4.9, 1.2 Hz, 1H), 6.83 (d, *J* = 8.8 Hz, 2H), 3.76 (s, 3H). <sup>13</sup>C NMR (100 MHz, CDCl<sub>3</sub>) δ 160.1, 149.9, 143.7, 136.0, 133.5, 126.8, 122.4, 114.3, 114.0, 89.5, 87.6, 55.2.

**1-chloro-3-(phenylethynyl)benzene (4.48)<sup>23</sup>**

Following the general procedure, the reaction of 1-chloro-3-ethynylbenzene and bromobenzene using 0.01 mol% of **4.32** gave the desired product as a colourless oil (136 mg, 64%) after purification by flash chromatography on silica (40/60 petroleum ether). <sup>1</sup>H NMR (400 MHz, CDCl<sub>3</sub>) δ 7.58 – 7.52 (m, 3H), 7.45 – 7.40 (m, 1H), 7.39 – 7.35 (m, 3H), 7.34 – 7.25 (m, 2H). <sup>13</sup>C NMR (100 MHz, CDCl<sub>3</sub>) δ 134.2, 131.7, 131.4, 129.7, 129.5, 128.6, 128.5, 128.4, 125.0, 122.8, 90.6, 87.9.

**1,4-bis(phenylethynyl)benzene (4.49)**<sup>24</sup>

Following the general procedure, the reaction of phenylacetylene (1.1 mmol) and 1,4-dibromobenzene (0.5 mmol) using 0.01 mol% of **4.32** gave the desired product as a yellow solid (262 mg, 94%) after purification by flash chromatography on silica (1 : 10, EtOAc : 40/60 petroleum ether). Melting point: 169.3 - 172.4 °C. <sup>1</sup>H NMR (400 MHz, CDCl<sub>3</sub>) δ 7.57 – 7.52 (m, 4H), 7.51 (s, 4H), 7.36 (dd, *J* = 5.1, 2.0 Hz, 6H). <sup>13</sup>C NMR (100 MHz, CDCl<sub>3</sub>) δ 131.6, 131.5, 128.4, 128.4, 123.1, 123.0, 91.2, 89.1.

**1,4-bis(thiophen-2-ylethynyl)benzene (4.50)**<sup>25</sup>

Following the general procedure, the reaction of 1, 4 diethynylbenzene (0.5 mmol) and 2-bromothiophene (1.1 mmol) using 0.01 mol% of **4.32** gave the desired product as a yellow solid (204 mg, 70%) after purification by flash chromatography on silica. Eluent gradient: 0 : 1 to 1 : 1. EtOAc : 40/60 petroleum ether. Melting point: 197.8 - 199.4 °C. <sup>1</sup>H NMR (400 MHz, CDCl<sub>3</sub>) δ 7.48 (s, 4H), 7.33 – 7.28 (m, 4H), 7.02 (dd, *J* = 5.1, 3.6 Hz, 2H). <sup>13</sup>C NMR (100 MHz, CDCl<sub>3</sub>) δ 132.1, 131.3, 127.6, 127.1, 123.0, 122.9, 92.7, 84.6.



## 5.4 References

- (1) Chen, M.-T.; Vivic, D. A.; Chain, W. J.; Turner, M. L.; Navarro, O. *Organometallics* **2011**, *30*, 6770–6773.
- (2) Tessin, U. I.; Bantreil, X.; Songis, O.; Cazin, C. S. J. *Eur. J. Inorg. Chem.* **2013**, *2013*, 2007–2010.
- (3) Alacid, E.; Nájera, C. *J. Org. Chem.* **2009**, *74*, 8191–8195.
- (4) Gao, T.-T.; Jin, A.-P.; Shao, L.-X. *Beilstein J. Org. Chem.* **2012**, *8*, 1916–1919.
- (5) Sawoo, S.; Srimani, D.; Dutta, P.; Lahiri, R.; Sarkar, A. *Tetrahedron* **2009**, *65*, 4367–4374.
- (6) Moncomble, A.; Floch, P. L.; Lledos, A.; Gosmini, C. *J. Org. Chem.* **2012**, *77*, 5056–5062.
- (7) Wang, W.; Yang, Q.; Zhou, R.; Fu, H.-Y.; Li, R.-X.; Chen, H.; Li, X.-J. *J. Organomet. Chem.* **2012**, *697*, 1–5.
- (8) Yang, F.-L.; Ma, X.-T.; Tian, S.-K. *Chem. Eur. J.* **2012**, *18*, 1582–1585.
- (9) Sore, H. F.; Boehner, C. M.; MacDonald, S. J.; Norton, D.; Fox, D. J.; Spring, D. R. *Org. Biomol. Chem.* **2009**, *7*, 1068–1072.
- (10) Datta, G. K.; Schenck, von, H.; Hallberg, A.; Larhed, M. *J. Org. Chem.* **2006**, *71*, 3896–3903.
- (11) Arvela, R. K.; Leadbeater, N. E.; Sangi, M. S.; Williams, V. A.; Granados, P.; Singer, R. D. *J. Org. Chem.* **2005**, *70*, 161–168.
- (12) Sore, H. F.; Boehner, C. M.; Laraia, L.; Logoteta, P.; Prestinari, C.; Scott, M.; Williams, K.; Galloway, W. R. J. D.; Spring, D. R. *Org. Biomol. Chem.* **2011**, *9*, 504–515.
- (13) Rahaim, R. J., Jr; Maleczka, R. E., Jr. *Org. Lett.* **2011**, *13*, 584–587.
- (14) Ke, C.-H.; Kuo, B.-C.; Nandi, D.; Lee, H. M. *Organometallics* **2013**, *32*, 4775–4784.
- (15) Mu, B.; Li, T.; Xu, W.; Zeng, G.; Liu, P.; Wu, Y. *Tetrahedron* **2007**, *63*, 11475–11488.
- (16) Landers, B.; Navarro, O. *Eur. J. Inorg. Chem.* **2012**, *2012*, 2980–2982.
- (17) Hu, H.; Yang, F.; Wu, Y. *J. Org. Chem.* **2013**, *78*, 10506–10511.
- (18) Park, K.; Bae, G.; Moon, J.; Choe, J.; Song, K. H.; Lee, S. *J. Org. Chem.* **2010**, *75*, 6244–6251.
- (19) Li, X.; Yang, F.; Wu, Y. *J. Org. Chem.* **2013**, *78*, 4543–4550.

- (20) Kaae, B. H.; Harpsøe, K.; Kvist, T.; Mathiesen, J. M.; Mølck, C.; Gloriam, D.; Jimenez, H. N.; Uberti, M. A.; Nielsen, S. M.; Nielsen, B.; Bräuner-Osborne, H.; Sauerberg, P.; Clausen, R. P.; Madsen, U. *ChemMedChem* **2012**, *7*, 440–451.
- (21) Zou, L. H.; Johansson, A. J.; Zuidema, E.; Bolm, C. *Chem. Eur. J.* **2013**, *19*, 8144–8152.
- (22) Rao, M. L. N.; Jadhav, D. N.; Dasgupta, P. *Org. Lett.* **2010**, *12*, 2048–2051.
- (23) Moon, J.; Jang, M.; Lee, S. *J. Org. Chem.* **2009**, *74*, 1403–1406.
- (24) Finke, A. D.; Elleby, E. C.; Boyd, M. J.; Weissman, H.; Moore, J. S. *J. Org. Chem.* **2009**, *74*, 8897–8900.
- (25) Arroyo, C. R.; Tarkuc, S.; Frisenda, R.; Seldenthuis, J. S.; Woerde, C. H. M.; Eelkema, R.; Grozema, F. C.; van der Zant, H. S. J. *Angew. Chem. Int. Ed.* **2013**, *52*, 3152–3155.